Engin. Library

MAR 24 1932

U. S. DEPARTMENT OF COMMERCE

BUREAU OF STANDARDS JOURNAL OF RESEARCH

Vol. 8 FEBRUARY, 1932 No. 2

CONTENTS

RP. No.	TITLE AND AUTHOR	Page
407.	Deteriorative effect of sulphur dioxide upon paper in an atmosphere of constant humidity and temperature. Arthur E. Kimberly	159
408.	Tensile properties of rail steels at elevated temperatures. G. Willard Quick	173
409.	The resistance to impact of rail steels at elevated temperatures. G. Willard Quick	191
410.	Kaolins; effect of firing temperature on some of their physical properties. R. A. Heindl, W. L. Pendergast, and L. E. Mong	199
411.	Composite-coil electrodynamic instruments. Francis B. Silsbee	217
412.	Some studies of radio transmission over long paths made on the Byrd Antarctic expedition. L. V. Berkner	265
413.	Phase equilibra in the system SiO_2-ZnO-Al_2O_3. E. N. Bunting	279
414.	System CaO-Na_2O-Al_2O_3. L. T. Brownmiller and R. H. Bogue	289
415.	Determination of tin in irons and steels. J. A. Scherrer	309

BUREAU OF STANDARDS JOURNAL OF RESEARCH

CONTENTS OF RECENT NUMBERS

September, 1931 (Vol. 7, No. 3)

RP348. The resistance to wear of carbon steels. Samuel J. Rosenberg. Price, 10 cents.
RP349. Permanence studies of current commercial book papers. John O. Burton. Price, 5 cents.
RP350. Thermomagnetic investigation of tempering of quenched 0.75 per cent carbon steel. George A. Ellinger. Price, 10 cents.
RP351. Hyperfine structures in the first spectra of krypton and xenon. C. J. Humphreys. Price, 5 cents.
RP352. Accelerated aging test for paper. Royal H. Rasch. Price, 10 cents.
RP353. Cryoscopic constant, heat of fusion, and heat capacity of camphor. Mikkel Frandsen. Price, 5 cents.
RP354. The passage of gas through the walls of pyrometer protection tubes at high temperatures. Wm. F. Roeser. Price, 5 cents.
RP355. An experimental study of several methods of representing photographic sensitivity. Raymond Davis and Gerald Kent Neeland. Price, 10 cents.
RP356. Some experimental studies of the vibrations of quartz plates. R. B. Wright and D. M. Stuart. Price, 20 cents.
RP357. Aqueous solutions of ethylene, glycol, glycerin, and sodium silicate as quenching media for steels. T. E. Hamill. Price, 15 cents.
RP358. Optical rotation and atomic dimensions—halogeno-tetra acetyl derivatives of manose. Their configurational peculiarities. D. H. Brauns. Price, 10 cents.
RP359. Soil-corrosion studies: Nonferrous metals and alloys, metallic coatings, and specially prepared ferrous pipes removed in 1930. K. H. Logan. Price, 10 cents.
RP360. Isolation and determination of the cyclohexane in a midcontinent petroleum. Johannes H. Bruun and Mildred M. Hicks-Bruun. Price, 10 cents.

October, 1931 (Vol. 7, No. 4)

RP361. Relation between the twist and certain properties of rayon yarns. Homer A. Hamm and Richard S. Cleveland. Price, 5 cents.
RP362. The hydrolysis of chestnut and quebracho tanned leathers by sulphuric acid. E. L. Wallace. Price, 5 cents.
RP363. Correlation of certain soil characteristics with pipe line corrosion. I. A. Denison. Price, 5 cents.
RP364. Further description and analysis of the first spectrum of krypton. Wm. F. Meggers, T. L. deBruin, and C. J. Humphreys. Price, 10 cents.
RP365. A correlated color temperature for illuminants. Raymond Davis. Price, 10 cents.
RP366. Quartz plate mountings and temperature control for piezo oscillators. Vincent E. Heaton and E. G. Lapham. Price, 10 cents.
RP367. An improved audio-frequency generator. E. G. Lapham. Price, 10 cents.
RP368. The porosity of electroplated chromium coatings. W. Blum, W. P. Barrows, and A. Brenner. Price, 10 cents.
RP369. The use of saturated ammonium chloride in the elimination of contact potentials. C. N. Murray and S. F. Acree. Price, 5 cents.
RP370. A balanced thermocouple and filter method of ultra-violet radiometry, with practical applications. W. W. Coblentz, R. Stair, and J. M. Hogue. Price, 10 cents.
RP371. Radiation from probe surfaces bombarded by electrons. F. L. Mohler and C. Boeckner. Price, 5 cents.

November, 1931 (Vol. 7, No. 5)

RP372. Highly purified wood fibers as paper-making material. Royal H. Rasch, Merle B. Shaw, and George W. Bicking.
RP373. Preliminary note on an automatic recorder giving a continuous height record of the Kennelly-Heaviside layer. T. R. Gilliland and G. W. Kenrick.
RP374. The relative spectral energy distribution and correlated color temperature of the N. P. L. white-light standard. Raymond Davis and K. S. Gibson. Price, 5 cents.
RP375. Isolation and determination of methylcyclopentane in a midcontinent petroleum. Mildred M. Hicks-Bruun and Johannes H. Bruun. Price, 5 cents.

Research papers, where price is given, are already available, and others will be available in the near future, as separates for purchase from the Superintendent of Documents, United States Government Printing Office, Washington, D. C.

U. S. DEPARTMENT OF COMMERCE
R. P. LAMONT, Secretary
BUREAU OF STANDARDS
GEORGE K. BURGESS, Director

BUREAU OF STANDARDS JOURNAL OF RESEARCH

February, 1932
Vol. 8, No. 2

UNITED STATES
GOVERNMENT PRINTING OFFICE
WASHINGTON : 1932

For sale by the Superintendent of Documents, Washington, D.C. - - - Price 40 cents; $3 Per Year on Subscription

For a partial list of previous research papers appearing in BUREAU OF STANDARDS JOURNAL OF RESEARCH see pages 2 and 3 of the cover

DETERIORATIVE EFFECT OF SULPHUR DIOXIDE UPON PAPER IN AN ATMOSPHERE OF CONSTANT HUMIDITY AND TEMPERATURE [1]

By Arthur E. Kimberly [2]

ABSTRACT

A preliminary survey of the causes of the deterioration of record papers in libraries having indicated atmospheric sulphur dioxide as an important factor in the deterioration, 14 different commercial book and writing papers were exposed for 240 hours to air containing 2 to 9 parts of sulphur dioxide per 1,000,000 parts of air. The temperature and relative humidity were kept constant at 30° C. and 65 per cent. Upon determining the physical and chemical characteristics of the selected papers after this treatment, the following effects were observed: A marked loss of folding endurance, accompanied by little change in tensile breaking strength, was observed. The total acidity and copper number increased considerably, while relatively little change in alpha cellulose content was observed, thus indicating that the modified forms of cellulose present in the original substance were the main points of attack. Initial quality was apparently no criterion of resistance to sulphur dioxide, since some of the low-grade papers unsuitable for permanent record use, as determined by the usual tests, suffered less from exposure to this gas than did high-grade papers. These facts add to the evidence in favor of the modification of library ventilating systems so as to eliminate acid pollution.

CONTENTS

		Page
I.	Introduction	159
II.	Description of apparatus	161
III.	Description of papers used	163
IV.	Description of test methods	165
V.	Procedure	166
VI.	Results	166
VII.	Discussion of results	168
VIII.	Summary	169
IX.	Acknowledgment	171

I. INTRODUCTION

The injurious effect of smoke upon vegetation [3] and building materials [4] in industrial localities has been well recognized for some time, as has the deleterious action of the sulphur dioxide present in the fumes emanating from certain types of smelters.[5] [6] In recent years atmospheric pollution has become of increasing concern to the inhabitants of cities, and many investigations have been conducted

[1] This is one of a series of investigations concerning the preservation of written and printed records which are being made at the Bureau of Standards with the assistance of a fund granted for the purpose by the Carnegie Corporation to the National Research Council.
[2] Research associate, National Research Council.
[3] The Effect of Smoke on Vegetation, Mellon Institute Smoke Bulletin No. 7.
[4] The effect of Smoke on Building Materials, Mellon Institute Smoke Bulletin No. 6.
[5] Report of the Selby Smelter Commission, U. S. Bureau of Mines, Bulletin No. 98.
[6] Haywood, J. K., J. A. Am. Chem. Soc., vol. 29, p. 998.

to determine the extent of the nuisance as well as means of abating it.[7 8 9 10 11 12] A study of statistics from 15 American and European cities showed air pollutions ranging from 0.2 to 3.0 parts of sulphur dioxide per 1,000,000 parts of air and an annual precipitation of sulphuric acid averaging from 11 to 190 tons per square mile. A further discussion of this problem has been given in a previous paper.[13] Additional evidence of the increasing pollution of modern urban atmospheres is given by a recent investigation by the Bureau of Standards of the causes of "winter damage" or the rotting of damp cotton fabric upon exposure to outside air experienced by laundries throughout New England.[14] Atmospheric sulphur dioxide, which is oxidized on the fabric to sulphuric acid, was found to be the cause of the phenomenon. The action is accelerated by the presence of minute quantities of iron or of chlorine bleaching residues.

Despite the great amount of evidence at hand to show the increase in the acidic nature of modern atmospheres but one attempt to determine the effect of sulphur dioxide upon paper has been found described in the literature. This work, by Richter,[15] involved the exposure of representative papers to the action of air-sulphur dioxide mixtures containing 1, 2, and 5 per cent sulphur dioxide, respectively, for periods up to 240 hours. The change of folding endurance incident to this exposure was then determined. In the concentrations of sulphur dioxide used, the decrease in folding endurance was found to be of considerable magnitude for each of the various types of paper tested. Exposures to 5 per cent sulphur dioxide for 240 hours resulted in decreases in folding endurance ranging from 48 to 68 per cent. All of these experiments were carried out in an atmosphere saturated with moisture at 20° C. (68° F.).

Although the work of Richter shows conclusively that relatively high concentrations of sulphur dioxide acting upon paper in a water-saturated atmosphere produce a large decrease in folding endurance, it seemed desirable to obtain further information of the effect of concentrations more nearly approaching those likely to be present in libraries. Therefore a series of commercial book and writing papers of various fiber compositions were exposed to the action of a sulphur-dioxide air mixture, in which the sulphur-dioxide content was maintained at 2 to 9 parts of sulphur dioxide per 1,000,000 parts of air, the exposure taking place at 30° C. (86° F.) and 65 per cent relative humidity for 240 hours. The concentration of sulphur dioxide used was the closest to actual conditions that could be accurately maintained with the equipment at hand. An elevated temperature was needed in order to produce a definite effect in a short time, so 30° C. (86° F.) was chosen. This temperature and the humidity used (65 per cent relative humidity) are representative of average summer conditions in the United States as determined by the United States Weather Bureau.

---

[7] Smoke abatement, Report of Committee of Chicago Chamber of Commerce; 1915.
[8] Recent Progress in Smoke Abatement in Manchester, Mellon Institute Smoke Bulletin No. 10.
[9] Meller, H. B., Mech. Engr., vol. 48, pp. 11a, 1275; 1926.
[10] Burrell, B. A., Proc. Leeds Phil. and Lit. Soc., Sci. Sec., vol. 1, pt. 3, p. 116; 1926.
[11] Monnett, Osborne, U. S. Bureau of Mines Technical Paper No. 273.
[12] Monnett, Parrott, and Clark, U. S. Bureau of Mines Bulletin No. 254.
[13] Kimberly, A. E., and Hicks, J. F. G., A Survey of Storage Conditions in Libraries Relative to the Preservation of Records, B. S. Misc. Pub. No. 128.
[14] Laundry "Winter Damage," Wilkie, John B., B. S. Jour. Research, vol. 6, p. 593; 1931.
[15] Richter, Geo. A., Ind. and Eng. Chem., vol. 23, No. 4, p. 371; 1931.

No analyses of air within libraries were made, as a survey of library conditions recently completed [16] showed that the acid constituents of the air are not generally removed. It was therefore assumed that the sulphur-dioxide content of air in the average library is practically the same as that of the outside air.

II. DESCRIPTION OF APPARATUS

A diagram showing the plan of the apparatus used is given in Figure 1. The cabinet, *A*, in which the exposure of the paper to the action of sulphur dioxide was made, was a double-walled box, fashioned of sheet metal and glass, the inside dimensions being 18 by 30 by 20 inches. Access to the interior was provided for by a circular door (18 inches in diameter) in the rear of the cabinet. This door

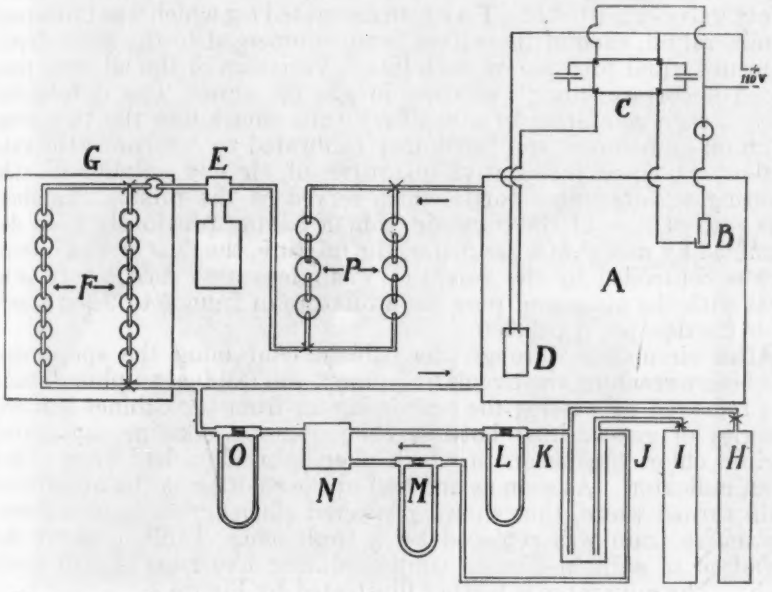

FIGURE 1.—*Diagram of apparatus for exposure of paper to sulphur dioxide*

was secured by clamps when the apparatus was in operation. In the front of the cabinet two armholes fitted with rubber gauntlets afforded a means of manipulating the specimens without disturbing conditions of temperature and humidity within the apparatus.[17]

Control of temperature was accomplished by means of a bimetallic strip, *B*, so adjusted that a slight decrease in temperature caused the strip to actuate a mercury relay, *C*, which in turn closed another circuit supplying current to a 600 w open-coil heater, *D*, within the cabinet. The heat supplied then caused the bimetallic strip to break contact, thus automatically severing the heater circuit. Even distribution of heat throughout the cabinet was assured by the use of an electric fan.

---

[16] See footnote 13, p. 160.
[17] Carson, F. T., A Small Constant Humidity Testing Cabinet, Paper Trade J., vol. 82, No. 8, p. 231; 1926.

The air was withdrawn from the cabinet by means of a small motor-driven centrifugal pump, *E*, passed through a train of gas-washing bottles, *F*, containing an aqueous solution of glycerin (specific gravity 1.1813 at 25° C.), and then returned to the cabinet. The humidity train was immersed in a water bath, *G*, held at the cabinet temperature to eliminate excessive heat losses and to aid in keeping the humidity as nearly constant as possible. The relative humidity was maintained constant to within ±1 per cent.

The mechanism used to introduce the sulphur dioxide into the cabinet consisted of a source of sulphur dioxide, *H*, and air, *I*, a safety valve for each gas, *J*, *K*, a differential valve for each gas, *L*, *M*, a mixing chamber, *N*, and a master differential valve, *O*, to govern release of the mixture into the cabinet itself. The sources of the sulphur dioxide and of air used were cylinders containing these gases, equipped with valves permitting fine adjustment. Each safety valve consisted of a T with an elongated leg which was immersed in mineral oil, each of the valves being submerged to the same depth to insure equal pressure on each line. Variation of the oil level produced a corresponding variation in gas pressure. The differential valves, each consisting of a capillary tube connecting the two arms of an oil manometer and previously calibrated to determine the rate of flow, governed the relative quantities of air and sulphur dioxide entering a 2-liter glass bottle which served as the mixing chamber. The rate of flow of the pure air from *F* having previously been determined by means of a gas meter, the mixture, the flow of which from *N* was controlled by the valve, *O*, was released at such a rate as to form with the stream of pure air a mixture of from 2 to 9 parts sulphur dioxide per 1,000,000.

After circulating through the cabinet containing the specimens, but before reaching the circulating pump, the residual sulphur dioxide was removed by passing the outcoming air from the cabinet through a series of gas-washing bottles, *P*, containing alkaline, saturated barium chloride solution to which phenolphthalein had been added as an indicator. As soon as one-half of the solution in the absorption train turned white, thus showing lowered efficiency as an absorbent, the entire train was replaced by a fresh one. Table 1 shows the variation of sulphur-dioxide content during five runs of 240 hours each. The apparatus is further illustrated by Figure 2.

TABLE 1.—*Variation of sulphur-dioxide content of air in cabinet*[1]

	Run No. 1	Run No. 2	Run No. 3	Run No. 4	Run No. 5
	Parts per million	*Parts per million*	*Parts per million*	*Parts per million*	*Parts per million*
Maximum	9.0	9.2	8.6	8.7	8.0
Minimum	3.0	3.0	2.6	2.2	4.6
Average[2]	6.2	5.4	5.8	5.8	5.8

[1] Computed from control data.
[2] Average of readings taken at hourly intervals.

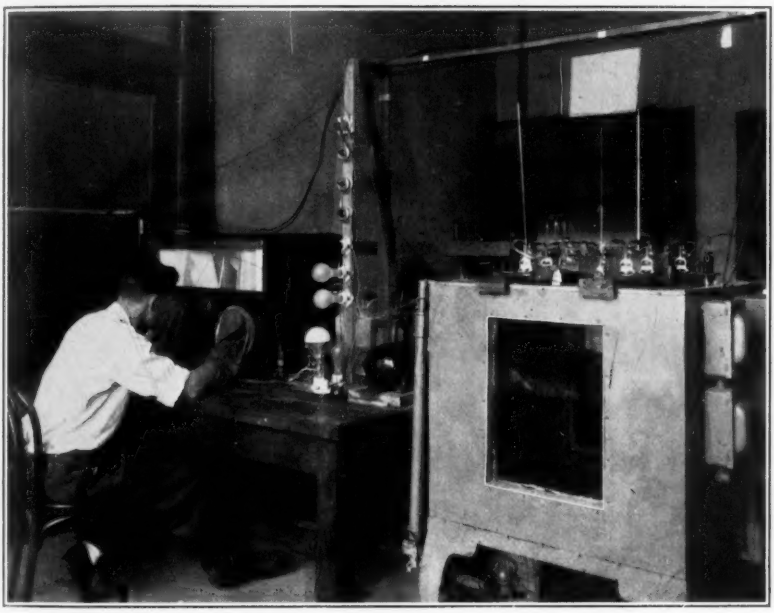

FIGURE 2.—*Apparatus for exposing the paper to polluted air showing means of manipulating samples*

Note rubber gauntlets allowing inclosed manipulation.

III. DESCRIPTION OF PAPERS USED

The papers exposed to the action of sulphur dioxide were carefully chosen with the view of having them as representative of the current type of both printing and writing record papers as was possible with the necessarily limited number used. The characteristics of these papers are shown by the test data given in Table 2. In those types generally having a wide range of quality, papers representative of the usual highest and lowest quality were included as far as possible. The properties considered most indicative of high quality in record papers are fiber purity, indicated by a high alpha cellulose content and a low copper number, minimum amounts of acid and rosin, and sufficient strength. In any consideration of strength it must be noted that writing papers are usually made stronger than book papers in order to withstand the greater stresses to which they are subjected.

TABLE 2.—*Characteristics of paper as shown by test data*

BOOK PAPERS[1]

Sample No.	Fiber composition: Rag	Highly purified wood fiber	Sulphite	Soda	Ground wood	Sizing material	Physical tests: Folding endurance: Machine direction	Folding endurance: Across machine direction	Tensile breaking strength: Machine direction	Tensile breaking strength: Across machine direction	Chemical tests: Acidity as sulfuric anhydride	Copper number	Alpha cellulose content
	Per cent	*Per cent*	*Per cent*	*Per cent*	*Per cent*		*Double folds*	*Double folds*	*kg*	*kg*	*Per cent*		*Per cent*
94001			40	60		Rosin	53	32	3.8	1.8	0.24	4.76	71.1
94001-H72[2]							3	4	3.6	1.6		5.56	58.6
94002			50	50		do	36	27	3.9	2.2	.02	3.25	76.5
94002-H72[2]							29	19	3.9	2.1		3.64	76.3
94003			30		70	do	33	16	3.5	2.1	.12	(3)	(3)
94003-H72[2]							16	10	3.5	2.2			
94004			30	20		do	118	35	3.3	1.6	.20	3.07	83.3
94004-H72[2]	50						9	8	2.7	1.4		4.17	67.7
94005			50			do	171	66	4.0	2.0	.09	2.94	83.4
94005-H72[2]	50						77	43	3.8	2.0		3.28	81.4
94006						do	177	74	6.1	3.7	.06	.77	93.4
94006-H72[2]	100						158	87	6.2	3.7		1.02	92.2
94014						do	740	289	9.3	5.3	.03	.40	95.0
94014-H72[2]	100						702	203	9.2	5.5		.93	92.5

WRITING PAPERS[4]

94007		100				Rosin and glue	1,855	1,180	11.4	5.3	0.11	1.71	85.3
94007-H72[2]							985	705	11.5	5.5	.14	1.91	83.7
94008						Rosin	102	71	7.6	4.5	.08	3.14	79.8
94008-H72[2]	60		40				16	23	7.3	4.4	.13	3.71	73.6
94009						Rosin and glue	206	107	8.4	4.4	.12	3.25	78.9
94009-H72[2]	60		40				18	24	7.8	4.1	.16	3.67	73.9
94010						Rosin	150	157	7.8	4.2	.03	2.85	78.9
94010-H72[2]							10	27	7.3	3.8	.06	3.44	73.9
94013			100			do	510	191	9.0	4.7	.08	3.67	78.5
94013-H72[2]							1	46	6.9	4.0	.14	4.03	75.2
94011						Rosin and glue	3,639	2,814	11.3	7.4	.09	1.06	91.0
94011-H72[2]	100						2,593	2,601	10.4	7.1	.14	1.32	89.7
94012						do	22	20	7.0	5.1	.08	2.34	82.4
94012-H72[2]	100						8	14	7.2	5.5	.13	2.57	79.8

[1] Tests performed by J. O. Burton. [2] Heated 72 hours at 100° C. [3] These data are not significant for ground-wood papers. [4] Tests performed by R. H. Rasch.

IV. DESCRIPTION OF TEST METHODS

The test data for fiber composition, folding endurance, and tensile breaking strength given in Table 2 were obtained by the official methods of the Technical Association of the Pulp and Paper Industry.[18] The folding endurance data given in Table 3, however, were not obtained with a Schopper type of tester and a fixed initial tension of 1 kilogram, as specified in the association method, a M. I. T. type of folding endurance tester being used for these data, since it facilitates variation in the tensile stress. Such variation was desirable, as with a tension of 1 kg. some of the book papers would not have a significant number of folds, while, on the other hand, unnecessary time would be consumed in testing some of the stronger writing papers. Folding data obtained with different tensions are not comparable, but this is immaterial where the percentage loss in folding endurance is the only required information. As an aid in determining the relative stability of the specimens to be treated, they were heated at 100° C. (212° F.) for 72 hours. Further details of this test and of its use in the classification of papers have been given in previous bureau publications.[19] [20]

The determination of alpha cellulose content and of copper number was made by modified procedures developed by the bureau specifically for testing paper,[21] except that ¼-inch squares were substituted for ground specimens in order to eliminate any possible contamination of the treated samples through action of the acid on the metallic grinder. The alpha cellulose content of the cellulosic material is that part which is insoluble in a sodium hydroxide solution of mercerizing strength (17.5 per cent NaOH) under certain specified conditions, and is regarded as a measure of the amount of unmodified cellulose which the material contains. The modified forms of cellulose possess the quality of reducing copper from alkaline copper solutions, and owing to their unstable nature are considered as deleterious impurities.

The determination of acidity was made as follows: A sample of air-dry paper cut into ¼-inch squares and weighing approximately 1 g. was well mixed with 150 ml of boiling distilled water in an Erlenmeyer flask. The resulting mixture was then heated to boiling and allowed to boil for one minute. After cooling to room temperature, the flask was swept out for 15 minutes with air free from carbon dioxide after which phenolphthalein was added and the mixture titrated with hundredth normal alkali to a faint pink color, persisting one minute. The sweep was kept in operation during the titration. The results were expressed as per cent sulphuric anhydride, being the number of milliliters of 0.01*N* alkali times 0.04 divided by the weight in grams of the sample, dried to constant weight ± 10 mg at 105° C.

[18] Copies of the official paper-testing methods of the Technical Association of the Pulp and Paper Industry may be obtained from the secretary, at 370 Lexington Avenue, New York, N. Y.

[19] Rasch, R. H., A Study of Purified Wood Fibers as a Paper-Making Material, B. S. Jour. Research, vol. 3, p. 469; 1929.

[20] Burton, J. O., Permanence Studies of Current Book Papers, B. S. Jour. Research, vol. 7, p. 429; 1931.

[21] Burton, J. O., and Rasch, R. H., The Determination of the Alpha Cellulose Content and Copper Number of Paper. B. S. Jour. Research, vol. 6, p. 603; 1931.

V. PROCEDURE

Twenty sheets (8 by 10½ inches) of each paper to be tested were conditioned at 65 per cent relative humidity and 21° C. (70° F.) for 48 hours, after which they were removed to the test cabinet, where they were suspended and exposed as previously described. They were then removed from the cabinet and placed in a closed vessel, through which a stream of nitrogen at 65 per cent relative humidity was passed to eliminate any adhering sulphur dioxide. After washing in this manner for 24 hours, the sample was removed in a closed vessel to an air-conditioned testing chamber, maintained at 65 per cent relative humidity and 21° C. (70° F.), where strips for the determination of folding endurance and tensile strength were cut and tested as rapidly as possible. Untreated specimens of each paper were tested simultaneously with the treated specimens in order that the results might be strictly comparable. The decrease in folding endurance as shown in Table 3 was then computed. The remainder of the sample was cut into ¼-inch squares for use in determinations of moisture content, copper number, alpha cellulose content, and total acidity. Four papers were treated simultaneously in the cabinet.

VI. RESULTS

The results of the experimental work are given in Table 3, which shows the physical and chemical changes induced by exposure to sulphur dioxide. It will be noted that in every case a marked decrease in folding endurance and an increase in acidity occurred. The color of the treated sheets was also affected, the specimens becoming dull gray.

Table 4 contains data showing the reproducibility of the effect of the exposure. Two series of independent tests were made on duplicate test specimens from five different papers. It should be noted that the data on folding endurance show the embrittling effect produced by each of two runs to be approximately the same. The experimental data on acidity and alpha cellulose content also agree very well, considering the nature of the material under examination. The copper numbers vary rather widely in all but one instance where excellent agreement was obtained.

TABLE 3.—*Change in physical and chemical properties of the papers upon exposure to sulphur dioxide*

BOOK PAPERS

Sample No.	Fiber composition					Sizing material	Decrease in folding endurance			Decrease in tensile breaking strength				Increase in SO_3		Increase in copper number		Decrease in alpha-cellulose content	
	Rag	Highly purified wood fiber	Sulphite	Soda	Ground wood		Machine direction		Across machine direction	Average	Machine direction		Across machine direction		Average				
	Per cent	*Per cent*	*Per cent*	*Per cent*	*Per cent*		*Double folds*	*Per cent*	*Double folds*	*Per cent*	*Per cent*	*kg*	*Per cent*	*kg*	*Per cent*	*Per cent*	*Units*	*Per cent*	*Units*	*Per cent*	*Units*	*Per cent*
94001			40	60		Rosin	2.7	7.5	4.7	13.7	−4.0	−0.16	−4.0	0.01	0.0	−2.0	0.10	37.5	0.198	5.2	0.96	1.3
94002			50	50		do	7.9	20.8	3.8	18.0	4.7	.18	4.7	.01	.7	2.7	.08	390.0	.14	5.0	−.09	−.1
94003			30		70	do	.2	1.6	5.7	16.9	4.4	.16	4.4	.08	4.0	4.2	.19	343.6	.27	8.7	.83	.9
94004		50	30	20		do	1.4	6.9	−2.6	.2	3.5	.11	3.5	−.04	−2.7	.4	.16	134.2	.11	3.6	1.18	1.4
94005		50	50			do	48.8	25.6	2.1	14.8	3.4	.13	3.4	.05	2.6	3.0	.05	117.4	.12	4.9	.29	.3
94006		100				do	22.6	13.2	6.7	10.9	−1.5	−.10	−1.5	.10	2.8	.7	.05	385.7	.05	8.8	.30	.3
94014		100				do	15.5	27.4	9.6	20.6	2.0	.20	2.0	.30	5.0	3.5	.07	202.7	.22	106.9	−.04	−.0
						WRITING PAPERS																
94007		100				Rosin and glue	15.9	14.4	14.6	17.2	0.12	1.2	0.36	6.8	4.0	0.08	144.4	0.04	4.3	0.12	0.1
94008	60		40			Rosin	1.2	9.3	2.0	7.2	.03	.4	.03	.6	.5	.05	101.0	.04	1.4	−.04	−.7
94009	60		40			Rosin and glue	1.2	2.1	.4	1.8	.36	4.2	.06	1.2	2.7	.08	129.0	.25	10.8	.52	.6
94010			100			Rosin	8.9	20.2	−1.1	8.6	.46	5.8	.27	6.4	6.1	.05	150.0	.03	1.3	.75	.9
94013			100			do	2.6	14.9	−.3	5.8	.44	5.0	.13	2.8	3.9	.07	117.2	.17	5.0	.25	.3
94011	100					Rosin and glue	15.5	4.1	42.5	14.2	.52	4.2	.25	3.3	3.7	.07	98.6	.02	3.0	.52	.5
94012	100					do	.9	7.1	2.2	11.2	−.08	−1.2	.02	.4	.4	.06	138.1	.24	12.0	.42	.5

TABLE 4.—*Reproducibility of effect of sulphur dioxide upon the papers*

Sample No.	Run No.	Loss of folding endurance		Loss of tensile breaking strength		Increase in per cent SO_3	Increase in copper number	Decrease in alpha cellulose content
		Machine direction	Across machine direction	Machine direction	Across machine direction			
		Per cent	*Per cent*	*Per cent*	*Per cent*	*Per cent*	*Per cent*	*Per cent*
94002	4	20.0	14.2	5.3	−1.4	450	−5.6	−1.4
	5	21.5	16.2	.0	2.8	330	5.0	−.1
94003	4	−1.6	26.0	1.4	6.1	373	−12.1	.9
	5	4.9	34.4	7.4	1.9	314	8.7	.9
94008	3	6.7	9.5	−.5	1.8	90	1.5	−.6
	5	2.2	10.0	1.3	−.5	112	1.4	−.9
94009	3	−3.4	4.2	1.9	2.6	132	−9.5	.9
	5	7.6	−1.1	6.4	−.2	126	10.8	.4
94014	4	27.7	27.0	−1.8	−1.5	100	51.0	.0
	5	27.0	36.7	5.8	11.4	306	162.8	.0

VII. DISCUSSION OF RESULTS

The data contained in Table 3 show that the acidity (expressed as per cent of sulphuric anhydride) of each sample treated increased upon exposure. This increase in acidity, while significant in any event, is more so if caused by sulphuric acid formed by the oxidation of sulphur dioxide upon the sheet. There are good grounds for such an assumption, since Wilkie [22] showed that such an oxidation takes place upon cotton fabric, especially in the presence of iron, [23] [24] [25] and since both cotton fabric and paper are essentially cellulose. The analogy is completed by the fact that most paper contains small amounts of iron derived from iron equipment, water, and reagents used in the paper-making processes. Sulphuric acid, being nonvolatile, would remain upon the paper and exert a continuous effect. Either sulphurous or sulphuric acid is capable of promoting acid hydrolysis,[26] which results in the embrittlement of paper fibers and their eventual crumbling.

Further consideration of the data in Table 3 shows that exposure to sulphur dioxide caused a distinct increase in the copper number, accompanied by relatively small changes of the alpha cellulose content (that is, 7 of 14 specimens show changes of 0.3 per cent or less). This seems to indicate that the main point of attack is that portion of the material of the sheet which had originally been partially modified by "hydration" in the beaters or otherwise. The embrittlement shown by decrease in folding endurance is added evidence for this point of view, as folding endurance is commonly considered to be partially dependent on the cementing action of the gel-like portion of the paper fiber. It is not known whether or not a longer exposure to the action of sulphur dioxide would result in more pronounced changes of alpha cellulose content. Further study of the nature of the embrittling reactions is planned for the future.

On comparing the embrittlement of the papers with their qualities for permanent record use as shown by the data in Table 2, it will be

[22] See footnote 14, p. 160.
[23] Cooke, S. F., Rôle of Certain Metallic Ions as Oxidation Catalysts, J. Biol. Chem., vol. 10, p. 289; 1926.
[24] Wilson, L. P., Catalytic Action in the Oxidation of Cellulose, J. Soc. Chem. Ind., vol. 39, p. 177T; 1920.
[25] Baudisch, O., and Davidson, D., Catalytic Oxidation by Means of Complex Iron Salts, J. Biol. Chem., vol. 11, p. 50; 1927.
[26] Heuser, West, and Esselen, Textbook of Cellulose Chemistry, p. 121, McGraw-Hill Book Co.; 1926.

noted that there is no constant relation between their quality and their resistance to the action of sulphur dioxide. This may be readily seen in the case of the book papers by a comparison of the data in Tables 2 and 3 on papers Nos. 94003, 94004, and 94014. It will be noted that paper No. 94003, a low-grade paper containing 70 per cent ground wood, possessed low initial strength, which decreased considerably on artificial aging by heat. This specimen also suffered a marked decrease in folding endurance upon treatment with sulphur dioxide. Paper No. 94004, a medium-quality paper having an alpha cellulose content of 83 per cent and a copper number of 3.07, failed completely under the heat test, but showed practically no change upon exposure to sulphur dioxide. The opposite was observed in sample No. 94014, having an alpha cellulose content of 95 per cent and a copper number of 0.40, which withstood the heat test with very little change, but lost about 30 per cent of its folding endurance upon treatment with sulphur dioxide. The writing papers examined show a similar effect. For instance, sample No. 94009, having an alpha cellulose content of 78.9 per cent and a copper number of 3.25, and sample No. 94013, with an alpha cellulose content of 78.5 per cent and a copper number of 3.67, both low-grade papers, show low stability under the heat test, but are relatively unaffected by sulphur dioxide, while the opposite is true of No. 94007 (alpha cellulose content 85.3 per cent, copper number 1.71) and No. 94011 (alpha cellulose content 91.0 per cent, copper number 1.06). These findings show that even the best grades of the papers examined were not proof against the deteriorating action of air polluted with sulphur dioxide, thus corroborating the results obtained by Richter.[27] In this connection it may be noted that in the case of Nos. 94008 and 94009, which are identical except for sizing, No. 94009, sized with rosin and glue, appears to be more resistant to sulphur dioxide. The difference is very slight, however.

Figures 3 and 4 compare the relative order of stability as established by per cent decrease in folding endurance after artificial aging by heat with the order established by change in folding endurance, acidity, and copper number after treatment with sulphur dioxide. It should be noted that in Figure 4 the order of stability as shown by resistance to heat is exactly the reverse of that obtained after treatment with sulphur dioxide. A similar tendency may be observed in Figure 3.

Regardless of the mechanism of the reactions and of relative resistance to sulphur dioxide, the mere fact that pronounced chemical and physical deterioration of paper may be produced by concentrations of sulphur dioxide approaching those actually encountered in urban communities in so short a period as 10 days indicates that measures to prevent acid pollution of the air in libraries are very necessary.

VIII. SUMMARY

1. Exposure of book and writing papers to air containing 2 to 9 parts of sulphur dioxide per 1,000,000 for 240 hours at 30° C. (86° F.) and 65 per cent relative humidity resulted in embrittlement of the papers, as evidenced by decrease in folding endurance, usually of considerable magnitude.

[27] See footnote 15, p. 160.

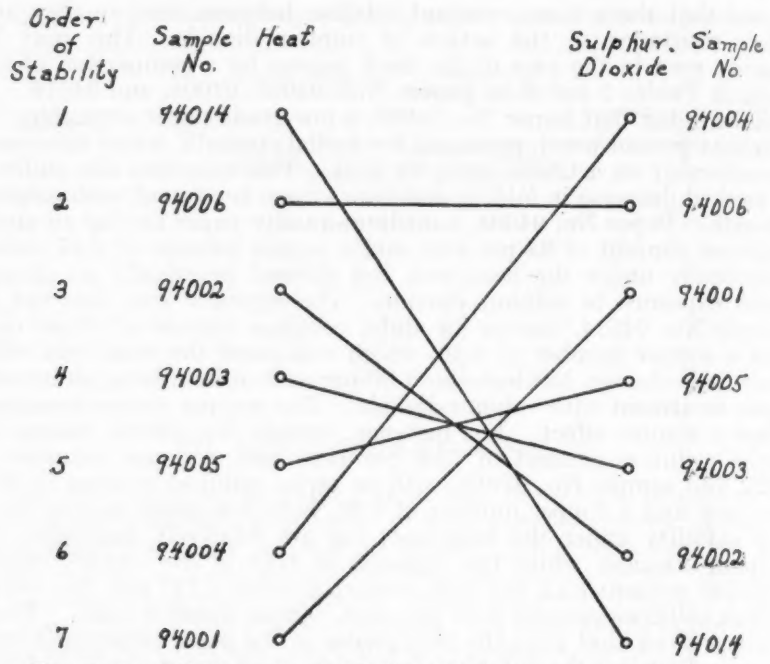

FIGURE 3.—*Relative order of stability of book papers as established by decrease in folding endurance under heat and sulphur dioxide*

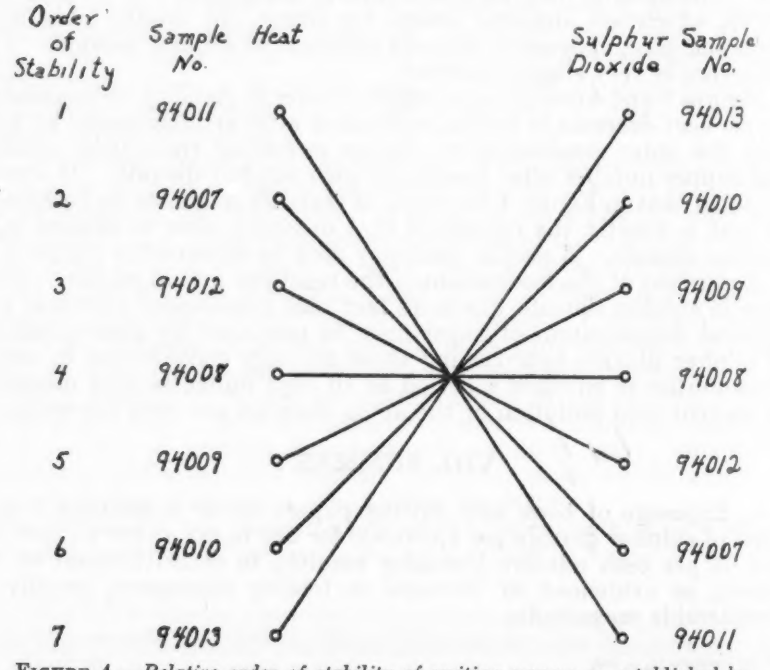

FIGURE 4.—*Relative order of stability of writing papers as established by decrease in folding endurance under heat and sulphur dioxide*

2. The embrittlement of the papers was accompanied by large increases in acidity and significant increases in copper number, but with slight decreases in alpha cellulose content. The possibility that the hydrolyzed portions of the paper fibers were further hydrolyzed, causing a loosening of the cementing "gel" which is formed particularly in beating the fibers, is suggested.

3. The effects noted bore no constant relation to the initial quality of the papers; some of the lower-grade papers, unsuitable in other respects for permanent records, showed the greatest resistance to the action of sulphur dioxide.

4. While the results obtained are considered quite convincing direct evidence of the desirability of preventing acid pollution of library air, further study of the nature of the deteriorative reactions s planned.

IX. ACKNOWLEDGMENT

The assistance of W. L. Holt [28] throughout this work is hereby gratefully acknowledged.

WASHINGTON, November 25, 1931.

[28] Assistant research associate, National Research Council.

RP408

TENSILE PROPERTIES OF RAIL STEELS AT ELEVATED TEMPERATURES

By G. Willard Quick

ABSTRACT

In continuation of previously reported work on a study of transverse fissure failures in railroad rails, a further series of tensile tests at elevated temperatures has been made on a number of rails representing different conditions of manufacture and service to determine the extent to which secondary brittleness occurred in these materials. Slower cooling from the hot saw tended to reduce the secondary brittleness at some sacrifice of tensile strength. No difference in tensile strength or secondary brittleness was found between fissured and unfissured rails that had been subjected to the same service. No appreciable difference in ductility was found in rails made at a certain mill when their rails were yielding poor service records and rails made subsequently which had improved service records; although secondary brittleness was not marked in either series, the ductility was rather low in the higher temperature range. Shatter cracks were found in all rails examined, which had failed in service. Secondary brittleness was manifest in both used and unused sorbitized rails. Shatter cracks were found in both.

CONTENTS

	Page
I. Introduction	173
II. Scope of present work	174
III. Results of elevated temperature tensile tests	175
1. Effect of different rates of cooling	175
2. Fissured *v.* unfissured rails	181
3. Rails from same mill rolled at different periods	183
4. Sorbitized rails	186
5. Medium manganese rails	186
IV. Discussion	186
V. Summary	189
VI. Acknowledgments	189

I. INTRODUCTION

Failures in railroad rails have been of vital concern to engineers, railroad executives, rail manufacturers, and the general public for years. Failure from transverse fissures originating from internal nuclei, have received particular attention in the past 20 years. J. E. Howard first reported this type of failure in 1911 as being responsible for a wreck on the Lehigh Valley Railroad in which several lives were lost. Since then many transverse fissures have been found. In 1919 Waring and Hofammann [1] etched longitudinal sections of rails in hot acid and found cracks extending both longitudinally and transversely in certain used rails as well as in some new rails. Since then

[1] F. M. Waring and K. E. Hofammann, Deep Etching of Rails and Forging, Am. Soc. Testing Materials, vol. 19, pt. 2, p. 183; 1919.

it has been thought by many that these "shatter" cracks are the nuclei from which transverse fissures subsequently develop in service. Methods for reducing the rate of cooling rails on the hot bed have been devised to decrease the temperature gradient and consequently the stress gradient in the rails. A study of the tensile properties of rails at elevated temperatures was made by Freeman and Quick,[2] who investigated the properties at temperatures through which rails pass on the cooling bed after leaving the hot saw. In their investigation a special study was made of the ductility of the steels in the temperature range 400° to 700° C. In this temperature range it was found that certain rail and other steels showed a marked decrease in elongation and reduction of area. The phenomenon was called "secondary brittleness" and the temperature range the "secondary brittle range." A tentative explanation was presented that internal failures, such as "shatter cracks" and "hair cracks" in rails, are the result of thermal stresses developed in the steel structure while cooling through the secondary brittle range. The investigation showed that the magnitude of the phenomenon varies for different heats, but that it did not differ for specimens from different ingots or for different rails in a particular ingot. It was also shown that annealing rail steel at a temperature, either above or below the critical range, markedly reduced the degree of the secondary brittleness. It was suggested that rapid cooling through the secondary brittle range was the cause of the formation of shatter cracks which, it was believed, were the nuclei of transverse fissures.

II. SCOPE OF PRESENT WORK

In 1929 arrangements were made for certain railroads to furnish the bureau with samples of rails for elevated temperature tensile tests. They included rails that had been cooled at different rates on the cooling beds; samples from fissured and unfissured rails; a new and a used sorbitized rail; a medium manganese rail deoxidized with zirconium; and rails from a particular mill, rolled prior to July, 1927, just after July, 1927, and at a more recent date. Many transverse fissures developed in rails rolled by this particular mill prior to July, 1927, and in rails rolled at a recent date, whereas in rails rolled just after July, 1927, relatively few fissures developed. A fissure had been discovered in the used sorbitized rail with the Sperry detector car.

This paper reports the results of elevated-temperature tensile tests on specimens from these rails. The procedure of testing was the same as described in the previous paper. Table 1 gives the designation, the chemical composition, and source of the materials studied.

[2] John R. Freeman, jr., and G. Willard Quick, Tensile Properties of Rail and Other Steels at Elevated Temperatures, B. S. Jour. Research, vol. 4 (RP 164), April, 1930, p. 549; A. I. M. E. Iron and Steel Division, p. 225; 1930.

TABLE 1.—*Materials studied*

Designation	Chemical Composition					Remarks
	C	Mn	P	S	Si	
	Per cent	*Per cent*	*Per cent*	*Per cent*	*Per cent*	
AL1	0.69	0.70	0.023	0.027	0.14	100-pound standard rail, heat No. 2435; cooled normally.
AL2	.69	.70	.023	.027	.14	100-pound standard rail, heat No. 2435; cooled slowly in mill scale.
PR1	.86	.65	.021	.038	.20	100-pound standard rail, heat No. 214562; cooled normally.
PR2	.86	.65	.021	.038	.20	100-pound standard rail, heat No. 214562; cooled slowly under a cover.
S1	.60	1.36	.027	.029	.13	120-pound medium manganese rail, heat No. 11588; cooled slowly in mill scale.
S2	.60	1.36	.027	.029	.13	120-pound medium manganese rail, heat No. 11588; cooled in air until magnetic, then mill scale.
S3	.60	1.36	.027	.029	.13	120-pound medium manganese rail, heat No. 11588; cooled normally.
S4	.54	1.51	.018	.025	.17	120-pound medium manganese rail, heat No. 6523; cooled slowly in mill scale.
S5	.54	1.51	.018	.025	.17	120-pound medium manganese rail, heat No. 6523; cooled in air until magnetic, then mill scale.
S6	.54	1.51	.018	.025	.17	120-pound medium manganese rail, heat No. 6523; cooled normally.
S7	.78	.85	.026	.036	.19	120-pound standard rail, heat No. 43050; cooled slowly in mill scale.
S8	.78	.85	.026	.036	.19	120-pound standard rail, heat No. 43050; cooled in air until magnetic, then mill scale.
S9	.78	.85	.026	.036	.19	120-pound standard rail, heat No. 43050; cooled normally.
S10	.77	.82	.029	.034	.28	120-pound standard rail, heat No. 55013; cooled slowly in mill scale.
S11	.77	.82	.029	.034	.28	120-pound standard rail, heat No. 55013; cooled in air until magnetic, then mill scale.
S12	.77	.82	.029	.034	.28	120-pound standard rail, heat No. 55013; cooled normally.
LN1	.76	.75	.039	.051	.18	100-pound rail, heat No. 874163; rolled January, 1927.
LN2	.75	.72	.025	.055	.22	100-pound rail, heat No. 815420; rolled January, 1928.
LN3	.83	.77	.033	.037	.23	100-pound rail, heat No. 885445; rolled December, 1928.
MP1	.74	.76	.020	.052	.20	85-pound rail, heat No. 856284; rolled 1926, A rail.
MP2	.77	.73	.018	.021	.18	90-pound rail, heat No. 829732; rolled 1929, G rail.
NC	.74	.91	.026	.035	.24	90-pound rail, heat No. 42249; rolled December, 1924, C rail.
CP1	.66	1.00	.072	.037	.14	Used standard rail, fissured.
CP2	.68	1.02	.039	.038	.11	Used standard rail, not fissured.
DL1	.68	1.40	.019	.022	.35	Used 130-pound medium manganese rail, fissured.
DL2	.70	1.36	.025	.015	.55	Used 130-pound medium manganese rail, not fissured.
DH1	.77	.74	.022	.030	.30	New 90-pound sorbitized rail, heat No. 86607, C–5.
DH2	.82	.79	.011	.029	.24	Used 90-pound sorbitized rail, heat No. 86666, C–11. Fissure detected by Sperry detector car.
K [1]	.65	1.59	.014	.032	.32	New 130-pound medium manganese rail, deoxidized with zirconium; F rail.

[1] Zr 0.09 per cent.

III. RESULTS OF ELEVATED TEMPERATURE TENSILE TESTS

1. EFFECT OF DIFFERENT RATES OF COOLING

Some of the first 16 materials listed in Table 1 were cooled in the normal way from the hot saw, whereas comparison rails from the same heats were cooled at a slower rate. Specimens from these rails were tested in tension at temperatures ranging from room temperatures to 700° or 750° C. Rails AL1 and AL2 were new rails from the same heat. Rail AL1 cooled on the hot bed in the normal manner showed blue brittleness in the range 200° to 300° C. with improved ductility at 400° C. At 550° and 600° C., secondary brittleness was quite marked and above 600° C., the ductility increased. The results were similar to many reported previously.[3] Rail AL2 from the same heat after leaving the hot saw was cooled slowly by burying in mill scale. The slower cooling caused a reduction of from 5,000 to 10,000

[3] See footnote 2, p. 174.

lbs./in.^{2} in tensile strength throughout the range of the elevated temperature tensile tests. There was less difference between the maximum and minimum elongation and reduction of area for the slowly cooled rail than for the normally cooled rail from 300° to 700° C. The results of the tests on rail steels AL1 and AL2 are given in Figure 1. The higher ductility of AL2 in the secondary brittle range was similar to the effect of annealing at 1,000° and 700° C. previous to testing as reported in the previous paper.[3]

Rails PR1 and PR2 were 120-pound rails which had been in service. PR1 was cooled from the hot saw in the normal manner and PR2 was cooled slowly under a preheated hood. The results of tests on specimens from these rails plotted in Figure 2 show that the manner

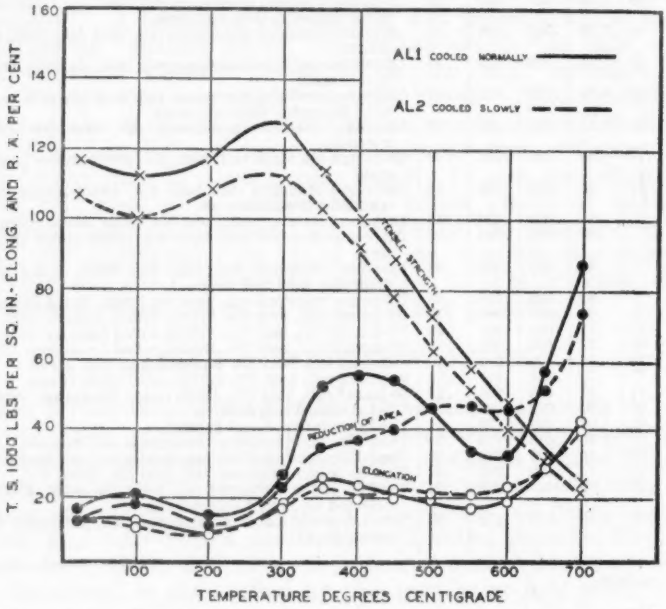

FIGURE 1.—*Results of tensile tests of specimens from new rails of the same heat*

AL1 cooled normally and AL2 cooled slowly in mill scale from the hot saw.

in which the curves were modified by slow cooling was similar to those given in Figure 1 for AL1 and AL2.

Three samples of rails from each of two duplicate heats of medium-manganese rail steel (S1 to S6, inclusive, Table 1) and three samples from each of two duplicate heats of standard rail (S7 to S12, Table 1), were secured through the courtesy of the test department of the Atchison, Topeka & Santa Fe Railroad. One sample from each heat had been cooled normally from the hot saw, one was cooled while buried in mill scale, and one was cooled in air until the head became magnetic and then buried in mill scale. The third method of cooling will be referred to as "interrupted cooling." Records of the temperatures of the air in the mill and the rails were not obtained for the medium manganese rails, but for the standard rails the following information was obtained: The atmospheric temperature of the mill

[3] See footnote 2, p. 174.

was 14° F. The temperature of the rails when they came through the finishing pass was about 1,950° F. The temperature at which the rails became magnetic when cooled in air was determined with an optical pyrometer to be between 1,275° and 1,300° F. The rails were uniformly heated and were handled in accordance with the best rolling-mill practice. The pieces that were buried in scale had about 3 inches of scale under them and at least 4 inches above the top of the head. The tensile strength of the more slowly cooled medium-manganese rails was lower than that of the normally cooled rails (figs. 3 and 4), from room temperature to 400° C., but above 400° C. the effect of slow cooling was not so noticeable. The results plotted in Figures 5 and 6 for the standard heats show

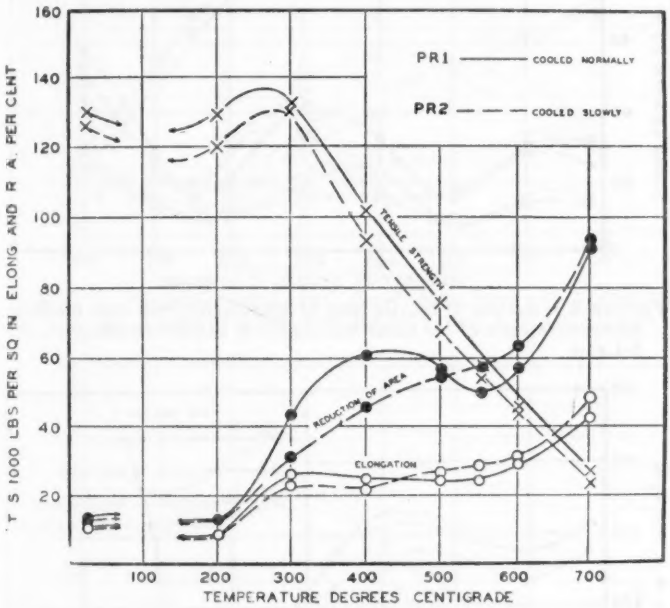

FIGURE 2.—*Results of tensile tests of specimens from used rails of the same heat*

PR1 cooled normally and PR2 cooled slowly under a preheated hood from the hot saw.

that the tensile strength of the more slowly cooled rails was lower than that of the normally cooled rails over the entire range of test.

The tensile tests at elevated temperature on the standard rails (S7–S12) did not show as marked secondary brittleness for the normally cooled rails as was shown for the normally cooled AL and PR rails or the medium manganese rails (S1–S6). This is seen by comparing Figures 1 and 2 with Figures 3, 4, 5, and 6. The ductility curves of the rails cooled slowly (in mill scale) did show less difference between maximum and minimum from 300° to 700° C. than those of the rails cooled normally. The ductility curves of the medium-manganese rails after "interrupted cooling" followed closely those for the medium manganese rails cooled normally (figs. 3 and 4), whereas the ductility curves of the standard rails cooled in the same manner followed closely those for the standard rails cooled in mill scale (figs. 5 and 6). This

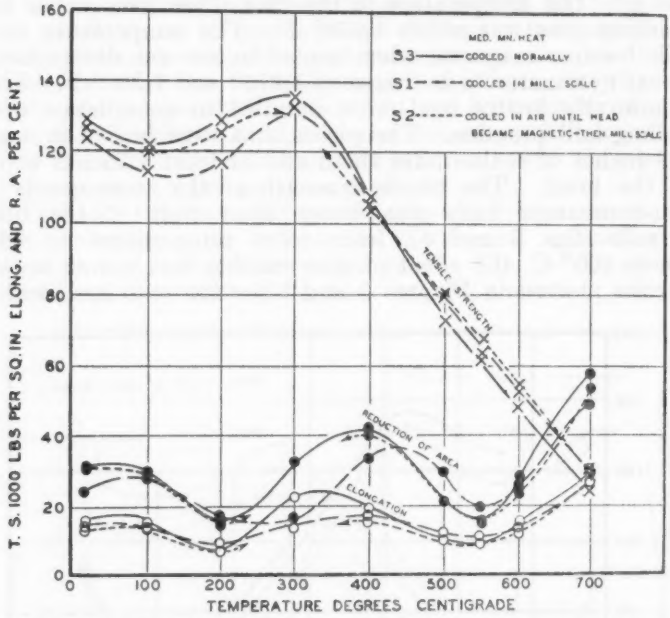

FIGURE 3.—*Results of tensile tests of specimens from new medium manganese rails of the same heat cooled at different rates from the hot saw*

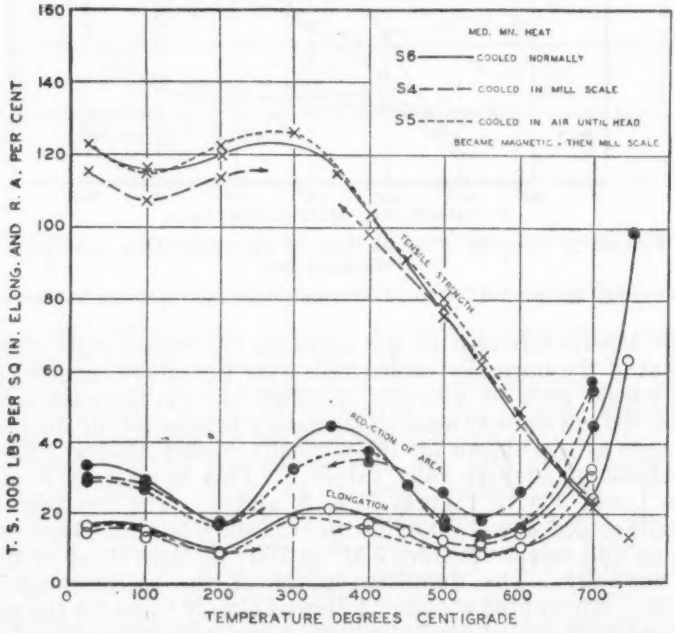

FIGURE 4.—*Results of tensile tests of specimens from new medium manganese rails of the same heat cooled at different rates from the hot saw*

This was from a duplicate heat to the one given in Figure 3.

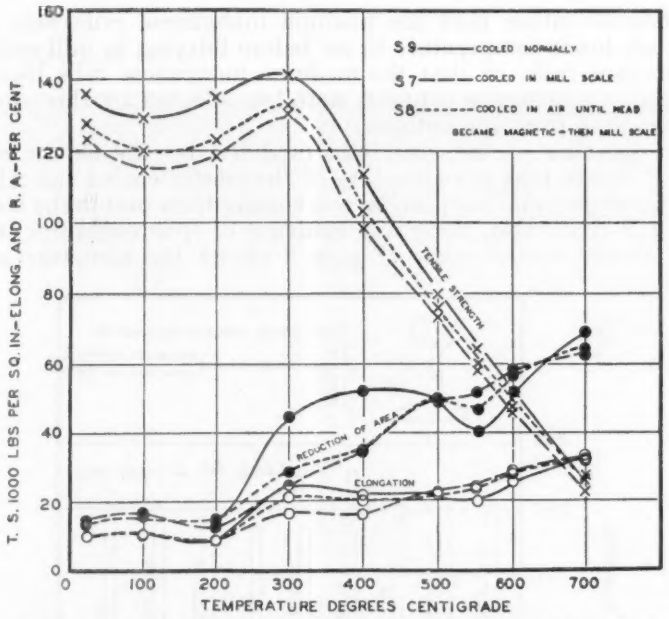
S 9 COOLED NORMALLY
S 7 COOLED IN MILL SCALE
S8 COOLED IN AIR UNTIL HEAD BECAME MAGNETIC - THEN MILL SCALE
TENSILE STRENGTH
REDUCTION OF AREA
ELONGATION
T. S. 1000 LBS PER SQ. IN.-ELONG AND R. A.-PER CENT
TEMPERATURE DEGREES CENTIGRADE
0 20 40 60 80 100 120 140 160
0 100 200 300 400 500 600 700

FIGURE 5.—*Results of tensile tests of specimens from new "standard" rails of the same heat cooled at different rates from the hot saw*

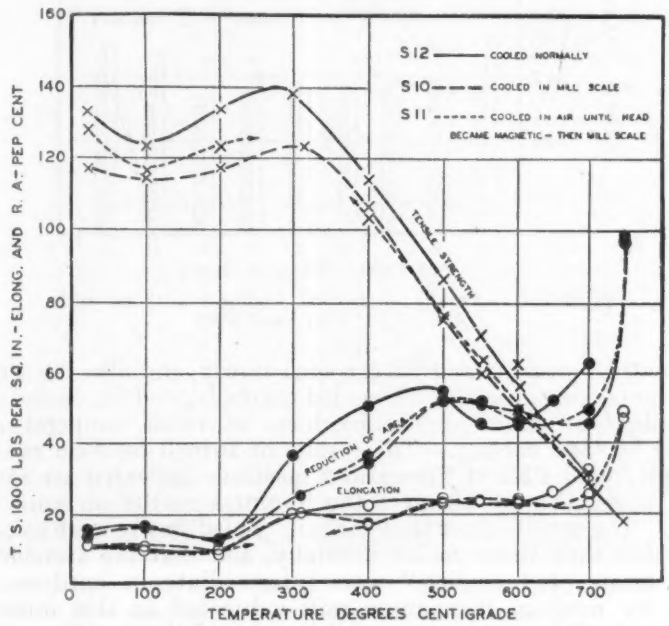
S12 COOLED NORMALLY
S10 COOLED IN MILL SCALE
S11 COOLED IN AIR UNTIL HEAD BECAME MAGNETIC - THEN MILL SCALE
TENSILE STRENGTH
REDUCTION OF AREA
ELONGATION
T. S. 1000 LBS PER SQ. IN. - ELONG. AND R. A.- PER CENT
TEMPERATURE DEGREES CENTIGRADE
0 20 40 60 80 100 120 140 160
0 100 200 300 400 500 600 700

FIGURE 6.—*Results of tensile tests of specimens from new "standard" rails of the same heat cooled at different rates from the hot saw*

This was from a duplicate heat to the one given in Figure 5.

may indicate either that the medium manganese rails were cooled to a much lower temperature in air before burying in mill scale than the standard rails, or that the medium manganese rails because of their higher manganese content, were less affected by this somewhat slower cooling from the hot saw.

The structure of the steel was modified by the slower cooling. Figure 7 shows that the structure of the slowly cooled rail AL2 was better developed and the pearlite was coarser than that in the normally cooled rail AL1; also, there was evidence of spheroidization in some of the slowly cooled rails. Figure 8 shows the structure of rails

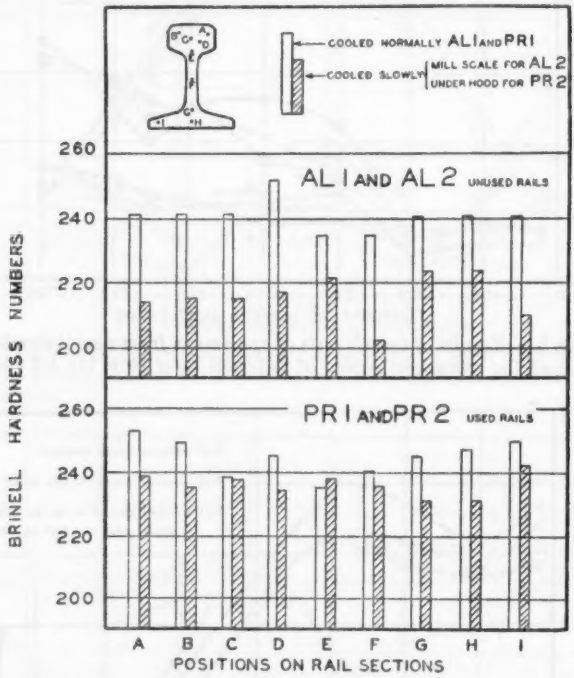

FIGURE 9.—*Results of Brinell hardness tests on rails AL1, AL2, PR1, and PR2*

PR1, cooled normally, and PR2, cooled slowly, and also the structure of medium manganese rails S6, cooled normally, and S4, cooled slowly.

As might be expected, the hardness at room temperature was reduced by slow cooling. The results of Brinell tests on rails AL1, AL2, PR1, and PR2 at the various positions indicated are shown in Figure 9, and Figure 10 gives the hardness results on some of the S rails. The results show that the rails cooled slowly were softer over the section than those cooled normally, and that the standard rails after "interrupted cooling" were intermediate in hardness. The results for medium manganese rails subjected to this interrupted cooling were less consistent and for most of the positions were as hard or harder than the corresponding positions on the rail cooled normally.

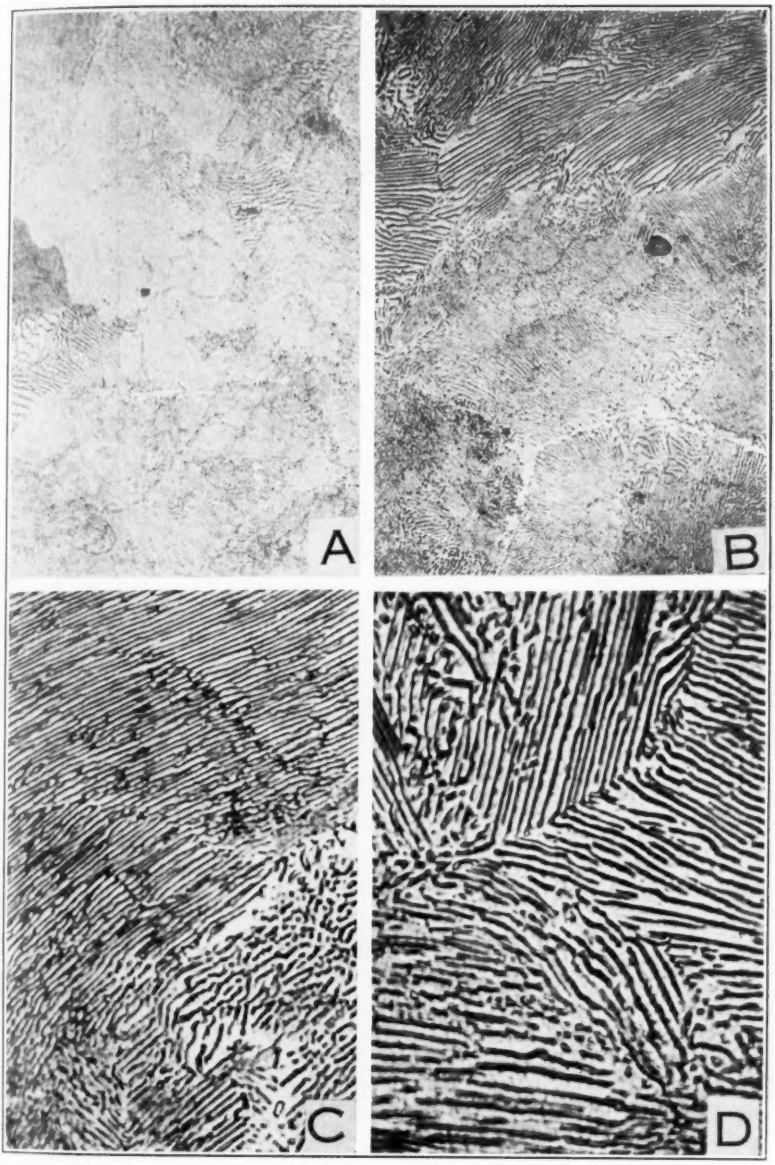

FIGURE 7.—*Structure of new "standard" rails AL1 cooled normally and AL2 cooled slowly from the hot saw in mill scale*

A, AL1, × 500; *B*, AL2, × 500; *C*, AL1, × 2,000; *D*, AL2, × 2,000. Etchant, 2 per cent nitric acid in alcohol.

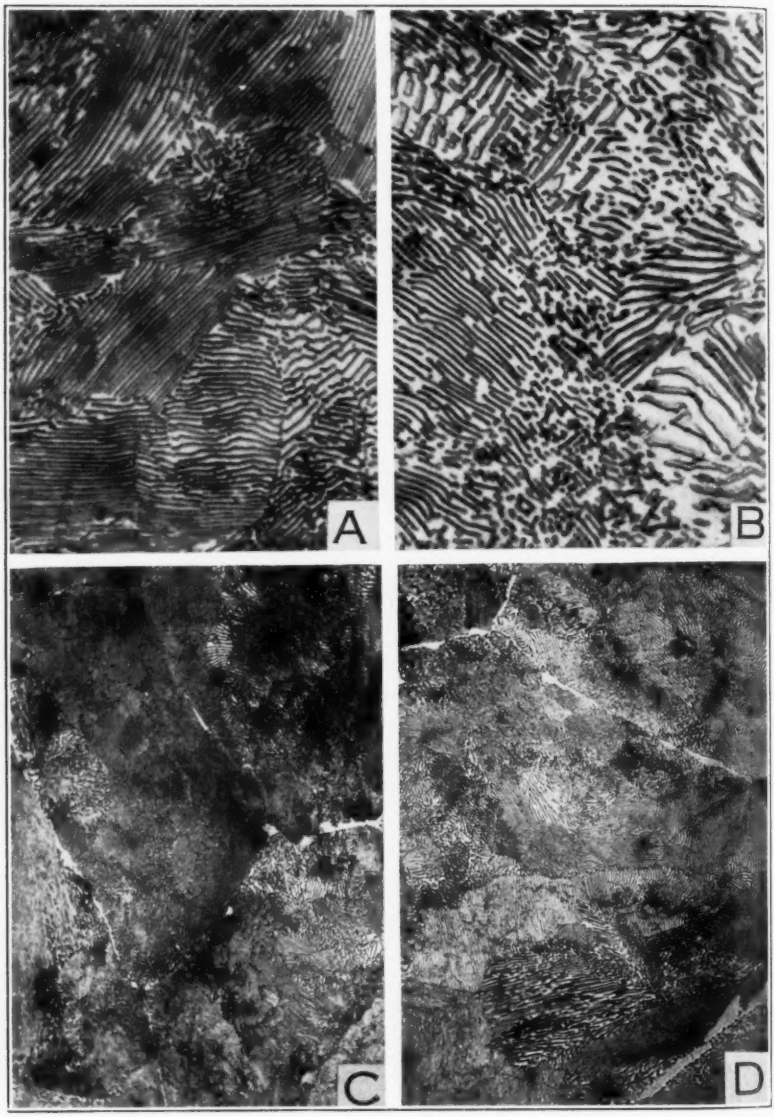

FIGURE 8.—*Structure of rails*

A, "Standard" PR1 cooled normally, × 2,000; *B* "Standard" PR2 cooled slowly from hot saw under a hood, × 2,000; *C*, S6 medium manganese cooled normally, × 500; and *D*, S4 medium manganese cooled slowly from hot saw in mill scale, × 500. Etchant, 2 per cent nitric acid in alcohol.

UNIV. OF MICH.

2. FISSURED *v.* UNFISSURED RAILS

Two pieces of medium manganese rail of 130-pound section, which had served in track for the same length of time, were obtained through the courtesy of the Delaware, Lackawanna & Western Railroad. Transverse fissures had been detected in the rail designated DL1, whereas no fissures had been detected in the rail designated DL2. Elevated-temperature tensile tests were made on both of these rails to ascertain if these differences in service behavior were accompanied by differences in the properties. From the results shown in Figure 11, it is evident that there were no appreciable differences in the tensile

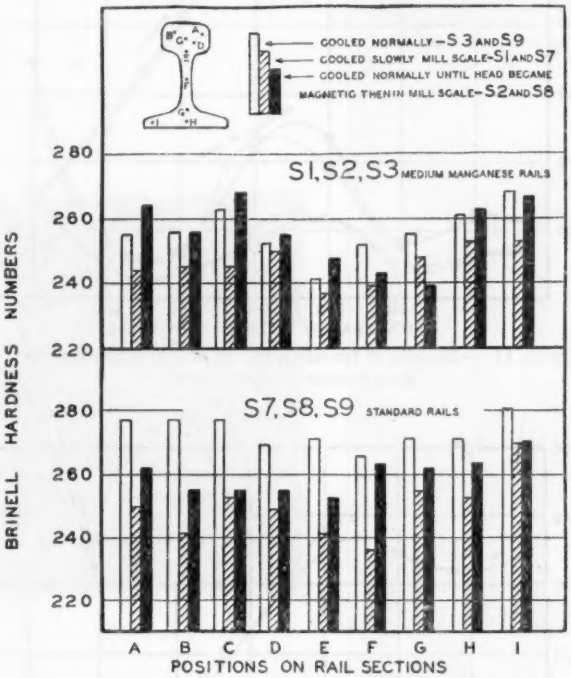
COOLED NORMALLY—S3 AND S9
COOLED SLOWLY MILL SCALE—S1 AND S7
COOLED NORMALLY UNTIL HEAD BECAME MAGNETIC THEN IN MILL SCALE—S2 AND S8
S1, S2, S3 MEDIUM MANGANESE RAILS
S7, S8, S9 STANDARD RAILS
BRINELL HARDNESS NUMBERS
280
260
240
220
A B C D E F G H I
POSITIONS ON RAIL SECTIONS

FIGURE 10.—*Results of Brinell hardness tests on rails S1, S2, and S3 medium manganese and S7, S8, and S9 "standard" rails*

properties. Similar tests were made on two 90-pound rails, from the Canadian Pacific Railroad (CP1 and CP2), in one of which a transverse fissure had been detected whereas in the other no fissures were detected. The results are shown in Figure 12, and it is seen that there was only a small difference in the properties and that CP2, the fissured rail, showed slightly greater secondary brittleness.

An examination of longitudinal deep-etched sections of rail DL1 (transverse fissured) revealed three longitudinal cracks, whereas the unfissured rail, DL2, when etched, revealed no cracks. Figure 13 shows a crack at natural size and at 20 magnifications. It is seen that the defect is an irregular crack with a general longitudinal direction. Similarly, shatter cracks were found in rail CP1 (fissured), but no cracks were found in rail CP2 (not fissured).

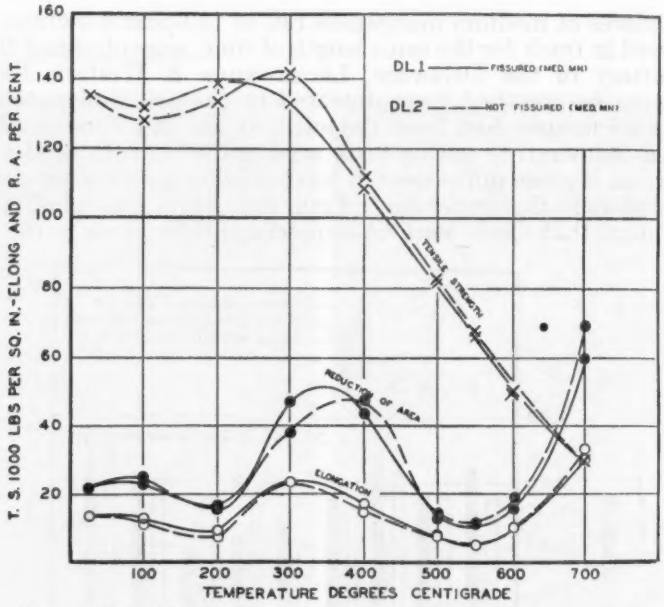

FIGURE 11.—*Results of tensile tests on medium manganese rails*
DL1, fissured; DL2, not fissured.

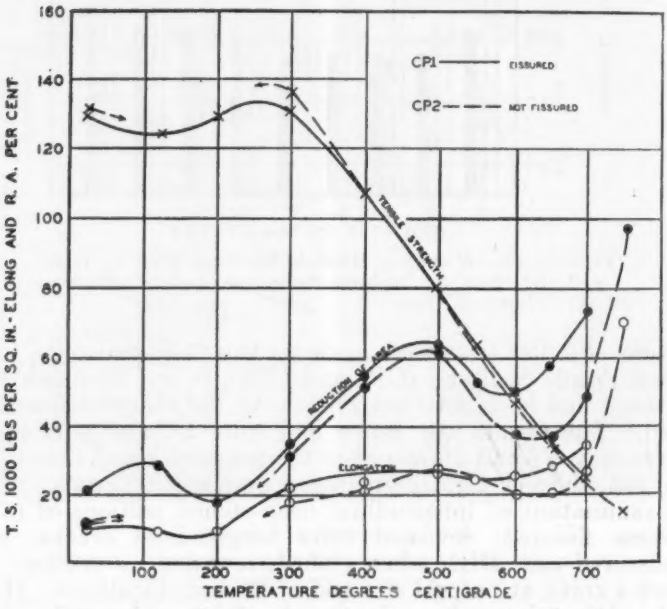

FIGURE 12.—*Results of tensile tests on "standard" rails*
CP1, fissured; CP2, not fissured.

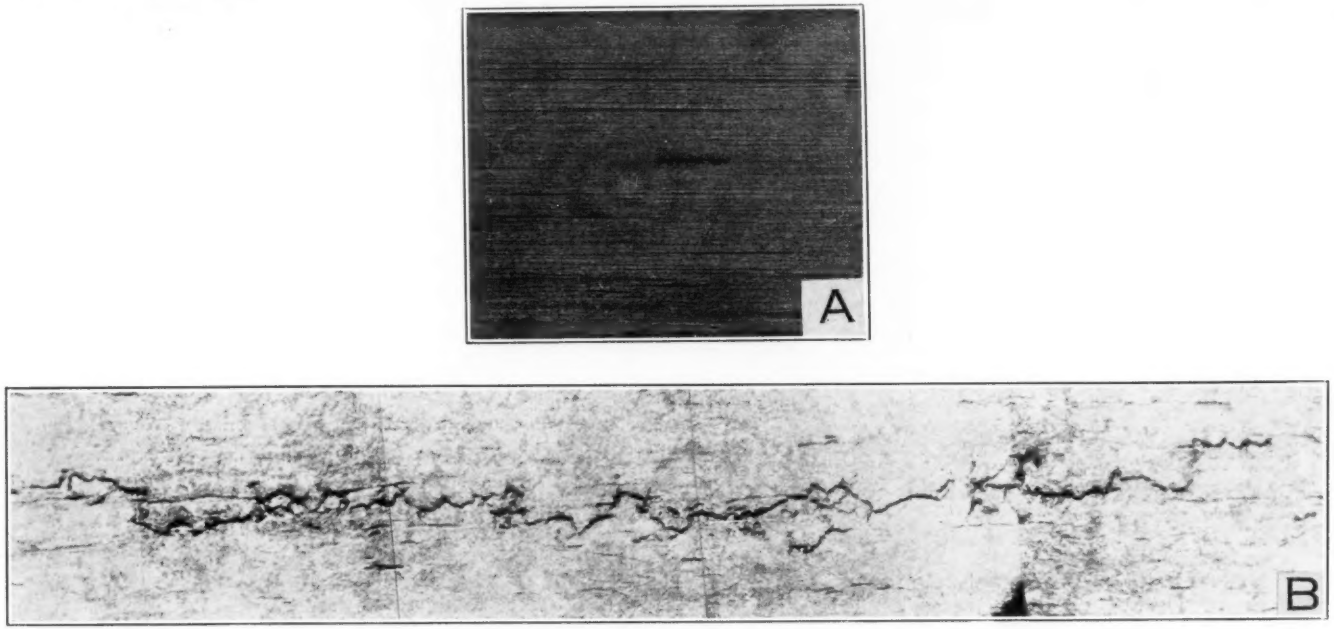

FIGURE 13.—*Crack in medium manganese rail DL1, fissured*

A, × 1; *B*, × 20.

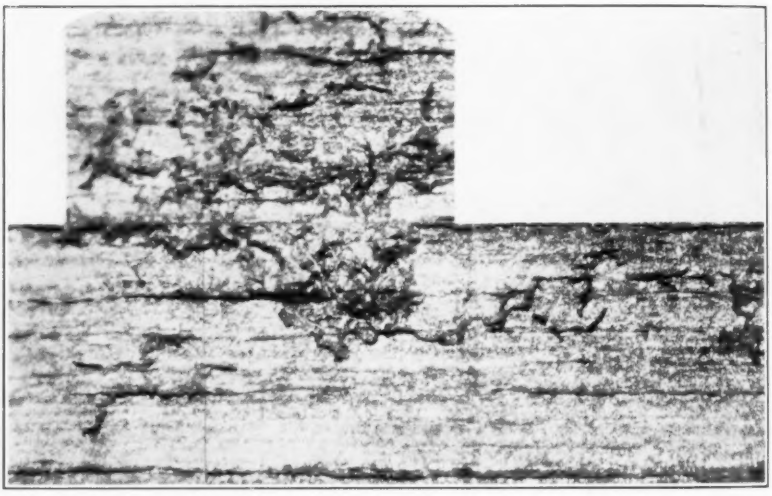

FIGURE 14.—*Shattered area in used rail LN1.* × *35*

OF MICH.

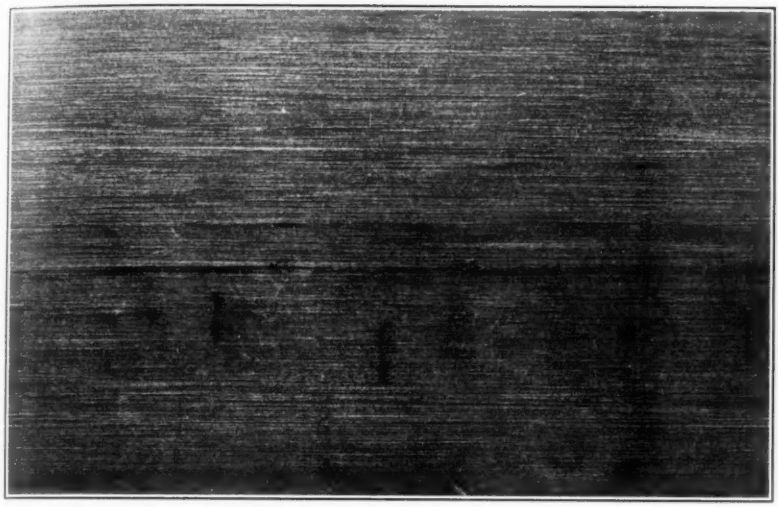

FIGURE 15.—*Longitudinal horizontal section three-fourths inch below the tread of used rail LN3.* × *1 showing shatter cracks*

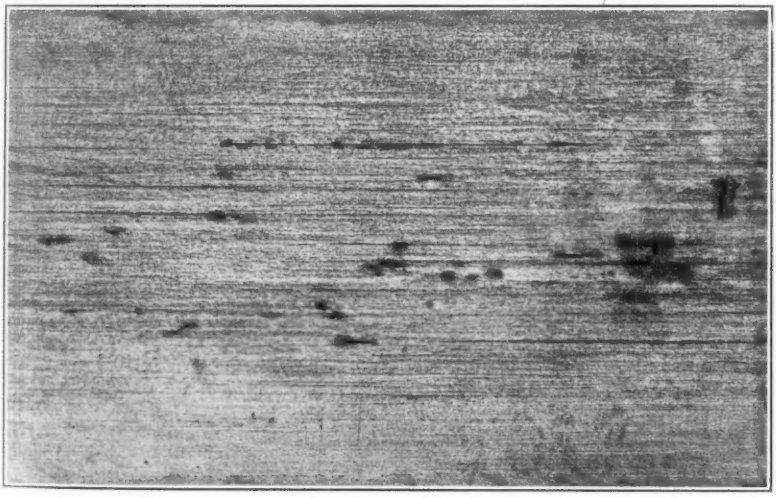

FIGURE 16.—*Longitudinal horizontal section three-fourths inch below the tread of used rail NC.* × *1 showing shatter cracks*

3. RAILS FROM SAME MILL ROLLED AT DIFFERENT PERIODS

Statistics [4] on transverse fissure show that the total accumulated number of transverse fissures per year has been increasing gradually and uniformly. There have been greater numbers of failures in rails rolled in certain years, particularly 1917, 1923, 1925, 1926, and 1927 than in other years. The greater number of failures in 1925, 1926, and 1927 were attributed principally to the excessive rate of failure in the output of a particular mill for those years. Fissure failures reported by the American Railway Engineering Association during the last few years as occurring in the first year of service are given in Table 2.

TABLE 2.—*Fissure failures occurring in first year of service*

29 failures in 1925 from 1925 rollings, all mills.
50 failures in 1926 from 1926 rollings, all mills.
114 failures in 1927 from 1927 rollings, all mills.
58 failures in 1928 from 1928 rollings, all mills.
106 failures in 1929 from 1929 rollings, all mills.

The improvement in the 1928 rollings shown above, according to Mr. Barnes' report, is due to the fact that only 3 out of a total of 58 failures were from this one mill, while in the first year of service of 1927 they produced 56 out of a total of 114 failures. This marked improvement in their rails from the fissure standpoint appears to be the result of changes in practice which were put into effect starting with July, 1927. Table 3 shows this more clearly.

TABLE 3.—*Fissure failures in rails from a particular mill (all roads) showing improvement attributable to changes in mill practice*

Year of failures	When rolled (year, months)				
	1925, January–December	1926, January–December	1927, January–June	1927, July–December	1928, January–December
1928	123	140	56	0	
1929	131	210	160	3	3
Total	254	350	216	3	3

Through the cooperation of Mr. Barnes, rails made at this mill were secured before and after July, 1927, as given in Table 4.

TABLE 4.—*Rails tested from a particular mill*

Railroad	Designation	Year rolled	Heat No.	Remarks
Louisville & Nashville	LN1	January, 1927	874163	
	LN2	January, 1928	815429	
	LN3	December, 1928	885445	Failed from transverse fissure; 100-pound "C" rail.
Missouri Pacific	MP1	1926	856284	85-pound "A" rail.
	MP2	1929	829732	90-pound "G" rail.
Nashville & Chattanooga	NC	December, 1924	42249	Failed from transverse fissure; 90-pound "C" rail.

[4] R. E. Barnes, Engr. of Tests, Rail Com., A. R. E. A., Transverse Fissure Statistics, A. R. E. A., vol. 31; p. 1485; 1930, vol. 32, p. 365; 1931.

Of the rails shown in Table 4, rails LN3 and NC had failed from a transverse fissure. Longitudinal sections of each of the six rails were deep etched. A small shattered area was found in rails LN1 and LN3, but in rail LN2 no shatter was found. These isolated observations check the service results in Table 3 which shows that rails rolled shortly after July, 1927, were better than those rolled previously or subsequently. Figure 14 shows the shattered area in the LN1 section and an etched longitudinal section of LN3 is shown in Figure 15. In this figure are seen a number of transverse and longitudinal cracks.

No shatter cracks were found in deep-etched sections of either MP1 or MP2. Many streaks were revealed in MP1 ("A" rail) while in MP2 ("G" rail) this condition was absent. A number of

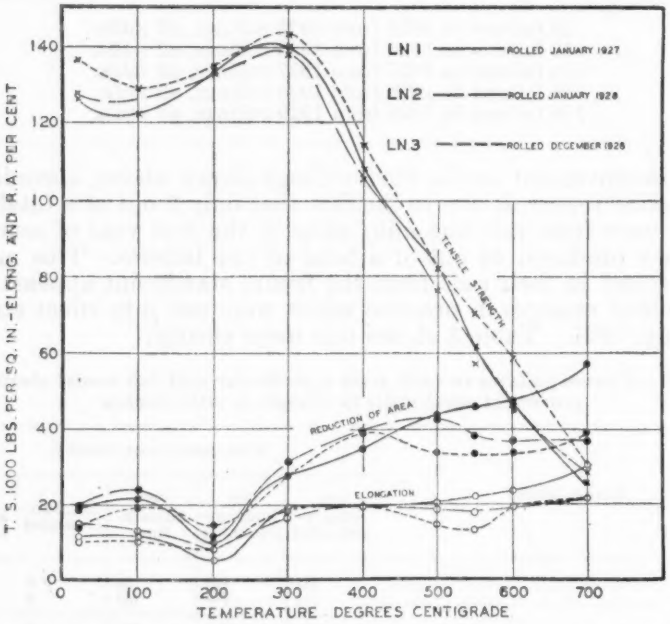

FIGURE 17.—*Results of tensile tests of specimens from used rails LN1, LN2, and LN3*

transverse and longitudinal cracks shown in Figure 16 were found in a deep-etched section from rail NC which was a 90-pound "C" rail, rolled at this mill in 1924. This section was taken longitudinally five-eighths inch below the tread. The rail, which had a transverse fissure on the end, was from a heat of which five rails broke between January 28 and March 9, 1925.

Elevated-temperature tensile tests were made on specimens from all of these rails and the results are given in Figures 17, 18, and 19. Although these specimens did not have a marked decrease in ductility in the secondary brittle range the values were generally somewhat lower from 400° to 700° C. than given for other rails in this or the previous publication. As shown in Figure 17 there were differences in ductility of these rails between 400° and 700° C. and the ductility curves of LN2 which revealed no cracks on deep etching lie between

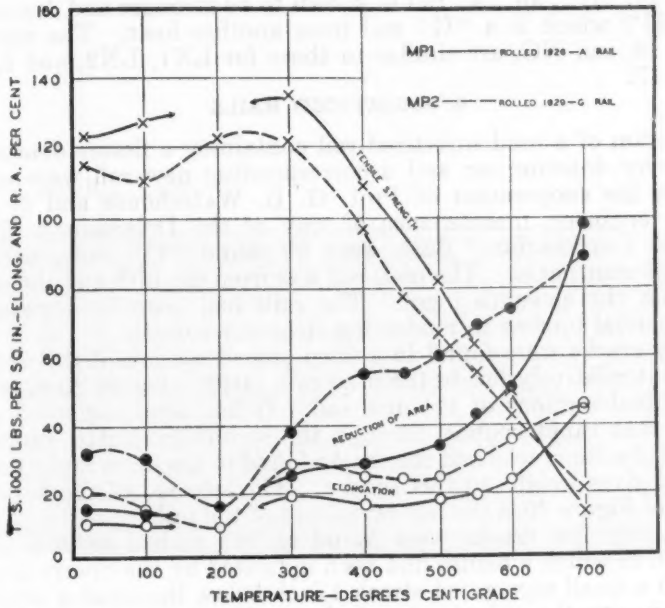

FIGURE 18.—*Results of tensile tests of specimens from used rails MP1 and MP2*

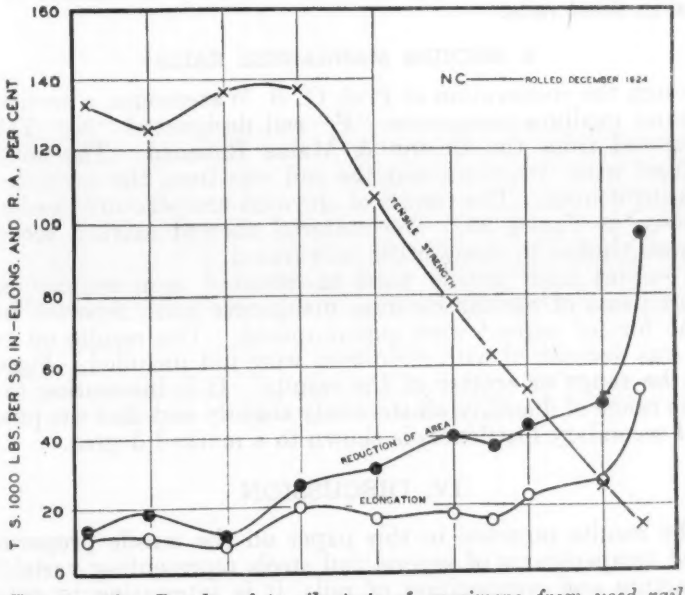

FIGURE 19.—*Results of tensile tests of specimens from used rail NC*

those of LN1 and LN3 which were presumably inferior rails. In Figure 18, MP1, an "A" rail is shown to be stronger and less ductile than MP2 which is a "G" rail from another heat. The curves in Figure 19, rail NC, are similar to those for LN1, LN2, and LN3 in Figure 17.

4. SORBITIZED RAILS

A section of a used sorbitized rail containing a fissure detected by the Sperry detector car and a corresponding new rail were secured through the cooperation of Prof. G. B. Waterhouse and of H. S. Clarke, engineer, maintenance of way of the Delaware & Hudson Railroad Corporation. Both were 90-pound "C" rails, but were from different heats. The used rail was from the fifth and the unused one from the eleventh ingot. The rails had been heat treated by a commercial process to render the structure sorbitic.

Many cracks were found in a deep-etched section of the new rail, DH1, but relatively few in the used rail, DH2. Figure 20 shows two longitudinal sections of the new rail. It has been suggested previously [5] that rapid cooling through the secondary brittle range is a cause of shatter cracks and the cracks found in the more rapidly cooled new rail gives weight to this theory. The left end of the horizontal section of Figure 20 is the hot sawed end of the rail.

Relatively few cracks were found in two etched sections of the DH2 rail in which a fissure had been indicated by the Sperry detector car. In a small segregated streak 1 inch below the tread a crack was observed with the aid of a hand glass. Figure 21 shows the crack and the structure of both the segregated streak and the area adjacent to it. The results of tensile tests at elevated temperatures on these two rails are shown in Figure 22. Secondary brittleness is very marked in these rails.

5. MEDIUM MANGANESE RAILS

Through the cooperation of Prof. G. B. Waterhouse, a section of a 130-pound medium manganese "F" rail designated "K," Table 1, was secured from the Boston & Maine Railroad. The steel was deoxidized with zirconium and the rail was from the seventh ingot of a 14-ingot heat. The results of elevated temperature tensile tests are shown in Figure 23. The material showed marked secondary brittleness similar to many other rails tested.

The curves from tensile tests at elevated temperatures on six different heats of regular medium manganese rails, reported in this and the former paper [5] were superimposed. The results on rail K which was deoxidized with zirconium were not included. Figure 24 shows the range or scatter of the results. It is interesting to note that the range of ductility scatters only slightly and that the phenomenon of secondary brittleness is shown to a marked degree.

IV. DISCUSSION

In the results reported in this paper on the tensile properties at elevated temperatures of several rail steels representing variables in manufacture and composition of rails, it is interesting to note the effect of these variables on the quality, structure, and the properties

[5] See footnote 2, p. 174.

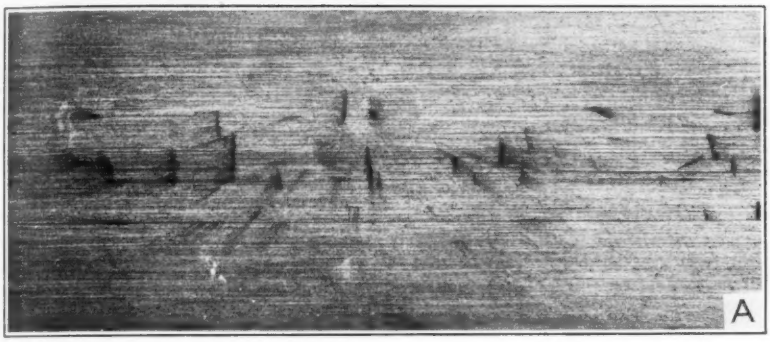

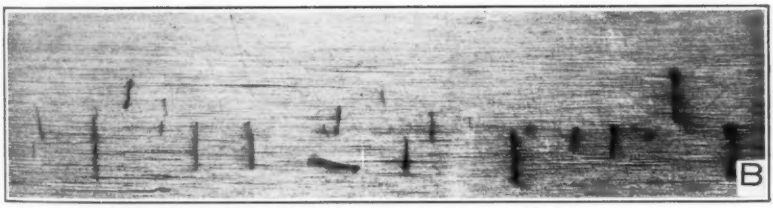

FIGURE 20.—*Sections of new sorbitized rail DH1.* × ⅔

A, Longitudinal horizontal section three-fourths inch below the tread. The left is the hot sawed end; *B*, longitudinal vertical section through the center of the head. The tread is at the top of the photographs. This section is some distance from the hot sawed end.

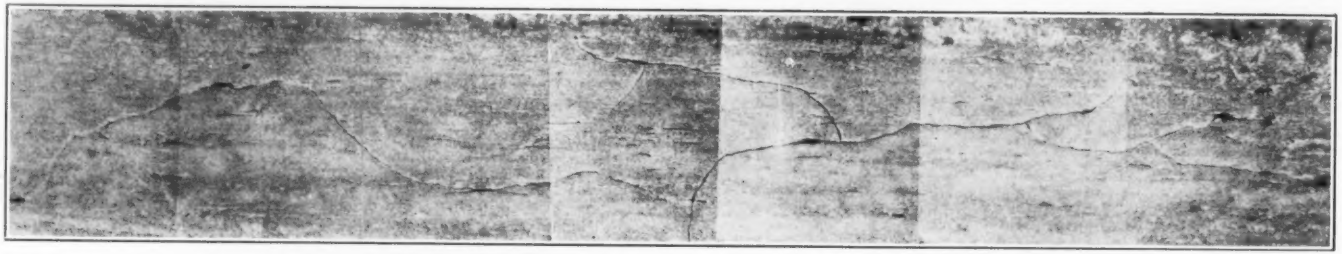

FIGURE 21.—*Crack in a segregated spot in used sorbitized rail DH2, 1 inch below the tread.* × 20

A, Structure of segregated area (× 1,200); *B*, structure of the rail just off the segregated area (× 1,200).

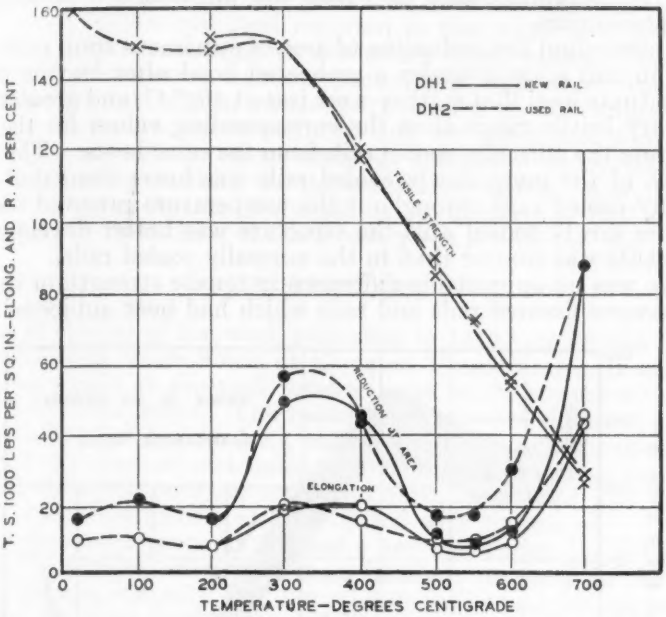

FIGURE 22.—*Results of tensile tests on specimens from sorbitized rails* DH1, new rail; DH2, used rail.

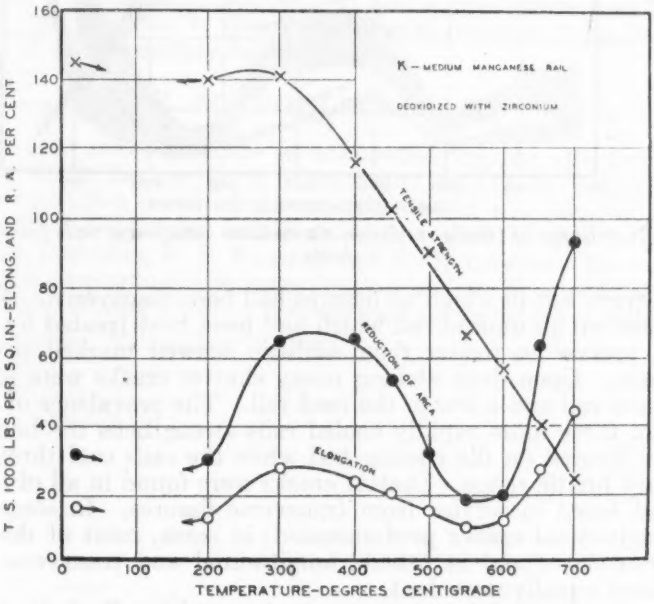

FIGURE 23.—*Results of tensile tests on specimens from a medium manganese rail deoxidized with zirconium*

in the temperature range in which the phenomenon of secondary brittleness occurs.

The elongation and reduction of area of specimens from rails cooled slowly in mill scale or under a preheated hood after leaving the hot saw fluctuate less; that is, they were less at 400° C. and greater in the secondary brittle range than the corresponding values for the specimens from the normally cooled rails from the same heats. The tensile strength of the more slowly cooled rails was lower than that of the normally cooled rails throughout the temperature range of test. In the more slowly cooled rails the structure was better developed and the peralite was coarser than in the normally cooled rails.

There was no appreciable difference in tensile strength or ductility of transverse fissured rails and rails which had been subjected to the

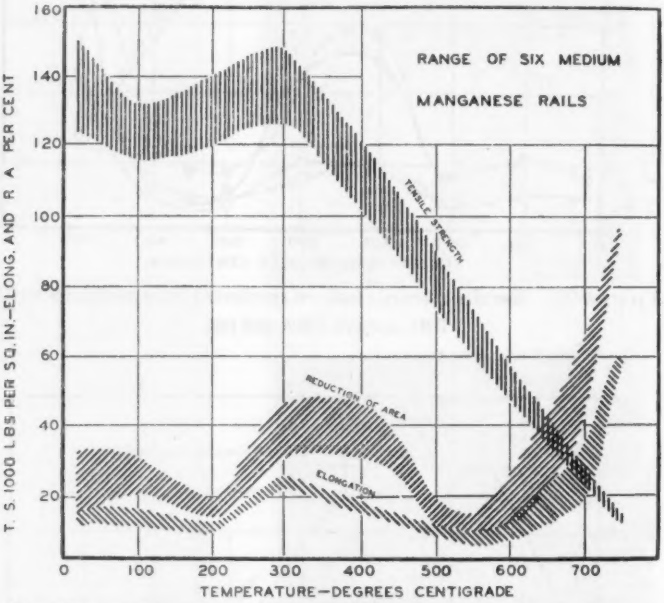

FIGURE 24.—*Range of tensile results on six medium manganese rails from different heats*

same service, but in which no fissures had been discovered. Tests on a used and on an unused rail which had been heat treated by a commercial process to render them sorbitic showed marked secondary brittleness. Upon deep etching many shatter cracks were found in the unused rail and a few in the used rail. The prevalence of shatter cracks in these more rapidly cooled rails strengthens the belief that they are formed on the cooling bed while the rails cool through the secondary brittle range. Shatter cracks were found in all of the rails that had failed in service from transverse fissures. In some of the rails longitudinal cracks predominated; in some, most of the cracks were transverse; and in others, longitudinal and transverse cracks were about equally prevalent.

Marked secondary brittleness was observed in all of the medium manganese rails tested, including one from a heat which had been deoxidized with zirconium. A composite figure of the results of ele-

vated temperature tests on specimens from six different heats of medium manganese rail steel reported in this paper and previously showed very little scatter in the secondary brittle range. The results of elevated temperature tests on specimens of rails which were rolled at a particular mill and in which many failures resulted subsequently in service from transverse fissures, and on specimens which were rolled at a subsequent period when the rails were improved showed little decrease in ductility in the secondary brittle range, but the ductility values at certain temperatures, particularly at 400° and 700° C., were lower than those of other rails given in this and the previous paper.

V. SUMMARY

In continuation of the work published in 1930 [6] on Tensile Properties of Rail and Other Steels at Elevated Temperatures, tensile tests have been made at elevated temperatures on 28 specimens of rails from 18 different heats. The material represented different rates of cooling on the hot bed for both carbon and medium manganese rails; samples from fissured and unfissured rails; rails from the same mill rolled at different periods; sorbitized rails, both used and unused; and a medium manganese rail deoxidized with zirconium.

From the results given in this and a previous paper, the indications are that secondary brittleness is an inherent property in the steels used at present for rails, but that the ductility may be appreciably improved by slow cooling through the temperature range in which this phenomenon occurrs.

Inasmuch as shatter cracks have been found in all transverse fissured rails and occasionally in new rails, it is believed that they are the nuclei of transverse fissures. It seems that transverse fissures would be less frequent in slowly cooled rails because of the increased ductility in the secondary brittle range.

VI. ACKNOWLEDGMENTS

The author takes pleasure in acknowledging the effective cooperation of R. E. Barnes, G. B. Waterhouse, and O. W. Ellis through whose cooperation much of the material tested was secured. He is also indebted to several members of the staff of the Bureau of Standards, including H. S. Rawdon and W. H. Swanger, for valuable suggestions throughout the investigation and to K. A. Milliken for carefully performing most of the elevated temperature tensile tests.

WASHINGTON, November 28, 1931.

[6] See footnote 2, p. 174.

THE RESISTANCE TO IMPACT OF RAIL STEELS AT ELEVATED TEMPERATURES

By G. Willard Quick

ABSTRACT

Charpy impact tests were made in the temperature range 20° to 700° C. on V notch specimens cut transversely and longitudinally from a medium manganese rail, and on longitudinal specimens cut from two standard rails, one cooled normally and the other cooled slowly after leaving the hot saw, two heat-treated rails and one untreated comparison rail, and a commercial bar stock steel containing 0.60 per cent carbon. The energy absorbed in breaking the specimens from all these materials inceased as the temperature increased from 20° to about 400° C., then decreased to a minimum at about 600° C., after which it increased rapidly to 700° C. Tensile tests on the rail steels, reported previously, had shown a marked decrease in elongation and reduction of area for all of the rail steels between 400° and 700° C., with the minimum values at 550° or 600° C., but not for the bar stock. The tensile test had also shown somewhat higher ductility in the secondary brittle range for the slowly cooled rail and the heat-treated rails than for the normally cooled and the untreated comparison rail, but the impact test did not distinguish between them. The path of the fractures in the impact specimens was transcrystalline at all temperatures. It is believed that the minimum values for impact strength occurring at 550° or 600° C. may be ascribed to the same phenomenon as the low ductility disclosed by the tensile tests at the same temperatures, namely, that of secondary brittleness rather than to the phenomenon of blue brittleness which some believe occurs at a higher temperature in dynamic tests than in tensile tests.

CONTENTS

	Page
I. Introduction	191
II. Materials tested and procedure	193
III. Results	193
1. Medium manganese rail	193
2. Rails cooled normally and cooled slowly after leaving the hot saw	195
3. Bar stock, 0.60 per cent carbon steel	195
4. Heat-treated rails	196
5. Fractures under impact at high temperatures	197
IV. Discussion of results	197
V. Summary	198
VI. Acknowledgments	198

I. INTRODUCTION

Tensile tests of rail steels at elevated temperatures [1] [2] have shown that certain rails, in addition to having low ductility in the well-known blue brittle range in the neighborhood of 200° C., have marked reduction in elongation and reduction of area in the temperature range from 400° to 700° C. This range of low ductility was called "the

[1] John R. Freeman, jr., and G. Willard Quick, Tensile Properties of Rail and Other Steels at Elevated Temperatures. B. S. Jour. Research, vol. 4 (RP164), April, p. 549; 1930. Also, A. I. M. E. Iron and Steel Division, p. 225; 1930.

[2] G. Willard Quick, Tensile Tests on Rail Steels at Elevated Temperatures. B. S. Jour. Research, vol. 8 (RP408), p. 173; 1932. Also, A. I. M. E. Iron and Steel Division; 1932.

secondary brittle range" and the phenomenon, "secondary brittleness."

The question naturally arises as to whether this property of the steels would be shown by impact tests performed in the same range of temperature. If so, the impact test, as suggested by Gillett [3] would be a simpler and quicker method for the routine examination of steels at elevated temperature than the tensile test.

A number of investigators have reported results of impact tests on steels at elevated temperatures, in which the energy absorbed decreased with increase of temperature above 200° or 300° C. Langenberg [4] performed Charpy impact tests on several steels at temperatures ranging from room temperature up to 1,000° F. (538° C.). His results showed an increase in the energy absorbed in specimens tested in the range from room temperature to 200° or 300° C. and then a gradual decrease in the range, 300° to 538° C., the maximum temperature used. Greaves and Jones [5] reported Charpy impact tests on several steels at elevated temperatures up to 1,000° C. Their results excepting those for "stainless" steel (12.37 per cent Cr) were similar to Langenberg's in that the energy used in breaking the specimen decreased at temperature above 300° C. to a minimum value at about 600° C.; then increased markedly to about 700° C. At higher temperatures the values were again lower. For "stainless" steel, however, the values were approximately constant from 200° to 600° C. and then became somewhat higher. Monypenny [6] has given results of Charpy impact tests at elevated temperatures for plain carbon and a number of alloy steels which are similar to those of Greaves and Jones.

Other investigators,[7 8 9] recently have made impact tests on iron and steels at low temperatures and, in general, the results show that the impact resistance falls off rapidly as the temperature is reduced from 20° C. to sub zero values. In the work of the previous investigators referred to, the tests at elevated temperatures were either not carried through the temperature range in which secondary brittleness has been shown by the tensile test, or else, when they were carried through this temperature range, the decrease in energy absorbed was ascribed to the phenomenon of blue brittleness.

Accordingly, in order to determine to what extent the changes in ductility as revealed by tensile tests would be duplicated by impact tests, a series of impact tests were made at elevated temperatures on a number of rail steels of which the tensile properties in the same range of temperature had already been determined.

---

[3] H. W. Gillett, Trans. A. I. M. E. Iron and Steel Division, p. 270; 1930. Discussion.

[4] F. C. Langenberg, An Investigation of the Behavior of Certain Steels under Impact at Different Temperatures. J. Iron & Steel Institute, Carnegie Scholarship Memoirs, vol. 12, p. 75; 1923. F. C. Langenberg, Investigation of the Influence of Temperature on the Charpy Impact Value of a Group of Steels of Varying Composition, Yearbook of Am. Iron & Steel Institute, vol. 12, p. 349; 1923.

[5] R. H. Greaves and J. A. Jones, The Effect of Temperature on the Behavior of Iron and Steel in the Notched Bar Impact Test, J. Iron & Steel Institute, vol. 112, No. 11, p. 123; 1925.

[6] J. H. G. Monypenny, Stainless Iron and Steel. John Wiley & Sons, Inc., N. Y., 1926.

[7] H. W. Russell, Effect of Low Temperatures on Metals and Alloys, Symposium on Effect of Temperature on the Properties of Metals, Joint Meeting of A. S. M. E. and A. S. T. M., Chicago, Ill.; June, 1931.

[8] Robert Sergeson, Behavior of Some Irons and Steels Under Impact at Low Temperatures, Preprint No. 16, A. S. S. T., for Boston meeting; Sept. 21-25, 1931.

[9] J. F. Cunningham and J. Gilchrist, Impact Characteristics of Steel Rails at Low Temperatures, Preprint No. 26, A. S. S. T., for Boston meeting; Sept. 21-25, 1931.

II. MATERIALS TESTED AND PROCEDURE

The chemical compositions and types of steel from which the impact specimens were taken are given in Table 1. All of the steels except one were rail steels.

TABLE 1.—*Materials tested*

Designation [1]	Chemical composition					Remarks
	Carbon	Manganese	Phosphorus	Sulphur	Silicon	
	Per cent	*Per cent*	*Per cent*	*Per cent*	*Per cent*	
M2D	0.59	1.30	0.053	0.040	0.20	130-pound medium manganese, "C" rail.
AL1	.69	.70	.023	.027	.14	100-pound standard rail, cooled normally.
AL2						100-pound standard rail, cooled slowly in mill scale.
H1	.73	.60	.026	.050	.25	Heat-treated "C" rail. Quenched 30 seconds in water, in furnace at 510° C., 1½ hours, then air cooled.
H2	.74	.62	.043	.063	.31	Heat-treated "C" rail. Quenched 15 seconds in water; in furnace at 510° C., 1½ hours, then air cooled.
H3	.60	.66	.040	.033	.32	Comparison "C" rail; not heat treated.
9A	.60	.65	.050	.025	.12	¾ by 2¼ inch bar stock.

[1] The designation of the material is the same as that used in the tensile tests reported previously, see footnotes 1 and 2, p. 191.

The impact tests were carried out on an American-made Charpy machine of 160 foot-pounds capacity. The specimens were 1 cm square in cross section, and had a 45° notch 0.079 inch deep, with a radius of 0.01 inch at the bottom. From 10 to 20 specimens were used for determining each of the curves given to show the variation in impact resistance with increase in temperature. The notches were cut in all of the specimens of a series at one time on a milling machine while the specimens were clamped side by side in a jig. In conducting the test, the specimens were heated slowly in an electric resistance furnace to the desired temperature which was determined by means of a base metal thermocouple and portable potentiometer. The bead or hot junction of the thermocouple was located in the notch of the specimen. After holding for 15 minutes at the desired temperature, the specimen was transferred with insulated tongs to the machine and broken. The time required for the transfer was about three seconds, and preliminary tests had shown that the maximum temperature drop from the time of removal from the furnace until the specimen was broken was not more than 5° C. No correction was made for this change in temperature since the significance of the results would not be appreciably affected by so small a change.

III. RESULTS

1. MEDIUM MANGANESE RAIL

Tests were made on specimens taken both longitudinally and transversely from rail M2D. The longitudinal specimens were taken from either side of the head. One set of transverse specimens was taken across the top of the head with the notch on the portion just under the tread while the second series of transverse specimens was cut from the middle of the head and the notch was cut on the side toward the tread of the rail.

The results of the impact tests are plotted in Figure 1, together with the results of tensile tests which have been reported previously.[10] The curve for the Charpy results on longitudinal samples rose from room temperature to a maximum at about 350° C. and then fell to a minimum at a temperature of 550° or 600° C., after which it rose steeply to 750° C., the maximum temperature used. The shape of the curve was similar to that of the curves summarizing the values for elongation and reduction of area determined in tensile tests in the secondary brittle range. The results of the tests on the two sets of transverse specimens also are plotted in Figure 1. These curves were similar to those for the longitudinal specimens except that the energy absorbed throughout the temperature range was less. The transverse

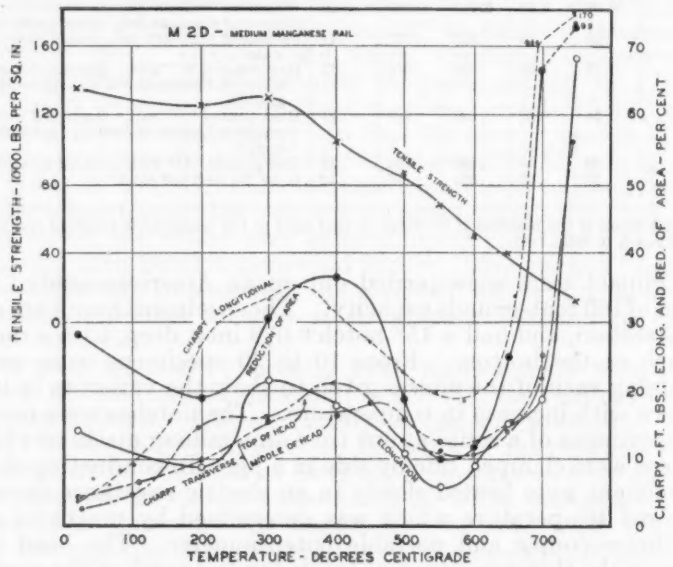

FIGURE 1.—*Results of Charpy impact tests of specimens taken both longitudinally and transversely, and tensile tests of specimens taken longitudinally from rail M2D*

Transverse Charpy specimens were from both the top and middle of the head.

specimens from the top of the rail absorbed more energy between 150° and 450° C. than those from the middle of the head, but from 450° to 700° C. the specimens from the middle of the rail absorbed slightly more energy. The fractured longitudinal specimens and the transverse specimens taken just under the head of the rail are shown in Figure 2. The longitudinal specimens tested above 670° C. did not break completely apart, but bent over the tup sufficiently to permit passage through the supports of the machine. The unbroken specimens formed an angle of about 55°. Although the values for the energy absorbed by the specimens that did not break completely are not strictly comparable with the values obtained for the completely broken specimens, the results for both have been plotted in the figures. Any errors introduced in the values on the partly broken

[10] See footnote 1, p. 191.

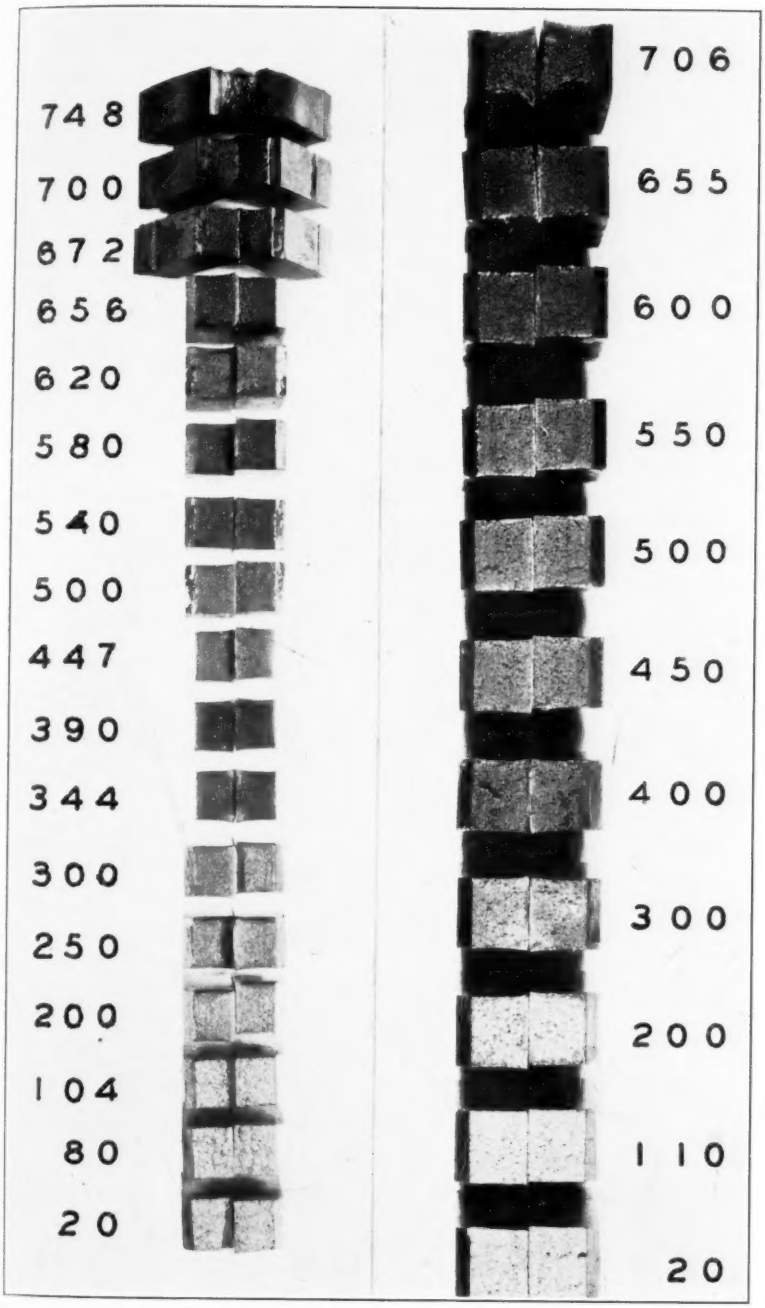

FIGURE 2.—*Fractured Charpy impact specimens showing the temperature in °C. at which they were broken*

A, Specimens taken longitudinally; *B*, specimens taken transversely.

UNIV OF

specimens would modify the results only very slightly because the temperatures at which incomplete fractures occurred were above the range of secondary brittleness.

2. RAILS COOLED NORMALLY AND COOLED SLOWLY AFTER LEAVING THE HOT SAW

The results of impact and tensile tests at elevated temperatures on rail AL1 cooled normally and rail AL2 cooled slowly are given in Figure 3. The Charpy impact results on longitudinal specimens showed secondary brittleness for both AL1 and AL2 to about the same degree, whereas the results of the tensile tests showed that the elongation and reduction of area were modified by slow cooling. Although the Charpy impact test showed secondary brittleness in

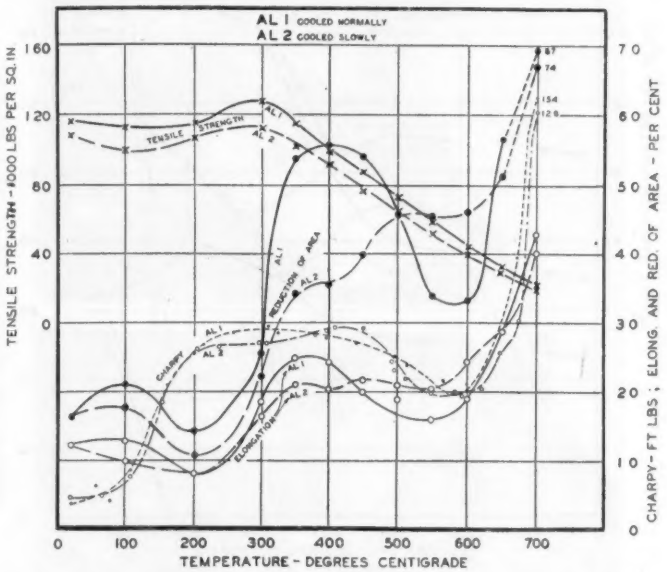

FIGURE 3.—*Results of Charpy impact tests and tensile tests of specimens from new rails of the same heat*

AL1 cooled normally and AL2 cooled slowly in mill scale from the hot saw.

the rails, it did not distinguish between the two which had been cooled at different rates after leaving the hot saw.

3. BAR STOCK, 0.60 PER CENT CARBON STEEL

This material in the annealed condition was reported in a previous paper [11] to show no secondary brittleness in tensile tests at elevated temperature. These results along with those of the impact tests of the material in both the annealed and "as received" conditions are shown in Figure 4. It will be noted that marked secondary brittleness was indicated by the impact test for the steel in both the annealed and "as received" conditions. In this case, the dynamic test showed

[11] See footnote 1, p. 191.

decreased ductility in the secondary brittle range whereas the tensile test did not.

4. HEAT-TREATED RAILS

Impact tests at elevated temperatures were made on specimens cut from two heat-treated "C" rails and a comparison rail made in the usual manner. The heat treatments were as follows: Rail H1, quenched from about 750° C., for 30 seconds, in water.

Rail H2, quenched from about 750° C., for 15 seconds, in water.

Both of the above rails after quenching were held one and one-half hours in a furnace at 510° C., then air cooled.

The tensile results, which have been reported previously [12] showed that the untreated rail had marked secondary-brittleness; the rail

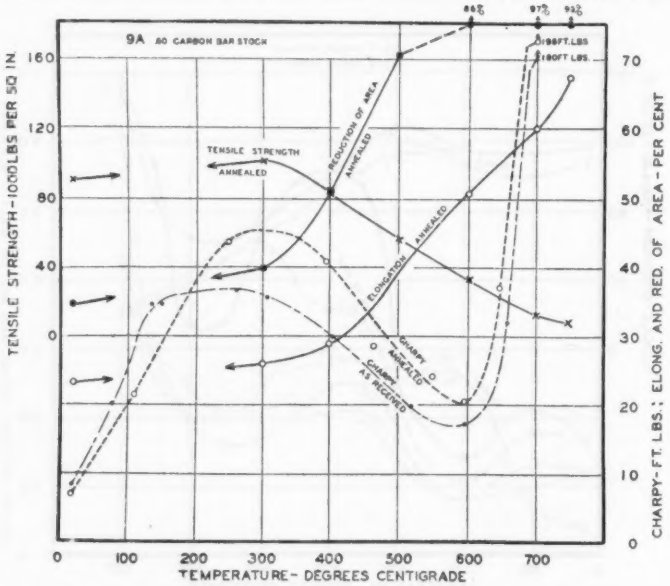

FIGURE 4.—*Results of Charpy impact tests in the "as received" and annealed conditions, and tensile tests in the annealed condition of specimens from 0.60 per cent carbon bar stock, 9A*

quenched for 30 seconds was somewhat less brittle; and the rail quenched for 15 seconds showed the greatest improvement in ductility in the secondary brittle range. Secondary brittleness in all three rails was shown by the results of the impact tests, Figure 5. The untreated rail, H3, absorbed less energy in the temperature range, 200° to 400° C., than the heat-treated rails, and less than H2 but more than H1 in the range, 450° to 600° C. Rail H2 showed a peculiar irregularity between 250° and 350° C. In general, the results of the impact tests on these rails were similar to those shown in Figure 3 for normally and slowly cooled rails in that the effect of the rate of cooling did not manifest itself as markedly in the impact resistance as in the tensile properties.

[12] See footnote 1, p. 191.

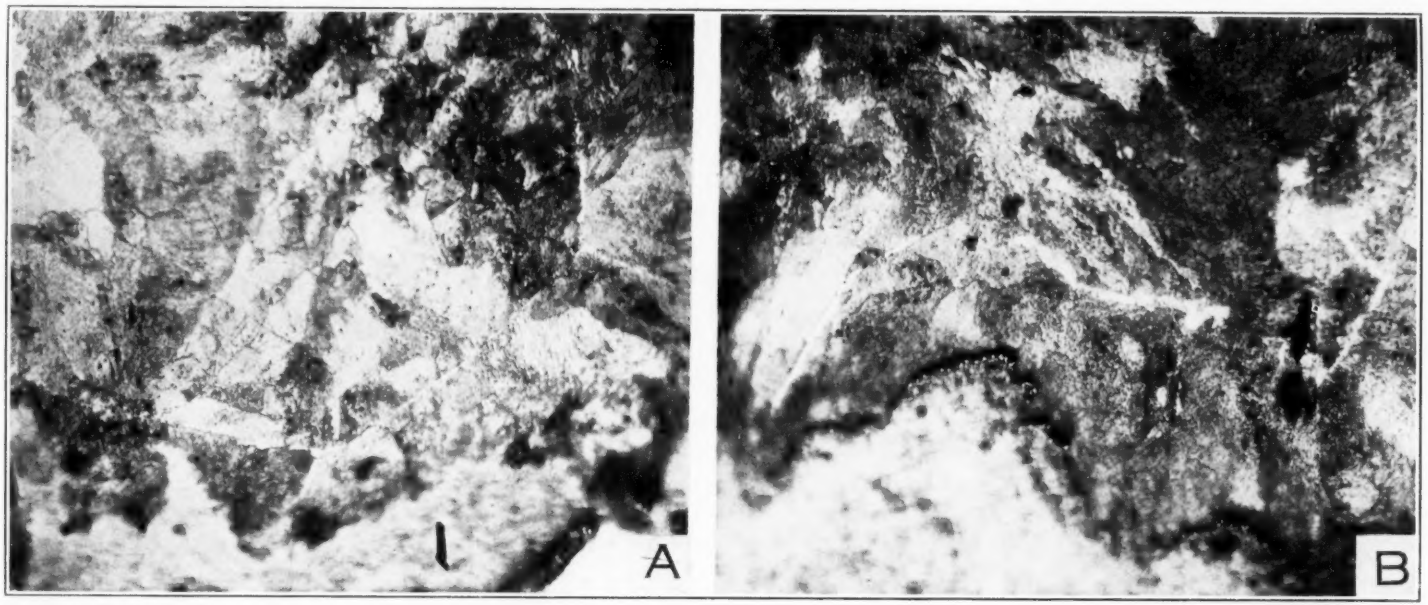

FIGURE 6.—*Fractures of Charpy impact specimens from medium manganese rail M2D.* × *500*

A, Broken at 309° C.; *B*, broken at 540° C. Etchant, 2 per cent nitric acid in alcohol.

5. FRACTURES UNDER IMPACT AT HIGH TEMPERATURES

Metallographic examinations were made to determine whether the path of the fracture was transcrystalline or intercrystalline. To preserve the face of the fracture during the polishing operation a heavy coating of copper was electroplated on the specimens. To obtain good adherence of the copper at the extreme edges of the fracture, it was necessary to remove all traces of the oxide film formed during the impact test without altering the surface of the steel. This was done by making the specimen the cathode in a 5 per cent (by weight) solution of sulphuric acid while a current of about 100 milliamperes at about 4 volts was applied for two or three minutes. A plate of high silicon cast iron formed the anode of the cell. The plated specimens were split longitudinally in a plane perpendicular to the notch and the cut surface was polished for examination. The

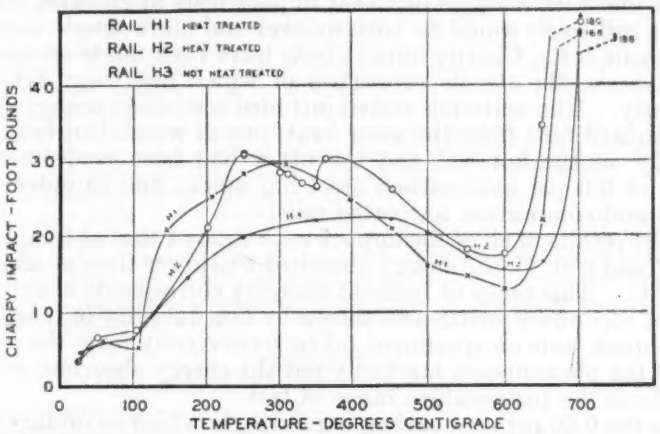

FIGURE 5.—*Results of Charpy impact tests of specimens from heat-treated rails H1 and H2, and rail H3, not heat treated*

Rail H1, quenched 30 seconds in water.
Rail H2, quenched 15 seconds in water.
Both rails after quenching were held one and one-half hours in a furnace at 510° C. (950° F.), than air cooled.

fractures were found to be transcrystalline for all temperatures of test from 20° C. to the critical temperature. Those heated above the Ac range had recrystallized. Micrographs of two of the fractured specimens from medium manganese rail M2D are shown in Figure 6.

IV. DISCUSSION OF RESULTS

The results of Charpy impact tests on rail steels at elevated temperature were in agreement with those given by other investigators for various carbon steels.

The energy absorbed by the notched specimen when broken under impact increased from room temperature to 300° or 400° C., showed no decrease at the "blue-brittle" temperature, and then gradually decreased as the temperature of test was raised to about 600° C. From 600° to 700° C. there was a sharp and marked increase of several hundred per cent. A few tests at higher temperatures have shown that the energy absorbed again decreased. It appears that

this decrease does not represent brittleness, but should be attributed rather to the increased plasticity and decreased tensile strength of the steel at the higher temperatures. It has been suggested by some investigators [13] that blue brittleness, manifested in tensile tests at about 200° C., extends to higher temperatures in dynamic tests and is represented by the low impact values at 500° and 600° C. It is seen from the results of tests in this paper that the low impact resistance in the temperature range 400° to 700° C., corresponds to the low values of elongation and reduction of area from tensile tests in the secondary brittle temperature range. It would appear reasonable that the low values in both tests are properly to be regarded as manifestations of the same phenomenon.

V. SUMMARY

1. In line with a suggestion that impact tests at elevated temperatures on rail steels would be both quicker and more simple to perform than tensile tests, Charpy impact tests have been made on specimens of rail steels, the tensile properties of which had been determined previously. The materials tested included a medium manganese rail; two standard rails from the same heat, one of which had been cooled normally on the hot bed and the other had been cooled slowly; a sample of 0.6 per cent carbon steel bar stock; and samples of heat treated and comparison untreated rails.

2. The results of all of the impact tests showed that at temperatures of 500° and 600° C. the energy absorbed was lower than at either 400° or 700° C. This range of reduced ductility corresponds closely to the range of secondary brittleness shown by low ductility in tensile tests.

3. Impact tests on specimens taken transversely from the rails also showed the phenomenon markedly but the energy absorbed was lower throughout the temperature range of test.

4. In the 0.60 per cent carbon bar stock, in which secondary brittleness was not shown in tensile tests, marked decrease in energy absorbed in the secondary brittle range was shown in the impact tests. This was true for the material in both the "as received" and the annealed condition.

5. A reduction in the energy absorbed at 500° and 600° C. was shown by impact tests on heat-treated rails and a comparison normal rail. The impact tests did not discriminate as closely between the heat treatments as well as previously reported tensile tests on the rails had done.

6. Longitudinal specimens tested in impact at temperatures above 660° C. did not fracture completely.

7. The fractures of the impact specimens were found to be transcrystalline throughout the range of temperature of the tests.

VI. ACKNOWLEDGMENTS

The author is indebted to several members of the staff of the Bureau of Standards, particularly H. S. Rawdon and W. H. Swanger for valuable suggestions in the preparation of the manuscript, and to P. Devaney, who carefully machined all of the test specimens.

WASHINGTON, December 28, 1931.

[1] See footnote 5, p. 192.

KAOLINS; EFFECT OF FIRING TEMPERATURES ON SOME OF THEIR PHYSICAL PROPERTIES

By R. A. Heindl, W. L. Pendergast, and L. E. Mong

ABSTRACT

North Carolina, Delaware, Georgia, and Zettlitz kaolins and English china clay were fired to eight different temperatures ranging from 1,100° to approximately 1,650° C. For the unfired clays the pyrometric cone equivalents were determined and the chemical and petrographic analyses made; on the fired clays the porosity, specific gravity, petrographic analyses and thermal expansion measurements were made. X-ray diffraction patterns made of mullite and cristobalite were compared with those obtained on the North Carolina and Georgia kaolins fired to 1,300° C. The results of the petrographic and chemical analyses show that three of the kaolins contain a greater amount of impurities than the other two, and the effect on the development of mullite and cristobalite through progressive heat treatments is consequently quite different. This difference in the development of mullite and cristobalite is indicated by both the petrographic examination and thermal expansion data. X-ray diffraction patterns show the presence of cristobalite in one of the fired clays. The beginning of the change in the rate of thermal expansion attributed to the alpha to beta inversion of cristobalite occurs approximately 75° C. below the usually accepted lower limit of temperature range of this inversion. A limited amount of data are given on dickite (Mexican kaolin), halloysite, and silica.

CONTENTS

		Page
I.	Introduction	199
II.	Materials	200
III.	Preparation of specimens	200
IV.	Methods of testing	200
V.	Results	201
	1. Chemical analyses	201
	2. Petrographic analyses	201
	3. Pyrometric cone equivalents	204
	4. Specific gravity and porosity	204
	5. Thermal expansion	205
	6. X-ray studies	211
VI.	Similarity of expansion between 100° and 200° C. of precipitated silica and the Georgia and Zettlitz kaolins	212
VII.	Summary	214
VIII.	Acknowledgments	215

I. INTRODUCTION

The effect of temperature of firing on the mineralogical composition of fire clays was discussed briefly in a report[1] recently published dealing with fire clays. Because of the interesting results obtained with such clays it was considered desirable to continue the study with clays of the kaolin type in order to gain information on the effect of heating materials whose composition more nearly approaches

[1] "Fire Clays; Some Fundamental Properties at Several Temperatures." B. S. Jour. Research, vol. 5 (RP194); also J. Am. Ceram. Soc., vol. 13 (10), pp. 725–750, 1930.

that of pure kaolinite. Even though kaolins are relatively pure clays, they differ quite appreciably in composition, depending on the source of supply and purifying process involved; and the results obtained in a study of them vary accordingly.

II. MATERIALS

The materials studied were taken from the regular stock available at the bureau, and included Georgia (soft), Delaware, North Carolina, and Zettlitz kaolins and English china clay. A few tests were also made on dickite, Georgia (hard) kaolin, halloysite, silicic acid, and flint.

III. PREPARATION OF SPECIMENS

Specimens suitable for expansion measurements with the interferometer, and bar specimens 2 inches long and 1 inch in cross section, were made of each of the five kaolins. These were fired in a furnace whose temperature was increased at the rate of 20° C. an hour up to 1,400° C. Two of the specimens for expansion studies and one of the bar specimens of each kaolin were withdrawn at each of the following temperatures: 1,100°, 1,150°, 1,200°, 1,250°, 1,300°, and 1,400° C. and placed in a second furnace having a temperature of approximately 600° C. At the end of 15 hours, when the temperature was approximately 100° C., the specimens were removed (referred to hereafter as "cooled rapidly"). The remaining specimens of the five clays were fired to cone 18½ (approximately 1,500° C.) at the rate of approximately 10° C. an hour and allowed to cool slowly with the furnace. With the exception of the English china clay, specimens for expansion studies were also fired at 1,200° and 1,300° C. for two hours, and at 1,400° C. for five hours, and in each instance were cooled with the furnace in approximately 48 hours (referred to hereafter as "cooled slowly"). In addition, specimens of Georgia kaolin containing 5, 10, and 15 per cent of muscovite were prepared and fired at 1,400° C. for five hours.

Specimens were also prepared of a mixture of kaolin and precipitated alumina and fired at 1,300° C. for two hours and others at cone 30 (approximately 1,650° C.) for one-half hour. Alumina was added to secure the proper alumina-silica ratio (3:2) in order to obtain a body consisting entirely of mullite after firing. This was done with all five of the kaolins and the amount added was dependent on the percentage of silica found by chemical analysis.

IV. METHODS OF TESTING

Thermal expansivity measurements of the materials were made from atmospheric temperature to 900° C. with the interferometer.[2] The procedure followed in making chemical analyses was, in general, the method of analysis for refractories described by Lundell and Hoffman.[3] The specific gravities were determined according to the method of test for pigments,[4] promulgated by the American Society for Testing Materials. The procedure for making the porosity determinations was as follows: The specimens were saturated by boiling

[2] Described in B. S. Sci. Paper No. 485, by G. E. Merritt.
[3] Analysis of Bauxite and of Refractories of High Alumina Content, B. S. Jour. Research, vol. 1 (RP 5); July, 1928.
[4] American Society for Testing Materials Standards 1930, Pt. II, A. S. T. M. Designation D 153-27.

in water under reduced pressure for two hours and permitting them to remain over night under a gradually increasing pressure. The volume was obtained by water displacement. The porosity expressed in per cent was computed by dividing the weight of water absorbed (dry weight minus saturated weight) by the volume of the specimen. The pyrometric cone equivalents [5] "softening points" were determined according to the A. S. T. M. standard method, serial designation C 24-28.[6]

TABLE 1.—*Chemical analyses of kaolins*

Name of material	Georgia kaolin [1]	North Carolina kaolin [1]	Delaware kaolin [1]	English China clay [1]	Zettlitz kaolin [2]	Dickite [3]	Halloysite [3]
	Per cent	*Per cent*	*Per cent*	*Per cent*	*Per cent*	*Per cent*	*Per cent*
Ignition loss	13.71	13.03	11.84	12.37	12.95	14.08	14.64
SiO_2	45.30	48.46	48.53	47.00	46.90	45.04	41.62
Fe_2O_3	.27	.51	1.57	.96	.65	Trace.	.62
Al_2O_3	39.14	36.53	35.79	37.72	37.40	40.70	38.66
TiO_2	1.54	.06	.33	.15	.18	Trace.	----------
CaO	.13	.13	.15	.19	.29	.22	.10
MgO	.04	.03	.22	.18	.27	Trace.	.08
K_2O	.15	1.34	1.80	1.57	.84	----------	----------
Na_2O	.10	.21	.19	.23	.44	Trace.	----------
H_2O	----------	----------	----------	----------	----------	----------	4.26

[1] Analysis made by J. F. Klekotka.
[2] Analysis made by Dr. J. I. Hoffman and taken from Bureau of Standards Technical News Bulletin 138, p. 146; 1928.
[3] These materials and chemical analyses were furnished by C. S. Ross, of the U. S. Geological Survey. The dickite originated in Chihuahua, Mexico, and the halloysite in Adams County, Ohio.

V. RESULTS AND DISCUSSION

1. CHEMICAL ANALYSES

The chemical analyses of the five kaolins on which the greater part of this study was made are given in Table 1. Considering kaolinite ($Al_2O_3 \cdot 2SiO_2 \cdot 2H_2O$) as approximately 14.0 per cent water, 46.5 per cent silica, and 39.5 per cent alumina, it is found that the composition of the Georgia and Zettlitz kaolins approaches the composition of the kaolinite more closely than do any of the other three. This point is of importance because the data obtained in the several tests vary quite decidedly for the different kaolins.

2. PETROGRAPHIC ANALYSES

Petrographic analyses were made of both the unfired clays and of the same clays after firing at progressively increasing temperatures. The petrographic examinations were made to obtain information on the foreign materials present and to determine, if possible, the temperature at which the clay when fired is converted to mullite with the excess silica remaining free in accordance with the following equations:

$$3\ (Al_2O_3 \cdot 2SiO_2 \cdot 2H_2O) + \text{heat} = 3\ (Al_2O_3 \cdot 2SiO_2) + 6H_2O$$
$$3\ (Al_2O_3 \cdot 2SiO_2) + \text{heat} = 3Al_2O_3 \cdot 2SiO_2 + 4SiO_2$$

[5] In this report the expression pyrometric cone equivalent (P. C. E.) is to be interpreted according to the tentative definition given in the Proceedings of the American Society for Testing Materials, pt. 1, vol. 30, 1930, p. 473, which is "In the case of refractories the number of that standard cone whose tip would touch the supporting plaque simultaneously with a cone of the material being investigated when tested in accordance with the standard method of test for softening point of fire-clay brick of the A. S. T. M.
[6] Described in American Society for Testing Materials Standards for 1930, Pt. II, p. 210.

The analyses follow:

GEORGIA KAOLIN.—*Unfired.*—Contains approximately 2 per cent mica and less than 1 per cent quartz. No feldspar noted, but a small amount of a fine-grained mineral (possibly rutile) present.

Fired to 1,100° C. (cone 1) and to 1,150° C. (cone 6).—No mullite noted. Made up largely of isotropic grains having an index of refraction of about 1.55. Occasional needles having a very high index and a very high birefringence (possibly rutile) present.

Fired to 1,200° C. (cone 10).—No visible mullite development. The amorphous grains have an index of refraction of about 1.57. The high index, highly birefringent aggregates appear to be smaller and less numerous.

Fired to 1,250° C. (cone 12) and 1,300° C. (cone 13).—The faintest trace of mottled structure noted which, perhaps, indicates the beginning of mullite development. The mottled structure becomes fairly distinct after firing at 1,300° C. The grains are made up of bundles of subparallel fibers showing low birefringence.

Fired to 1,400° C. (cone 16).—Fine, somewhat irregular fibers of mullite are visible. Material made up of only two visible phases, namely, mullite and a low index interstitial material.

Fired at cone 18–19 (approximately 1,500° C.).—Mullite fibers are perceptibly larger and better developed than in the material fired at 1,400° C.

Fired at cone 30 (approximately 1,650° C.).—The average thickness of the mullite fibers is increased to approximately 4μ. The material containing the added alumina consists almost entirely of large, well-developed mullite crystals. Only a very small amount of glass and uncombined alumina present.

ENGLISH CHINA CLAY.—*Unfired material.*—Estimated to contain from 9 to 11 per cent of muscovite, less than 1 per cent of quartz, and a small amount of feldspar (probably less than 2 per cent).

Fired to 1,100° C.—Material somewhat heterogeneous in composition and largely composed of platy, colorless grains.

Fired to 1,150° C.—Not much change from the preceding firing. The stained grains show a mottled structure.

Fired to 1,200° C.—A faint but unmistakable mottled structure perceptible in all the platy grains.

Fired to 1,250 ° C.—The material is more uniform in structure and in index of refraction than that fired at the lower temperatures. Bundles of subparallel fibers with low birefringence noted.

Fired to 1,300° C.—Mottled structure of lower fired samples replaced by irregular and extremely thin fibrous structure (probably mullite).

Fired to 1,400° C.—The sample consists of only mullite and an interstitial, low index, isotropic material.

Fired at cones 18–19 (1,500° C.).—Very little change from the 1,400 ° C. firing except that the mullite needles are better developed.

Fired at cone 30 (approximately 1,650° C.).—Very similar to the material fired at 1,500° C., except that the mullite needles are somewhat larger and better developed. The mixture of kaolin and alumina consists almost entirely of large, well-developed mullite crystals. Only a very small amount of uncombined glass and alumina noted.

NORTH CAROLINA KAOLIN.—*Unfired material.*—Estimated to contain from 7 to 9 per cent of muscovite, 10 to 12 per cent quartz, and, perhaps, as much as 10 per cent feldspar (largely microcline).

A small amount of an unidentified mineral with a high index of refraction (probably hematite or hydrated ferric oxide) present.

Fired to 1,100° C.—Heterogeneous in structure. Kaolinite and mica grains still retain their platy structure. Feldspar grains have been largely fused to a glass. Quartz grains appear unchanged.

Fired to 1,150° C. and to 1,200° C.—Quartz remains unchanged. A mass of short fibers developed within the fused feldspar grains which are only visible with the highest magnification, indicating the beginning of the formation of mullite.

Fired to 1,250° C.—Mullite development has begun in the kaolinite grains and progressed further in the fused feldspar grains. The quartz grains are surrounded by a narrow rim of low index material either the result of transformation or solution.

Fired to 1,300° C. and 1,400° C.—Triangular networks of mullite have developed in the kaolinite grains which continued to develop with the 1,400 ° C. firing.

Fired to 1,500° C. (approximately).—A marked change in the structure and microscopic appearance of the material noted. Only fibers of mullite imbedded in an interstitial low index material (probably glass) present.

Fired at 1,650° C. (approximately).—The mullite grains show definite evidence of solution. The specimen originally containing the mixture of kaolin and alumina after firing consists almost entirely of large, well-developed crystals of mullite. Small amounts of glass and uncombined alumina noted.

DELAWARE KAOLIN.—*Unfired material.*—Estimated to contain from 15 to 17 per cent of mica, from 12 to 14 per cent of quartz, and an indeterminate quantity of feldspar (probably less than 5 per cent). Very small amounts of what may be rutile and hematite noted.

Fired to 1,100° C.—Kaolinite grains still retain a platy structure. Quartz grains unaltered from the raw material.

Fired to 1,150° C.—No visible development of mullite in the kaolinite grains. Edges of quartz grains indicate incipient fusion.

Fired to 1,200° C.—Mottled structure in kaolinite grains indicates the initial development of mullite.

Fired to 1,250° C. and to 1,300° C.—Further gradual development of mullite grains.

Fired to 1,400° C.—Small fibers of mullite embedded in a low index, interstitial material (probably glass) are the only two phases present.

Fired at 1,500° and 1,650° C. (approximately).—The mullite and glass phases are similar to that noted in the 1,400° C. firing except that the mullite needles show much better development. The kaolin with the added alumina after firing to approximately 1,650° C. shows a much greater percentage of mullite crystals, but considerable amounts of uncombined alumina and glass also present.

ZETTLITZ KAOLIN—*Unfired material.*—Estimated to contain from 1 to 2 per cent of muscovite and less than 1 per cent of quartz. No feldspar noted, but very small amounts of hornblende, hematite, and dolomite present.

Fired to 1,100° C.—The original kaolinite grains largely converted to isotropic masses with a few remnants of the original platy structure remaining. No visible mullite development and no mottled structure noted.

Fired to 1,150°, 1,200°, and 1,250° C.—The material after firing at 1,150° C. appears very similar to that fired to 1,100° except that cloudy birefringent areas have largely disappeared. After firing at 1,200° C. the grains show a mottled structure indicating the possible presence of mullite and with the 1,250° C. firing a fairly distinct fiber formation evident.

Fired to 1,300° C.—Grains not uniform in structure, but the mullite structure and fiber development have progressed decidedly. Isotropic low index inclusions, irregular in shape, persist and appear to be more abundant than in preceding firings.

Fired to 1,400°, 1,500°, and 1,650° C.—Mullite and an interstitial material of lower index are the only two phases present. The mullite needles grow in size as the temperature of firing is raised. The kaolin-alumina mix composed principally of large, well-developed crystals of mullite. Appreciable amounts of glass and uncombined alumina noted.

3. PYROMETRIC CONE EQUIVALENTS

The P. C. E. of each of the five kaolins was 35 (approximately 1,785° C.).

No change in the P. C. E. of Georgia kaolin was observed by additions of either 5, 10, or 15 per cent of muscovite, the P. C. E. of which was 14 (equivalent, under the conditions of our test, to approximately 1,400° C.). This was the only kaolin to which muscovite was added.

4. SPECIFIC GRAVITY AND POROSITY

The true specific gravity and the apparent porosity of the specimens of kaolins after firing at each of six temperatures, namely, 1,150°, 1,200°, 1,250°, 1,300°, 1,400°, and 1,500° C., are given in Table 2.

TABLE 2.—*Specific gravity and porosity* [1] *after firing*

Kaolin identity	Temperature of firing °C.											
	1,150		1,200		1,250		1,300		1,400		1,500	
	Specific gravity	Porosity	Specific gravity	Porosity	Specific gravity	Porosity	Specific gravity	Porosity	Specific gravity	Porosity	Specific gravity	Porosity
		Per cent		*Per cent*		*Per cent*		*Per cent*		*Per cent*		*Per cent*
North Carolina	2.709	46.45	2.711	45.78	2.732	43.50	2.696	41.18	2.706	34.60	2.707	31.80
Delaware	2.712	39.47	2.724	37.18	2.719	32.10	2.705	24.02	2.675	6.79	2.689	1.50
Georgia	2.748	39.00	2.787	33.32	2.801	32.30	2.815	30.18	2.781	9.10	2.793	2.57
Zettlitz	2.748	37.17	2.755	34.42	2.762	30.70	2.733	22.12	2.695	1.74	2.749	.64
English	2.714	41.15	2.723	37.00	2.725	28.40	2.734	22.72	2.702	10.04	2.700	.50

[1] For method of determining, see J. Am. Ceram. Soc., vol. 11, No. 6, p. 456; 1928.

North Carolina kaolin shows the smallest change in porosity over the range of firing temperatures used and English china clay the largest, although there is not a great deal of difference between the English china clay and the Georgia, Zettlitz, and Delaware kaolins. The values given represent determinations on one specimen only for each of the firings.

In general, the specific gravity slightly increases with increasing firing temperature to 1,250° C., decreases to 1,400° C., and increases again at 1,500° C.

The specific gravity values represent the average of two determinations and in no case was there a greater variation from the average than ±0.005.

5. THERMAL EXPANSION

The linear thermal expansion of the materials studied is shown in Table 3. Values are given for three different ranges of temperature obtained for each of the kaolins after firing at several different temperatures. Curves representing the expansion data are shown in Figures 1 to 5, inclusive.

TABLE 3.—*Coefficient of linear thermal expansion of kaolins fired at different temperatures*

Kaolins fired to ° C.—	Average coefficient of expansion [1] of kaolin														
	North Carolina			Delaware			Georgia			Zettlitz			English		
	Temperature range (° C.)														
	100 to 200	550 to 600	20 to 900 [2]	100 to 200	550 to 600	20 to 900 [2]	100 to 200	550 to 600	20 to 900 [2]	100 to 200	550 to 600	20 to 900 [2]	100 to 200	550 to 600	20 to 900 [2]
1,100 [3]	3.7	10.1	4.6	4.2	7.2	4.5	3.8	4.7	4.5	3.3	5.0	4.2	3.7	5.6	4.4
1,150 [3]	3.3	9.3	4.1	4.0	6.4	4.4	3.7	4.7	4.0	5.7	5.3	4.6	4.4	5.4	4.3
1,200 [3]	3.5	7.8	4.4	4.6	6.9	4.7	5.8	4.5	4.7	9.9	5.2	5.8	4.9	5.4	4.5
1,200 (slow cooling) [4]	4.6	7.3	4.8	5.1	5.8	5.0	11.2	5.2	6.4	13.0	5.5	6.4			
1,250 [3]	4.9	7.0	4.5	4.1	5.4	4.6	13.3	5.0	5.9	10.5	3.7	5.3	4.3	4.8	4.4
1,300 [3]	4.5	6.8	4.5	3.5	4.9	4.4	15.7	5.4	6.5	6.1	5.1	4.7	3.9	5.0	4.3
1,300 (slow cooling) [4]	6.2	7.5	4.9	4.4	5.5	4.5	15.7	5.8	6.8	13.9	5.5	6.4			
1,300 (plus alumina) [5]	6.6	9.5	6.9	5.8	7.4	6.2	7.5	6.3	6.4	5.0	6.5	5.8	4.5	6.3	5.6
1,400 [3]	4.7	5.7	4.4	3.6	4.8	4.3	15.7	5.7	6.5	3.6	4.1	4.2	3.8	4.5	4.2
1,400 (slow cooling) [4]	4.2	5.7	4.6	3.7	4.9	4.4	19.9	5.9	7.1	11.0	5.6	6.0			
1,500 [4]	3.7	4.4	3.9	3.8	4.5	4.3	16.4	5.3	6.5	5.7	5.1	5.1	3.8	4.4	4.2
1,650 [4]	3.7	4.1	4.1	4.0	4.8	4.6	3.6	4.5	4.0	3.8	4.8	4.0	3.8	4.5	4.3
1,650 (plus alumina) [5]	4.5	5.8	5.2	4.7	6.0	5.5	3.6	4.6	4.4	4.4	5.7	5.3	4.4	5.8	5.3

[1] Values to be multiplied by 10^{-6}.
[2] To obtain percentage expansion at 900° C., multiply the value given in the column headed "20 to 900" by 880 and divide by 10^4.
[3] Specimens were withdrawn at the temperatures indicated and cooled comparatively rapidly.
[4] Specimens held at the temperatures indicated for a short time as noted in the text and then were allowed to cool with the furnace, therefore, cooled comparatively slowly.
[5] Specimens contained added percentages of precipitated alumina.

In general, the curves for North Carolina and Delaware kaolins and the English china clay are similar and for convenience may be classified in one group and those for the Georgia and Zettlitz kaolins in a second. The curves on the left in Figures 1 and 2 represent the expansion data of the kaolins after rapid cooling, while those on the right are the same kaolins after slow cooling. The curves in Figure 1, which give the expansion data of the first group, show very little difference in either the type or the total expansion of the three clays. The North Carolina kaolin shows the greatest increase in expansion between 575° and 600° C., due to the inversion of α to β quartz. Both the Delaware and English clays show this same inversion at the

lower firings, but to a lesser degree. The data for the North Carolina and Delaware kaolins indicate that the rate of cooling has compara-

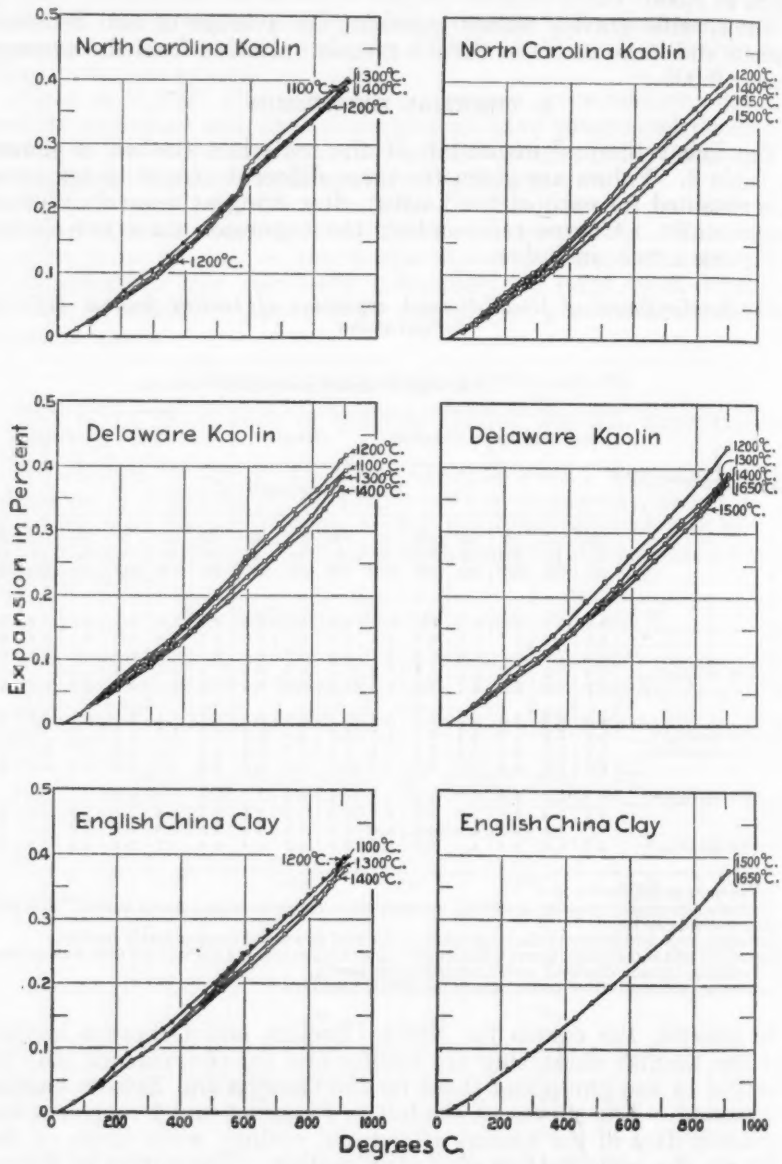

FIGURE 1.—*The thermal expansion curves of one group of kaolins after firing at several different temperatures*

The curves on the left were obtained when the clays were cooled rapidly and those on the right when held at the maximum temperature for a short time and cooled slowly.

tively little effect on the thermal expansion of these clays after having been fired to the same temperatures.

The thermal expansions of the Georgia and Zettlitz kaolins which are shown in Figure 2 are decidedly different from the three kaolins shown in Figure 1. Progressively increasing the temperature of firing has a marked effect on the expansivity of the Georgia and Zettlitz kaolins below 200° C. The pronounced variation in rate is undoubtedly due to mineralogical changes occurring in the clays which, in

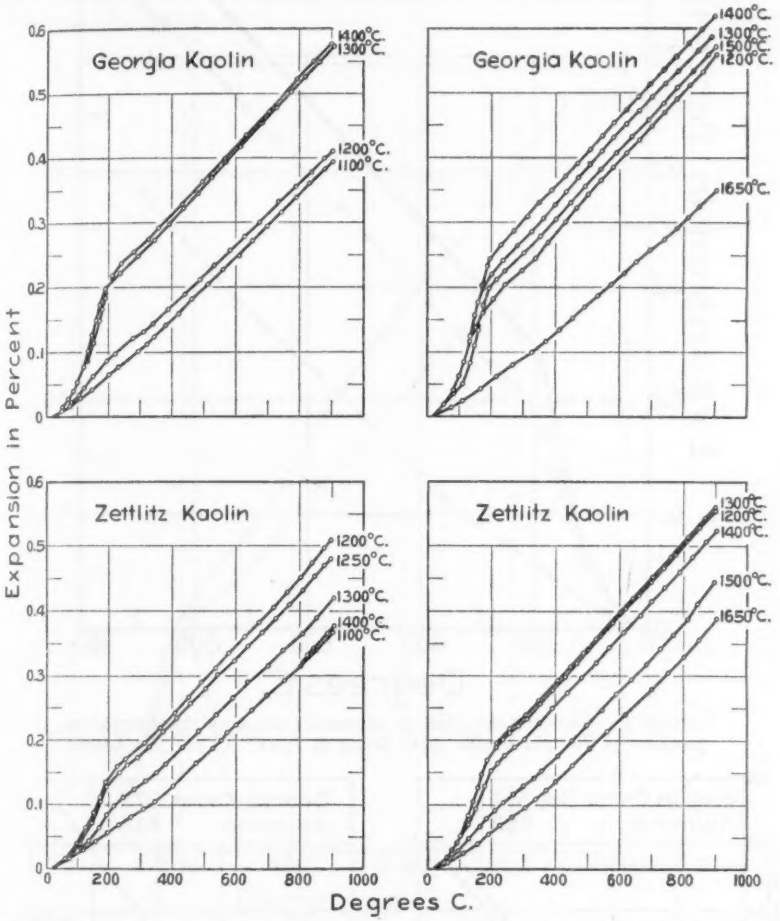

FIGURE 2.—*The thermal expansion curves of a second type of kaolins after firing at several different temperatures*

The rate of cooling (rapid cooling on the left) after firing at certain temperatures has a decided effect on the expansion.

turn, are affected by the relative purity. As shown by the curves on the left in Figure 2, the Georgia kaolin shows a slightly higher total expansion after firing at 1,200 °C. than after 1,100° C. However, after firing at 1,250° (not shown in the figure), 1,300°, and 1,400° C., the expansion below 200° C. has increased to its maximum, but is practically the same for the three firings. The Zettlitz kaolin under corresponding conditions of firing shows the greatest increase in expansion after the firing to 1,200° C. As the temperature of firing

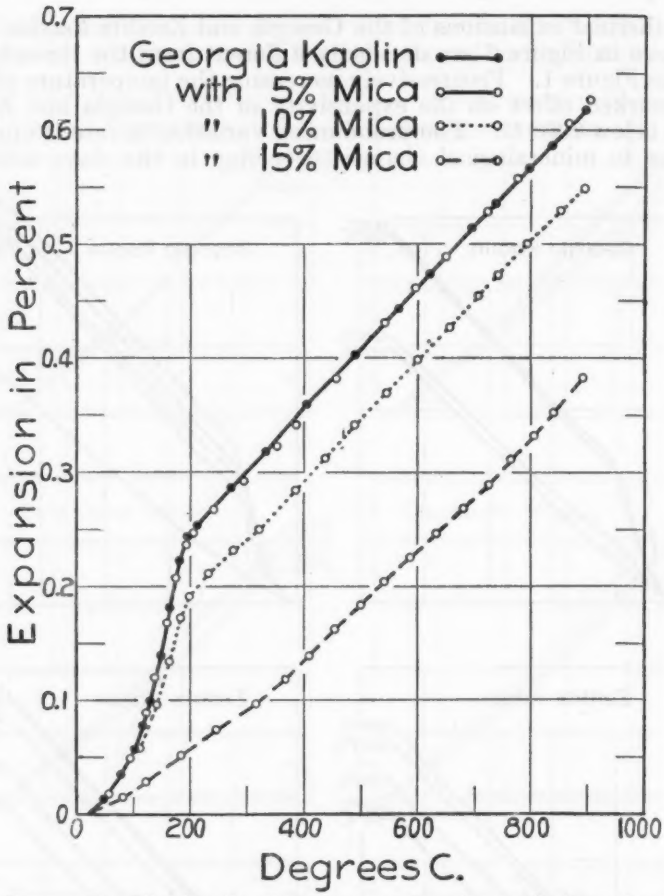

FIGURE 3.—*Showing the effect of muscovite mica on the thermal expansion of Georgia kaolin after firing at 1,400° C. for five hours*

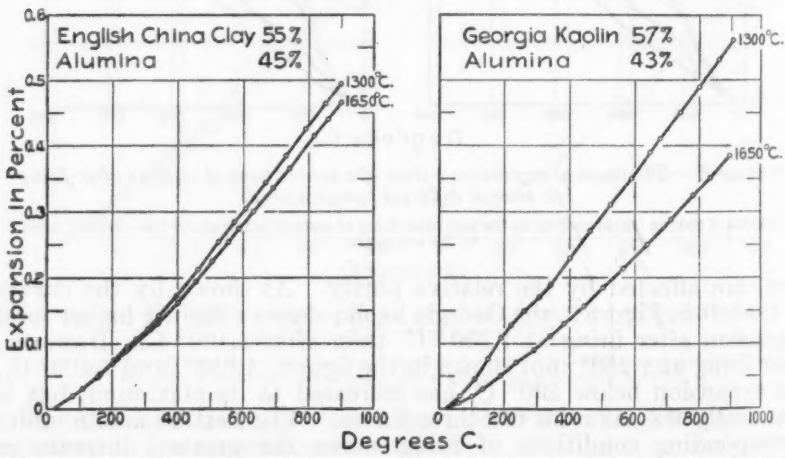

FIGURE 4.—*The effect of alumina on the thermal expansion of kaolins having two different types of expansion after firing*

was increased the total thermal expansion gradually decreased so that after firing at 1,400° C. the expansion was practically the same as after the firing at 1,100° C. The petrographic examination shows the Georgia and Zettlitz kaolins to be very nearly the same as far as clay content, mica, quartz and feldspar are concerned. The chemical analysis shows the Georgia kaolin to have appreciably more titanium oxide (rutile) than the Zettlitz kaolin, but the alkalies are decidedly greater in the latter.

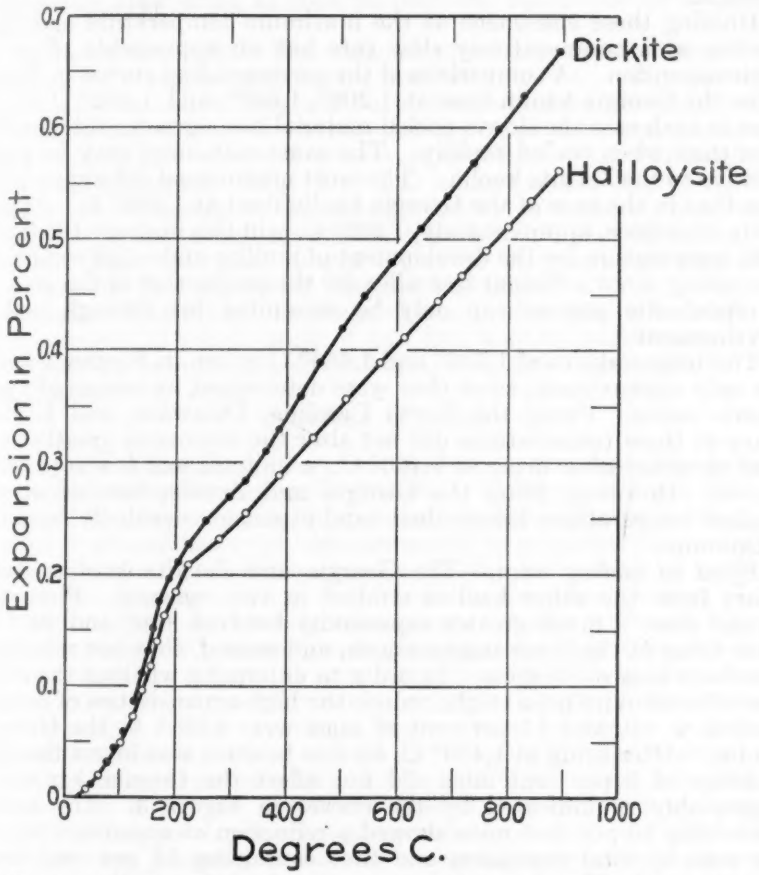

FIGURE 5.—*Thermal expansion curves of dickite and halloysite after firing at 1,300° C. for two hours*

The sample of dickite was hand-picked and unusually pure.

Comparing the information obtained from the petrographic analysis and thermal expansion data of these two fired kaolins, the following differences are noted. In all probability these differences are the result largely of the greater amount of alkalies present in the Zettlitz kaolin.

1. The first indication of the formation of cristobalite in the Zettlitz clay from the excess of silica developed as a result of the conversion of the clay to mullite, occurred at 1,200° as against 1,250° C. in the Georgia kaolin.

2. The temperature at which the maximum amount of cristobalite is formed in the Zettlitz kaolin is approximately 200° C. below that at which the maximum was formed in the Georgia kaolin.

3. The maximum amount of cristobalite present in the Zettlitz kaolin after any firing is decidedly less than that obtained in the Georgia kaolin.

4. The cristobalite is changed to a glass at a considerably lower temperature and at a greater rate in the Zettlitz kaolin than in the Georgia.

Holding these specimens at the maximum temperature and then cooling at a comparatively slow rate has an appreciable effect on their expansion. A comparison of the corresponding curves in Figure 2 for the Georgia kaolin fired at 1,200°, 1,300°, and 1,400° C. shows that in each case the slower cooled material has a greater total expansion than when cooled rapidly. The same statement may be made relative to the Zettlitz kaolin. The most pronounced difference noted was that in the case of the Georgia kaolin fired at 1,200° C. Apparently, therefore, approximately, 1,200° C. is in this instance the favorable temperature for the development of mullite under the conditions prevailing, since sufficient free silica for the production of the amount of cristobalite present can only be accounted for through such a development.

The temperatures of 1,500° and 1,650° C. given in Figures 1 and 2 are only approximate, since they were determined by means of pyrometric cones. Firing the North Carolina, Delaware, and English clays at these temperatures did not alter the expansion greatly from that obtained after firing at 1,400° C., a uniform and low rate being shown. However, firing the Georgia and Zettlitz kaolins at the highest temperatures lowers their total expansion decidedly from the maximum.

Effect of adding mica.—The Georgia and Zettlitz kaolins stand apart from the other kaolins studied in two respects. First, the former show a much greater expansivity between 100° and 200° C. after firing at the lower temperatures, and second, they are relatively free from muscovite mica. In order to determine whether the addition of muscovite mica might reduce the high expansivities of certain kaolins, 5, 10, and 15 per cent of mica were added to the Georgia kaolin. After firing at 1,400° C. for five hours it was found that the addition of 5 per cent mica did not affect the thermal expansion appreciably as indicated by the curves in Figure 3. The kaolin containing 10 per cent mica showed a reduction of approximately 12 per cent in total expansion and that containing 15 per cent mica approximately 37 per cent reduction, thereby bringing the expansion close to that of North Carolina, Delaware, and English kaolins after firing at the same temperature. These data indicate that the mica present in kaolins evidently has a decided effect on their expansion. This is an effect which might be expected if the added mica dissolves or prevents the cristobalite formation.

Effect of adding alumina.—The purpose of adding alumina to the kaolins was (1) to permit the formation of mullite by a combination of the added alumina and free silica resulting during the firing of clays and (2) to determine its effect on the thermal expansion. The data obtained on the thermal expansion after firing at two different temperatures are given in Table 3 and expansion curves of the English

and Georgia kaolins are given in Figure 4. The alumina tends to make the rate of expansion uniform throughout the entire range from 20° to 900° C. for the two kaolins showing a high rate of expansion below 200° C. after firing at 1,200° C. and by so doing causes the average coefficient of expansion to be lowered. The three kaolins which do not have the high rate of expansion below 200° C. show an increased rate of expansion because of the added alumina. In all cases the kaolins with the added alumina show a slightly higher expansivity after firing at cone 30 than the kaolin having no added alumina.

Additional materials.—The thermal expansion was measured of a specimen of Georgia hard kaolin fired at 1,300° C. The data obtained were so nearly identical with those obtained on the Georgia soft kaolin included in this study that no other data were obtained. Samples of dickite [7] and halloysite were also fired at 1,300° C. and the expansion measured. (Fig. 5.) The halloysite has practically the same total expansion as the Georgia kaolin, but the dickite has a decidedly greater total expansion than any of the other kaolins studied. Both materials have a high rate of expansion below 200° C. similar to that shown by the Georgia kaolin.

Duplicate determinations of the thermal expansions were made on 27 specimens in which each of the five kaolins were represented. The greatest variation in data obtained on the same material was less than ± 2½ per cent.

6. X-RAY STUDIES

Although it has long been assumed that the increased rate of expansion often observed in clay products between 100° and 200° C. is caused by the inversion of one form of cristobalite to another, no definite evidence has ever been presented to establish that assumption as a fact. A question arises as to the correctness of such an assumption because existing data [8] indicate that the inversion of the low cristobalite to high cristobalite occurs between 200° and 275° C. approximately. Westman [9] made computations from expansion data to show that the inflections occurring below 200° C. in the thermal expansion curves of fire-clay brick were probably due to the presence of cristobalite. The expansion curve given in Figure 5 for the form of kaolinite known as dickite shows the high rate of expansion to occur between approximately 110° and 210° C. The petrographic examination of the raw material indicated it to be free from impurities. The increased rate of expansion between 110° and 210° C. is therefore very probably due to the excess silica occurring as a result of the development of mullite from the clay. The petrographic microscope has failed to indentify the cristobalite as such because of its fine-grained state and because it is present as an interstitial material. X-ray diffraction patterns were made of the North Carolina kaolin, which showed a uniform rate of expansion throughout the range (20° to 900° C.) studied, and of both the Georgia and Mexican (dickite) kaolins, which show a high rate of expansion between approximately 100° and 210° C. and a comparatively low and uniform

[7] Described in detail in "The Kaolin Minerals," by C. S. Ross and P. F. Kerr, U. S. Geological Survey Professional Paper 165E.
[8] Robert B. Sosman, The Properties of Silica.
[9] A. E. R. Westman, The Thermal Expansion of Fire-Clay Bricks, Univ. Ill. Bull. No. 181.

rate from 210° to 900° C. For purposes of comparison X-ray diffraction patterns were also made of mullite and cristobalite.

The patterns of the North Carolina kaolin fired at 1,300° C. showed nothing but the typical mullite pattern indicating that the silica was present in noncrystalline form, a condition which would account for the fact that there is no inflection in the expansion curve below 200° C. The Georgia kaolin as well as the dickite fired at 1,300° C. showed the diffraction pattern of mullite as well as that of cristobalite. The X-ray patterns of the Georgia kaolin (center), mullite (top), and cristobalite (bottom) are given in Figure 6. The Georgia kaolin shows only the patterns of mullite and cristobalite. The information thus obtained definitely establishes the fact that the high and increased rate of expansion between approximately 100° and 200° C. in refractory clays is primarily caused by the presence of cristobalite.

VI. SIMILARITY OF EXPANSION BETWEEN 100° AND 200°C. OF PRECIPITATED SILICA AND THE GEORGIA AND ZETTLITZ KAOLINS

Specimens prepared from silicic acid and also from potters flint were fired at 1,300° C. for two hours and a second set at 1,400° C. for five hours. The silicic acid was the C. P. grade and the flint, which was ground to pass a 200-mesh sieve, came from Illinois.

The petrographic examination indicated that the silicic acid or precipitated silica had been apparently wholly converted to cristobalite. The powder X-ray diffraction pattern confirmed the results of the petrographic examination. No lines other than those of cristobalite were noted in the pattern.

The petrographic examination of the flint fired at 1,300° C. showed it to be composed almost entirely of crystalline quartz with some indications of initial formation of what apparently was cristobalite. The X-ray diffraction pattern gave similar information. Examination after firing at 1,400° C. showed less quartz and more cristobalite.

The expansion data obtained on these materials are represented by the curves in Figure 7. Greatly increased rates of expansion of the specimen of flint occur between 200° and 240° C. and again between 555° and 575° C. These increases in the rate of expansion begin presumably with or just before the cristobalite and quartz inversions. The curve for silicic acid after firing at 1,300° C. shows that a very high rate of expansion occurs between 150° and 195° C., but from 200° to 900° C. the rate is much lower and, in general, the entire curve is about the same as that obtained of the Georgia and Zettlitz kaolins after firing at certain temperatures. (See fig. 2.) Various investigators [10] have reported the transformation of precipitated silica to cristobalite at comparatively low temperatures. Houldsworth and Cobb [11] reported expansion data on precipitated silica after the transformation to cristobalite similar to those obtained on the silicic acid fired at 1,300° C.

The high rate of expansion and greatly increased total expansion observed between 175° and 230° C. approximately, in the specimen

[10] Robert B. Sosman, The Properties of Silica, pp. 166–176.
[11] H. S. Houldsworth and J. W. Cobb; The Reversible Thermal Expansion of Silica, Trans. Eng. Cer. Soc., vol. 21, pp. 227–276; 1921.

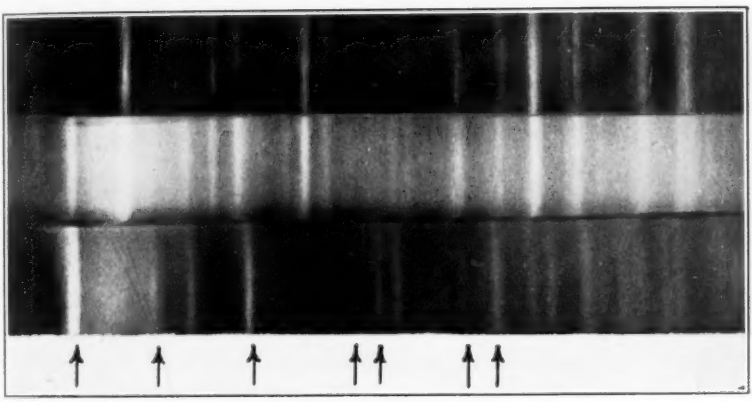

FIGURE 6.—*X-ray diffraction patterns of Georgia kaolin (center), mullite (top), and cristobalite (bottom)*

Arrows point to the lines of cristobalite which are clearly visible in the diffraction pattern of the kaolin. Unmarked lines in the cristobalite pattern are either so faint that they are not definite or are coincident or nearly coincident with mullite lines. The mullite lines in the kaolin pattern may readily be matched with those in the pattern of the pure mullite.

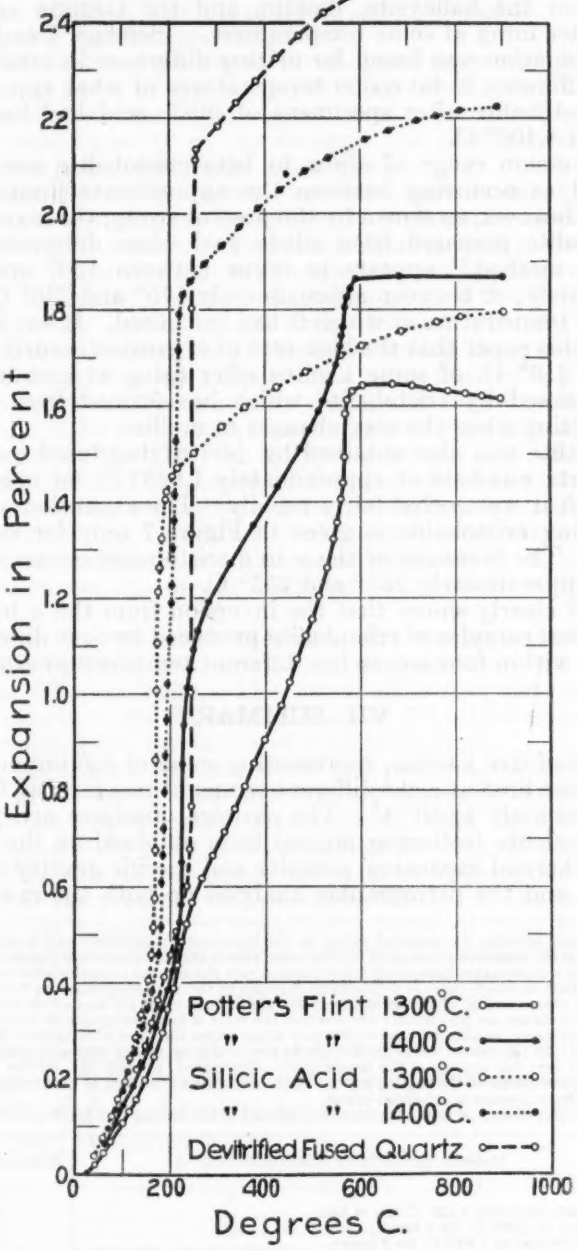

FIGURE 7.—*The thermal expansion of precipitated amorphous silica, crystalline silica (flint) after firing at 1,300° and 1,400° C., and devitrified fused quartz*

fired at 1,400° C. are also comparable to some extent to the expansion obtained on the halloysite, dickite, and the Georgia and Zettlitz kaolins after firing at some temperatures. (See figs. 2 and 5.)

An explanation was found for neither difference in total expansion nor the difference in inversion temperatures of what apparently was wholly cristobalite after specimens of silicic acid had been fired at 1,300° and 1,400° C.

The inversion range of alpha to beta cristobalite has long been recognized as occurring between the approximate limits 200° and 275° C. However, as shown by the present study, the inversion range of cristobalite prepared from silicic acid when determined by the expansion method [12] appears to occur between 150° and 195° C., approximately, or between approximately 175° and 230° C., depending on the temperature at which it had been fired. It has been shown earlier in this paper that the high rate of expansion occurring between 100° and 210° C. of some kaolins after firing at certain temperatures is caused by cristobalite which has formed from the excess silica resulting when the clay changes to mullite.

Cristobalite was also obtained by devitrifying fused quartz. The fused quartz was held at approximately 1,625° C. for one-half hour, after which it was cooled fairly rapidly. The expansion obtained on the resulting cristobalite is given in Figure 7 only for comparative purposes. The inversion of the α to β cristobalite occurs in this case between approximately 235° and 255° C.

Figure 7 clearly shows that the inversion from the α to β form of four different samples of cristobalite produced by four different methods occur within four somewhat different temperature ranges.

VII. SUMMARY

Samples of five kaolins, representing some of the important world sources, were fired at eight different temperatures ranging from 1,100° to approximately 1,650° C. The chemical analyses and pyrometric cone equivalents (softening points) were obtained on the raw materials, the thermal expansion, porosity and specific gravity on the fired materials, and the petrographic analyses on both the raw and fired.

[12] This difference between the accepted values for the inversion temperatures and those which might be chosen in view of the temperature range of the increased rate of thermal expansion probably arises from the fact that there is a measurable increase in the expansion rate throughout a considerable temperature range just preceding that in which there is a detectable increase in the heat absorption on heating.

The accepted values for the inversion temperatures are usually based on heat effect determinations and the temperatures chosen are presumably those where the rates of heat absorption or evolution are greatest and these temperatures usually fall reasonably near those where the rates of expansion or contraction are at their maxima. In the case of clear-cut heat effects the maximum rate of heat absorption or evolution is always within a very few degrees of the temperatures determined, respectively, by the minimum of the heating and the maximum of the cooling curve. Such maxima and minima as determined by A. Q. Tool for four of the above specimens are given below.

Temperatures corresponding to the maxima and minima of the cooling and heating curves, respectively:

Material (presumably cristobalite from—)	Maximum	Minimum
	°C	°C
Fused quartz heated at 1,625° C. for ½ hour	219	259
Flint heated at 1,400° C. for 5 hours	221	235
Silicic acid heated at 1,400° C. for 5 hours	203	220
Silicic acid heated at 1,300° C. for 2 hours	196	204

The heat effects both on heating and cooling were large and very clear-cut in the case of the fused quartz specimen. For the flint they were much smaller and only reasonably clear-cut. In the cases of both silicic acid specimens they were somewhat smaller still, and the minima of the heating curves were not well defined. This lack of definiteness was of such a character that it suggests the possibility of a mixture of crystal forms.

X-ray diffraction patterns were made of Georgia, North Carolina, and Mexican (dickite) kaolins, mullite, and cristobalite.

The following results were noted:

1. The chemical and petrographic analyses show the Georgia and Zettlitz kaolins to be of greater purity than the North Carolina and Delaware kaolins or the English china clay.

2. The specific gravity of the Georgia and Zettlitz kaolins is, in general, higher than that of the other three.

3. The porosity of the North Carolina kaolin is the highest and shows the least change over the range of temperature used.

4. After firing the purer Georgia and Zettlitz kaolin at some temperatures, the linear thermal expansion between approximately 100° and 200° C. is decidedly greater than that of the other three.

5. Progressively increasing the firing temperature of the kaolins affects the thermal expansion of those containing the greater amount of foreign material to a less extent than it does those of higher purity. The former are also affected less by changes in the rate of cooling.

6. Addition of 15 per cent muscovite to the Georgia kaolin did not measurably affect its P. C. E. (softening point), but after firing at 1,400° C. the thermal expansion of the mixture was greatly reduced when compared with that obtained on the kaolin alone after firing at the same temperature. Addition of alumina in amounts based on the quantity of free silica present increased the mullite to almost 100 per cent when certain of the materials were fired at the highest temperature.

7. Evidence is given which indicates that the high rate of expansion shown by certain fired refractory clays is primarily caused by the presence of cristobalite. This cristobalite may form as a result of (*a*) free quartz in the unfired material or (*b*) excess silica from the reaction involving the formation of mullite from clay.

8. X-ray diffraction patterns show the presence of cristobalite in one of the fired clays. The high rate of expansion caused by the inversion of the α to β form begins approximately 75° C. below the usually accepted lower limit of the temperature range of this inversion.

9. The high rate of expansion between approximately 100° and 210° C. due to the presence of cristobalite in some of the fired kaolins is similar to the expansion of cristobalite prepared from precipitated amorphous silica which also occurs between approximately 100° and 210° C.

VIII. ACKNOWLEDGMENTS

Acknowledgment is due Dr. Herbert Insley for making the X-ray photographs and interpreting the diffraction patterns and also for his work and that of R. H. Ewell on the petrographic analyses.

WASHINGTON, December 5, 1931.

RP411

COMPOSITE-COIL ELECTRODYNAMIC INSTRUMENTS

By Francis B. Silsbee

ABSTRACT

This paper describes a new type of electrodynamic instrument suitable for the precise measurement of alternating current, voltage, or power at power frequencies. The principles of operation and the limitations in the accuracy both of ordinary wattmeters and of the new type of instrument are discussed in detail. An experimental ammeter of the new type, having a range of 5 amperes and readable to 0.01 per cent, is described. The general equations on which the design of this type of instrument is based are worked out, and, as an illustration, the design of a wattmeter is carried through. The appendixes contain the more mathematical portions of the design, a discussion of temperature errors, and some suggestions as to the winding of coils so that two independent windings will have very nearly equal magnetic effects.

CONTENTS

		Page
I.	Introduction	217
II.	The simple wattmeter	219
III.	The composite-coil wattmeter	221
IV.	Description of experimental instrument	229
V.	Experimental results with composite-coil ammeter	235
VI.	Fundamental considerations in design	238
VII.	An illustrative design	241
VIII.	Conclusion	250
IX.	Appendix A. Optimum winding of the coils of a composite-coil wattmeter	250
X.	Appendix B. Temperature compensation	257
XI.	Appendix C. Intermingling of coils for composite windings	260
XII.	Notation	262

I. INTRODUCTION

The progress of the electrical industry has been marked throughout its existence by a corresponding development of instruments and of methods of measurement of greater and greater accuracy. The tangent galvanometer of the pioneers has given way to the permanent-magnet moving-coil voltmeter and to the potentiometer, and the Edison electrolytic meter to the modern induction watthour meter.

In the field of direct-current measurements the development of methods has been pushed to the point where the final limits of accuracy are fixed by the definition or realization of the fundamental units. For example, a potentiometer and standard cell with suitable auxiliary apparatus and reasonable care in operation can yield results of an accuracy as great as is needed in almost any industrial or scientific work.

In the alternating-current field, however, the situation is far less satisfactory. There is no such thing as an "a. c. standard cell," and the operation of determining alternating currents and voltages in terms of direct-current quantities involves considerable difficulty.

This is especially the case in power measurements, because effective a. c. power is not given by the simple product of the voltage and current as is the case with direct current. A great many devices for accomplishing the transfer from a. c. to d. c. have been proposed, but all leave something to be desired. Thermal devices [1] are slow and liable to uncertainty, because the flow of heat is so much less susceptible of control than is the flow of electric current. Electrodynamic instruments of high sensitivity, and consequently slow period, are most generally used in this country,[2] while quadrant electrometers are used in Great Britain [3] for this purpose. Instruments of either of these types can be calibrated with direct current and then used to measure alternating current, voltage, or power. With careful work an accuracy approaching 0.01 per cent can be obtained, but the procedure necessary to minimize various errors is rather slow and laborious, and the apparatus is in no sense portable.

The a. c. potentiometer is capable of giving with high accuracy the relative values and phase differences of alternating voltages or currents, and certain specialized types of it form the basis for the highly precise methods for measuring the ratio and phase angle of instrument transformers. For the absolute measurement of voltage or current, the a. c. potentiometer can be no more accurate than the transfer instrument used to refer its indications to the direct-current standards. It is also not readily applicable to power measurement, particularly if the wave forms are distorted.

The passage from the portable d. c. indicating instrument to the potentiometer, with its increased accuracy, unfortunately results in a corresponding and unavoidable increase in the cost and delicacy of the apparatus and a decrease in the speed and convenience of its operation. An intermediate stage in the case of d. c. measurements is occupied by the deflection potentiometer.[4] This instrument is substantially equivalent to an indicating instrument having 1,500 scale divisions instead of the usual 150 divisions. The various sources of error present in ordinary indicating instruments can here affect only a small fraction of the indication, and the major part of the indication is subject only to the errors in resistance coils and standard cells, as in the conventional type of potentiometer. Such an instrument has proved very useful in the calibration of direct-current indicating instruments and in the precise measurement of direct-current voltage and power, especially in cases where fluctuations in the supply voltage have made the usual null potentiometer unworkable.

There seems to be a need [5] in the electrical industry for a type of apparatus which functions on alternating current in much the same way that the deflection potentiometer does on direct current. Among the possible applications of such an instrument would be the calibration of a. c. indicating instruments, the measurement of power in alternating-current circuits during important acceptance tests of large generating units, and perhaps the measurement of power at points

[1] Northrup, E. F., Standardization Apparatus for Measuring Volts, Amperes, and Watts, J. Franklin Inst., vol. 166, p. 115; 1908.

[2] E. B. Rosa, The Compensated, Two-Circuit Electrodynamometer, B. S. Bull., vol. 3, p. 43; 1906. F. K. Harris, A Suppressed-Zero Electrodynamic Voltmeter, B. S. Jour. Research, vol. 3, p. 445; 1929.

[3] Paterson, Rayner, and Kinnes, J. Inst. Elec. Eng., vol. 51, p. 294; 1913.

[4] Brooks, H. B., Deflection Potentiometers for Current and Voltage Measurements, B. S. Sci. Paper No. 172; June, 1911.

[5] It is interesting to note that this same need was voiced by Dr. L. T. Robinson in his paper on Electrical Units and Their Application, presented at the A. I. E. E. summer convention, June 24, 1931, when the manuscript of this paper was nearly completed.

where large interchange of power occurs between plants belonging to different corporations. The sums of money involved are often so great that a very considerable expenditure of money and time on the measurements is justified if a definite increase in accuracy can thereby be secured.

The instrument should be capable of being transported from place to place and connected in circuit with moderate ease through the conventional instrument transformers. It should be convenient to read on moderately fluctuating loads. It should have a precision of reading of 0.01 per cent, and a sustained accuracy at least approaching this value. It should be possible for the user to assure himself, by making proper auxiliary checks, that the instrument has not been thrown out of calibration since its last previous laboratory test.

In an effort to meet the requirements just outlined, a new form of electrodynamic instrument has been devised at the Bureau of Standards. It is the purpose of this paper to discuss the major features in the design of such instruments and to describe the construction and method of use of an experimental instrument of this type which has been built and used in this laboratory. It is hoped that it may prove of value as a guide to instrument makers in the development of a commercially practical instrument which will meet the growing demands of the industry for more precise alternating-current measurements.

The basic idea on which the operation of this instrument rests is a close intermingling of the windings which carry alternating current with those carrying direct current; hence the name "composite coil." This type of construction was proposed to the author a number of years ago by Dr. H. B. Brooks, who had originally conceived the idea and who fully realized the great advantages of such an arrangement in insuring constancy in the relative torque coefficients of the a. c. and d. c. windings. On page 262 will be found a list giving the meanings of the various symbols used in this paper.

II. THE SIMPLE WATTMETER

The composite-coil wattmeter can, perhaps, be best understood by comparing it with a single-phase electrodynamic wattmeter of the usual portable type. The essential element of such a portable wattmeter consists of a fixed coil, which is connected in series with the load to be measured, and a moving coil, which, in series with a high resistance, is connected across the terminals of the load. The electrodynamic action of the currents in the coils tends to move them so that the magnetic fields produced by the currents will aid one another. The moving coil is pivoted so that it can rotate about an axis perpendicular to the magnetic axis of the fixed coil, but this rotation is restrained by a pair of spiral springs which also serve to conduct current and to from the moving coil. The instantaneous torque produced by such a mechanism is proportional to the product of the instantaneous currents in the two coils. The constant of proportionality, G_{fm}, when the currents are expressed in amperes and the torque in dyne-centimeters given numerically in practical units by $\frac{dM_{fm}}{d\alpha} \times 10^7$ where M_{fm} is the mutual inductance in henries between the fixed and moving coils and α is the angle (in radians) turned through by

the moving coil. When the currents are alternating and of frequency f the torque pulsates with a frequency $2f$. Because of its inertia, the moving coil can not follow the pulsations, but moves in response to the average electrical torque given by

$$\tau = fG_{fm}\int_0^{1/f} i_m i_f dt \tag{1}$$

Now

$$i_m = \frac{e}{R_p + R_m} \tag{2}$$

where e is the instantaneous voltage across the load and $R_p + R_m$ is the total resistance of the moving-coil circuit. Also the control torque of the spring is given by

$$\tau_U = U\alpha \tag{3}$$

where U is the stiffness of the spring.

The moving coil will, therefore, turn until these torques are balanced and

$$U\alpha = \frac{fG_{fm}}{(R_p + R_m)}\int_0^{\frac{1}{f}} e_m i_f dt \tag{4}$$

Now by definition the average power delivered to the load is

$$P = f\int_0^{\frac{1}{f}} e i_f dt \tag{5}$$

Hence we obtain

$$P = \frac{\alpha U(R_p + R_m)}{G_{fm}} \tag{6}$$

If the pointer length is Z, the angular motion for a deflection X is

$$\alpha = \frac{X}{Z} \tag{7}$$

and we get in terms of the deflection X

$$P = \frac{U(R_p + R_m)}{G_{fm}Z} X \tag{8}$$

which may be considered the basic equation of the electrodynamic wattmeter, since it gives a definite relation between the pointer position and the power for any alternating-current wave form and for any relation between M_{fm} and α. In many commercial instruments the shapes of the coils have been carefully chosen so as to make $\frac{dM_{fm}}{d\alpha}$ nearly independent of α over the range used, with the result that the angular deflection α, and hence the motion of the pointer, is approximately proportional to the power P, and the scale is substantially uniform. Such a condition is, however, not essential to the accuracy of the instrument, since, even if it does not hold, the scale divisions can be laid off so as to correspond to equal increments in power.

The limitations in the accuracy of portable wattmeters are introduced by a variety of factors, among the most important of which are (1) errors in reading the position of the pointer with respect to the scale, (2) imperfection in the elastic properties of the springs, (3) friction between the pivots and jewels, (4) effect of the self-inductance of the moving coil, (5) effects of the mutual inductance between the fixed and the moving coils, (6) changes in the instrument constant $\left(\frac{dM_{fm}}{d\alpha}\right)$ as a result of side play in the bearings, (7) secular change in the resistance of the moving-coil circuit, (8) changes in room temperature, and (9) changes in coil temperature and spring temperature resulting from the heat produced by the currents. The effect of some of these factors, such as (5) and (7), are negligible in almost all cases, and those of others, such as (4) and (8), can be allowed for, if necessary, by applying proper corrections. The first three, however, together with (9), form the most serious limitations on accuracy.

The refinements of modern instrument design have pushed the uncertainty introduced by these effects down to about the limit which it is reasonable to expect with present-day materials. This limit is about the same for all of the first three effects listed above, and a modification which reduces one source of error (as, for example, the lengthening of the pointer as in a laboratory standard instrument) often serves merely to make the presence of the other limitations more obvious.

III. THE COMPOSITE-COIL WATTMETER

To pass from the simple wattmeter to a composite-coil wattmeter, one may imagine a succession of constructional changes to be made. The first of these is that each coil (moving and fixed) of the ordinary instrument becomes one which has two windings, insulated from each other, but so thoroughly intermingled that the magnetic field produced by a current in either winding is identical with that produced by the same ampere turns acting in the single coil of the original instrument. One winding of each coil has the same number of turns as did the corresponding original coil and is connected to the a. c. circuit in the same way. These will be called the a. c. windings. The other winding of each coil is connected through suitable resistances to a battery or other convenient source of direct current, so that the currents in these d. c. windings can be adjusted in steps to a series of values which are accurately measured in terms of the voltage of a standard cell and of the resistances of certain manganin coils.

The direction of the currents through the d. c. windings is so chosen that the torque produced by their interaction is opposite to that produced by the alternating currents. Since the interaction of alternating current in one coil with direct current in another gives no net contribution to the average torque, the moving element will deflect in response to only the difference between the torques of the a. c. and the d. c. windings. If the d. c. torque is adjusted to be nearly equal to the a. c. torque, both may be made very large in comparison to their difference, which alone is effective in producing a deflection of the instrument. The natural limits to this process lie in the heating of the windings by the current and in the increase in the period of the

instrument which would result from an excessive weakening of the control springs. In the particular apparatus described below, however, it has been found possible to carry the process to the point where the full a. c. torque is fifty times that which, if unopposed, would produce full-scale deflection (75 mm), and still to have the natural period as short as 3.5 seconds.

The second constructional change in the passage from the simple wattmeter to the composite-coil type is that the composite-coil wattmeter is made astatic by the use of two elements; that is, two sets of moving and of fixed coils. The two moving coils are mounted one above the other on the same spindle with their axes parallel. Each of the two moving coils and each of the two fixed coils is of the composite-coil construction with its intermingled a. c. and d. c. windings.

There are two reasons for going to this more complicated form of construction; the first is because the effect of the earth's magnetic field in producing a torque on the d. c. moving coil is thereby greatly reduced and can be more readily eliminated entirely by using the mean of readings taken before and after reversing the direction of the d. c. current. The second and more important reason is that the mutual inductance between the a. c. and the d. c. windings in one coil is neutralized by that in the corresponding coil of the other element, so that there is no net tendency for alternating currents to be induced and to circulate in the d. c. network. This second object could be attained by the use of fixed mutual inductors suitably connected, but such an instrument would have only one-half the torque of the type here described.

There are, of course, a great variety of possible arrangements of d. c. network which will serve to supply and measure the currents in the d. c. windings, which furnish the opposing torque. Perhaps the simplest form of d. c. circuit would be obtained by connecting the two d. c. windings in series with each other and with a resistance adjustable in steps of known value. If the voltage drop in the known resistance is balanced against a standard cell by suitable control of the current, the value of the current, and hence that of the opposing torque, would be known. Such an arrangement requires that successive steps of the precision resistor, if they are to correspond to equal steps in torque, have different values, none of which would be simple multiples of an ohm. A still greater objection is that the normal current rating of the fixed and the moving d. c. windings must be alike, which means that the fixed d. c. winding would have to have an inconveniently large number of turns, and consequently a high resistance.

An alternative circuit which is probably the one best suited to most applications is shown in Figure 1. Here 1 and 2 are the a. c. and d. c. windings, respectively, on the upper moving coil; 3 and 4 are the a. c. and d. c. windings on the upper fixed coil. Coils 1′, 2′, 3′, and 4′ constitute the corresponding windings of the lower element. R_p is the usual series resistor which makes the total resistance of the potential (moving coil) circuit suitable for the rated a. c. voltage.

A B C is an Ayrton-shunt dial, having a total resistance R_D between *A* and *C*, formed of D_m equal steps each of resistance R_A. The d. c. moving coils in series with the resistor R_T are shunted across the terminals *A C*. The compensating resistance R_c with steps approxi-

mately equal to R_A serves to keep the total resistance of the battery circuit constant when the main dial contact is moved.

A standard cell of voltage E_s is connected in series with the galvanometer and key across a resistance R_s. The fine rheostat R_a is used to adjust the main d. c. current to the exact value

$$I_4 = \frac{E_s}{R_s} \tag{9}$$

as shown by a balance of the galvanometer. If the setting on the

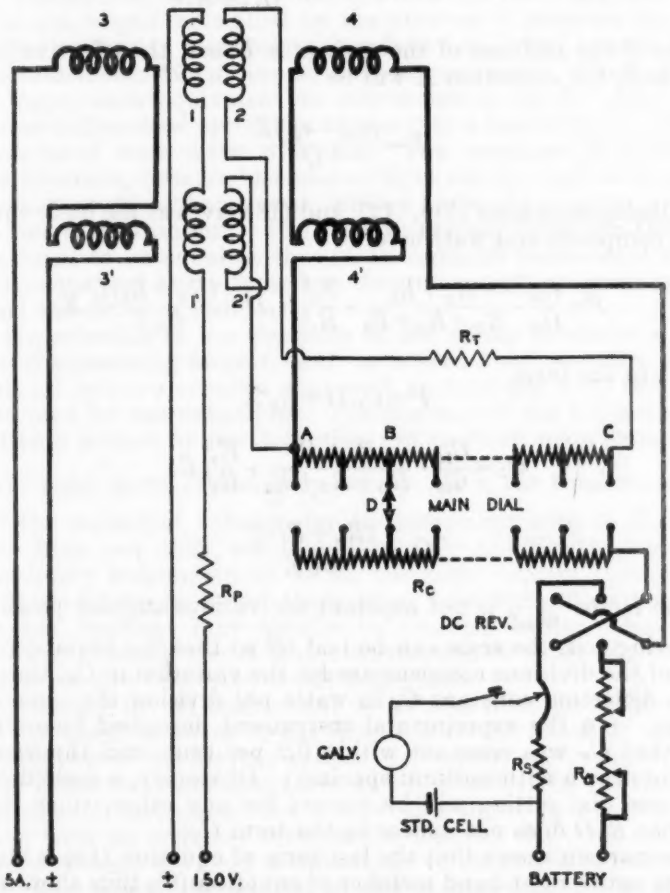

FIGURE 1.—*Schematic diagram of circuits of a composite-coil wattmeter*

dial is D, the resistance between A and B is R_A $D = R_w$ and the moving-coil current is

$$I_2 = \frac{R_A D\, I_4}{R_D + R_T + R_2} \tag{10}$$

where R_2 is the total resistance of the two d. c. moving coils, the springs and leads being here considered as part of R_T. The d. c.

torque is therefore

$$\tau_{dc} = G_{24} I_2 I_4 = \frac{G_{24} R_A D\, E_s^2}{R_s^2 (R_D + R_T + R_2)} \tag{11}$$

where $G_{24} = \frac{dM_{24}}{d\alpha} \times 10^7$ is the torque constant for the complete d. c. windings (both elements).

The a. c. torque is given by

$$\tau_{ac} = G_{13} I_1 I_3 \cos \varphi = \frac{G_{13} P}{(R_p + R_1)} \tag{12}$$

Hence if the stiffness of the springs is U and the effective pointer length is Z, the deflection X will be

$$X = \frac{(\tau_{ac} - \tau_{dc}) Z}{U} \tag{13}$$

Combining equations (11), (12), and (13) gives as the basic equation for the composite-coil wattmeter

$$P = \frac{G_{24}}{G_{13}} \cdot \frac{R_p + R_1}{R_D + R_T + R_2} \cdot \frac{E_s^2}{R_s^2} R_A D + \frac{(R_p + R_1) U}{G_{13} Z} X \tag{14}$$

which is in the form

$$P = C_D D + C_X X$$

where

$$C_D = \frac{G_{24}}{G_{13}} \cdot \frac{R_p + R_1}{R_D + R_T + R_2} \cdot \frac{E_s^2}{R_s^2} R_A \tag{16}$$

and

$$C_X = \frac{(R_p + R_1) U}{G_{13} Z} \tag{17}$$

If the factor $\frac{U}{G_{13} Z}$ is not constant for various angular positions of the moving coil, the scale can be laid off so that the variation in the length of the divisions compensates for the variation in C_X, thus keeping the deflection constant C_s in watts per division the same for all readings. (In the experimental instrument described below it was found that C_X was constant within 0.2 per cent, and the scale was therefore drawn with uniform spacing.) Obviously, a scale drawn to fit for one dial setting will be correct for any other, since the dial resistance $R_A D$ does not appear in the term C_X.

A comparison shows that the last term of equation (14) is identical with the entire right-hand member of equation (8), thus showing that the deflection X of the composite-coil wattmeter measures the portion $C_X X$ of the total power in exactly the same way as would a simple wattmeter whose constant $\frac{U(R_p + R_1)}{G_{fm} Z}$ was equal to C_X. To avoid circumlocution, we will call $C_X X$ the "deflection part" and $C_D D$ the "null part" of the total indication.

In mathematical terms a composite-coil instrument differs from an ordinary one by having C_X much smaller than the usual wattmeter constant. This may be obtained by making U much smaller, by

permitting somewhat more heating, which renders (R_p+R_1) smaller, and by making G_{13} larger. The flattening of the coils, which is permissible if the angular deflection is to be small, also increases G_{13}, and the use of a spot of light in place of a pointer permits an increase in Z.

Let us now compare the composite-coil wattmeter with one of the ordinary type as regards the various limitations on accuracy already mentioned. Since each step on the main dial corresponds to the same number of watts as does a deflection over the greater part of the actual instrument scale, it is evident that the instrument is equivalent as regards precision of reading to one in which the scale length is equal to the actual length multiplied by the number of steps on the main dial. The particular instrument described below has a scale 18 cm long graduated into 120 divisions, each 1.5 mm long. The main dial has 25 steps, each equivalent to 100 divisions on the scale. The instrument is therefore equivalent to one with a scale 375 cm (12 feet) long graduated with 2,500 divisions. The precision of reading is reduced, however, because the spot of light can be read with ease to only the nearest fifth of a division, while a knife-edge pointer could be read to one-tenth division. The relative reading error can therefore be considered to be equal to that in an ordinary instrument having 1,250 divisions and hence to be less than one-eighth as great as with the usual 150-division scale.

Any imperfection in the elasticity of the spring produces a direct effect in the restoring force U and, as is seen from equation (14), a proportional relative error in that part $C_X X$ of the total indication which is read by the deflection. The fraction of the full-scale indication which is read by the deflection (up or down scale from a central zero) need never exceed $\frac{1}{2\ D_m}$, where D_m is the total number of steps in the main dial. Hence, for an instrument with 25 dial steps the error from zero shift, etc., would be only one-fiftieth as great as in an ordinary instrument in which the same control springs were used. It may also be noted that, when used for calibrating other instruments, readings may usually be confined rather closely to a succession of nominal values which correspond to exact dial settings and hence involve only very small deflections.

The tendency for an instrument to be free from pivot friction is usually expressed in terms of the ratio τ/w of the full-scale torque τ to the weight w of the moving system, or, better, τ/w^p, where p is an exponent taken by various authors as 1.5 or 1.33. In the design of a composite-coil instrument there may be a slight gain in torque as compared with an ordinary instrument, because the requirement of uniformity of scale law over a wide range of deflection is less severe. On the other hand, the weight of the moving system is at least doubled because of the need for the d. c. moving coils. The quantitative study of these relations given below indicates that for the higher accuracy sought the use of a strip suspension is imperative. With such a construction, pivot friction is, of course, entirely eliminated, although at the expense of bulkiness in construction and of slightly increased indefiniteness in the position of the axis of the moving system.

Coming now to those limitations in accuracy which are usually less serious, we have first the possibility of changes in the operating con-

stant G as a result of distortion or relative displacement of the coils. In an ordinary electrodynamic instrument any such change in G will make a proportional error in the indication. In a composite-coil instrument such an effect on the null part of the indication can be produced only by a change in the ratio G_{13}/G_{24}. From the intermingled construction of both the fixed and the moving coils in this type of instrument it would seem highly probable that any change in this ratio would be very much smaller than the relative change produced in either G_{13} or in G_{24} separately by the same displacement or distortion. Of course, that fraction of the entire indication which is based on the deflection is directly affected by any change in G_{13} as in an ordinary instrument.

The principal effect of change in room temperature on the indication of electrodynamic instruments is twofold. An increase in temperature of 1° C. weakens the elastic constant of the control springs by about 0.04 per cent, and also increases the resistance of the copper (or aluminum) coils by about 0.4 per cent. The effects of temperature in expanding and distorting the instrument are usually negligible. If in an ordinary wattmeter the resistance of the entire potential circuit is made ten times that of the copper moving coil by the addition of resistors having low temperature coefficient, these two principal effects neutralize each other and the indications of the instrument are very little influenced by the ambient temperature. As shown in Appendix B, a similar situation exists in a composite-coil instrument, and it is possible to design the circuits so that the effect of the increased resistance of the a. c. potential circuit at high temperature tends to be balanced by the combined action of the increased resistance of the d. c. moving-coil circuit and the weakening of the control springs, at least if the Ayrton-shunt type of d. c. circuit is used.

The compensating action just described will be theoretically perfect only if the springs are at the same temperature as the copper windings of the moving coil. Any self-heating of these coils as a result of the currents flowing in them tends to upset this ideal condition. It will be noted, however, that the intermingled construction insures excellent opportunity for thermal equalization between the a. c. and d. c. moving-coil windings. It would therefore appear that these two windings would have substantially the same temperature even when the power dissipated in them is different. If this equality of temperature exists, the only error in the indication arises from the effect of temperature on the springs, and this affects only the deflection and not the null part of the indication. This gives a distinct advantage in cases where constructional difficulties have prevented the designer from giving a sufficiently small ratio of copper to manganin in the moving-coil circuits. The self-heating of the fixed coils, which is greater than that of the moving coils, produces no direct effect on the indication of the instrument, but tends somewhat to raise the temperature of the moving coils and springs.

The error arising from the self-inductance of the a. c. moving coil is substantially the same in a composite-coil instrument as in an ordinary one. If necessary, the correction for this error can be computed and applied. An alternative procedure, which might well be justified by the greater accuracy of the new instrument, is to connect a condenser of suitable value in parallel with a part of the series resistance R_p, and thus make the effective inductance of the potential

circuit zero. Self-inductance in the a. c. fixed coil and in the d. c. coils has no effect upon the indications.

Because of the intimate mingling of the a. c. and d. c. windings the mutual inductance between the individual pairs of coils is relatively large. The use of two sets of coils connected so that these mutual inductances are opposed serves to reduce M_{34} and M_{12} to small residuals comparable to M_{13} and M_{24}.

An exact analysis of the error produced by such inductive actions while possible, is very laborious. An approximate estimate can be found by directly computing the current induced in coils 2 and 4 by the a. c. currents normally flowing in coils 1 and 3. The direct coupling between 2 and 4 also causes the fraction $\frac{R_w}{R_2'}$ of the current induced in coil 4 to circulate in coil 2, and conversely. Each disturbing effect can be computed by multiplying each of these induced currents by the current in one of the a. c. coils and by the appropriate torque constant (G), with regard, where necessary, for any phase displacement between the interacting currents.

Thus in the experimental instrument the interaction constants G_{23} and G_{14} were found to be about 0.001 G_{13} and 0.01 G_{24}, respectively. The principal error was found to arise from the interaction of the current induced in coil 4 with that circulating in coil 2 as a result of the direct coupling between circuits 2 and 4. The error amounted to 0.025 per cent at full dial and fell off in proportion with decrease in the dial setting.

Secular changes in the resistance of the various circuits will, of course, introduce error into the indications in direct proportion as shown by equation (14) in much the same way as does a change in the series resistor of an ordinary wattmeter. Such changes are, however, usually very small in properly constructed manganin resistance coils and should not prove to be an appreciable limitation on the accuracy of the instrument.

In the composite-coil instrument a certain difficulty is encountered which has no very close analogue in the case of the ordinary wattmeter. This arises from the fact that the factor $\frac{G_{24}}{G_{13}}$ enters directly into the null part of the indication, and hence must be definite and constant to the full accuracy of the instrument. The intermingling of the coils, of course, tends very strongly to produce this desired condition, but it is always possible that the reaction, G_{24}, between the d. c. coils may vary with the position of the moving coil in a manner different from that of the reaction, G_{13}, between the a. c. coils. If this condition exists, the factor $\frac{G_{24}}{G_{13}}$ would depend upon the deflection X, and the correction of the readings for this effect, though possible, would be very cumbersome.

To a first (and fairly close) approximation the factor $\frac{G_{24}}{G_{13}}$ changes linearly with the rotation of the moving coils. Consequently a satisfactory device for compensating for this discrepancy can be obtained by using a pair of compensating coils D D placed as shown in the section on B–B in Figure 5 and connected in series with either of the fixed coils. It will be seen that when the moving coil is in its zero position it lies in the same plane as the compensating coils, and hence

experiences no torque from the current in them, because the mutual inductance between them is a maximum. However, as the moving coil turns to either side from this mid-position the torque constant between it and the compensating coils which is given by

$$G_{2c}=\frac{dM_{2c}}{d\alpha}\times 10^{7}$$

ceases to be zero and introduces a small torque which is opposite in direction on the two sides of the mid-position. By adjusting the distance of the compensating coils from the moving coil, or, more conveniently, by adjusting the fraction of the d. c. current flowing in them by a suitable shunting resistance, the compensating torque can be readily adjusted to have any desired rate of increase with the deflection of the moving coil.

In an instrument of the suspension type with a taut suspension, a change in level will, in general, produce three effects—(*a*) a shift of zero, (*b*) a change in the apparent stiffness of the suspension, and (*c*) a change in the torque constant $\frac{G_{24}}{G_{13}}$. If the instrument is perfectly balanced statically (that is, if the center of gravity lies in the line joining the points at which the suspensions are attached to the moving system), effects (*a*) and (*b*) will vanish. It is therefore quite desirable to provide a "cross" or similar device on which balancing weights can be adjusted to approximate this condition. If a slight lack of balance exists in a composite-coil instrument, the adjustment of the instrument constant C_s will eliminate the effect (*b*) so long as the level remains the same as that at which the mirror adjustment was made. Effect (*a*) is, of course, eliminated by setting the zero, with no current flowing, at the beginning of each set of measurements. Because of the composite-coil construction the change in the ratio G_{24}/G_{13} will be decidedly smaller than the change likely to occur in G_{13} of an ordinary wattmeter of the suspension type. (In the experimental composite-coil ammeter the effect of change of level was found to be less than 0.03 per cent for a tilt of 1° in any direction. It thus appears that while a level should be attached to any such instrument, no extreme accuracy is required in its adjustment.)

The close juxtaposition of the a. c. and d. c. windings, of course, introduces a certain capacitance between these circuits. In the case of the instrument described below these capacitances were 0.05 and 0.002 μf for the fixed and moving coils, respectively. It will be evident that at 60 cycles the currents flowing in the condensers thus formed will be entirely negligible, although this may not be the case at materially higher frequencies.

As in any other problem in engineering design, the advantage of high accuracy, which is inherent in the composite-coil instrument, is obtainable only by the deliberate sacrifice of certain other desirable features in construction or operation. In the present case the cost of the accuracy may be reckoned as including the constructional difficulties involved in the pair of duplicate elements, the multiplicity of resistance coils, and the complexity of the circuits. The composite-coil ammeter described below contains 31 resistors adjusted to the full accuracy of the instrument and 45 others which require only approximate adjustment. This assemblage might be expected to be about equivalent in cost to a potentiometer.

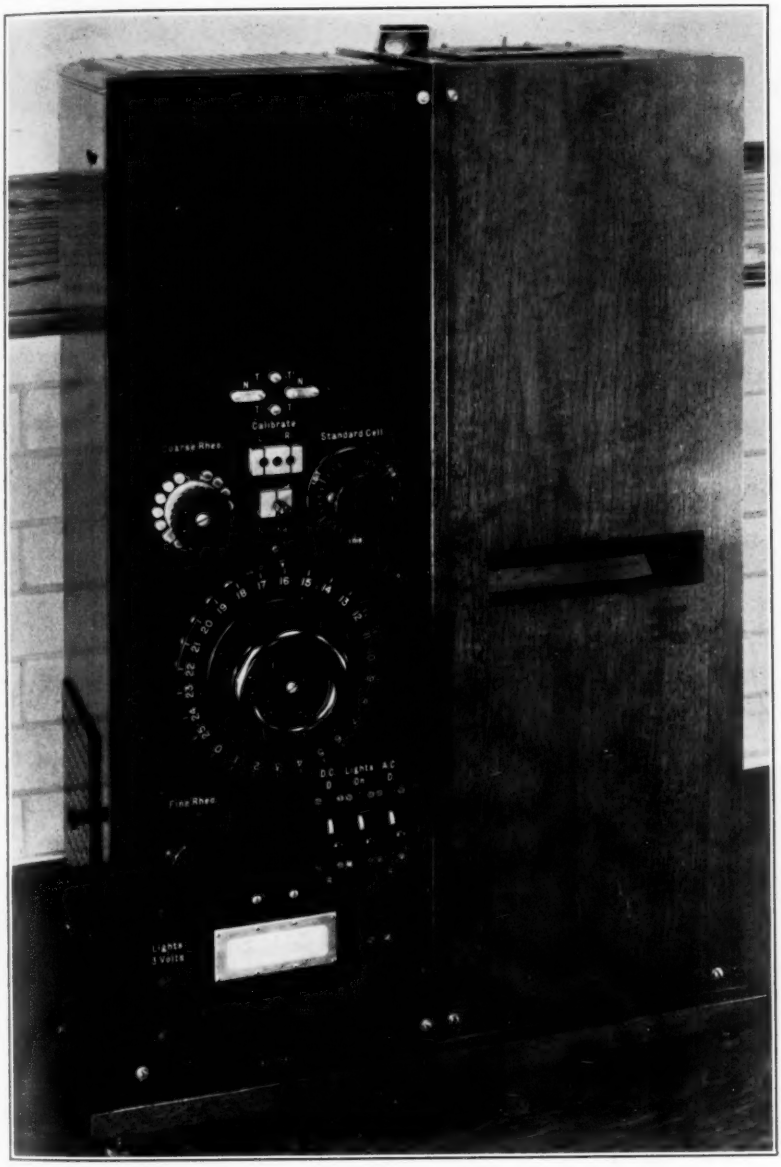

FIGURE 2.—*Front view of experimental composite-coil ammeter*

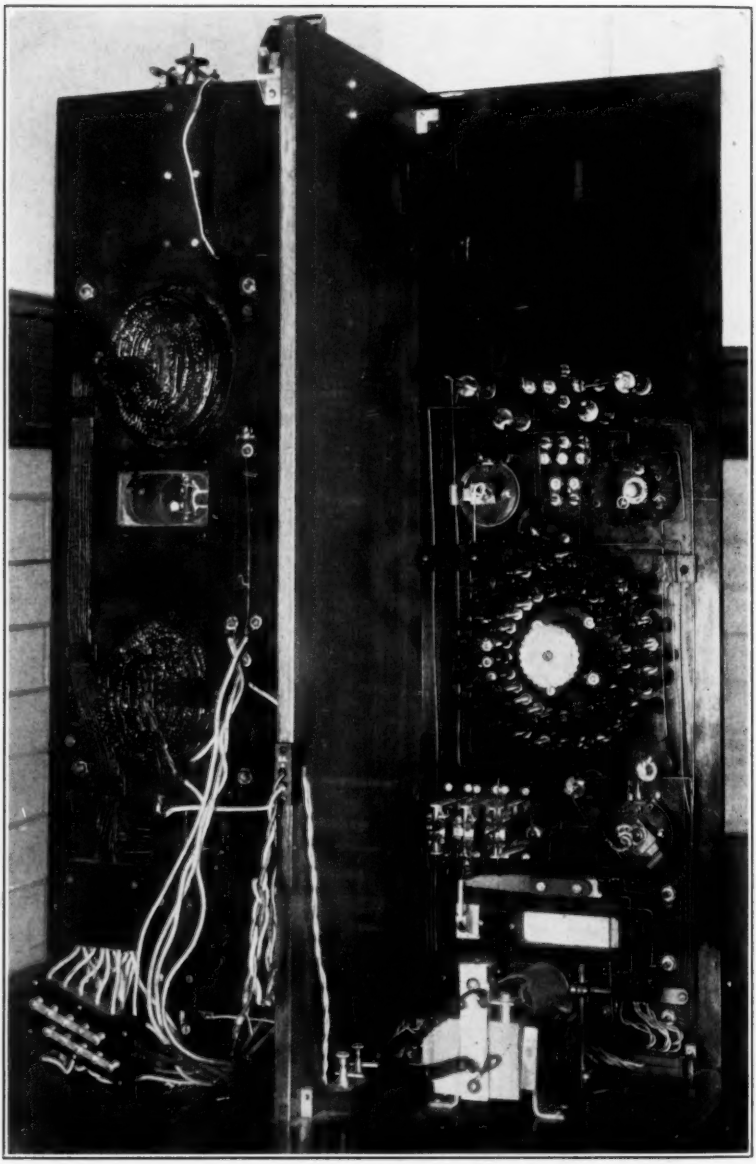

FIGURE 3.—*Experimental composite-coil ammeter. View from rear with protecting wooden covers removed*

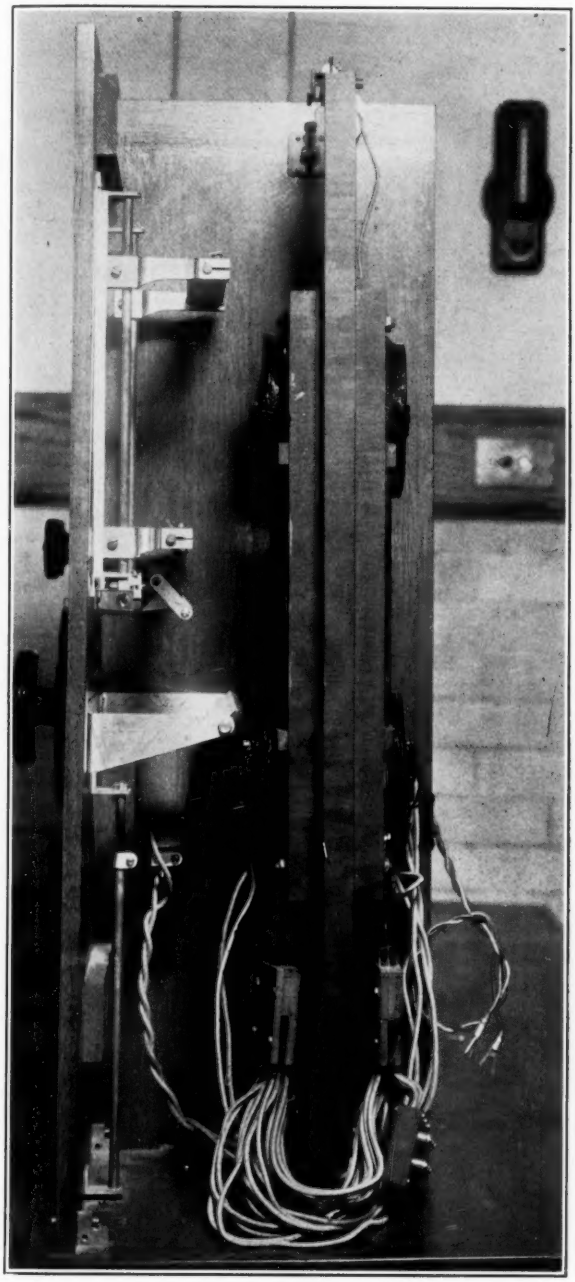

FIGURE 4.—*Experimental composite-coil ammeter. Side view showing instrument proper and optical system*

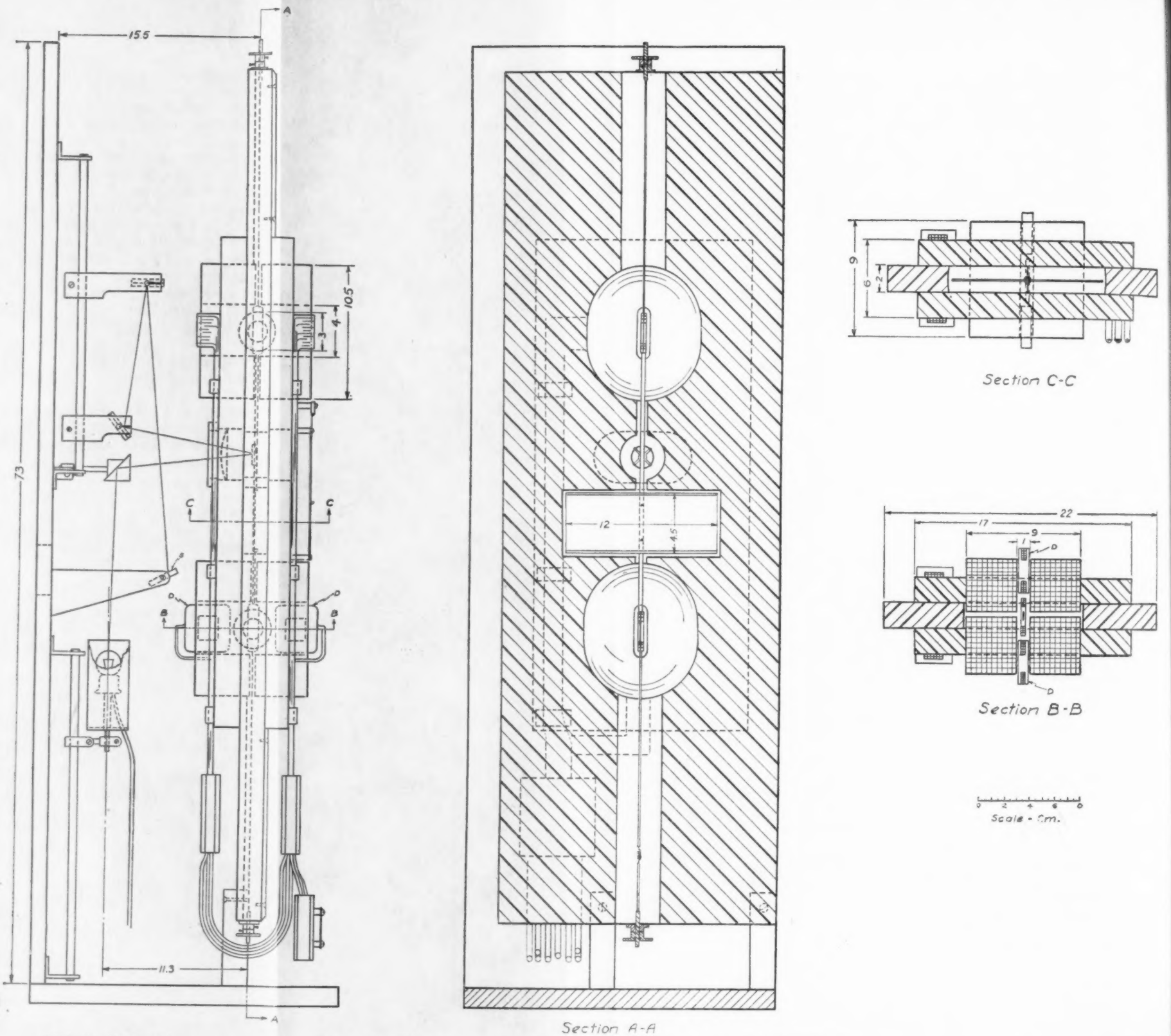

94173—32. (Face p 229.)

FIGURE 5.—*Side view and typical sections of experimental composite-coil ammeter*

In inconvenience of operation there must be charged up a number of items. The standard-cell circuit must be balanced even more frequently than in the case of a potentiometer, both because the circuit resistance may change with changes in dial setting, if the compensating resistors are not in exact adjustment, and also because the drain of about 1 ampere from the storage battery supplying the d. c. circuits will cause its voltage to drop off more rapidly than would the much smaller corresponding current of a potentiometer. Thus in testing a 3-phase generator, where two or three such instruments would be used for power measurement, it would probably be found convenient to connect the d. c. circuits of all the instruments in series and have one observer hold the current in this circuit at the correct value while the other observers read the instruments at regular intervals, reversing the d. c. or the a. c. circuits after each reading.

Pairs of readings or, better still, sets of four readings should be taken to eliminate the effects of such a. c. and d. c. magnetic fields as may be present.

The burdens which the a. c. circuits impose on the instrument transformers are somewhat larger than for an ordinary wattmeter, but are not excessive.

Economy of space and portability have also been sacrificed to a considerable extent in the quest for accuracy. The first experimental instrument, in which to be sure no attempt was made to economize on space and weight, occupies about 3½ cubic feet and weighs 75 pounds. The presence of the suspended coil also invites breakage from rough handling in transportation. It is probable, however, that a suitable coil clamp can eliminate this risk, and that attention to considerations of space and weight will yield a design which is as easily moved as a potentiometer or oscillograph. The 12 or 18 volt battery needed for supplying the d. c. circuit and lights must also be considered.

IV. DESCRIPTION OF EXPERIMENTAL INSTRUMENT

In order to determine the practicability of an instrument of the composite-coil type and to obtain experimental values for design constants to be used in the theoretical discussions in this paper, an experimental instrument was built in 1928–29 in the instrument shop of the Bureau of Standards. The mechanical construction was done by J. M. S. Kaufman and E. A. Tibbals. The winding and painstaking adjustment of the various resistance coils was done by Miss N. L. Forman.

This instrument was designed as a 5-ampere ammeter, rather than as a wattmeter, primarily because such an instrument was the more urgently needed in the instrument-testing laboratory, but also because in an ammeter the errors from mutual-inductance effects are greater, and a more crucial test of the composite-coil type is obtained.

Figures 2, 3, and 4 show the general appearance of the complete instrument, the protecting wooden covers being removed from the rear in Figures 3 and 4. Figure 5 shows the instrument proper in elevation and in cross section, while Figure 6 is a representative diagram of the electrical connections used. The essential dimensions and other data will be found in Table 2 at the end of the paper.

The instrument is divided into two distinct compartments by a vertical partition extending from front to back and serving as a mechanical support for the other parts. To the right of this partition (as seen in fig. 2) is the electrodynamic instrument proper,

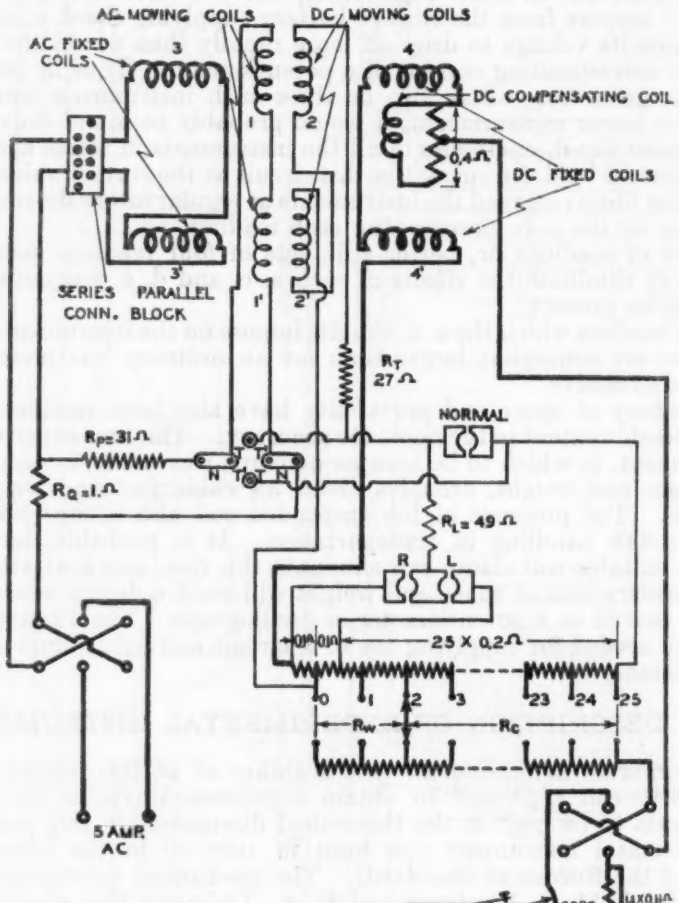

FIGURE 6.—*Schematic diagram of connections of experimental composite-coil ammeter*

including the coils and the optical system for indicating the position of the moving mirror. To the left of the partition is the bakelite panel which supports the various resistors, switches, dial rheostats, etc. The d. c. galvanometer used in setting the current is fastened to the bottom of the instrument on this side. The spot of light re-

flected from the mirror of this galvanometer is viewed on the ground-glass scale inserted in the bakelite panel.

As is indicated in Figure 5, the electrodynamic instrument proper is formed of three slabs of bakelite, which are clamped together at the corners by four brass studs not shown in the figure. The large central slab, which is anchored to the base and to the partition, supports the other two slabs and carries the moving system. It is pierced with apertures for the coils, the mirror, and the damping vane, and slots for accommodating the spindle and suspension strips are milled from the front three-fourths of the way through the slab. The front and the rear slabs are pierced with holes for the beam of light and for the four fixed coils, two of which are firmly anchored in each of these slabs by being embedded in plaster of Paris. The axial length of each fixed coil is considerably greater than the thickness of the slabs, and the coils are arranged to project inward into the larger holes in the center slab so as to nearly meet, leaving only a small clearance for the spindle of the moving system. The coils also project somewhat on the outer side of the slabs, thus affording more cooling surface.

Each of the four fixed coils was wound with No. 15 A. W. G. (1.45 mm) silk-enameled wire. Ten such wires were wound side by side on the form and transposed at the end of each layer so as to obtain as thorough a mixing as possible. Each of the 10 wires makes 50 turns in each coil. Corresponding wires of the upper and lower coils on each slab were connected in series, with due regard to polarity, so as to give 20 windings of 100 turns each, half of each winding being on the upper and half on the lower element. The coils on the two slabs were then connected by flexible leads so as to give 10 windings each having 200 turns equally distributed in the upper and lower, front and back coils. Five of these 200-turn windings were then permanently connected in series to constitute the main fixed d. c. winding of 1,000 turns. The terminals of the remaining five windings were brought to a terminal board provided with gold-plated studs and links, whereby the five can be connected either in series or in parallel. The parallel connection gives a 5-ampere winding of 200 turns for normal a. c. measurements. The series connection gives a 1,000-turn winding which is used with direct current in the initial calibration of the instrument and in the checking of its constancy.

The choice of which of the 40 original windings shall be assigned to a given group (a. c. or d. c.) may be based on the relative electrodynamic effectiveness of the two windings in either of two ways—either so that the average torque constant shall be very closely the same, or so that the average rate of change of torque constant with change in the position of the moving coil shall be very closely the same for the two groups. However, such a selection, involving many crossovers, would lead to a very complex and unsightly condition at the junction points; and it is probably always preferable to join the winding in a systematic fashion, allowing for any residual differences in torque constant or in scale law by a suitable adjustment of the resistances and the compensating coils. As the coils in the d. c. group should produce magnetic fields in opposite directions in the upper and lower elements, while those in the a. c. group should produce fields in the same direction, the decision as to the group to

which a given winding is to be assigned must be made at the time the windings in the upper and the lower elements of a slab are joined in series.

The compensating coils (*DD*, fig 5), which serve to offset any difference in the respective scale laws of the a. c. and d. c. windings, are located inside the axial apertures of the two fixed coils of the lower element. Each coil consists of 10 turns of No. 15 wire wound into an approximately square coil of rectangular cross section, the outside dimensions of the coil being 3.5 by 3.5 cm. They are cemented to the fixed coils with sealing wax, their axes being horizontal and perpendicular to that of those coils. The distance between their adjacent faces is enough to avoid interference with the motion of the moving coil.

The moving coils are mounted at the ends of a bakelite spindle 21 cm long and 0.3 cm in diameter. Each coil consists of two windings each having 75 turns of No. 28 (0.32 mm) silk-enamel wire. The two wires are wound side by side to form a coil of 15 layers with 10 wires (5 turns of each) per layer. Each coil has an outside diameter of about 3.2 cm and a weight of 11.0 g. One winding of one coil is joined in series with one winding of the other coil with polarity such that both produce magnetic field in the same direction. These constitute the a. c. moving coil, and their terminals are brought out through two spiral springs to a pair of terminal blocks fastened on the central slab of the instrument. The other two windings are also joined in series but with opposite relative polarity and constitute the d. c. winding. Their terminals lead through the suspension strips to the top and bottom terminal blocks.

Between the two moving coils there is fastened to the bakelite spindle a thin silvered mirror, about 2 cm in diameter, and a damping vane, of thin sheet aluminum, 4.5 cm high and 12 cm wide. This vane is stiffened by being rolled up along the top and bottom edges to form a tiny bead. The vane swings, with a small clearance, in a rectangular opening in the central slab. The front and back slabs form the walls of the damping box and carry small partitions which extend inward nearly to the central bakelite spindle. Adjustment of the clearance between these partitions and the spindle affords a convenient means for adjusting the damping of the instrument. The suspensions as well as the spiral springs are of "phonoelectric"[6] strip, about 17 cm long and 0.056 by 0.006 cm in cross section. This material has a resistivity of only 3.4×10^{-6} ohm-cm at 20° C. and has rather good elastic properties. The lower end of the lower suspension is anchored to a short helical brass spring which can be stretched to exert a tension of perhaps 50 or 100 g, thus serving to make the location of the moving coil fairly definite.

The position of the moving coil is indicated by a spot of light reflected from the mirror on the spindle and focused on the scale. In spite of the lower precision of reading of such a spot as compared with a knife-edge pointer, it was felt that this arrangement was to be preferred to a pointer principally because the effective pointer length Z of equation (17) could be readily adjusted to correspond to any change in the spring stiffness U, such as might result from repairs to a broken suspension. It also greatly reduces the moment of inertia. All parts of the optical system, except the lens and the moving mirror,

[6] This is a silicon-copper alloy developed for use in trolley wire.

are mounted together on the mahogany board which forms the front of this compartment of the instrument, so that this compartment can be completely opened without permanently disturbing the optical adjustments.

As shown in Figure 5, the light passing upward from a 4-volt, 0.5-ampere straight-filament lamp is reflected almost horizontally by a 90° prism having faces 2.5 cm square into the instrument through the plano-convex lens which forms its front window. After being reflected by the moving mirror the light again traverses the lens, strikes a fixed mirror (10 by 2.5 cm), passes upward to a second mirror, horizontal and fixed, and thence to the scale. The scale is set at a slight angle with the horizontal so that it can be viewed comfortably through a horizontal slot about 4 cm high extending across nearly the full width of the wooden panel. As the scale is set back about 9 cm from the panel it is so shaded that the image of the lamp filament and the scale markings are both comfortably visible. The use of the two fixed mirrors gives, in a fairly compact space, a light path of considerable length, adjustable from 25 to 60 cm (thus varying the length (Z) of the effective pointer from 50 to 120 cm). Focusing is done by sliding the lamp mounting along its supporting rod. The opening in the rear bakelite slab opposite the mirror is closed by a plane glass window which permits of inspection of the spiral springs and also facilitates the initial adjustment of the optical system.

The bakelite control panel (fig. 2) carries the main dial, coarse and fine rheostat dials for controlling the d. c. current, and a standard-cell dial by which the resistance across which the cell electromotive force is balanced may be adjusted so as to have in ohms a value numerically equal to the electromotive force of the cell in volts. It also carries three telephone-type switches, which serve, respectively, for reversing the d. c. current, for connecting the galvanometer and instrument lights to their "4-volt" binding posts, and for reversing the a. c. current. The last-mentioned switch is so arranged that when it is in mid-position the "5-ampere a. c." binding posts are short-circuited, thus avoiding risk of injury to any current transformer which may be supplying the alternating-current circuit. A key is also mounted on the panel to close the circuit of the d. c. galvanometer and standard cell. On the back of the panel are mounted the various resistance coils shown in Figure 6, including the resistor R_q which forms the a. c. shunt. This has a resistance of 1 ohm and, being made of manganin strips 0.023 cm thick, has a cooling surface of about 1,500 cm^2. It is placed at the top of the panel just under a grating, so that the heat resulting from the 25 watts which is dissipated in the resistor at full current can be carried out of the instrument by a rising air current without heating other parts of the circuit. This shunt forms the major part of the burden which this instrument imposes on a current transformer, namely, a resistance of 1.1 ohms and an inductance of 370 microhenries.

The experimental instrument is provided with two self-checking features which will probably be found worthy of inclusion in a commercial design.

The first of these is intended to test the accuracy of the constant C_X which fixes the deflection part of the indication. This is accomplished by a tapered plug which normally is inserted in the hole

marked "Normal" in Figure 6 and connects the d. c. moving-coil circuit to span 25 units on the main dial. If this plug is removed from "normal" and inserted at L or R the moving-coil circuit will then span only 0.5 unit, and with the a. c. circuits open the insertion of the plug should produce a deflection, due to the direct current only, of 50 divisions to the left or to the right, respectively. In order that the factor $R_D+R_T+R_2$ may still have its normal value of 35 ohms, an additional resistance, R_L, of 4.9 ohms is so connected as to be in series with the moving coil when the plug is in L or R.

The second calibrating scheme provides for a determination of the ratio G_{24}/G_{13} which enters the constant C_D of equation (15). The terminals of the a. c. fixed coils on the connection block allow of connecting the five individual windings in series, thus giving the a. c. fixed coil the same number of turns as the d. c. fixed coils, and multiplying the constant G_{13} by exactly 5. The a. c. binding posts can then be connected in series with the d. c. posts so that the same direct current (I_4) will pass through both sets of fixed coils. Provision is also made by which the a. c. moving coil may be disconnected from the potential terminals of the a. c. shunt (by removing the pair of links from NN, fig. 6) and instead connected in series with the d. c. moving coil (by placing the links at TT, fig. 6, and removing the plug from the hole marked "Normal"). Changing the links from TT to $T'T'$ reverses the a. c. moving coil with respect to the d. c. moving coil, while both moving coils still form a shunt circuit in parallel with the main dial.

With this arrangement it is evident that the current I_2 in both sets of moving coils is given by

$$I_2=\frac{R_s}{R_1+R_2+R_T+R_D}I_4 \tag{18}$$

where I_4 is the current in the fixed coils.

Hence with the links connected at TT we have

$$\tau=I_2\,I_4\,(5\,G_{13}-G_{24}+G_{14}+5\,G_{23})=\frac{UX}{Z} \tag{19}$$

while with the links at $T'T'$, which reverses coil 1 with respect to coil 2, and with the a. c. fixed coil reversing switch in the opposite position, we have for the same currents

$$\tau'=I_2\,I_4\,(5\,G_{13}-G_{24}-G_{14}-5\,G_{23})=\frac{UX'}{Z} \tag{20}$$

whence

$$\frac{\tau+\tau'}{2}=I_2\,I_4\,(5\,G_{13}-G_{24})=\frac{(X+X')}{2}\frac{U}{Z} \tag{21}$$

or, in terms of the observed deflections X and X'

$$5\,G_{13}-G_{24}=\frac{U\,(X+X')}{2\,I_2\,I_4\,Z} \tag{22}$$

For an ammeter the deflection constant is given by

$$C_X=\frac{(R_1+R_p+R_g)\,U}{G_{13}R_gZ} \tag{23}$$

Using this equation to eliminate U and Z from equation (22) and using equation (18) to eliminate I_2 gives, on rearranging the terms,

$$\frac{G_{24}}{G_{13}} = 5\left[1 - \frac{C_X R_q (R_1 + R_2 + R_T + R_D)}{10\, I_4^2 R_D (R_1 + R_p + R_q)} (X + X')\right] \tag{24}$$

Since G_{24} and $5\ G_{13}$ are in practice very nearly equal, the second term in equation (24) is very small and can be read with sufficient accuracy from the deflections X and X', provided the current I_4 used in the calibration has at least the normal value, 1 ampere.

In practice it is desirable to take a number of deflections X and X', each of these being the mean of a pair of readings between which the current is reversed, with the instrument zero shifted to different parts of the scale. The observed mean deflections can then be plotted as ordinates against the mean deflected positions as abscissas. The factor $X + X'$ can then be computed from ordinates read from both curves for the same abscissa, and used in equation (24) to give the ratio G_{24}/G_{13} for the particular coil position corresponding to that abscissa. Any change in this ratio with coil position indicates the need for adjustment of the compensating coils, while the mean value of the ratio is to be taken as a basis in finally adjusting R_p to fit C_D to its correct value.

V. EXPERIMENTAL RESULTS WITH COMPOSITE-COIL AMMETER

The indications of this experimental ammeter when used on direct current were compared with those of a carefully calibrated potentiometer, and were found to agree to better than 0.01 per cent when proper allowance was made for the errors in adjustment of the resistance coils of the main dial. In such a test it is, of course, necessary to take the mean of the four readings observed with the current flowing in each direction in both the a. c. and d. c. coils. A typical calibration at the 11 cardinal scale points with the dial set at 25 is given in Table 1.

TABLE 1

Setting of composite-coil ammeter	Current by ammeter corrected for resistance adjustments	Current by potentiometer	Error
Amperes[3]	*Amperes*	*Amperes*	*Amperes*
24.500	4.9432	4.9437	−0.0005
24.600	4.9532	4.9537	−.0005
24.700	4.9632	4.9635	−.0003
24.800	4.9732	4.9741	−.0009
24.900	4.9832	4.9835	−.0003
25.000	4.9932	4.9932	.0000
25.100	5.0032	5.0039	−.0007
25.200	5.0132	5.0132	.0000
25.300	5.0232	5.0232	.0000
25.400	5.0332	5.0330	+.0002
25.500	5.0432	5.0430	+.0002
Average			±.0003
Per cent			±0.006

Comparisons were also made between this instrument and an electrodynamic wattmeter of the suspension type which is regularly used by the Bureau of Standards as a transfer instrument from direct

to alternating current. For the purpose of this test the composite-coil instrument was made into a wattmeter by disconnecting the a. c. shunt R_s and using a noninductive resistance of 714 ohms in series with the a. c. moving coils. Tests were first made at 110 volts, 5 amperes, 60 cycles, with the current lagging the voltage by about 90°. In these experiments the angle of lag was adjusted until the composite-coil wattmeter read zero; the standard instrument then read merely the power which was required to offset the spurious torques produced by the various inductive effects. When both the fixed and the moving d. c. circuits were open the standard instrument showed a negative deflection corresponding to 0.02_2 per cent of the volt amperes. The effect to be expected from the self-inductance of the a. c. moving-coil circuit was a phase displacement of 0.5 minute, which would correspond to a deflection of 0.01_6 per cent of the volt amperes. This agrees with the observed value to within 0.00_8 per cent and even this slight difference may, perhaps, be in part accounted for by the mutual inductance M_{13}. It thus appears that the use of a considerable volume of copper in the thick fixed coils has not introduced any appreciable eddy current error.

When the main dial was set at zero, the closing of the d. c. moving-coil circuit while the d. c. fixed-coil circuit was open produced less than 0.01 per cent change. Conversely, closing the d. c. fixed-coil circuit, the usual storage battery being omitted, changed the torque by an amount corresponding to 0.01_2 per cent of the volt amperes. This change (observed with the d. c. moving-coil circuit open) is evidently the result of the reaction between the current in the a. c. moving-coil circuit and that induced in the d. c. fixed-coil circuit (this induction coming mainly from the a. c. fixed coil). The magnitude of this effect computed from the expression $\frac{G_{14}\omega M_{34}R_4}{G_{13}(R'_4{}^2+\omega^2L^2_4)}$ is 0.01_3 per cent.

When both the moving-coil and the fixed-coil d. c. circuits were closed, the main dial still being on zero, a further slight change (-0.00_8 per cent) was noted, and presumably is the result of the interaction between the currents separately induced in the two circuits. Changing the main dial setting to 25 introduces a coupling resistance of 5 ohms in common with both circuits and materially increases the a. c. current I_2' circulating in the d. c. moving-coil circuit, by shunting ing into that circuit a fraction $\frac{R_w}{R_2+R_w}$ of the induced current I_4'. The effect of this change expressed as a fraction of the applied volt amperes is given approximately by the expression $\frac{G_{24}\omega^2M^2_{24}R_w(R_1+R_p)I_3}{G_{13}Z^2_4R'_2E_1}$ and for the experimental instrument has the computed value of 0.01_8 per cent. The observed effect was found to be 0.02_9 per cent. This effect is always a tendency for the composite-coil instrument to deflect down scale with a torque proportional to the square of the a. c. fixed-coil current and independent of the voltage or power factor. This is the preponderating inductive effect in the case of the experimental ammeter and will probably be larger than the others in other instruments.

Further tests were made to determine the effect of possible uncompensated mutual inductance between the various coils. While operating as a wattmeter at 60 cycles, 115 volts, 4 amperes it was

found that the insertion of a mutual inductance between the a. c. and the d. c. moving-coil circuits (that is, M_{12}) as great as 2.5 millihenries produced a change of 0.03_5 per cent at unity power factor and 0.01_2 per cent at zero power factor. The effects computed from the circuit constants are 0.03_2 and 0.01_2 per cent, respectively. The insertion of 0.25 millihenry between the a. c. and the d. c. fixed-coil circuits (that is, M_{34}) produced an effect which amounted to 0.11_5 per cent (the calculated effect is 0.14_8 per cent). As the values of mutual inductance thus artificially inserted are much larger than those likely to exist as a result of slight imperfections in the balance of the coils, it seems evident that these latter inductive effects do not constitute a serious source of error.

In the course of these measurements pairs of repeated settings of the composite-coil ammeter were frequently made at intervals of several minutes under supposedly identical conditions. An examination of a considerable number of data sheets shows that the difference between two such settings, averaged without regard to sign, is less than 0.005 per cent, which is equivalent to 0.1 division. The error introduced by a single reading would, therefore, not be expected to greatly exceed this value.

The data quoted in the foregoing paragraphs indicates only the initial accuracy of the instrument, and it is of course the sustained accuracy after continued handling under service conditions which gives the true measure of instrument quality. However, in view of the fact that conditions in a standardizing laboratory like those of the Bureau of Standards are materially different from the conditions to which an instrument would be subjected in test work in generating and substations, and also in view of the probably greater ruggedness which could be built into an actual composite-coil instrument by an experienced instrument manufacturer, it was felt that little would be gained by holding up the present descriptive paper until a report could be made of the effect of some years of use in the laboratory.

The following experiment was tried to give an indication of the reliability of the instrument constants. The experimental ammeter was set up, leveled, and checked against a Wolff 5-dial potentiometer, using direct current and taking the mean of the four readings obtained with the four possible combinations of directions of current flow through the coils. The mean current required for full deflection was 4.993_4 amperes. The instrument was then lifted onto a truck; wheeled over a threshold into another room; certain resistances in it were measured and it was then moved back and again set up in the original location. The current for full deflection was then found to be 4.993_5 amperes. The rear fixed coils and the bakelite slab supporting them were removed, exposing the damping vane and moving coils for inspection. After replacing the coils, the current was 4.993_7 amperes. The backplate carrying the coils was then moved back about 6 mm and clamped against some temporary spacers. This had the effect of reducing the deflection constant C_X by about 10 per cent, because of the reduction in the torque constant G_{13}. The current for full deflection was then found to be 4.986_7 amperes. On restoring normal conditions, the current returned to 4.993_8 amperes. It thus appears

that the change in the ratio $\frac{G_{24}}{G_{13}}$ was 0.14 per cent or only one-seventieth of the change in G_{24} or in G_{13} separately.

VI. FUNDAMENTAL CONSIDERATIONS IN DESIGN

The basis for the design of a composite-coil instrument is, of course, identical with that of an electrodynamic instrument of the ordinary type. Because of the need for pushing certain operating conditions to the limit, it may not be amiss to consider first the basic factors which determine the design of an ordinary wattmeter. The designer must consider in any case the following factors: (1) Absolute size, (2) shape (or relative size) of the major parts, (3) the numbers of turns required to make the windings suitable for the ranges desired, and (4) mechanical details of construction.

The basic relation for the torque τ produced by an electrodynamic instrument when currents I_m and I_f are flowing in the moving and the fixed coils respectively is

$$\tau = I_f I_m \cos \phi \frac{d M_{fm}}{d\alpha} \times 10^7 \tag{25}$$

when ϕ is the phase angle between the currents and M_{fm} is the mutual inductance between the coils, while α is the angle through which the moving coil is deflected from its zero position.

If the numbers of turns N_f and N_m in the two coils are varied without changing the size or arrangement of the space filled by the windings, the mutual inductance M_{fm} and consequently its derivative will vary in proportion to the product $N_f N_m$, the constant of proportionality g_{fm} being defined by the equation

$$g_{fm} = \frac{1}{N_f N_m} \cdot \frac{dM_{fm}}{d\alpha} \times 10^7 \tag{26}$$

Though g_{fm} is independent of the number of turns in either coil it is a function of both the size and the shape of the coils. Inserting equation (26) in (25) gives

$$\tau = g_{fm} \cos \phi \cdot I_f N_f I_m N_m \tag{27}$$

This equation indicates clearly that the torque acting (for any particular phase angle) is proportional to the product of the ampere-turns of the two coils and hence shows that a proper choice of the turns will fit the instrument for almost any ranges of current. Decision as to the number of turns in the coil may, therefore, be postponed until the design has been completed on a basis of ampere turns.

The principal limitations met in an attempt to obtain large torque in such a system are the effects of the heating of the windings by their respective currents. To express this heating quantitatively we may write

$$P_f = I_f^2 R_f = \frac{I_f^2 L_f}{T_f} \tag{28}$$

and

$$P_m = I_m^2 R_m = \frac{I_m^2 L_m}{T_m} \tag{29}$$

where P_f, R_f, L_f, and T_f are, respectively, the rate of heat development in, and the resistance, inductance, and time constant of the fixed coil, while the corresponding letters with subscript m designate the corresponding values for the moving coil. We may also introduce a constant k_{fm} which indicates in the usual way the closeness of the inductive coupling between the two coils. This coefficient of coupling is defined by the equation

$$k_{fm} = \frac{M_{fm}}{\sqrt{L_f L_m}} \tag{30}$$

Inserting these relations into equation (25) gives

$$\tau = \cos\phi \sqrt{P_f P_m T_f T_m}\, \frac{d}{d\alpha} k_{fm} \times 10^7 \tag{31}$$

In this form of the equation, the numbers of turns in the windings do not appear explicitly, and the absolute size of the instrument affects only the four factors under the radical sign, the last factor $\frac{d}{d\alpha} k_{fm}$ depending only on the shape of the instrument and not on its size.

To visualize the effect of the absolute size of an instrument upon its sensitivity we may consider two geometrically similar instruments A and B, each linear dimension of the various parts of B being m times the corresponding dimension of A. As is well known the two time constants T_f and T_m of B will each be m^2 times as great as those of A. Also, the principal obstacle to the dissipation of heat from an instrument coil lies at the surface where the heat passes from the solid material to the surrounding air, consequently the power losses, P_f and P_m, which can be dissipated by the coils of B will, for equal temperature rise, be proportional to the area of its cooling surfaces and hence m^2 times those of A. Since k_{fm} and its derivative and also $\cos\phi$ are the same for both instruments it follows that for the same self-heating instrument B will develop m^4 times as much torque as A.

The moment of inertia of the moving system of B will, however, be m^5 times as great as that of A because its mass is m^3 and its radius of gyration is m times as great. Therefore, if the control springs of the two instruments are so constructed as to make the periods of the instruments equal, the stiffness of B will have to be m^5 times that of A and the angular deflection produced by full-scale torque will be only $1/m$ times that of A. If the pointer length of B is made m times that of A the linear indication produced by full-scale torque will be equal in the two instruments.

If we consider the quality of the instruments as regards error from pivot friction, and take as a criterion the ratio of torque to weight,[7] then that of instrument B would be m times that of A. However, if the criterion taken is that suggested by Keinath [8] (viz, torque divided by $\sqrt[3/2]{\text{weight}}$) instrument B would have a figure of merit only $m^{-1/2}$ as great as A, while for Fichter's [9] criterion using the 4/3 power of the weight, both A and B would have equal merit. It may, there-

[7] F. Janus, E. T. Z., vol. 26, p. 560, 1905.
[8] G. Keinath, Die Technik electrischer Messgeräte, 3d ed., vol. I, p. 27.
[9] Fichter, Rev. Gen. de l'Electricité, vol. 15, p. 1042; 1924.

fore, be concluded that no material gain in performance as regards either sensitivity at a fixed period or freedom from friction errors, can be obtained by even a radical change in the size of the coils of a wattmeter of constant proportions.

An increase in the size of the fixed coil alone, however, increases both P_f and T_f and does not require any change in the controlling springs to maintain the desired period. Consequently, such a modification of the usual design would seem to give promise of increased sensitivity, albeit at the cost of total weight, and of power consumption in the fixed coils.

As additional turns are added to the fixed coils, they must be placed at a greater and greater distance from the moving coil and are hence less effective in producing torque. This fact is shown in mathematical form by a decrease in the factor k_{fm} and in its derivative. This decrease would set an ultimate limit to the sensitivity which could be obtained. Still another limiting factor is the lack of perfect heat transmission through the thickness of the coil to the outer surface where it is taken up by the ambient air. This tends to make the permissible value of P_f increase at a less rapid rate than does the square of the linear dimensions of the coil.

In a composite-coil instrument there is less need for providing a large range of angular motion of the moving coil, since the deflections serve only to bridge the steps of the main dial. This is particularly true if the coil position is indicated by a beam of light instead of a pointer. Consequently it becomes possible to shape the opening of the fixed coil so that its width is considerably less than its height parallel to the axis of rotation. This has the effect of bringing the fixed coil closer to the moving coil and thus increasing the factor $\frac{dk_{fm}}{d\alpha}$. In a preliminary experiment it was found that the substitution of such a flattened fixed coil in an ordinary wattmeter movement increased the factor $\frac{dk_{fm}}{d\alpha}$ from the value 0.38 to 0.46. In this case the flattened coil had about three times the volume of the original circular coil and about the same time constant. The width of the opening permitted the moving coil to turn 30° in either direction from its mid-position. At the extreme positions the value of $\frac{dk_{fm}}{d\alpha}$ was only 4 per cent less than at the center. The possibility of increasing the torque by such a modification of the shape of the fixed coil is, however, rather limited. If the factor $\frac{dk_{fm}}{d\alpha}$ does have a large and fairly constant value from the mid-position, where $k_{fm}=0$, to the extreme deflected position α_m, the value of k_{fm} at this extreme position is $\alpha_m \frac{dk_{fm}}{d\alpha}$. Now k_{fm} can never exceed unity and, consequently, $\frac{dk_{fm}}{d\alpha}$ can not exceed $1/\alpha_m$. Although $1/\alpha_m$ may be fairly large all the electrodynamic instruments analyzed by the author have shown values of $\frac{dk_{fm}}{d\alpha}$ less than the value unity which corresponds to the case in which the fixed coil produces a uniform magnetic field.

To justify the complication of its operation a composite-coil instrument must have a precision at least 10 times that of an ordinary wattmeter. Since, however, only one-half of the working material of each coil is available for producing up-scale torque, the net effectiveness is only one-fourth of that of the simple instrument which would be formed by connecting its a. c. and d. c. coils in series. The design must, therefore, be such as would yield a simple instrument of 40 times the usual sensitivity.

The flattening of the fixed coil may, perhaps, give a factor of 1.2. The increase in size of the fixed coil, in the case of the experimental instrument described in Section IV, yields a net gain of 2.4 and a further factor of 1.2 might have been obtained by forcing the fixed coils to a higher operating temperature. These increases in torque when combined may give a factor of 3.5, still leaving a factor of 12 to be sought elsewhere.

The obvious ways to gain sensitivity are by reducing the stiffness U of the control springs or by increasing the effective length Z of the pointer. If the entire step were covered by a decrease in U, the period would be increased by $\sqrt{12}$ (that is, about 3.5 times). This is a not impossible basis for a design, particularly if the pointer is made as long as that in an instrument of the laboratory standard type.

An increase in pointer length to 12 times the normal value is impracticable unless recourse is had to the use of a beam of light reflected from a mirror attached to the moving system. The precision of reading such a spot of light on a scale is considerably less than that of reading a knife-edge pointer, so that the sensitivity required in the instrument is still further increased. It is, however, easily feasible to obtain very long effective pointer lengths by employing a mirror and scale, and this type of construction is probably most desirable for composite-coil instruments.

In the experimental instrument both the period and pointer length were increased. If the performance of this instrument is compared quantitatively with a typical high-grade wattmeter it appears that the modification of the fixed coil in size and in shape has increased the torque by a factor of 2.9. An increase in period from 1.2 to 3.5 seconds has given a factor of 8.5 and the use of a beam of light about 50 cm long ($Z = 100$ cm) has given a factor of 8.8. Since two sets of coils are used the torque is doubled. On the other hand, the use of a rather heavy copper moving coil has produced a loss in effectiveness by a factor of 0.44 and a more conservative rating of the working moving-coil current to keep its temperature rise below 2° C. has cost a factor of 0.41. The loss arising from the composite-coil construction is by a factor of 0.25. Consequently, the final result is an intrument having about 20 times the sensitivity and about 10 times the precision of reading of the conventional wattmeter.

VII. AN ILLUSTRATIVE DESIGN

In illustration of the various factors which must be considered in the design of composite-coil instruments, a specific case, namely, the design of a composite-coil wattmeter having a full-scale range of 600 watts and intended for use on a 120-volt, 5-ampere circuit under conditions of fairly high power factor, will now be outlined. A convenient arrangement would be to use a main dial of 30 steps,

each corresponding to 20 watts, and a scale covering a range of 10 watts on either side of the zero and having ±50 divisions, each corresponding to 0.2 watt. If the spot of light on the scale is readable to one-fourth division, the precision of reading would be 0.01 per cent. If each division has a width of 1.5 mm, we get for the various scale constants, $C_X = 1.333$ watts per centimeter; $C_s = 0.2$ watt per division; $C_D = 20$ watts per step; $D_m = 30$.

Although the general reasoning of the foregoing paragraphs has shown that in his choice of dimensions of the moving coil the designer is not limited by the need for sensitivity, he is limited by certain constructional difficulties. Since the direct current used in the instrument will in most cases be supplied from a portable storage battery, it is evidently desirable to keep the voltage of this battery, and hence the number of cells, as low as possible. This means that the voltage drop E_D in the main dial must be decidedly smaller than the a. c. line voltage E_1. From equation (53A) of Appendix A it follows that the d. c. moving-coil current I_2 must be decidedly larger than the a. c. current I_1; yet I_2 must not be made so large as to produce any appreciable heating of the control springs. On the other hand, equation (53A) also shows that the wire diameter d_1 must at the same time be decidedly smaller than d_2; yet d_1 can not be indefinitely decreased because of the difficulty of winding excessively fine wire without breakage and also because of the decrease in space factor s_m with decrease in wire diameter. Equation (57A) of Appendix A shows clearly the balance of conflicting requirements between large wire diameter on the one hand and small moving-coil current and battery voltage on the other. It may be rearranged to give

$$\frac{b_m c_m}{b_m + c_m} = \frac{\pi^2 K \theta_R d_1^4 E_1^2}{8 \rho_m s_m I_2^2 E_D^2} \tag{32}$$

Assuming the cooling coefficient $K = 0.002$ watt per square cm per ° C., the resistivity of the aluminum wire $\rho_m = 2.9 \times 10^{-6}$ ohm-cm, and the space factor $s_m = 0.25$, this becomes

$$\frac{b_m c_m}{b_m + c_m} = 3{,}400 \frac{d_1^4 E_1^2 \theta_R}{I_2^2 E_D^2} \tag{33}$$

where b_m and c_m are the axial length and radial depth, respectively, of the moving-coil winding. If we also choose as limiting values $E_D = 15$ volts, $E_1 = 120$ volts, $I_2 = 0.1$ ampere, $\theta_R = 3°$ C., and d_1 as 0.008 cm (that is, No. 40 A. W. G.), we get

$$\frac{b_m c_m}{b_m + c_m} = 0.27 \text{ cm} \tag{34}$$

which for a coil of square cross section ($b_m = c_m$) gives $b_m = 0.54$ cm.

This, of course, is a reasonable value for the side of a coil of the general proportions of those used in ordinary wattmeters, but the foregoing analysis shows plainly that any decrease in I_2 or E_D or any increase in d_1 or in operating temperature θ_R beyond the values here assumed must be paid for by a corresponding increase in the bulk and weight of the moving coil. In fact, if it were not for this limitation, the operating temperature rise might well be chosen decidedly greater than 3° C.

As indicated by equation (31) the torque involves the factor $\sqrt{P_m T_m}$. Although the classic relation of Maxwell as modified by Shawcross and Wells [10] indicates that for a given mass of coil of square cross section, T_m is a maximum if $a_m/b_m = 1.5$. The torque will be greatest for a value of a_m/b_m considerably greater than 1.5 because P_m increases roughly in proportion to $\sqrt[3]{a_m/b_m}$. Hence, in commercial instruments this ratio ranges from 3 to 6.

In view of the preceding, we may adopt tentatively for our illustrative design $b_m = c_m = 0.5$ cm; a_m to be four times this (2.0 cm); and $E_D = 12.5$ volts (although this departs slightly from giving a simple ratio between E_1 and E_D), retaining the values for E_1, E_2, and d_1 assumed in the preceding calculations. The working temperature rise on this basis is by equation (33) 1.9° C. The cooling surface of each moving coil is 25 cm² and, hence, $P_m = 0.1$ watt.

Equation (51A) of Appendix A shows that the foregoing assumptions have fixed h_1 as 12.5 and by equation (53A) $I_1 = 0.01$, approximately $d_2 = d_1\sqrt{9.6} = 0.025$ cm (that is, No. 30 A. W. G.).

Also assuming r_m for such a coil to be 6×10^{-4} ohms per (turn)², we get by equations (42A) and (43A) as an approximate estimate, $N_1 = 620$ and $N_2 = 65$.

We may assume that the winding space is filled with a succession of layers of No. 30 and No. 40 wire, the respective layers connected in accordance with the schedule of Table 3, Appendix C. However, since No. 30 winds with about 30 turns per centimeter, a coil having $b_m = 0.5$ would have 15 turns per layer and, for $N_2 = 65$, would require less than 5 layers. A better equalization of the magnetic effects can be obtained by using 8 layers and hence making a shorter and deeper coil. With 8 layers and 8 turns per layer in the d. c. winding, the coil length b_m would be 0.27 cm. The a. c. winding would have 16 turns per layer in this length and 40 layers would yield 640 turns. The total radial thickness of the two windings would be $8/30 + 40/60 = 0.93$ cm. These proportions give a reasonable design. An alternative design which would be easier to manufacture and which would probably be satisfactory as regards the balance of magnetic fields is obtained by using 4 layers of No. 30 wire, with 16 turns per layer and 20 layers of No. 40 with 32 turns per layer. These would make a coil 0.53 by 0.47 cm, only slightly larger than that originally assumed and of nearly square cross section.

On either basis the mean radius a_m may still be taken as 2.0 cm. The resistances (two elements in series) computed from the exact numbers of turns are $R_1 = 954$ ohms and $R_2 = 9.54$ ohms for either design. Since $I_2 = 0.1$ ampere and $I_1 = 0.01$ ampere $R_1 + R_p = 12{,}000$ ohms; $R_2 + R_T = 125$ ohms, and at rated conditions the heat generated in one element is $P_m = 0.095$ watt.

Coming now to the design of the fixed coils, a decision must first be made as to whether or not to secure the self-checking feature obtainable if the a. c. fixed coils when connected in series have the same number of turns as the d. c. fixed coils. The advantages of this feature are that the user of the instrument (without a potentiometer or other precise standard of measurement) can measure the ratio G_{12}/G_{24} of the constants of the a. c. and d. c. windings and assure

[10] Maxwell, Electricity and Magnetism, 3d ed., vol. 2, p. 345; Shawcross and Wells, Elec'n, vol. 75, p. 64; 1915.

himself of the presence or absence of any significant change which may have been produced by shipment or other rough handling. Also this feature makes it considerably easier for the manufacturer to determine this ratio which he must know in order to properly adjust the a. c. series resistor R_p.

If the instrument is self-checking in the manner described on p. 234 the ratio of fixed-coil currents and the inverse ratio of turns must be a small integer. With this construction the instrument may be used with series and various series-parallel connections thus obtaining current ranges in addition to that corresponding to a parallel connection of all the a. c. fixed windings, and the voltage drop E_4 in the d. c. winding is then usually rather small, but the current drain on the storage battery is large.

If the self-checking feature is abandoned and a single current range is used, it becomes permissible to wind the d. c. fixed coils with a wire of much smaller size than that used in the a. c. windings. If the entire fixed coil is formed by winding in alternating succession single layers of thick wire for a. c. and multiple layers of thinner wire for d. c. the intermingling should be quite satisfactory and the space factor fairly high. With this type of winding the normal d. c. current I_4, and hence the drain on the storage battery, may be much reduced, but the voltage drop E_4, and hence the number of storage cells needed will be increased.

It may be assumed for the purpose of this illustrative design that the self-checking feature is retained. Then if four sections are used in parallel in the a. c. coils ($I_3/I_4=4$) the current I_4 taken from the battery will be $I_3/4=1.25$ amperes, which is probably too great to give steady conditions. If $I_3/I_4=5$, only two ranges 5-ampere and 1-ampere will be obtained, while if $I_3/I_4=6$, the current $I_4=0.833$ ampere; and ranges of 100, 200, 300, and 600 watts, easily capable of being loaded to 1, 2, 3, and 6 amperes, respectively, will be available. This involves winding 6 wires in parallel in the fixed coil, which is not prohibitive and for $E_D=12.5$ volts requires a main-dial resistance of 15 ohms (or 0.5 ohm per step). Increasing the current ratio to 8 would, however, make the coil rather difficult to wind.

On the basis of $I_3/I_4=6$ the maximum permissible power dissipation, P_f in the fixed coils must next be assumed. In the experimental ammeter described above P_f is 2.4 watts for each element and produces a temperature rise of 6° C. It seems probable that the fixed coils in that instrument are too large for the highest efficiency, while on the other hand the temperature rise is very conservatively low. Therefore, in the new design it may be assumed that $P_f=3.0$ watts. From equation (52A) it follows that for unity power factor $E_4=P_f/I_4=3.0/0.833=3.6$ volts and from equation (49A) that $R_4=4.33$ ohms. Assuming that the mean length of turn is the same (23 cm) as in the experimental instrument, but that the cross section of the winding space on one element is only 6 by 4 cm instead of 9 by 4 cm, its resistance constant r_f will be about 1.5 times that for the experimental instrument, or 3.6×10^{-6} ohms per (turn)^2. From this figure there is obtained by equation (45A) the tentative estimate $N_3=91$ and $N_4=546$. The winding space available in one element for either winding has been assumed to be 12 cm^2, hence if the space factor $s_f=0.5$ the cross section of the wire can be $6/546=0.011$ cm^2. This suggests the use of No. 17 A. W. G. (1.15 mm) wire.

From the considerations discussed in Appendix C it appears that a satisfactory coil can be obtained by using entire layers for either the a. c. or the d. c. circuits, provided the assignment is made in accordance with the schedule of Table 3. On this basis each d. c. layer would consist of a simple continuous winding. Each a. c. layer would be wound with six wires laid side by side and capable of being connected in series or parallel at a terminal block external to the coil. All wires would be of the same size. A few trial calculations show that if the total of about 1,100 turns were wound in only 16 layers the ratio of length to depth of the coil would be over 4 to 1 which is much too great. On the other hand, if the coil has 32 layers it will be nearly square in cross section, and will probably be fairly efficient in producing torque. Since the fixed coil of one element is most conveniently made in two halves which are supported one on each side of the axis, it is essential that the number of turns per layer of the a. c. winding be an integral multiple of 12, and we may, therefore, assume 36 turns per layer, giving a total of 1,152 turns for both. If No. 17 A. W. G. single silk-enamel wire is used (allowing 0.004 cm for insulation thickness) the coil will have the dimensions $b_f = 4.5$ cm, $c_f = 4.0$ cm approximately.

The opening needed in the interior of the fixed coil depends, of course, on the size of the moving coil and the angular motion required for full deflection. Assuming the travel of the spot of light from zero to the maximum scale reading (± 60 divisions) to be 9 cm and the scale distance to be 50 cm, the angular motion of the reflected ray is about 0.18 radian and that of the coil is one-half this. If the maximum radius of the moving coil is 2.5 cm and its thickness is 0.5 we get, after allowing 0.25 cm clearance on each side, a width of opening of approximately 1.5 cm. The vertical height of the opening must be taken somewhat greater than the outside diameter of the moving coil. Therefore the entire fixed coil will consist of two semicircular portions of inner and outer radii 0.75 and 4.75 cm separated by rectangular portions 5 cm long. The mean length of turn is consequently $2\pi \times 2.75 + 10 = 27.3$ cm. From this and the total of 1,152 turns (in the d. c. winding of both elements) we get $R_4 = 5.32$ ohms at 25° C., $E_4 = 4.4$ volts and P_f (for one element at full rating) $= 3.7$ watts. The outer surface of such a coil, including the flat ends, has an area of 328 cm^2 and if not obstructed by supports should operate with a temperature rise of about 6° C.

For the design thus arrived at we may estimate approximately the inductance coefficients l_f and l_m by the usual formulas.[11] In the case of the flattened fixed coils it is natural to use as effective radius that of a circle which has a circumference equal to the mean length of turn. For the experimental instrument, this assumption gives an inductance 15 per cent too high, and a correction of this magnitude will probably suffice to allow for the flattening in the case of the present design also. On this basis we get $l_f = 47 \times 10^{-9}$ and $l_m = 57 \times 10^{-9}$ henries per (turn)^2. Assuming conservatively that $\frac{dk_{fm}}{d\alpha} = 0.3$ we can estimate the full rated torque by equation (13A) as

$\tau = 2 \times 640 \times 96 \times \sqrt{47 \times 57 \times 10^{-18}} \times 0.01 \times 5 \times 0.3 \times 10^{+7} = 954$ dyne-cm.

For the scale length and scale distance previously assumed, a coil

[11] B. S. Bull., vol. 8, p. 1; 1912.

motion of 0.075 radian corresponds to one-half step of the dial, and hence to 1/60 full indication and to 954/60 = 16 dyne-cm. The stiffness U of the control springs should, therefore, be 214 dyne-cm per radian. The division of this control among the four springs which are needed to lead current to the moving circuits is of little importance. Perhaps the best design is to supply the a. c. coils through slender spirals of fine strip since they are in a circuit of high resistance and need carry only a small current. The bulk of the control would then be provided by relatively thick and strong upper and lower suspension strips which would supply the lower resistance d. c. circuit and carry the weight of the moving system.

The mass of aluminum in the two elements of the moving system is 4.4 g and its moment of inertia is about 8.9 g-(cm)^2. Allowing a margin for the inertia of the insulation, spindle, mirror, etc., would make a total of perhaps 12 gm-(cm)^2. This inertia combined with the spring stiffness of 214 dyne-cm per radian corresponds to a free period of oscillation of 1.5 seconds, which is quite satisfactory.

In a composite-coil wattmeter of this design the accuracy of the deflection part of the indication may be checked in exactly the same way as in the experimental ammeter described above. The circuits needed are the same as shown in Figure 6, except that the resistances spanned by the R and L plugs should each be equal to one-half step on the main dial (that is, 0.25 ohm); and the resistance R_L should be 29.75 ohms.

The connections for checking the null part of the indication, which involves the ratio G_{13}/G_{24}, are, however, decidedly more complicated. This complication arises from the fact that the a. c. and the d. c. moving coils have very different numbers of turns, and therefore, can not be made to produce equal ampere-turns merely by being connected in series. The arrangement shown in Figure 7 should, however, furnish the desired self-checking feature. For the sake of simplicity, in this figure only one element of each winding is shown. Here 3 is the a. c. fixed coil the six sections of which have been connected in series at the connection block C and which thus has the same number of turns as the d. c. fixed coil 4.

This change alone gives the torque constant for the coils 1 and 3 a value $6G_{13}$. These two coils in series are supplied with a test current I_f' from the battery B. The main dial may be left out of the circuit for this test and this omission will more than compensate for the resistance added to the circuit by the insertion of the a. c. fixed coil. The calibrating current I_f' may be adjusted by the usual rheostats to the exact value fixed by the standard-cell dial, or may be merely read by an ammeter A_1 in the battery lead.

The moving coils 1 and 2 are supplied with currents which must have exactly the ratio $\frac{N_1}{N_2} = 10$. This may be accomplished by forming a Wheatstone bridge, two adjacent arms of which are fixed and have resistance R_g and R_h in the desired 10 : 1 ratio. Reasonable values are $R_g = 500$ ohms and $R_h = 50$ ohms. The other arm adjacent to R_h consists of the d. c. moving coil with its series resistance and has a resistance $R_2 + R_T$. The fourth arm of the bridge consists of the a. c. moving coil in series with about 300 ohms and an adjustable three-dial rheostat having 10, 1, and 0.1 ohm steps. The entire

bridge is supplied with a test current I_m' of about 0.11 ampere from the storage battery, the current being read on the milliammeter A_2.

The galvanometer for this Wheatstone bridge circuit may well be the one used in setting the d. c. current in the normal use of the instrument.

In making a check on the instrument constant C_D the first step is to balance the Wheatstone bridge by adjustment of the 3-dial

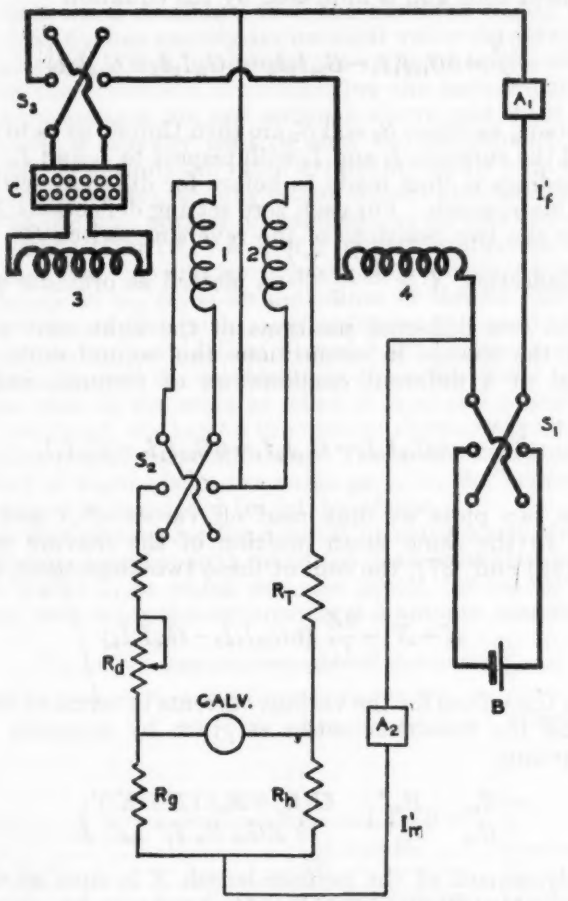

FIGURE 7.—*Connections to be used in determining G_{24}/G_{13}, in illustrative design of wattmeter*

rheostat. This serves to compensate for any change in the resistance of either moving coil whether caused by temperature changes or otherwise, and insures that the currents in the two moving coils have with high accuracy the ratio:

$$\frac{I_2}{I_1}=\frac{R_g}{R_h} \tag{35}$$

The deflections X_1 and X_2 of the instrument are then noted for the two positions of the reversing switch S_1. This process is then repeated

with the instrument zero shifted to a number of different positions on the scale. The mean deflection $X=\frac{X_1+X_2}{2}$ may then be plotted as ordinate against the mean of the two deflected positions of the light spot as abscissa. This mean deflection is a measure of the residual effect of the various torques resulting from the interaction of the several pairs of coils and is indicated by the equation

$$\frac{UX}{Z}=6G_{13}I_1I_3-G_{24}I_2I_4+6G_{23}I_2I_3+G_{14}I_1I_4 \tag{36}$$

The reversing switches S_2 and S_3 are then thrown so as to reverse the direction of the currents I_1 and I_3 with respect to I_2 and I_4. A second series of readings is then made as before for different settings of the zero of the instrument. For each zero setting deflections X_1' and X_2' are read for the two positions of the reversing switch S_1. As before the mean deflection $X'=\frac{X_1'+X_2'}{2}$ is plotted as ordinate against the mean of the two deflected positions of the light spot as abscissa. Because of the change in connections this second curve will show the residual of a different combination of torques, and we have

$$\frac{UX'}{Z}=6G_{13}I_1I_3-G_{24}I_2I_4-6G_{23}I_2I_3-G_{14}I_1I_4 \tag{37}$$

From these two plots we may read off values of X and X' which correspond to the same mean position of the moving coil. From equations (36) and (37), the sum of these two deflections, is given by

$$X+X'=\frac{2Z}{U}\ (6G_{13}I_1I_3-G_{24}I_2I_4) \tag{38}$$

Inserting the values for the various currents in terms of the ammeter readings and the resistance ratios as given by equation (35) gives, after transposing

$$\frac{G_{24}}{G_{13}}=6\frac{R_h}{R_g}\left(1-\frac{U(R_g+R_h)\ (X+X')}{12\ ZG_{13}\ R_h\ I_f'\ I_m'}\right) \tag{39}$$

If the adjustment of the pointer length Z is such as to give the deflection constant its proper value, C_X, as shown by equation (17), we have the additional relation

$$\frac{U}{ZG_{13}}=\frac{C_X}{R_p+R_1}$$

Whence we get for each deflected position of the coil

$$\frac{G_{24}}{G_{13}}=6\frac{R_h}{R_g}\left(1-\frac{(R_g+R_h)\ C_x\ (X+X')}{12\ (R_p+R_1)\ R_h\ I_f'\ I_m'}\right) \tag{40}$$

If R_h/R_g is close to its nominal value (1/10) the second term in the brackets will be very small as compared with unity and the quanti-

tities I_f', I_m', X, and X' need be known to only a moderate accuracy even though G_{24}/G_{13} is needed to the full relative acccuracy of the instrument.

The value of G_{24}/G_{13} computed by equation (40) from the values of X and X' corresponding to the normal zero of the instrument is to be taken as the value to use in equation (16) for computing C_D. In the final adjustment by the manufacturer R_p or R_T should be adjusted so that when combined with the observed G_{24}/G_{13} according to equation (16) C_D has exactly its nominal value (in this design 20 watts per dial step). This final observed value of G_{24}/G_{13} should also be entered on the certificate accompanying the instrument. A user who at any time repeats the test outlined above and finds the same value for G_{24}/G_{13} is thereby assured that the instrument is still in good condition. If he finds the value to be different by a small amount (say 0.2 per cent greater), he may either correct his values by adding 0.2 per cent to the null part of his readings, or he may reduce R_p by 0.2 per cent of the total (R_p+R_1), or if he prefers increase R_T by 0.2 per cent of $(R_D+R_T+R_2)$ and thus restore the instrument calibration. Any large change in G_{24}/G_{13} is an indication of serious damage, such as a short circuit between turns, and indicates the need for repairs.

If the compensating coils *DD* of Figure 5 are functioning properly, the value of G_{24}/G_{13} will be substantially the same when the spot of light is at the ends of the scale as when it is at the center. If this condition is not found, the tap on the resistor shunting these coils may be readjusted to restore this condition. The relative error introduced by a departure of G_{24}/G_{13} from the value given in the maker's certificate is, of course, proportional to the departure.

The values thus chosen for the various quantities required for this illustrative design, together with pertinent data computed from them, are given in Table 2, in which are also given, for comparison, the corresponding values for the experimental 5-ampere ammeter.

TABLE 2.—*Data on composite-coil instruments*

	Experimental ammeter		Illustrative design of wattmeter	
Rated current, I_1	5		5.	
Rated voltage, E_1			120.	
Battery voltage, E_B	10		18.	
Number of steps on main dial, (D_m)	25		30.	
Dial constant, (C_D)	1 amp.[2] per step		20 watts per step.	
Number of scale divisions	±60		±60.	
Length of 1 scale division, mm	1.5		1.5.	
Deflection constant, C_s	0.01 amp.[2] per division		0.2 watt per division.	
Equivalent total scale length, mm	3,750		4,500.	
	d. c. winding	a. c. winding	d. c. winding	a. c. winding on 5-ampere connection
Current in fixed-coil windings at full rating, amperes	1.0	5.0	0.833	5.0.
Total turns in fixed-coil winding for 2 elements	1,000	200	1,152	192.
Size of wire in fixed-coil windings, A. W. G. No.	15	15, 5 in parallel.	17	17, 6 in parallel.
Resistance of fixed-coil windings for 2 elements at 25° C, ohms	2.5	0.1	5.3	0.148.
Inductance of fixed-coil winding for 2 elements, microhenries		0.370		0.860.

	Experimental ammeter		Illustrative design of wattmeter	
	d. c. winding	a. c. winding	d. c. winding	a. c. winding
Current in moving-coil winding, full rating.....amperes..	0.14	0.14	0.1	0.01
Total turns in moving-coil winding.....	75	75	64	640
Size of wire in moving-coil windings.....A. W. G. No..	28	28	30	40
Resistance of moving-coil winding for 2 elements.....ohms..	2.2	2.2	9.5	954
Resistance of complete moving-coil circuit (including main dial or shunt).....	35.0	35	125	12,000
Inductance of moving-coil winding for 2 elements..millihenries..	0.30	0.30	0.468	46.8

	Experimental ammeter	Illustrative design of wattmeter
Dimensions of moving coil of 1 element: mean radius × axial length × radial thickness, cm.	2.5 by 0.4 by 0.8.....	2.0 by 0.53 by 0.47, or 2.0 by 0.27 by 0.93.
Dimensions of fixed coil of 1 element: mean radius × axial length × radial thickness.	3.7 by 9 by 4.....	4.3 by 4.5 by 4.0.
Weight of moving system, w.....g..	28.....	7.
Stiffness of suspensions, U.....dyne-cm per radian..	180.....	214.
Undamped period.....seconds..	3.5.....	1.5.
Torque at rated currents.....dyne-cm..	660.....	954.
Rotation of coil for deflection corresponding to one-half dial step, radians.	0.07.....	0.075.
Temperature rise of fixed coils.....° C..	6.....	6.
Temperature rise of moving coils above fixed coils.....° C..	1.5.....	1.9.
Power consumed in a. c. current circuit.....watts..	27.5.....	3.7.
Power consumed in a. c. voltage circuit.....watts..	.....	1.2.
Power consumed in d. c. circuit.....watts..	10.....	15.

VIII. CONCLUSION

The foregoing discussion, and the characteristics obtained in the experimental ammeter here described, have demonstrated the technical feasibility of this new type of a. c. instrument, which as regards accuracy is definitely in advance of present indicating instruments. The inconvenience of its operation appears to be no greater than that normally associated with present practice in high-accuracy tests, where a number of repeat measurements are always made.

The economic practicability of the new type of instrument must be decided by a balance between cost of manufacture and the value of accurate measurement to the electrical industry. It is hoped that the growing appreciation by the electrical engineers of the importance of accuracy in their tests, will induce American instrument makers to utilize and improve this new tool for precise electrical measurements.

IX. APPENDIX A. OPTIMUM WINDING OF THE COILS OF A COMPOSITE COIL WATTMETER

We may consider as given quantities the rated current I_3 and voltage E_1 for which the a. c. circuits of the instrument are to be suited. The average power factor of the a. c. circuit cos φ must also be considered, since it affects the ratio of the heating in the a. c. to that in the d. c. windings. The voltage drops E_4 in the d. c. winding and E_D in the main dial at full scale are at the disposal of the designer, but their sum is more or less definitely fixed by the excess of the battery voltage E_B over the voltage required for the standard-cell dial and by convenient control rheostats.

If each moving coil is circular and has a mean radius a_m, an axial length b_m, and a radial winding depth c_m, the cross section of the winding space will have an area $b_m\, c_m$. Let the fraction A_2 of this space be devoted to the N_2 turns of the d. c. winding of one element, while the fraction $1-A_2$ is assigned to the N_1 turns of the a. c. winding. If the resistivity of the wire is ρ_m, the space factor [12] for either winding is s_m and the wire diameters are d_1 and d_2, then we have the relations

$$N_1=\frac{4b_mc_m\,(1-A_2)\,s_m}{\pi d_1^{\,2}} \tag{1A}$$

$$N_2=\frac{4b_mc_mA_2s_m}{\pi d_2^{\,2}} \tag{2A}$$

and for the total resistance of the respective a. c. and d. c. windings, the corresponding coils in the two elements being connected in series

$$R_1=\frac{4\pi\rho_m a_m N_1^{\,2}}{b_mc_m\,(1-A_2)\,s_m}=\frac{64\rho_m a_m b_m c_m\,(1-A_2)\,s_m}{\pi d_1^{\,4}}=\frac{2r_m N_1^{\,2}}{(1-A_2)} \tag{3A}$$

$$R_2=\frac{4\pi\rho_m a_m N_2^{\,2}}{b_mc_mA_2s_m}=\frac{64\rho_m a_m b_m c_m A_2 s_m}{\pi d_2^{\,4}}=\frac{2r_m N_2^{\,2}}{A_2} \tag{4A}$$

where the coefficient r_m (= ohms per (turn)^2) is a constant for any given material and winding channel and does not depend on the number of turns used.

Similarly for the fixed coils we may write

$$R_3=\frac{2r_f N_3^{\,2}}{(1-A_4)} \tag{5A}$$

$$R_4=\frac{2r_f N_4^{\,2}}{A_4} \tag{6A}$$

where the coefficient r_f will be independent of the number of turns. Such a relation will exist even though the coils may not be circular in shape.

Assuming for the purpose of design that the current I_1 in the a. c. moving coil is in phase with the voltage E_1, we have for the deflecting torque

$$\tau=I_1I_3\cos\phi\frac{dM_{13}}{d\alpha}\times10^7 \tag{7A}$$

Let us denote by M_{fm} the mutual inductance which would exist between the fixed and the moving coils of one element if the total cross-section of each of its coils were devoted to single windings of N_f and N_m turns, respectively. We may denote by L_f and L_m the inductances, by R_f and R_m, the resistances and by T_f and T_m the time constants which these hypothetical coils would have.

[12] Strictly the space factors (defined as ratio of cross section of metal to cross section of entire coil) of the two moving-coil windings may be somewhat different unless both are wound with the same size of wire. The effect of such a difference is, however, quite negligible in the present discussion.

The resistance and inductance of a coil occupying a fixed winding space are each proportional to the square of the number of turns in the coil, and we may denote the respective proportionality constants by r_f and l_f for the fixed and r_m and l_m for the moving coil of one element. Since the mutual inductance between two coils is proportional to the product of the number of turns in each, we have for the two elements combined

$$M_{13}=2\frac{N_1N_3}{N_fN_m}M_{fm} \tag{8A}$$

Also we may let k_{fm} represent the coefficient of coupling between the fixed and moving coils, defined as usual by

$$M_{fm}=k_{fm}\sqrt{L_fL_m} \tag{9A}$$

Combining equations (9A) and (8A) gives

$$M_{13}=\frac{2N_1N_3k_{fm}}{N_fN_m}\sqrt{L_fL_m} \tag{10A}$$

or

$$M_{13}=2N_1N_3k_{fm}\sqrt{l_fl_m} \tag{11A}$$

Since k_{fm} is the only variable which is dependent on α we get for the derivative

$$\frac{dM_{13}}{d\alpha}=2N_1N_3\sqrt{l_fl_m}\frac{dk_{fm}}{d\alpha} \tag{12A}$$

Equation (7A) for the torque therefore becomes

$$\tau=2N_1N_3\sqrt{l_fl_m}I_1I_3\cos\varphi\frac{dk_{fm}}{d\alpha}\times10^7 \tag{13A}$$

To avoid errors from variations in room temperature it is desirable that the ratio of the total resistance of each moving-coil circuit to that part of each circuit which has a high temperature coefficient should have a particular value, h, which may be in some cases definitely fixed by the relative temperature coefficients of the resistance of the windings and of the stiffness of the control springs and which always should be nearly the same for both a. c. and d. c. circuits. Consequently we have the relation

$$h=\frac{R_p+R_1}{R_1}=\frac{R_T+R_2+R_D}{R_2} \tag{14A}$$

The fact that the d. c. torque is substantially equal and opposite to the a. c. torque gives us the additional relation

$$N_1N_3I_1I_3\cos\varphi=N_2N_4I_2I_4 \tag{15A}$$

We also have for the heating P_f and P_m in the fixed and moving coils, respectively, of each element

$$P_f=\frac{I_3^2R_3}{2}+\frac{I_4^2R_4}{2} \tag{16A}$$

$$P_m=\frac{I_1^2R_1}{2}+\frac{I_2^2R_2}{2} \tag{17A}$$

If in equations (15A), (16A), and (17A) we eliminate the currents I_1, I_2, and I_4 by expressing them in terms of the voltage acting in each of the circuits and its resistance, we get

$$\frac{N_1N_3E_1I_3\cos\varphi}{hR_1}=\frac{N_2N_4E_DE_4}{hR_2R_4} \tag{18A}$$

$$P_f=\frac{I_3^2R_3}{2}+\frac{E_4^2}{2R_4} \tag{19A}$$

$$P_m=\frac{E_1^2}{2h^2R_1}+\frac{E_D^2}{2h^2R_2} \tag{20A}$$

$$\tau=2N_1N_3\sqrt{l_fl_m}\,\frac{E_1I_3\cos\varphi}{hR_1}\,\frac{dk_{fm}}{d\alpha}\times10^7 \tag{21A}$$

Equations (3A), (4A), (5A), and (6A), enable us to eliminate the various resistances from the foregoing group of equations and on substitution give

$$\frac{N_3}{N_1}E_1I_3\cos\phi=\frac{E_DE_4A_2A_4}{2r_fN_2N_4(1-A_2)} \tag{22A}$$

$$P_f=\frac{r_fN_3^2I_3^2}{(1-A_4)}+\frac{A_4E_4^2}{4r_fN_4^2} \tag{23A}$$

$$P_m=\frac{E_1^2(1-A_2)}{4r_mh^2N_1^2}+\frac{E_D^2A_2}{4r_mh^2N_2^2} \tag{24A}$$

and

$$\tau=\frac{N_3(1-A_2)\sqrt{l_fl_m}E_1I_3\cos\varphi}{N_1hr_m}\,\frac{dk_{fm}}{d\alpha}\times10^7 \tag{25A}$$

In these four equations the designer has under his control six variables, viz, A_2, A_4, N_1, N_2, N_3, and N_4. The problem, therefore, is to choose the six variables so that the torque as given by equation (25A) is a maximum, while at the same time the limiting conditions indicated by equations (22A), (23A), and (24A) are satisfied.

Solving equation (22A) for N_3 and inserting the result in equation (23A) gives

$$N_4^2=\frac{E_4^2A_4}{4r_fP_f}\left(1+\frac{E_D^2A_2^2A_4N_1^2}{E_1^2\cos^2\phi\,(1-A_2)^2\,(1-A_4)\,N_2^2}\right) \tag{26A}$$

and equation (24A) can be rearranged to give

$$N_2^2=\frac{1}{4r_mh^2P_m}\left[E_1^2\,(1-A_2)\,\frac{N_2^2}{N_1^2}+E_D^2A_2\right] \tag{27A}$$

Now from equation (25A) it is evident that the torque will be a maximum when the quantity $\frac{N_3\,(1-A_2)}{N_1}$ is a maximum, since the other factors are constant. From equation (22A) we have

$$\frac{N_3\,(1-A_2)}{N_1}=\frac{E_DE_4A_2A_4}{2r_fE_1I_3\cos\phi N_2N_4} \tag{28A}$$

Squaring this equation and inserting the values of N_2^2 and N_4^2 from equations (26A) and (27A) gives

$$\left\{\frac{N_3}{N_1}(1-A_2)\right\}^2=\frac{4r_m h^2 P_m P_f A_2^2 A_4 (1-A_2)^2}{r_f I_3^2 E_D^2\left\{\frac{E_1^2}{E_D^2}(1-A_2)\frac{N_2^2}{N_1^2}+A_2\right\}} \tag{29A}$$

$$\times\frac{(1-A_4)\frac{N_2^2}{N_1^2}}{\left\{\frac{E_1^2}{E_D^2}\cos^2\phi\,(1-A_2)^2(1-A_4)\frac{N_2^2}{N_1^2}+A_2^2A_4\right\}}$$

The problem thus resolves itself to finding the values of A_2, A_4, and of the ratio $\frac{N_2}{N_1}$ which makes the right-hand member of equation (29A) (which is proportional to the square of the torque) a maximum.

Considering first the variable A_4, we see that the torque will be a maximum when the quantity

$$\frac{E_1^2}{E_D^2}\cos^2\varphi\,\frac{(1-A_2)^2}{A_4}\left(\frac{N_2}{N_1}\right)^2+\frac{A_2^2}{1-A_4} \tag{30A}$$

is a minimum. Differentiating this with respect to A_4 and setting the result equal to zero gives

$$\frac{E_1^2}{E_D^2}\cos^2\varphi\,(1-A_2)^2\left(\frac{N_2}{N_1}\right)^2\frac{1}{A_4^2}=\frac{A_2^2}{(1-A_4)^2} \tag{31A}$$

or

$$\frac{A_4}{1-A_4}=\pm\frac{E_1}{E_D}\cdot\frac{N_2}{N_1}\cos\varphi\,\frac{(1-A_2)}{A_2} \tag{32A}$$

Only the + sign is physically possible, and hence

$$A_4=\frac{\frac{E_1}{E_D}\frac{N_2}{N_1}\cos\varphi\left(\frac{1-A_2}{A_2}\right)}{1+\frac{E_1}{E_D}\frac{N_2}{N_1}\cos\varphi\left(\frac{1-A_2}{A_2}\right)} \tag{33A}$$

Inserting this value of A_4 into equation (29A) gives

$$\left\{\frac{N_3}{N_1}(1-A_2)\right\}^2=\frac{4r_m h^2 P_f P_m\,(1-A_2)^2\frac{N_2^2}{N_1^2}}{r_f I_3^2 E_D^2\left\{\frac{E_1^2}{E_D^2}(1-A_2)\frac{N_2^2}{N_1^2}+A_2\right\}}\times \tag{34A}$$

$$\frac{1}{\left\{\frac{E_1}{E_D}\cos\varphi\,\frac{N_2}{N_1}\frac{(1-A_2)}{A_2}+1\right\}^2}$$

Considering now as a single variable the turn ratio $\frac{N_2}{N_1}$ we see from equation (34A) that the torque will be a maximum when the quantity

$$\left\{\frac{E_1^2}{E_D^2}(1-A_2)+A_2\frac{N_1^2}{N_2^2}\right\}\left\{\frac{E_1}{E_D}\cos\phi\,\frac{(1-A_2)}{A_2}\frac{N_2}{N_1}+1\right\}^2$$

is a minimum. Differentiating this quantity with respect to $\frac{N_2}{N_1}$ and equating the result to zero gives as the optimum value for the turn ratio

$$\frac{N_2}{N_1}=\frac{E_D}{E_1}\left(\frac{A_2}{1-A_2}\right)^{\frac{3}{4}}\frac{1}{(\cos\phi)^{\frac{1}{4}}} \tag{35A}$$

Inserting this value in equation (34A) gives

$$\left\{\frac{N_3}{N_1}(1-A_2)\right\}^2=\frac{4r_m h^2 P_f P_m}{r_f I_3^2 E_1^2\{(1-A_2)^{-\frac{1}{4}}+A_2^{-\frac{1}{4}}(\cos\phi)^{\frac{3}{4}}\}^3} \tag{36A}$$

Coming now to the variable A_2, we may differentiate the denominator of the right member of equation (36A) and obtain, on equating the derivative to zero,

$$1-A_2=\frac{1}{1+\sqrt{\cos\phi}}\,,\quad A_2=\frac{\sqrt{\cos\phi}}{1+\sqrt{\cos\phi}} \tag{37A}$$

Inserting this value of A_2 in equation (36A) gives

$$\left\{\frac{N_3}{N_1}(1-A_2)\right\}^2=\frac{4r_m h^2 P_f P_m}{r_f E_1^2 I_3^2\{1+(\cos\phi)^{\frac{1}{2}}\}^4} \tag{38A}$$

Finally inserting this result in equation (25A) and noting that $\frac{l_f}{r_f}$ and $\frac{l_m}{r_m}$ are equal, respectively, to the time constants of the fixed and moving coils T_f and T_m we get for the maximum value of the operating torque

$$\tau_{ac}=\frac{2dk_{fm}}{d\alpha}\sqrt{T_f T_m P_f P_m}\,\frac{(\cos\phi)}{\{1+\sqrt{\cos\phi}\}^2}\times 10^7 \tag{39A}$$

For the optimum value of A_2 we also get from equation (35A)

$$\frac{N_2}{N_1}=\frac{E_D}{E_1} \tag{40A}$$

and from equation (33A)

$$A_4=\frac{\sqrt{\cos\phi}}{1+\sqrt{\cos\phi}}\;1-A_4=\frac{1}{1+\sqrt{\cos\phi}} \tag{41A}$$

If $\cos\phi=1$ equations (37A) and (41A) reduce to

$$A_2=0.5 \text{ and } A_4=0.5$$

It thus is evident that these equations are merely the expression in mathematical form of the fact that the heating of the a. c. windings when producing a given torque at unity power factor is equal to that in the d. c. windings, and hence that for this case each should be given an equal share of the available winding space.

The other optimum constants of the instrument may be determined by substituting the optimum values of A_2, A_4, and $\frac{N_2}{N_1}$ in the earlier equations (15A) to (28A).

We thus obtain for the turns in one element

$$N_1 = \frac{E_1}{2h\sqrt{r_m P_m}} \tag{42A}$$

$$N_2 = \frac{E_D}{2h\sqrt{r_m P_m}} \tag{43A}$$

$$N_3 = \frac{1}{I_3(1+\sqrt{\cos\phi})}\sqrt{\frac{P_f}{r_f}} \tag{44A}$$

$$N_4 = \frac{E_4}{2\sqrt{r_f P_f}} \tag{45A}$$

Similarly for the resistances of the two elements of each coil as connected in series

$$R_1 = \frac{E_1^2\,(1+\sqrt{\cos\varphi})}{2\,h^2\,P_m} \tag{46A}$$

$$R_2 = \frac{E_D^2\,(1+\sqrt{\cos\varphi})}{2\,h^2\,P_m\sqrt{\cos\varphi}} \tag{47A}$$

$$R_3 = \frac{2\,P_f}{I_3^2\,(1+\sqrt{\cos\varphi})} \tag{48A}$$

$$R_4 = \frac{E_4^2\,(1+\sqrt{\cos\varphi})}{2\,P_f\sqrt{\cos\varphi}} \tag{49A}$$

The corresponding currents are therefore

$$I_1 = \frac{2\,h\,P_m}{E_1\,(1+\sqrt{\cos\varphi})} \tag{50A}$$

$$I_2 = \frac{2\,h\,P_m\sqrt{\cos\varphi}}{E_D\,(1+\sqrt{\cos\varphi})} \tag{51A}$$

$$I_4 = \frac{2\,P_f\sqrt{\cos\varphi}}{E_4\,(1+\sqrt{\cos\varphi})} \tag{52A}$$

The inclusion of the variable cos φ in these equations permits the designer to fit the instrument more closely to the class of work for which it is intended. An instrument to be used for the most part at low power factor can be so wound that it will give more torque at rated volt-amperes than will an instrument of the same current and voltage ratings designed for unity power factor. However, the

gain in torque is only 38 per cent in the case of an instrument designed for a power factor of 0.5 and only 60 per cent for a power factor of 0.2. It is therefore probably seldom desirable to depart from the equal division of the coil volumes, which is called for at unity power factor.

For the case that $\cos \phi = 1$ the equations can be combined to give the following relations which exist under the optimum conditions:

$$\frac{I_2}{I_1} = \frac{N_1}{N_2} = \sqrt{\frac{R_1}{R_2}} = \frac{E_1}{E_D} = \frac{d_2^2}{d_1^2} \tag{53A}$$

and

$$\frac{I_4}{I_3} = \frac{N_3}{N_4} = \frac{P_f}{I_3 E_4} \tag{54A}$$

and by equations (17A) and (53A)

$$P_m = I_2^2 \, R_1 \, E_D^2 / E_1^2 \tag{55A}$$

Since the available cooling surface of the moving coil is approximately $4\pi a_m \, (b_m + c_m)$, the heat dissipated at a temperature rise θ_R will be

$$P_m = 4\pi a_m \, (b_m + c_m) \, K\theta_R \tag{56A}$$

where K is the emissivity in watts per square centimeter per degree. Inserting this value in equation (55A), eliminating R_1 by equation (3A), and noting that for $\cos \phi = 1$, $A_2 = \frac{1}{2}$, we get the relation

$$d_1^4 = \frac{8\rho_m b_m c_m s_m E_D^2 \, I_2^2}{\pi^2 K \, \theta_R (b_m + c_m) \, E_1^2} \tag{57A}$$

X. APPENDIX B. TEMPERATURE COMPENSATION

The basic equation for a composite-coil wattmeter (equation (14) above) is

$$P = \frac{G_{24}(R_p + R_1) E_s^2 R_A D}{G_{13}(R_D + R_T + R_2) R_s^2} + \frac{(R_p + R_1) U \, X}{G_{13} Z} \tag{1B}$$

Of the quantities appearing in this equation the only ones appreciably affected by temperature are U, R_1, R_2, and that part of the resistances R_p and R_T which are formed by the control springs (or suspensions). We may designate these last-mentioned items by R_{U1} and R_{U2}, respectively. Differentiating with respect to the temperature θ gives

$$\frac{dP}{d\theta} = \frac{G_{24}(R_p + R_1) E_s^2 R_A D}{G_{13}(R_D + R_T + R_2) R_s^2} \left\{ \frac{1}{(R_p + R_1)} \frac{d(R_1 + Ru_1)}{d\theta} - \frac{1}{(R_D + R_T + R_2)} \frac{d(R_2 + R_{U2})}{d\theta} \right\} \tag{2B}$$

$$+ \frac{U(R_p + R_1)X}{G_{13} Z} \left\{ \frac{1}{R_p + R^1} \quad \frac{d(R_1 + U_1)}{d\theta} + \frac{1}{U} \frac{dU}{d\theta} \right\}$$

Now we may define the temperature coefficients of the various elements by

$$\beta=\frac{1}{R_1}\frac{dR_1}{d\theta}=\frac{1}{R_2}\frac{dR_2}{d\theta} \tag{3B}$$

$$\gamma=\frac{1}{R_{U1}}\frac{dR_{U1}}{d\theta}=\frac{1}{R_{U2}}\frac{dR_{U2}}{d\theta} \tag{4B}$$

$$\eta=\frac{1}{U}\frac{dU}{d\theta} \tag{5B}$$

Inserting these values and also the value of the instrument constants C_D and C_X from equations (16) and (17) gives, if we also write

$$h_1=\frac{R_p+R_1}{R_1} \tag{6B}$$

and

$$h_2=\frac{R_D+R_T+R_2}{R_2} \tag{7B}$$

$$\frac{dP}{d\theta}=C_D D\left\{\frac{\beta}{h_1}+\frac{R_{U1}\gamma}{h_1R_1}-\frac{\beta}{h_2}-\frac{R_{U2}\gamma}{h_2R_2}\right\}+C_X X\left\{\frac{\beta}{h_1}+\frac{R_{U1}\gamma}{h_1R_1}+\eta\right\} \tag{8B}$$

The changes produced within the range of temperature met with in use may be considered linear. Therefore, if the coils 1 and 2 have a temperature rise of θ_R above normal, while the control springs have a rise θ_U, we may write for the change in the indicated power, expressed in terms of the full-scale indication $C_D D_m$

$$\begin{aligned}\frac{\Delta P}{P}=\frac{D}{D_m}&\left\{\left(\frac{1}{h_1}-\frac{1}{h_2}\right)\beta\theta_R+\left(\frac{R_{U1}}{h_1R_1}-\frac{R_{U2}}{h_2R_2}\right)\gamma\theta_U\right\}\\&+\frac{C_X X}{C_D D_m}\left\{\frac{\beta\theta_R}{h_1}+\left(\frac{B_{U1}\gamma}{h_1R_1}+\eta\right)\theta_U\right\}\end{aligned} \tag{9B}$$

The first term in the right-hand member of this equation represents the temperature error in the null part of the indication, while the second term is the error in the deflection part.

If the factor h_2 is chosen equal to h_1, the null part will be independent of coil temperature θ_R and will be affected by room temperature and self-heating of the springs only to the extent indicated by the expression

$$\frac{\gamma\theta_U}{h_1}\left(\frac{R_{U2}}{R_2}-\frac{R_{U1}}{R_1}\right)$$

Since the resistance temperature coefficient γ of the alloy springs is rather small and h is 10 or more, while the ratios $\frac{R_{U1}}{R_1}$ and $\frac{R_{U2}}{R_2}$ of spring to coil resistance are also small, it is evident that the compensation will be nearly perfect. However, if θ_R is nearly equal to θ_U a

slightly better condition is obtained by making

$$\frac{h_2}{h_1}=\frac{\beta+\gamma\dfrac{R_{U2}}{R_2}}{\beta+\gamma\dfrac{R_{U1}}{R_1}} \tag{10B}$$

In this case the resultant temperature error in the null part is given by

$$\frac{\gamma\left(\dfrac{R_{U2}}{R_2}-\dfrac{R_{U1}}{R_1}\right)(\theta_R-\theta_U)}{h_1\left(1+\dfrac{R_{U2}}{R_2}\cdot\dfrac{\gamma}{\beta}\right)}$$

This involves only the difference $(\theta_R-\theta_U)$ between the temperature of the coils and that of the springs; this difference, which is due to self-heating, can be kept smaller than the unavoidable room-temperature changes likely to occur in service. In case the condition $\frac{R_{U2}}{R_2}=\frac{R_{U1}}{R_1}$ is realized, as is possible in an ammeter, the two desirable values of h_2 for a given h_1 become the same, and compensation of the null part of the indication is perfect.

In equation (9B) the second term, which indicates the error in the deflection part of the indication, can be made zero for room-temperature changes if h_1 is chosen to satisfy the relation

$$h_1=-\left(\frac{\beta}{\eta}+\frac{R_{U1}}{R_1}\frac{\gamma}{\eta}\right) \tag{11B}$$

Since η is usually negative while β and γ are positive, this equation leads to a positive value for h_1. If this is done the self-heating error arising from a difference $(\theta_R-\theta_U)$ in the temperatures of the coils and spring is only

$$-\frac{C_X}{C_D}\frac{X}{D}\frac{\{(\theta_R-\theta_U)\eta\}}{\{1+R_{U1}\gamma\}}{R_1\beta}$$

The value of h_1 required to satisfy equation (11B) is about 10. In the design of an ammeter this condition is easily met. In the case of a wattmeter for use at voltages of 100 volts or more the value $h_1=10$ requires the use of an inconveniently fine wire in the moving-coil winding. However, even if h_1 and h_2 are made very large the temperature error still only amounts to

$$\frac{\Delta P}{P}=\frac{C_X}{C_D}\frac{X}{D}\eta\,\theta_U \tag{12B}$$

In a instrument having 25 steps on the main dial $\frac{C_X}{C_D}\times\frac{X}{D}=0.02$, and for most suspension materials $\eta=0.0004$. Hence the net temperature coefficient will be only 8×10^{-6} per °C.

XI. APPENDIX C. INTERMINGLING OF COILS FOR COMPOSITE WINDINGS

In the construction of windings for composite-coil instruments the primary requirement is that the ratio G_{13}/G_{24} of the torque constant of the a. c. to that of the d. c. coils shall be affected as little as possible by the rotation of the moving coil. A sufficient, though not necessary condition for satisfying this requirement is that the magnetic field produced at any point in space by a given current in the a. c. winding of each coil shall have a ratio to the field produced at the same point by the same current in the d. c. winding, which is the same for all points. It is also desirable, but not essential, that this ratio be a small integer.

An obvious construction is to form a cable of insulated wires and to wind the coil with such a cable. A certain number of the strands are then joined to form the d. c. winding, while the remainder form the a. c. winding. This gives a very perfect intermingling, but has a very low space factor, and in the case of a moving coil the end connections add excessive weight and bulk and are awkward to make.

In the experimental ammeter described in this paper the fixed coils were wound with 10 wires fed on to the coil side by side in a flat ribbon. At the end of each layer the wires were transposed alternately by fives and singly, so that a fairly thorough intermingling was obtained. The space factor, while better than that of a cable winding, was still rather poor as compared with a normal layer winding. When the first five wires were chosen for the a. c. winding, the ratio G_{13}/G_{24} was found to differ from unity by about 1 per cent and to change with rotation of the moving coil at the rate of about 1 per cent per radian of coil motion. By selecting coils so as to minimize this latter effect, the departure from unity was reduced to 0.2 per cent and the rate of change to 0.02 per cent per radian.

A third method, in which all the turns of a layer are devoted to a single winding and the layers are suitably apportioned between the two windings, gives a considerably better space factor; the winding process is also much easier. A logical basis for this apportionment of the layers can be deduced as follows:

Suppose that the a. c. and d. c. layers have equal numbers of turns and are connected in series opposition. Then the best apportionment is that which for this connection makes the net magnetic field most nearly zero. The magnetic potential arising from the kth layer can be expressed (by Taylor's theorem) in the form

$$y(k\delta) = Q_0 + Q_1 k\delta + Q_2(k\delta)^2 \tag{1c}$$

where δ is the ratio of the thickness of one layer to the maximum radius of the coil. The magnetic potential of the entire coil is the sum of the contributions of all the layers, those assigned to the a. c. winding being taken as $+$, while those carrying d. c. are $-$. We thus get

$$y = Q_0 \sum_{k=1}^{k=\lambda} (1) + Q_1\delta \sum_{k=1}^{k=\lambda} k + Q_2\delta^2 \sum_{k=1}^{k=\lambda} k^2 \tag{2c}$$

where λ is the total number of layers. To make the first term zero it is sufficient that there be an equal number of $+$ and $-$ layers. If there are four layers, the second term can also be made to vanish

if the signs are taken to give $Q_1\delta\{+1-2-3+4\}$. Moreover, since in general

$$(q+1)-(q+2)-(q+3)+(q+4)=0 \qquad (3c)$$

each successive, mutually exclusive quartet of this type will vanish and the entire second term will vanish if λ is any multiple of 4. Furthermore,

$$(q+1)^2-(q+2)^2-(q+3)^2+(q+4)^2=1^2-2^2-3^2+4^2=+4 \qquad (4c)$$

and is also independent of q; hence if any quartet is affected by a sign opposite to that of an immediately adjacent quartet, this octet of terms involving Q_2 will also vanish and the entire term will drop out if λ is a multiple of 8. Similar relations hold for the higher terms. Thus we get the sequence of signs and apportionment of layers shown in Table 3.

TABLE 3

Layer No. k	Sign of term	Assignment of layer	Number of entries in group
1	+	a. c.	2^0
2	−	d. c.	2^1
3	−	d. c.	2^2
4	+	a. c.	
5	−	d. c.	2^3
6	+	a. c.	
7	+	a. c.	
8	−	d. c.	2^4
9	−	d. c.	
10	+	a. c.	
11	+	a. c.	
12	−	d. c.	
13	+	a. c.	
14	−	d. c.	
15	−	d. c.	
16	+	a. c.	
.	.	.	
.	.	.	
.	.	.	

To form the second column, for $k=2^\circ=1$ write +; for $k=2^1=2$ write −; for the next two terms repeat these with reversed signs ending with $k=2^2=4$ and +; for the next group repeat these four, but with reversed signs ending with $k=2^3=8$ and −; and so on.

In a coil of 2^{n+1} layers an assignment according to this scheme will balance the a. c. and d. c. ampere turns up to and including the terms in equation (1c) involving Q_n. This will be true even if the ampere turns of one set of layers are obtained by a different number of turns, provided that the thickness of any multiple layer is the same as that of a layer of the other winding.

As an experimental check on the effectiveness of this scheme, one of the four fixed coils of the experimental ammeter was replaced with one wound in 20 layers according to Table 3. The torque constants between this coil and one of the moving coils showed an excess of a. c. over d. c. torque of only 0.16 per cent, and the ratio of torques changed at the rate of 0.7 per cent per radian motion of the moving coil.

XII. NOTATION

A_2, A_4 = fractions of cross section of moving and fixed coils used for windings 2 and 4, respectively.

a_f, a_m = mean radius of fixed and moving coils, respectively.

b_f, b_m = axial length of fixed and moving coil windings, respectively.

C_D = main dial constant, watts (or (amperes)^2) per dial unit.

C_s = deflection constant, watts (or (amperes)^2) per scale division.

C_X = deflection constant, watts (or (amperes)^2) per centimeter.

c_m, c_f = radial depth of winding of moving and fixed coils, respectively.

D = reading of main dial in dial units.

D_m = total number of steps on main dial.

d_1, d_2 = diameter of wire used in coils 1, 2.

E_B = voltage of battery supplying d. c. circuits.

E_D = voltage drop in main dial at maximum setting.

E_s = electromotive force of standard cell.

E_1 = voltage of a. c. moving-coil circuit.

E_2, E_4 = voltage drops in coils 2 and 4 (both elements being considered as in series).

e = instantaneous voltage.

f = frequency, cycles per second.

G_{fm} = torque constant $= \frac{dM_{fm}}{d\alpha} \times 10^7$ dyne = cm per radian.

G_{24}, G_{13}, etc. = torque constants pertaining to the interaction between coils 2 and 4, 1 and 3, etc., respectively, of both elements.

G_{2c} = torque constant of compensating coil action on coil 2.

g_{fm} = proportionality constant defined by $\frac{1}{N_f N_m} \cdot \frac{dM_{fm}}{d\alpha}$.

h = desired ratio of total resistance to copper resistance in a potential circuit to give temperature compensation.

h_1, h_2 = actual ratios of total resistance to coil resistance of a. c. and d. c. moving-coil circuits, respectively.

I_f, I_m = currents in fixed and moving coils, respectively.

I'_f, I'_m = currents in fixed and moving coils, respectively, during check test.

I_1, I_2, etc. = currents in coils 1, 2, etc., respectively.

I_2', I_4' = alternating current induced in coils 2 and 4, respectively.

i_f, i_m = instantaneous value of currents in fixed and moving coils.

K = emissivity, watts dissipated per square cm per °C.

k = integer indicating location of layer in coil.

k_{fm} = coefficient of magnetic coupling between fixed and moving coils, defined as $M_f/\sqrt{L_f L_m}$.

L_f, L_m = self-inductance of fixed and moving coils, respectively.

l_f, l_m = inductance per turn of fixed and moving coils, respectively.

M = mutual inductance.

M_{fm} = mutual inductance between fixed and moving coils of one element.

M_{13}, M_{24}, etc., = mutual inductance between coils 1 and 3, 2 and 4, respectively, the two elements being in series.

M_{2c} = mutual inductance between coil 2 and compensating coil.

m = dimensionless factor.

N_f, N_m = number of turns in fixed and moving coils, respectively.

N_1, N_2, etc., = number of turns of coils 1, 2, etc., of one element.

n = integral exponent in Appendix C.

P = power in a. c. circuit, watts.

P_f, P_m = rate of heat dissipation at rated current and voltage, in fixed and moving coils, respectively, of one element.

p = empirical exponent in torque-weight criterion.

Q, Q' = coefficients in equations (1c) and (2c).

q = any integer.

R_A = resistance per step of main dial.

R_a = resistance of fine adjustment rheostat.

R_c = resistance of main-dial compensating rheostat at any setting.

R_B = total resistance of main dial.

R_f, R_m = resistance of fixed and moving coils, respectively.

R_g, R_h = resistances used to adjust ratio of moving-coil currents.

R_L = resistance added in calibrating circuit.

R_p = resistance of series resistor in a. c. moving-coil circuit.

R_q = resistance of a. c. shunt used in composite-coil ammeter.

R_s = resistance of standard-cell dial resistor.

R_T = resistance of series resistor in d. c. moving-coil circuit.

R_{U1}, R_{U2} = resistances of a. c. and d. c. springs or suspensions, respectively.

R_w = resistance of part of main dial in use.

R_1, R_2, etc. = resistances of coils, 1, 2, etc., respectively (for both elements in series).

R_2' = $R_2+R_T+R_d$ = total resistance of d. c. moving-coil circuit.

R_4' = total resistance of d. c. fixed-coil circuit.

r_f, r_m = resistance per (turn)^2 of fixed and moving coils, respectively.

S = reading of scale in divisions.

s = space factor.

T_f, T_m = time constants (L/R) of fixed and moving coils, respectively.

t = time.

U = stiffness of control springs in dyne-cm per radian motion of coil.

w = weight of complete moving element.
X = deflection of pointer or light spot, in centimeters.
y = dependent variable.
Z = equivalent pointer length (2 × length of reflected ray from moving mirror to scale).
Z_4 = impedance of d. c. fixed-coil circuit.
a = angular displacement of moving coil, in radians.
a_m = maximum angular motion of coil from central position.
β = temperature coefficient of resistance of moving coil.
γ = temperature coefficient of resistance of spring material.
δ = thickness of layer of winding divided by maximum radius.
η = temperature coefficient of elasticity of spring material.
θ = temperature rise above standard condition.
θ_R = temperature rise of moving coils.
θ_U = temperature rise of control springs.
λ = number of layers.
$\rho_f \rho_m$ = resistivity of metal used in fixed and moving coils, respectively.
τ = torque.
τ_U = torque of control spring.
τ_{ac} = torque arising from electrodynamic action of currents in a. c. coils.
τ_{dc} = torque arising from electrodynamic action of currents in d. c. coils.
ϕ = power factor angle.
ω = $2\pi \times$ frequency.

WASHINGTON, September 3, 1931.

SOME STUDIES OF RADIO TRANSMISSION OVER LONG PATHS MADE ON THE BYRD ANTARCTIC EXPEDITION [1]

By L. V. Berkner

ABSTRACT

Field intensity measurements of high-frequency signals (9,000 to 15,000 kc) over long paths, taken at Dunedin, New Zealand, during 1929–30, are given. The relation of diurnal and seasonal changes in signal intensity to the changes of daylight and darkness along the path is discussed. The effect of prolonged darkness along a given path is investigated. Special cases of the variation of signal intensity contrary to that which might be expected from the nature of variation of daylight along the path (during which the increase in attenuation through the daylight portion of the path with time apparently predominates over a slow decrease in the darkness portion of the path) are illustrated. The possibility of a shift in direction of the path of high-frequency signals has been observed under certain circumstances. Evidence of correlation between magnetic disturbances and loss in signal strength along certain paths is indicated, while a lack of such correlation along other paths at nearly the same time and along a reciprocal path is mentioned.

CONTENTS

	Page
I. Introduction	265
II. Method of measurement	265
III. Experimental data	266
IV. Discussion of observed data	267
V. Correlation with magnetic activity	276
VI. Summary	277
VII. Acknowledgments	278

I. INTRODUCTION

During the radio operations of the Byrd Antarctic expedition (1928–1930), regular observations and measurements were made at the operating bases. This paper deals with the studies of radio signal intensities and fading observations taken on signals arriving over long paths at Dunedin, New Zealand. These observations were made in accordance with a program outlined by the radio section, Bureau of Standards.

The Dunedin field station was located at an altitude of about 500 feet on a mountainside sloping directly to the Pacific Ocean. It was selected because of low noise level and other natural advantages.

II. METHOD OF MEASUREMENT

The general method has been used for several years by the Bureau of Standards for similar recording purposes. The signals were re-

[1] Presented at May 1, 1931, meeting of the International Union of Scientific Radio Telegraphy, American Section, Washington, D. C.

ceived on a high-frequency receiver of the double-detection type. A low intermediate frequency was used because of available equipment. The output of the intermediate frequency amplifier was rectified by means of a square law rectifier and continuously recorded on a Shaw recorder, driven by a synchronous timing motor. The over-all receiver gain was determined by means of a well-shielded local radio-frequency generator, using the current-resistance drop method for the determination of the input voltage. The receiver gain was adjusted by means of a calibrated attenuator in the intermediate amplifier circuit. The over-all receiver gain was determined with a signal of known value from the local radio-frequency generator at regular intervals of about 10 to 15 minutes during operation.

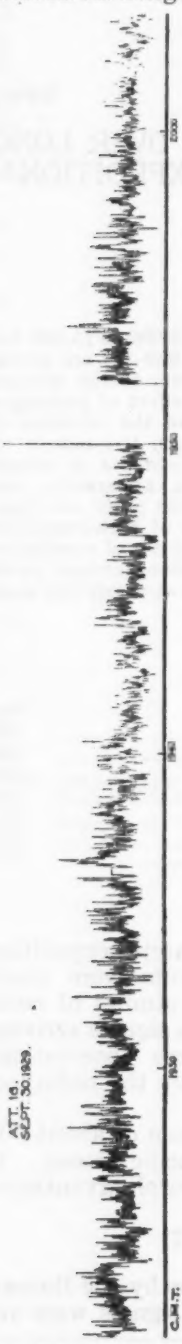

FIGURE 1.—*Typical record of signal intensity as recorded under steady conditions from station G5SW (11,750 kc), Chelmsford, England*

Because of the limitations in apparatus, absolute values of field intensity could be determined with only a moderate degree of accuracy. The comparative values, however, were determined to within about 10 per cent.

III. EXPERIMENTAL DATA

In Figure 1 is indicated the type of record obtained under normal steady conditions. Figures 2 and 3 show typical daily variations of field intensities based on 10-minute mean values taken from the actual records of the Shaw recorder, and smoothed as regards very rapid fading. Figures 4 to 9 show monthly averages of signal intensity measurements made on stations W2XAF, Schenectady, N. Y., U. S. A. (9,530 kc); PCJ, Eindhoven, Holland (9,580 kc); G5SW, Chelmsford, England (11,750 kc); W8XK, Pittsburgh, Pa., U. S. A. (11,800 kc); W6XN, San Francisco, Calif., U. S. A. (12,830 kc); and W2XAD, Schenectady, N. Y., U. S. A. (15,340 kc), for the period June, 1929, to October, 1929. The monthly averages embrace eight or more continuous daily measurements, so that short period disturbances do not greatly affect the averages. Where the number of observations is fewer, the curves have been dotted. Additional measurements of these stations were made during periods of occasional special transmission, occurring usually during the later evening hours, to obtain a more definite idea of the trends during these periods. These are not shown because of their irregularity.

IV. DISCUSSION OF OBSERVED DATA

Probably the simplest scheme for the study of these curves with regard to the nature of the daylight-darkness path traversed is a series of charts, such as is illustrated in Figures 11 and 12. These charts are based on a special projection of the earth, shown in Figure 10, with Dunedin, New Zealand, as a center, and the antipodal point as the boundary circle. A straight line drawn from the center of this

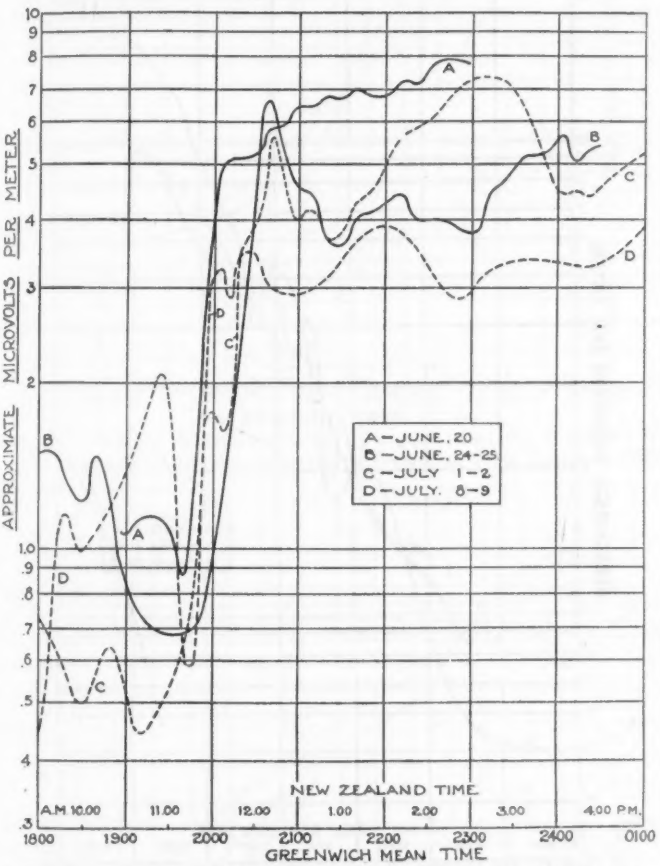

FIGURE 2.—*Typical daily variation of signal intensity of station G5SW, Chelmsford (11,750 kc), observed at Dunedin, New Zealand, 1929*

chart to any point shows the great-circle path and distance. Likewise, any straight line drawn from the center of the daylight-darkness charts to any point corresponding to a similar point on Figure 10 shows the conditions of daylight and darkness along the great-circle path to that point for the time of the chart. Similar studies have been made by Prescott [2] using a type of chart evolved on rectangular coordinates.

[2] M. L. Prescott, the Diurnal and Seasonal Performance of High-Frequency Radio Transmission Over Various Long-Distance Circuits. Proc. I. R. E.; November, 1930.

The effect of seasonal change upon signal intensities due to the change in the diurnal nature of the path is most marked with antipodal stations. The approximate three-dimensional graphs shown in Figures 13 and 14 are the result of the measurements of stations GBX (10,280 kc), G5SW (11,750 kc), and other southern English stations of about the same frequency, supplemented by about 10,000 aural observations of station GBX made by the Post and Telegraph

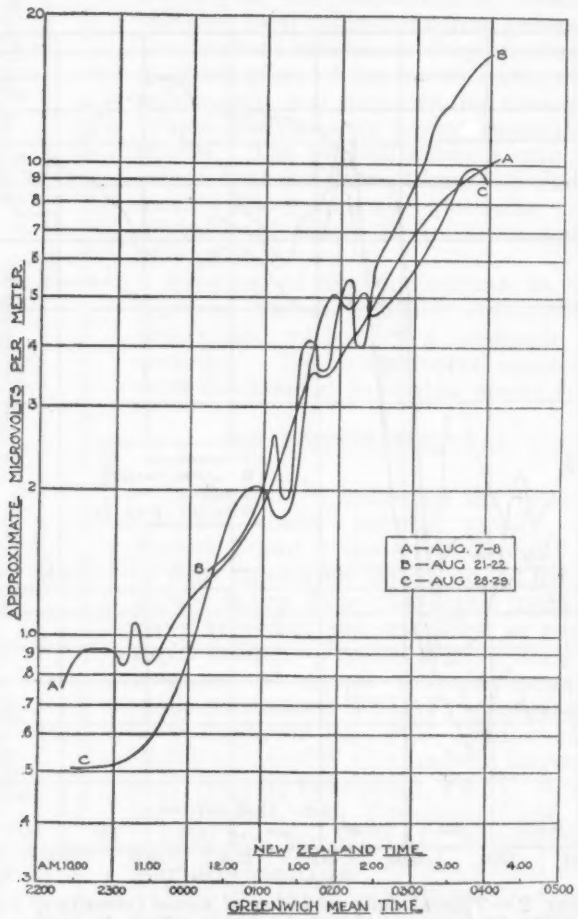

FIGURE 3.—*Typical daily variation of signal intensity of station W2XAD, Schenectady (15,340 kc), observed at Dunedin, New Zealand, 1929*

Department of the New Zealand Government at the Awarua radio station, and furnished through the courtesy of Mr. Gibbs, chief engineer. Small corrections determined by observation have been made to the measurements of G5SW to reduce them to approximate equivalents of GBX.

It is seen from Figures 13 and 14 that the signal intensity with respect to time of day is just inverted with season; that is, signals are received at noon (N. Z. T.) in June, fading out entirely at midnight

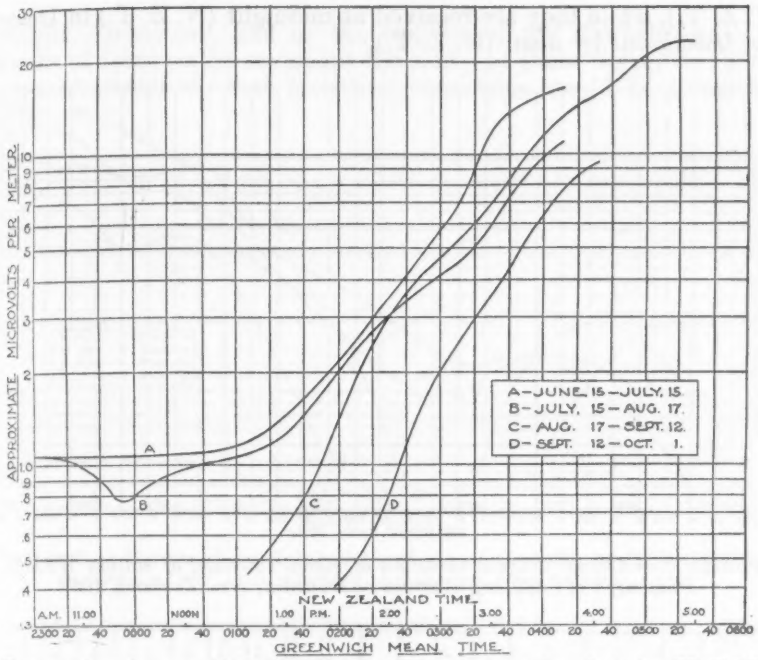

FIGURE 4.—*Average diurnal variation of signal intensity of station W2XAF Schenectady (9,530 kc), observed at Dunedin, New Zealand, 1929*

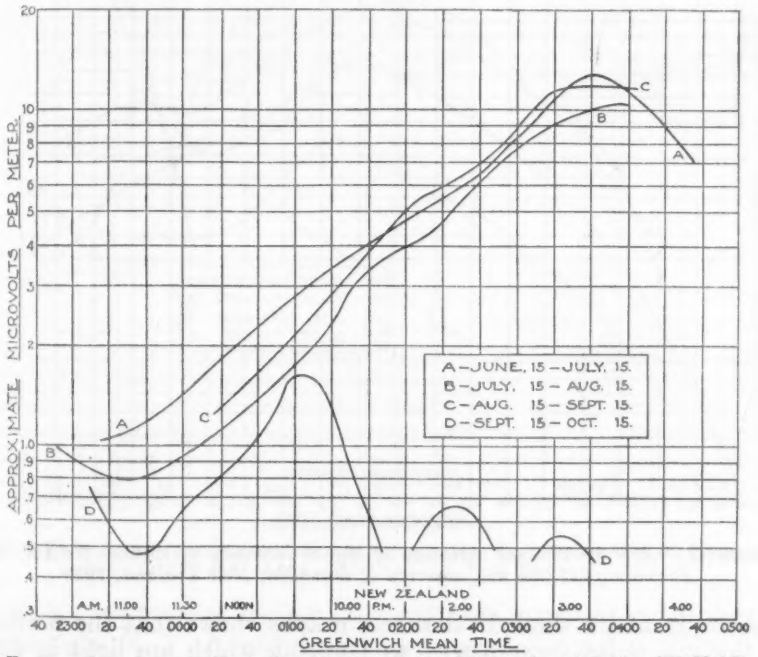

FIGURE 5.—*Average diurnal variation of signal intensity of station W2XAD, Schenectady (15,340 kc), observed at Dunedin, New Zealand, 1929*

(N. Z. T.), while they are received at midnight (N. Z. T.) in December, fading out by noon (N. Z. T.).

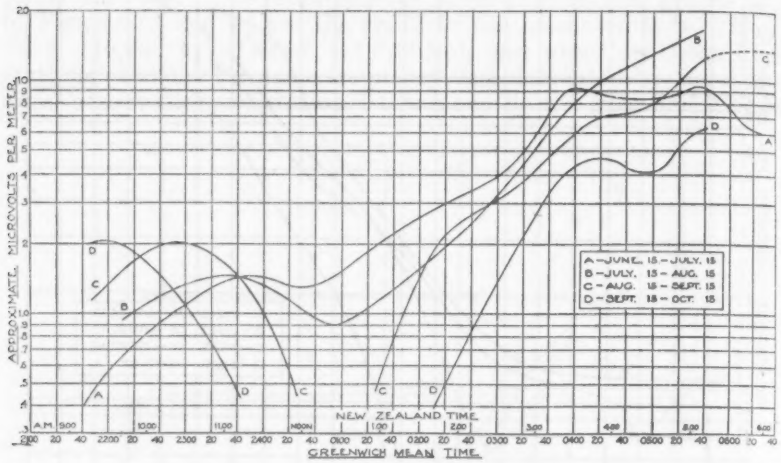

FIGURE 6.—*Average diurnal variation of signal intensity of station W8XK, Pittsburgh (11,880 kc), observed at Dunedin, New Zealand, 1929*

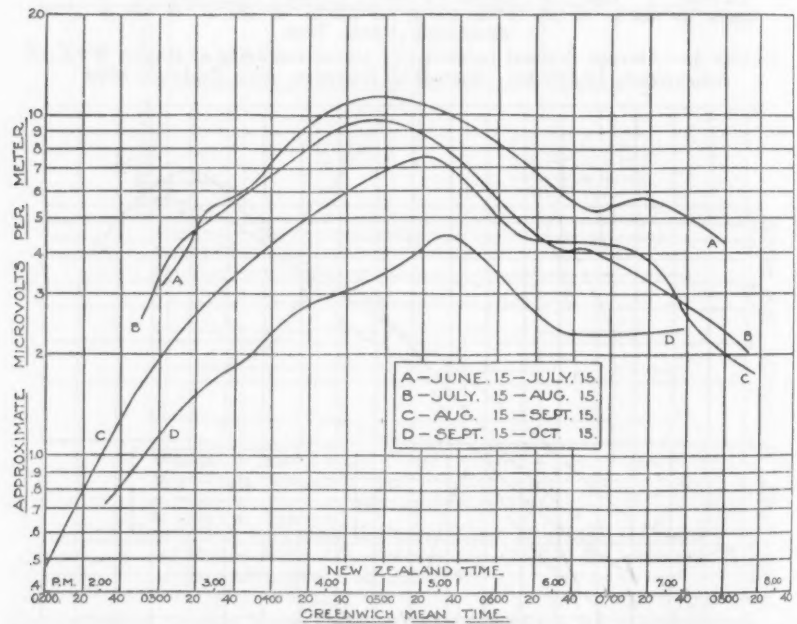

FIGURE 7.—*Average diurnal variation of signal intensity of station W6XN, San Francisco (13,830 kc), observed at Dunedin, New Zealand, 1929*

A study of the daylight-darkness graphs shows that the portions of the two paths from Rugby to Dunedin which are light in June at noon are dark in December at midnight. The signal, therefore, must traverse opposite paths around the earth at noon, June, and

midnight, December, and as the lengths of the daylight-darkness portions of these paths are about the same, at these times, we should expect, as observed, that reception conditions would be somewhat similar.

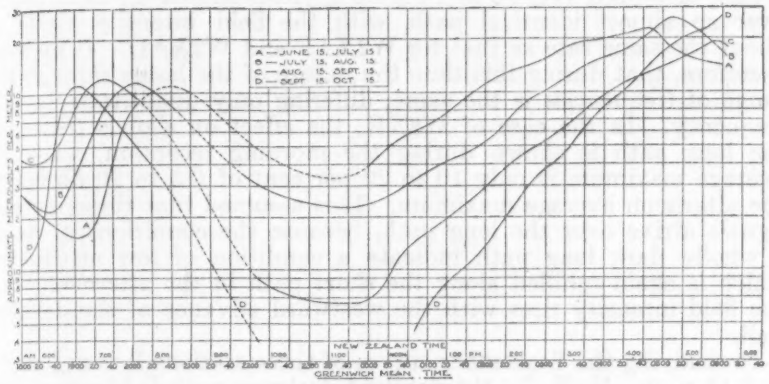

FIGURE 8.—*Average diurnal variation of signal intensity of station PCJ, Eindhoven (9,560 kc), observed at Dunedin, New Zealand, 1929*

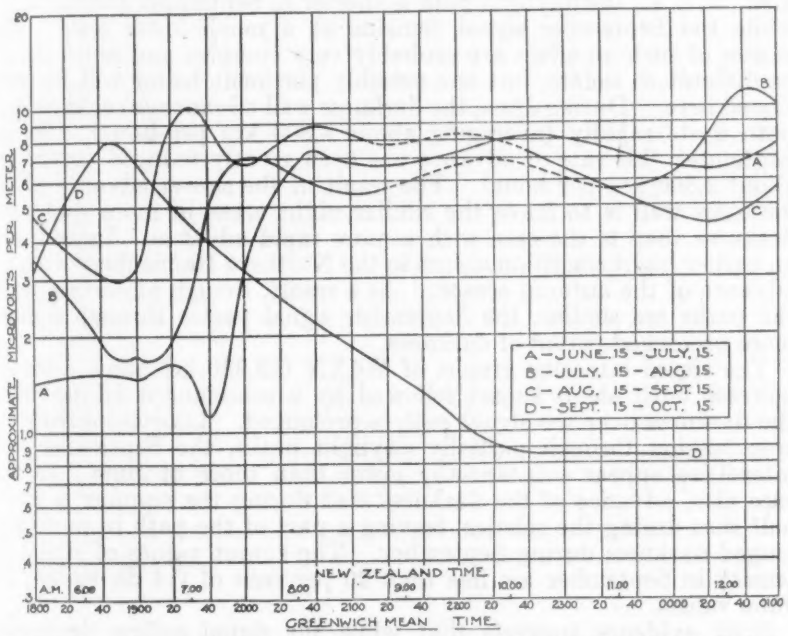
APPROXIMATE MICROVOLTS PER METER
A — JUNE 15 — JULY 15.
B — JULY 15 — AUG. 15.
C — AUG. 15 — SEPT. 15.
D — SEPT. 15 — OCT. 15.
NEW ZEALAND TIME
GREENWICH MEAN TIME

FIGURE 9.—*Average diurnal variation of signal intensity of station G5SW, Chelmsford (11,750 kc), observed at Dunedin, New Zealand, 1929*

Stations W2XAF (9,530 kc) and W2XAD (15,340 kc) located at Schenectady, N. Y., furnish an excellent comparison of two frequencies over the same path. It is seen that the higher frequency reaches a maximum much earlier in the day, as might be predicted. It is

of great interest, however, to note that field intensities at both frequencies rise at very nearly the same rate up to sunset. For any particular month, the rate of advance of the darkness wall is nearly uniform throughout the afternoon over this path. Study of the graphs of W8XK (11,800 kc), Figure 6, yields almost the same results over an almost identical path, with the field intensity rising at about the same rate as that for W2XAF and W2XAD. It appears, therefore, that during this time the nature of the losses through this range of frequencies is the same, differing only quantitatively with frequency. In the case of W8XK, the effect on signals traversing the long path is shown during the morning reception, when the average maximum is only 10 to 20 per cent of (15 to 20 db below) the afternoon average maximum. It is assumed that these morning signals arrive over the long path, because the conditions of nearly a wholly dark long path indicate a condition of low attenuation which is again fulfilled along the short path in the afternoon when the field intensity rises with the westward advance of the darkness wall.

In studying the September curves of these stations it is noted that at 2.15 p. m., N. Z. T., the daylight-darkness path is identical with that in June at the same time, while the signals are uniformly less than 20 per cent of (14 db below) the June values. Prior to 2.15 p.m., N.Z.T., the daylight path is shorter in September than in June, while the September signal remains at a much lower level. The causes of such an effect are probably very complex and must always be difficult to isolate, but one possibly pertinent factor will be mentioned here. During June, the darkness wall advances over the signal path quite rapidly (averaging about 4,800 km per hour). During September this rate of advance has been greatly reduced (averaging about 2,800 km per hour). The result of the slower advance of the darkness wall is to leave the similar night areas in more prolonged darkness than is the case with a more rapid advance. In addition, an earlier night condition occurs in the Northern Hemisphere with the advance of the autumn season. As a result, though at certain times the paths are similar, the September signal passes through a much more prolonged period of darkness.

The signal intensity graphs of W6XN (13,830 kc) show a steady increase until about sunset followed by a pronounced falling off as the darkness over the signal path is prolonged. Likewise during the transmission through partially daylight paths, the September field intensities appear substantially lower than those of June. In this case also, advance of the darkness wall during the equinox is about half that during the solstice, leaving a part of the path in more prolonged darkness during September. The sunset values of signal intensity in September are less than 20 per cent of (14 db below) the June values.

Such evidence suggests that while the signal suffers decreasing absorption in the ionized layer with the advance of the darkness wall, a second loss occurs, in darkness, increasing with frequency and as the darkness is prolonged. This loss becomes predominant after the maximum signal intensity has been reached, and causes a comparatively rapid drop in the signal intensities of the higher frequencies some time before sunset, becoming noticeable on the lower frequencies progressivley later.

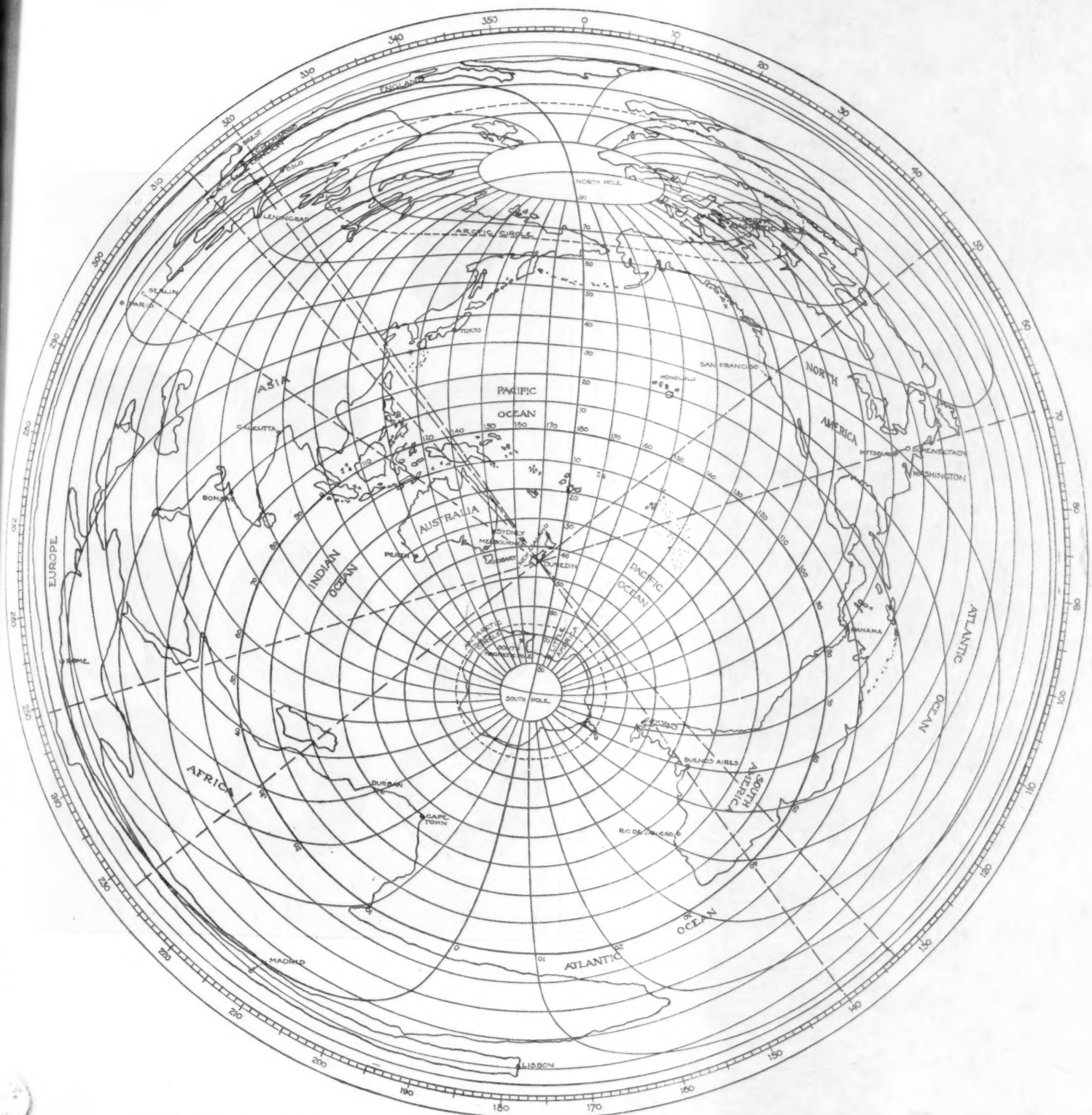

FIGURE 10.—*Chart of the world, showing great-circle distances and azimuths, from Dunedin, New Zealand*

94173—32. (Face p. 272.)

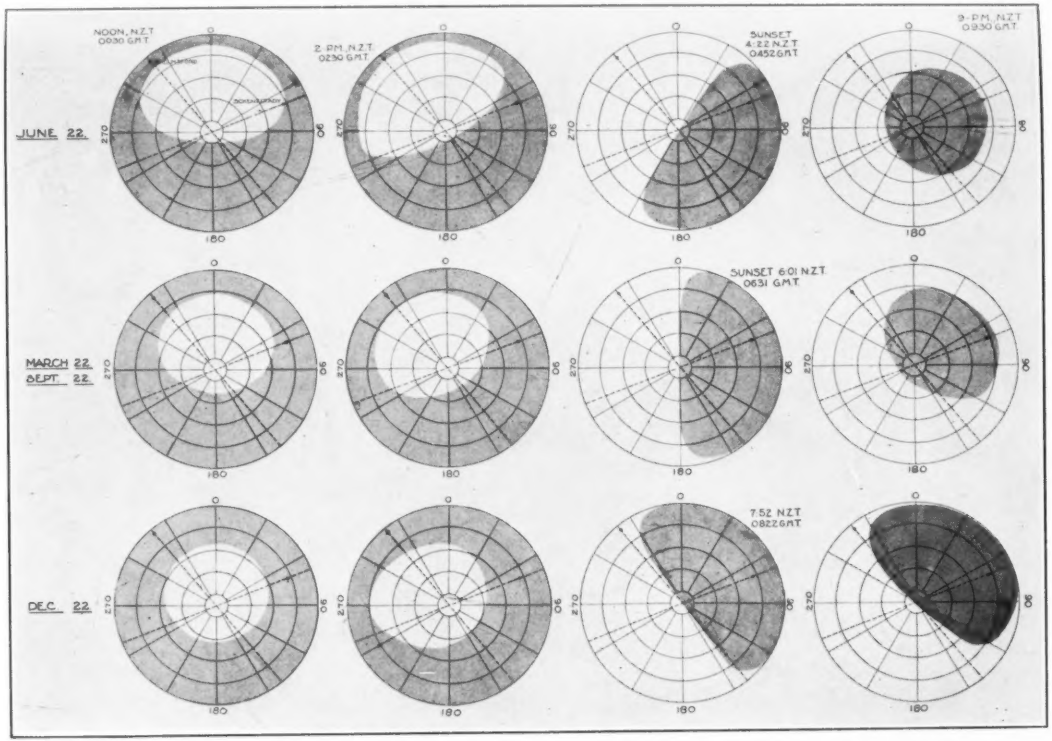

FIGURE 11.—*Diurnal and seasonal variation of daylight and darkness along any path from Dunedin, New Zealand (171 E. 46S.) Morning*

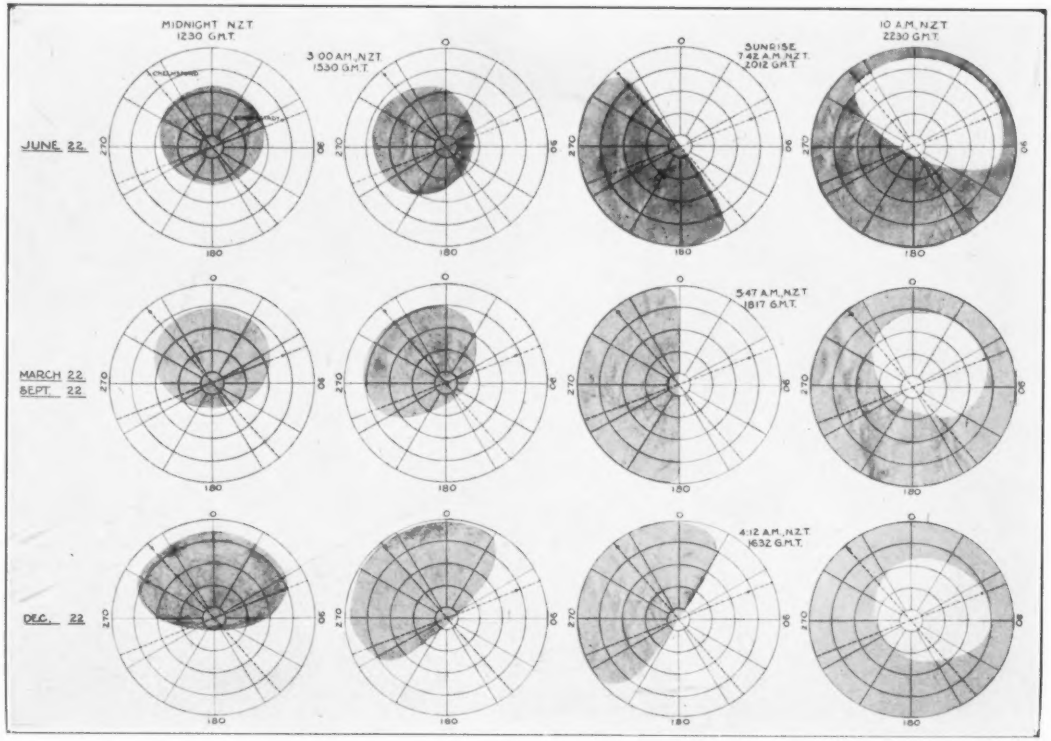

FIGURE 12.—*Diurnal and seasonal variation of daylight and darkness along any path from Dunedin, New Zealand. (171 E. 46 S.) Evening*

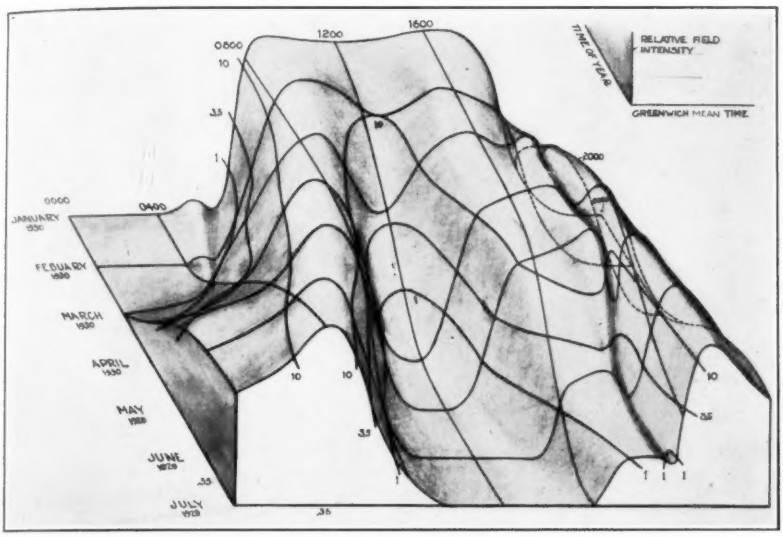

FIGURE *13.—Diurnal and seasonal variations of relative field intensity of GBX, Rugby (10,280 kc), observed at Dunedin and Awarna, New Zealand, 1929-1930*

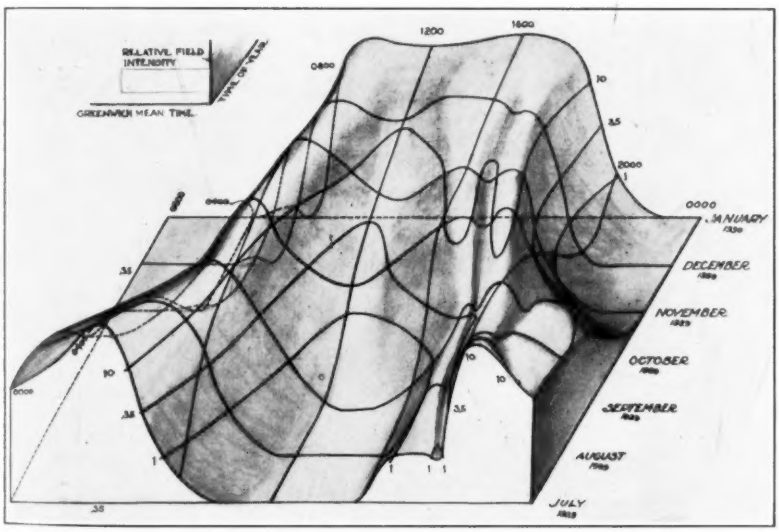

FIGURE *14.—Diurnal and seasonal variations of relative field intensity of GBX, Rugby (10,280 kc) observed at Dunedin and Awarna, New Zealand, 1929-1930*

UNIV. OF MICH.

It is to be noted in the case of PCJ (9,560 kc) that, in general, the variations in signal intensity follow the changes in daylight and darkness along the path. About midday (N. Z. T.), however, the length of the daylight path traversed starting at 10 a. m. to noon (N. Z. T.) decreases nearly uniformly, though slowly (averaging about 600 km per hour). At the same time the signal strength also decreases slowly. In the afternoon the darkness wall continues to approach at about the same rate while the signal rises quite rapidly, reaching fairly fixed values for given lengths of daylight and darkness paths during the period observed. For instance, at noon in June, the nature of the path is the same as at 3 p. m. in September, and the average signal at these times is the same. In this case the rate of change of daylight along the path is about the same in June as in September.

It appears that during the morning the advance of the darkness wall was so slow that the attenuation in the transmitting layer along the daylight portion of the path actually increased faster than the decrease in attenuation due to the advance of the darkness wall.

Another major deviation of change in signal intensity from the usual change with the daylight and darkness path will be mentioned in the case of G5SW. From Figures 2 and 9 it is seen that shortly before sunrise in June, the signal falls suddenly to a decided minimum, followed quickly by a very rapid rise of 10 to 20 times (20 to 25 db). Typical cases of original records are shown in Figures 15 and 16. This minimum occurs at about 7.10 a. m., N. Z. T., in June. By September this phenomenon has entirely disappeared. It is seen from Figures 11 and 17, that in June the signal path lies nearly parallel to the sunrise-sunset path. Up to 8 a. m., however, no marked variation is taking place in the retrogression of the darkness wall along the great-circle path, which might account for the sudden and large changes in signal intensity. In fact it might be expected from a general study of the daylight-darkness charts that a steady increase would take place throughout this period with a dip after 8 a. m., when the received signal would appear to change from the direct to the reverse path around the earth.

If the signal path is assumed to be shifted from 12° to 18° toward the poles, it appears that this phenomenon could be explained. Under these circumstances: (1) Up to 7.10 a. m., N. Z. T., the June signal rapidly decreases as the assumed path suddenly becomes all daylight; (2) at about 7.10 a. m., N. Z. T., the daylight along the two assumed paths becomes about equal and maximum, and the signal is a minimum; and (3) from 7.10 a. m., N. Z. T., to sunrise, the darkness rapidly increases along the assumed reverse path, reaching a maximum about 10 minutes after sunrise when the signal is a maximum.

This condition of fading becomes less and less marked as the season progresses until it has disappeared when the equinox is reached. There appears to be some indication, therefore, that some such shift in direction may take place, and that the signal may not necessarily travel along the great-circle path along the earth. Consideration of the earlier sunrise at the approximate Kennelly-Heaviside layer altitudes does not appear to alter the above discussion.

On the basis of this discussion, it might be predicted that a similar condition of fading would take place before sunset during midsummer. That this is actually the case is shown in Figures 13 and 14, a dip occurring about 7.15 p. m. N. Z. T. during December, whereas such

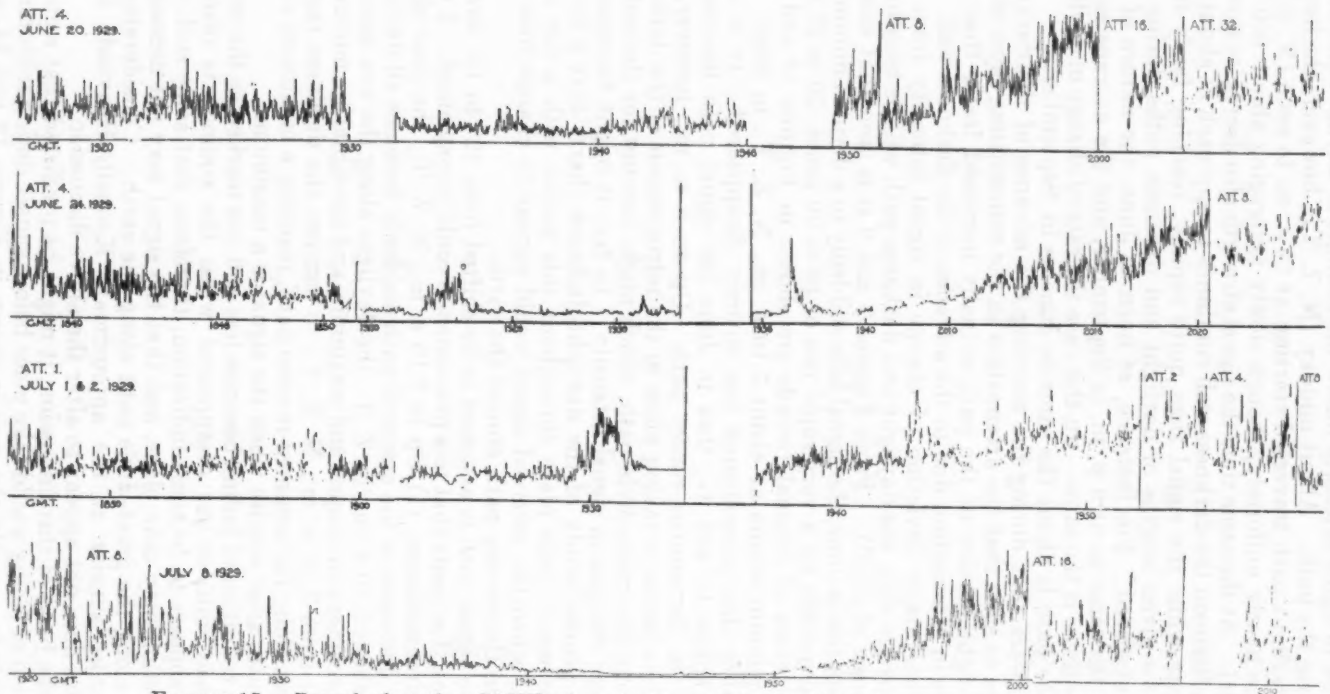

FIGURE 15.—*Record of station G5SW taken during period of critical change near sunrise (N. Z. T.)*

NOTE.—"ATT." indicates the value of attenuator step in the amplifier.

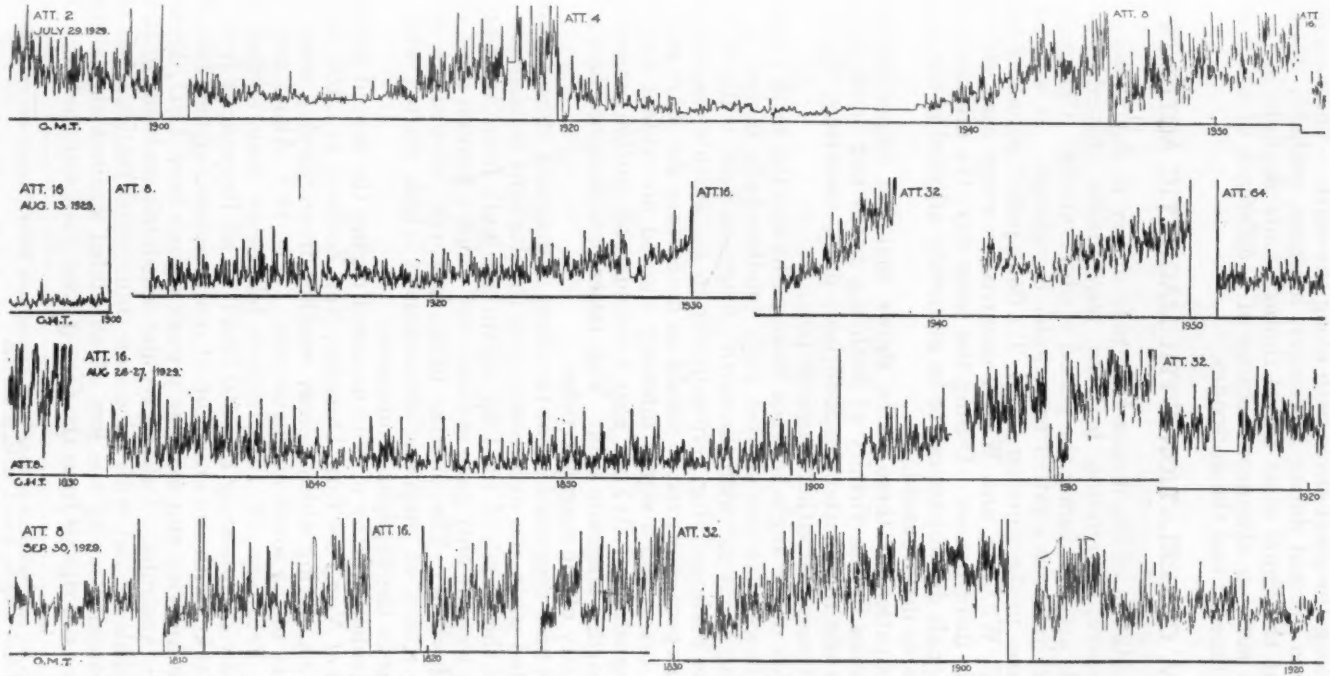

FIGURE 16.—*Records of station G5SW showing transition of period of critical change to a fairly steady condition with progression of season*

a change would be expected about an hour later were the signal to travel along the great circle path along the earth. These conditions are not so marked during December, however, probably due to the fact that the signal must travel through more daylight in the New Zealand summer afternoon because of a difference of about 9° between Dunedin and the antipodes.

V. CORRELATION WITH MAGNETIC ACTIVITY [3]

Examination of the measurements from day to day shows no evident general correlation between transmission disturbances and magnetic activity during the period of observations. One exception, however, indicates a rather remarkable correlation. It is noted that large losses in the morning (N. Z. T.) (long path)[4] signals of stations W2XAF, W2XAD, and W8XK occurred in every case with major magnetic disturbances. During the same day, the afternoon (short path) signals did not appear to be materially affected in the presence of the same disturbances.

Investigation of these paths shows that the longer (disturbed) path passes in the vicinity of both the north and south magnetic poles, while the shorter (undisturbed) path, traversing the Pacific, does not pass near either magnetic pole.

A study of the angle between these paths and the earth's magnetic field [5] shows that the shorter path (undisturbed) makes an angle averaging about 45° with the earth's magnetic field, while the longer path has portions lying perpendicular to the earth's magnetic field. In this respect, however, it should be noted that the short path from Europe (over which signal intensity showed no evident correlation with magnetic activity) has, also, a considerable portion perpendicular to the earth's magnetic field. This latter path does not pass so near the vicinity of the magnetic poles.

It has been suggested [6] that the effect of magnetic storms should be first noted when the path comes into the daylight hemisphere. Because of the length of the long (disturbed) path from American stations, it was the only path studied over which a portion must always be in daylight. The shorter path, however, showed no marked evident effects of magnetic dusturbances which started while this path was in the daylight hemisphere.

An incident worthy of note occurred during the second passage of the *City of New York* from Dunedin, New Zealand, to Little America, Antarctica, during which stormy weather drove the ship westward in proximity of the south magnetic pole. (Fig. 18.) About noon (0000 GMT), February 12, 1930, signals fell below their normal value, practically disappearing by 0600 GMT on all frequencies from 1,000 to 20,000 kc, with the exception of much reduced signals from WFA at Little America and extremely weak signals from LSD, Argentine, and VIS, Australia. Calls on regular schedule were made in an effort to establish contact with American commercial stations, but subsequent examination of the logs of scheduled stations shows that no indications of signals from the *City of New York* were heard. Condi-

[3] Anderson, C. N., Correlation of Long Wave Transatlantic Radio Transmission with Other Factors Affected by Solar Activity, Proc. I. R. E., p. 297; 1928.
[4] Anderson, D. N., Transatlantic Radio Transmission, Proc. I. R. E., p. 1528; 1929.
[5] Eckersley, T. L., An Investigation of Short Waves, J. I. E. E. (London), p. 992; 1929.
[6] Maris, H. B., and Hulburt, E. O., Wireless Telegraphy and Magnetic Storms. Proc. I. R. E., p. 494 1929.

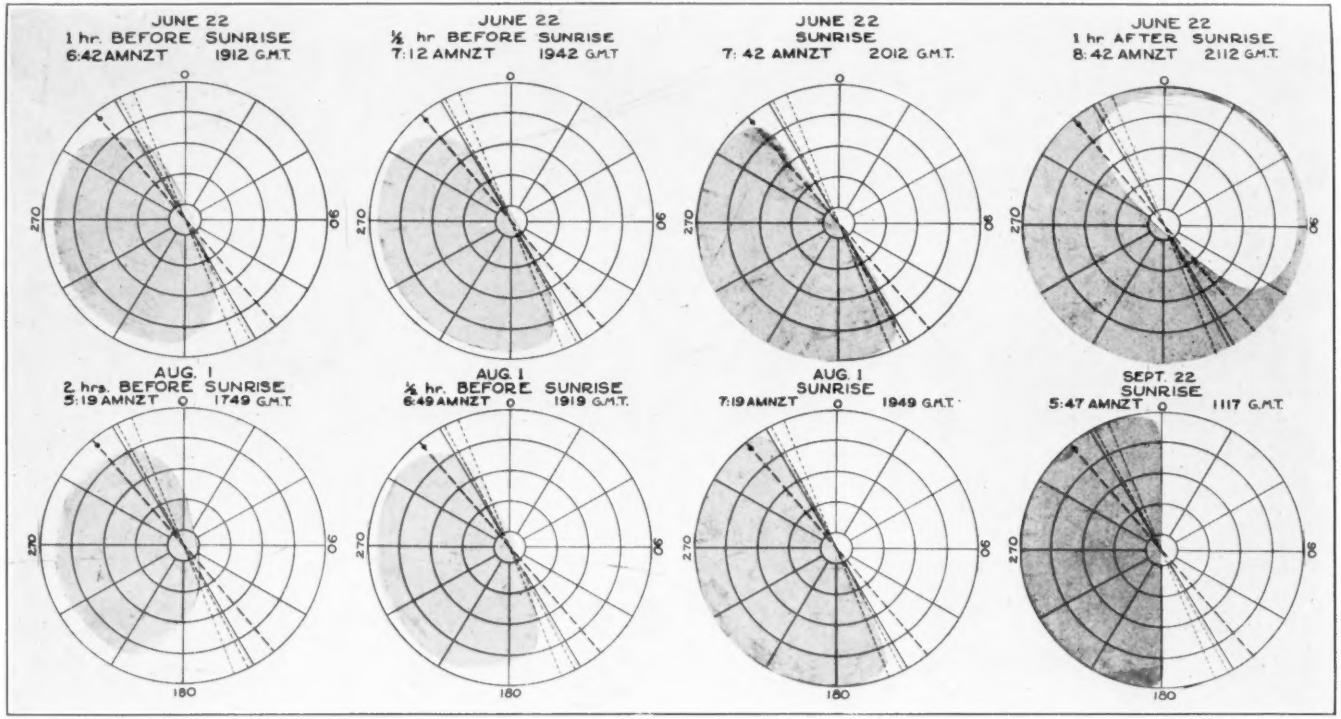

FIGURE 17.—*Seasonal variation of daylight and darkness along signal path through sunrise from Chelmsford, England, to Dunedin, New Zealand*

tions recovered slightly by noon, February 13, again becoming bad by 0600 GMT. General recovery was noted by the evening of February 14. During this period a major magnetic disturbance took place corresponding almost exactly to the disturbed transmission period. Though WFA, Little America, about 600 miles farther from the magnetic pole to the southeastward, noted much reduced signals, ordinary communications were carried on throughout the disturbed period. This would indicate that the effect was largely localized in the vicinity of the magnetic pole.

It is of interest that during September, 1929, when lower values of signal intensities were noted for all of the American stations, the

FIGURE 18.—*Position of "City of New York" during magnetic storm, Feb. 12 and 13, 1930*

Wolfer sun spot number was a minimum for the year. It is of equal importance, however, that European signals did not appear to show any marked variations in intensities during this time, so that it is doubtful if the low sun spot number had any bearing on the matters previously discussed.

VI. SUMMARY

It is, of course, impossible to draw any very general conclusions from the data obtained over such a limited period. It is known that these conditions are not exactly repeated from year to year, due to solar effects and, perhaps, other unknown factors. Mr. Shiel, of

Dunedin, for instance, reports the signals of 2XAD rather erratic during 1930–31; that is, not nearly as regular as during the period of measurement. However, certain repeated occurrences through the frequency ranges and paths considered may be mentioned:

1. In general, a signal minimum occurs over a wholly light path.
2. A rise in signal intensity generally occurs as the path becomes partially dark, higher frequencies rising and reaching a maximum progressively before the next lower frequency.
3. A steady fall in signal intensity occurs after the maximum has been reached, starting progressively down from the higher frequencies and becoming most pronounced after the path has become wholly dark. The transmission conditions do not appear to become fixed or steady either during daylight or darkness. A secondary rise and maximum is frequently observed as daylight approaches the transmitting end of the path.
4. An apparent diminution in signal intensity takes place generally for a given daylight-darkness path, when the darkness portion is prolonged.
5. A decrease in signal intensity appears to take place when the darkness wall is advancing so slowly as to apparently allow the attenuation along the prolonged daylight portion of the path to increase more rapidly than the diminution in attenuation at the advancing darkness wall.
6. A shift of the signal path may take place under certain circumstances, as suggested.

VII. ACKNOWLEDGMENTS

The writer wishes to acknowledge the support given this work by the Aeronautics Branch, Department of Commerce, through providing funds. He also acknowledges his indebtedness to Dr. J. H. Dellinger, T. Parkinson, S. S. Kirby, and T. R. Gilliland, of the Bureau of Standards, who made possible the project and supervised the assembly of the equipment; to the Post and Telegraph Department of the New Zealand Government, Mr. Gibbs, chief engineer, Mr. Macey, district telegraph engineer, and Mr. Head, chief operator of the Awarua radio station, who made possible the field station and lent their aid in making its operation successful; to Lalor Shiel, Dunedin, New Zealand, who very kindly aided in the measurements and made his factory shop facilities available; to Dr. Jack, University of Otago, for his assistance; and to the writers' colleagues on the expedition for their cooperation and assistance.

WASHINGTON, November 14, 1931.

RP413

PHASE EQUILIBRIA IN THE SYSTEM SiO_2-ZnO-Al_2O_3

By E. N. Bunting

ABSTRACT

A study of the phase equilibria in the system SiO_2-ZnO-Al_2O_3 shows that no ternary compounds are formed. Two ternary eutectics are present—one at 52 mole per cent SiO_4, 40 per cent ZnO, 8 per cent Al_2O_3 and $1,305 \pm 5°$ C., with tridymite, Zn_2SiO_4, and ZnO.Al_2O_3 as the solid phases; the other at 18.5 mole per cent SiO_2, 71.3 per cent ZnO, 10.3 per cent Al_2O_3, and $1,440 \pm 5°$ C., with ZnO, Zn_2SiO_4, and ZnO.Al_2O_3 as the solid phases. There are also two quintuple points which are not eutectics; one at 63 mole per cent SiO_2, 26 per cent ZnO, 11 per cent Al_2O_3, and $1,400 \pm 5°$ C., with tridymite, ZnO.Al_2O_3 and mullite as the solid phases; the other in the neighborhood of 40 mole per cent SiO_2, 23 per cent ZnO, 37 per cent Al_2O_3 at about 1,750° C. with Al_2O_3, ZnO.Al_2O_3, and mullite as solid phases.

From the standpoint of resistance to slag formation, an alumina retort containing as little silica as possible should give much better service than the ordinary clay retort as the container for the charge in the zinc retort furnace.

CONTENTS

		Page
I.	Introduction	279
II.	Materials and experimental procedure	280
III.	The binary systems	280
IV.	Experimental data	281
V.	Discussion	284
VI.	Acknowledgment	287

I. INTRODUCTION

In the recovery of zinc from its ores a mixture of coal and ore, in the form of impure zinc oxide, is heated in a clay retort to a temperature in the neighborhood of 1,300° C. At this temperature the retort is subjected to the slagging action of the zinc oxide and other oxides present as impurities, and in a month or two must be replaced. Since the retort is largely composed of silica and alumina, the study of the SiO_2-ZnO-Al_2O_3 system was undertaken to find out what reactions occur between the retort and the zinc oxide.

Previous work on this system has been limited to a study of deformation temperatures [1] [2] and glazes [3] and to the effect of reclaimed retort material and zinc oxide upon the physical properties of retort mixtures.[4]

[1] Kai Ching Lu, J. Am. Ceram. Soc., vol. 9, p. 29; 1926.
[2] Kallauner and Tykač, Stavivo, p. 113; 1929.
[3] Zimmer and Neff, J. Am. Ceram. Soc., vol. 12, p. 746; 1929.
[4] Wheeler and Kuechler, Bull. Am. Zinc Inst., vol. 10, No. 5–6, p. 97; 1927; Bull. Missouri School of Mines, vol. 10, No. 2; 1927.

II. MATERIALS AND EXPERIMENTAL PROCEDURE

A number of mixtures of SiO_2 (99.7 per cent), ZnO (99.9 per cent) and Al_2O_3 (99.7 per cent) were prepared in stick form and fused in the oxyhydrogen flame. The fused mixtures were pulverized in a diamond steel mortar and ground in an agate mortar. Three grindings and fusions of each mixture were made to obtain good homogeneity. Some ZnO was lost at each fusion, but the final product was sufficiently homogeneous to give reproducible results within 5° C. in the temperatures of crystallization. On analysis [5] all the mixtures were found to have been contaminated, on grinding, with from one to two tenths of a per cent of Fe_2O_3.

Small charges of these mixtures were placed in platinum or rhodium capsules and held at constant temperatures in an electric furnace [6] until equilibrium between the phases was obtained. The charge was then rapidly cooled by dropping into water, so that no change in the equilibrium could occur, and examined under the petrographic microscope to identify the phases present.

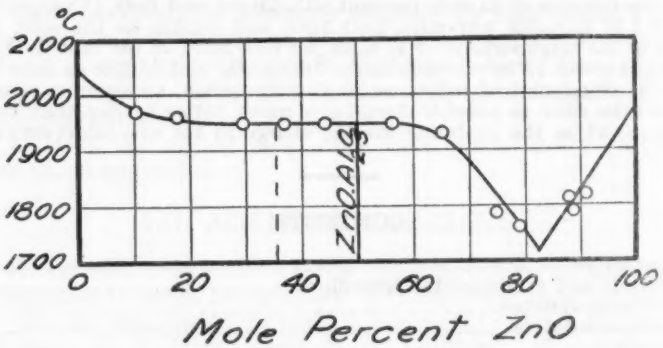

FIGURE 1.—*The binary system ZnO-Al_2O_3*

Temperatures were measured with a calibrated disappearing filament optical pyrometer and tolerances in temperature measurements are given within the limits of precision. The tolerances are probably about twice as large from the standpoint of accuracy of location on the temperature scale.

III. THE BINARY SYSTEMS

The data for the SiO_2-ZnO system are taken from a previous publication [7] and for the SiO_2-Al_2O_3 system from the work of Bowen and Greig.[8]

The ZnO-Al_2O_3 system was investigated by observing the melting points of various mixtures heated in a Pt-Ir button [9] by high-frequency induction. Figure 1 shows the melting point curve obtained, indicating a eutectic between ZnO and $ZnO.Al_2O_3$ at 1,720° ± 10° and 83 mole per cent ZnO. The melting point of $ZnO.Al_2O_3$ is 1,950° ± 10° C., at which temperature considerable vaporization of ZnO occurs.

[5] About one-third of the mixtures were analyzed by J. A. Scherrer.
[6] For a description of the furnace, see Bunting, B. S. Jour. Research, vol. 4, p. 131; 1930.
[7] See footnote 6.
[8] Bowen and Greig, J. Am. Ceram. Soc., vol. 7, pp. 238–254; 1924.
[9] See footnote 6.

$ZnO.Al_2O_3$ is found as a mineral, Gahnite, and has been prepared artificially in several ways, but no determination of its melting point is recorded in the literature. Although no definite location for the eutectic between $ZnO.Al_2O_3$ and Al_2O_3 could be found from the melting

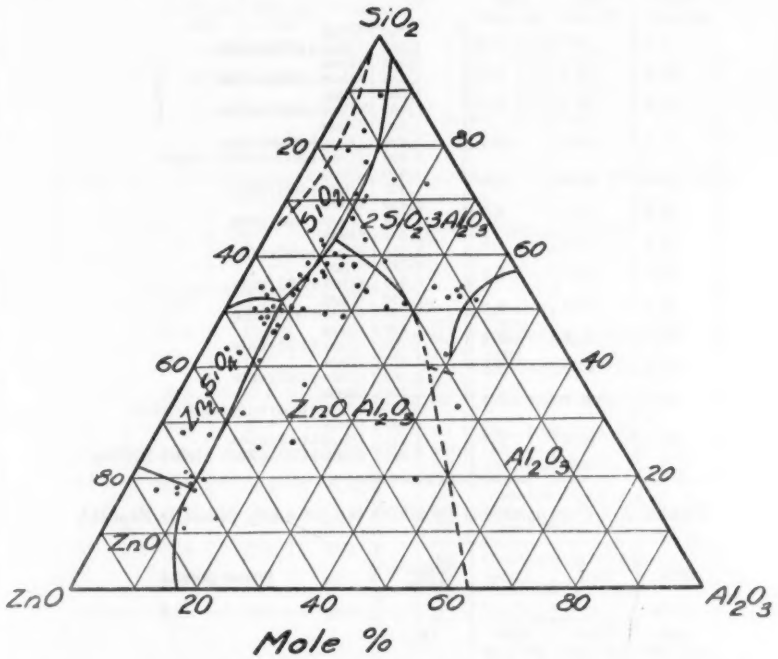

FIGURE 2.—*Diagram showing the compositions investigated and the fields of primary crystallization*

curve, it can not be much below 1,950° and its composition is probably between 30 and 40 mole per cent ZnO.

IV. EXPERIMENTAL DATA

The data obtained are given in Tables 1 to 6. Figure 2 shows the compositions investigated and the various fields within the equilibrium diagram.

TABLE 1.—*Compositions in which the primary phase is SiO_2*

SiO_2	ZnO	Al_2O_3	Temperature	Phases present
Mole per cent	*Mole per cent*	*Mole per cent*	°C.	
89.2	5.3	5.5	1,590	Glass.
			1,580	Glass+cristobalite.
83.0	11.1	5.9	1,595	Glass.
			1,585	Glass+cristobalite.
77.2	13.7	9.1	1,505	Glass.
			1,495	Glass+cristobalite.
71.7	18.2	10.1	1,500	Glass.
			1,490	Glass+cristobalite.
			1,480	Glass+SiO_2+$2SiO_2 \cdot 3Al_2O_3$.
63.1	28.0	8.9	1,430	Glass.
			1,420	Glass+tridymite.
62.2	28.1	9.7	1,410	Glass.
			1,400	Glass+tridymite.
58.6	32.6	8.8	1,395	Glass.
			1,385	Glass+tridymite.
56.9	34.7	8.4	1,380	Glass.
			1,370	Glass+tridymite.
54.7	37.3	8.0	1,330	Glass.
			1,325	Glass+tridymite.
55.0	41.6	3.4	1,400	Glass.
			1,390	Glass+tridymite.
53.5	40.9	5.6	1,370	Glass.
			1,360	Glass+tridymite.
53.7	37.2	9.1	1,370	Glass.
			1,360	Glass+tridymite+$ZnO \cdot Al_2O_3$.
53.2	38.0	8.8	1,340	Glass.
			1,335	Glass+tridymite.
			1,305	Glass+SiO_2+$ZnO \cdot Al_2O_3$+Zn_2SiO_4.

TABLE 2.—*Compositions in which the primary phase is Zn_2SiO_4*

SiO_2	ZnO	Al_2O_3	Temperature	Phases present
Mole per cent	*Mole per cent*	*Mole per cent*	°C.	
53.1	42.1	4.8	1,350	Glass.
			1,345	Glass+Zn_2SiO_4.
51.0	41.7	7.3	1,330	Glass.
			1,325	Glass+Zn_2SiO_4.
			1,305	Glass+Zn_2SiO_4+SiO_2+$ZnO \cdot Al_2O_3$.
50.8	45.0	4.2	1,390	Glass.
			1,385	Glass+Zn_2SiO_4.
50.3	43.1	6.6	1,340	Glass.
			1,335	Glass+Zn_2SiO_4.
49.3	43.7	7.0	1,335	Glass.
			1,330	Glass+Zn_2SiO_4.
49.0	44.7	6.3	1,345	Glass.
			1,340	Glass+Zn_2SiO_4.
48.1	44.9	7.0	1,345	Glass.
			1,340	Glass+Zn_2SiO_4.
43.8	52.8	3.4	1,425	Glass.
			1,420	Glass+Zn_2SiO_4.
42.8	51.2	6.0	1,415	Glass.
			1,410	Glass+Zn_2SiO_4.
32.1	59.7	8.2	1,440	Glass.
			1,435	Glass+Zn_2SiO_4.
28.5	67.6	3.9	1,495	Glass.
			1,490	Glass+Zn_2SiO_4.
27.9	63.9	8.2	1,475	Glass.
			1,470	Glass+Zn_2SiO_4.
21.0	70.9	8.1	1,490	Glass.
			1,480	Glass+Zn_2SiO_4.
20.6	70.8	9.1	1,480	Glass.
			1,475	Glass+Zn_2SiO_4.
18.5	71.5	10.0	1,450	Glass.
			1,445	Glass+Zn_2SiO_4.

TABLE 3.—*Compositions in which the primary phase is ZnO*

SiO_2	ZnO	Al_2O_3	Temperature	Phases present
Mole per cent	*Mole per cent*	*Mole per cent*	° *C.*	
18.8	73.5	7.7	1,490	Glass.
			1,480	Glass+ZnO.
17.9	77.3	4.8	1,590	Glass.
			1,580	Glass+ZnO.
17.5	74.1	8.6	1,530	Glass.
			1,520	Glass+ZnO.

TABLE 4.—*Compositions in which the primary phase is $2SiO_2.3Al_2O_3$*

SiO_2	ZnO	Al_2O_3	Temperature	Phases present
Mole per cent	*Mole per cent*	*Mole per cent*	° *C.*	
73.7	11.1	15.2	1,595	Glass.
			1,585	Glass+$2SiO_2.3Al_2O_3$.
70.7	17.2	12.1	1,505	Glass.
			1,500	Glass+$2SiO_2.3Al_2O_3$.
70.3	17.5	12.2	1,500	Glass.
			1,495	Glass+$2SiO_2.3Al_2O_3$.
62.5	22.5	15.0	1,515	Glass.
			1,505	Glass+$2SiO_2.3Al_2O_3$.
59.2	20.0	20.8	1,560	Glass.
			1,550	Glass+$2SiO_2.3Al_2O_3$.
54.5	14.5	31.0	1,780	Glass.
			1,770	Glass+$2SiO_2.3Al_2O_3$.
54.2	10.4	35.4	1,805	Glass.
			1,795	Glass+$2SiO_2.3Al_2O_3$.
53.4	11.6	35.0	1,800	Glass.
			1,790	Glass+$2SiO_2.3Al_2O_3$.
52.7	11.2	36.1	1,810	Glass.
			1,800	Glass+$2SiO_2.3Al_2O_3$.
41.9	19.0	39.1	1,810	Glass.
			1,800	Glass+$2SiO_2.3Al_2O_3$.

TABLE 5.—*Compositions in which the primary phase is $ZnO.Al_2O_3$*

SiO_2	ZnO	Al_2O_3	Temperature	Phases present
Mole per cent	*Mole per cent*	*Mole per cent*	°*C.*	
60.6	27.4	12.0	1,410	Glass.
			1,400	Glass+$ZnO.Al_2O_3$.
59.8	26.4	13.8	1,480	Glass.
			1,470	Glass+$ZnO.Al_2O_3$.
58.5	29.3	12.2	1,415	Glass.
			1,405	Glass+$ZnO.Al_2O_3$.
58.5	24.8	16.7	1,540	Glass.
			1,530	Glass+$ZnO.Al_2O_3$.
57.0	31.1	11.9	1,415	Glass.
			1,410	Glass+$ZnO.Al_2O_3$.
55.4	33.0	11.6	1,415	Glass.
			1,405	Glass+$ZnO.Al_2O_3$.
55.5	34.4	10.1	1,390	Glass.
			1,380	Glass+$ZnO.Al_2O_3$.
54.9	26.5	18.6	1,570	Glass.
			1,560	Glass+$ZnO.Al_2O_3$.
53.7	37.2	9.1	1,370	Glass.
			1,360	Glass+$ZnO.Al_2O_3$+SiO_2.
53.2	38.0	8.8	1,340	Glass.
			1,335	Glass+$ZnO.Al_2O_3$.
			1,305	Glass+$ZnO.Al_2O_3$+Zn_2SiO_4+SiO_2.
53.2	26.5	20.3	1,575	Glass.
			1,565	Glass+$ZnO.Al_2O_3$.
51.0	20.2	28.8	1,710	Glass.
			1,700	Glass+$ZnO.Al_2O_3$.
			1,690	Glass+$ZnO.Al_2O_3$+$2SiO_2.3Al_2O_3$.
50.9	24.0	25.1	1,590	Glass.
			1,580	Glass+$ZnO.Al_2O_3$.
50.8	39.3	9.9	1,395	Glass.
			1,385	Glass+$ZnO.Al_2O_3$.

TABLE 5.—*Compositions in which the primary phase is $ZnO.Al_2O_3$*—Con.

SiO_2	ZnO	Al_2O_3	Temperature	Phases present
Mole per cent	*Mole per cent*	*Mole per cent*	°C.	
50.8	40.8	8.4	1,340	Glass.
			1,330	Glass+$ZnO.Al_2O_3$.
			1,305	Glass+$ZnO.Al_2O_3$+Zn_2SiO_4+SiO_2.
50.3	37.9	11.8	1,435	Glass.
			1,425	Glass+$ZnO.Al_2O_3$.
49.6	34.2	16.2	1,520	Glass.
			1,510	Glass+$ZnO.Al_2O_3$.
49.1	31.7	19.2	1,580	Glass.
			1,570	Glass+$ZnO.Al_2O_3$.
47.6	43.1	9.3	1,350	Glass.
			1,340	Glass+$ZnO.Al_2O_3$.
45.6	42.8	11.6	1,440	Glass.
			1,430	Glass+$ZnO.Al_2O_3$.
41.6	48.9	9.5	1,390	Glass.
			1,380	Glass+$ZnO.Al_2O_3$.
32.0	56.2	11.8	1,450	Glass.
			1,440	Glass+$ZnO.Al_2O_3$.
26.0	57.1	16.9	1,560	Glass.
			1,550	Glass+$ZnO.Al_2O_3$.
24.5	37.6	37.9	1,650	Glass+$ZnO.Al_2O_3$.
19 5	35.4	45.1	1,700	Glass+$ZnO.Al_2O_3$.
19.4	69.2	11.4	1,500	Glass.
			1,495	Glass+$ZnO.Al_2O_3$.
18.1	71.3	10.6	1,450	Glass.
			1,445	Glass+$ZnO.Al_2O_3$.
			1,440	Glass+$ZnO.Al_2O_3$+ZnO+Zn_2SiO_4.
15.0	74.5	10.5	1,605	Glass.
			1,595	Glass+$ZnO.Al_2O_3$.
10.9	76.3	12.8	1,690	Glass.
			1,680	Glass+$ZnO.Al_2O_3$.
8.4	79.6	12.0	1,710	Glass.
			1,700	Glass+$ZnO.Al_2O_3$.

TABLE 6.—*Compositions in which the primary phase is Al_2O_3*

SiO_2	ZnO	Al_2O_3	Temperature	Phases present
Mole per cent	*Mole per cent*	*Mole per cent*	°C.	
52.0	9.2	38.8	1,825	Glass.
			1,815	Glass+Al_2O_3.
32.4	22.1	45.5	1,800	Glass+Al_2O_3.

V. DISCUSSION

From Figures 2 and 3 it is seen that no ternary compounds are formed. Two ternary eutectics are present; one (*E*, fig. 3) at 52 mole per cent SiO_2, 40 per cent ZnO, 8 per cent Al_2O_3 and 1,305 ± 5° C., with tridymite, Zn_2SiO_4, and $ZnO.Al_2O_3$ in equilibrium with liquid and vapor phases. The other eutectic (*E'*) is at 18.5 mole per cent SiO_2, 71.3 per cent ZnO, 10.3 per cent Al_2O_3 and 1,440 ± 5° C., with ZnO, Zn_2SiO_4, and $ZnO.Al_2O_3$ as the solid phases. There are also two quintuple points which are not eutectics; one (*Q*) at 63 mole per cent SiO_2, 26 per cent ZnO, 11 per cent Al_2O_3 and 1,400 ± 5° C., with tridymite, $ZnO.Al_2O_3$ and $2SiO_2.3Al_2O_3$ as the solid phases; the other (*Q'*) in the neighborhood of 40 mole per cent SiO_2, 23 per cent ZnO, and 37 per cent Al_2O_3 at about 1,750° C. with Al_2O_3, $ZnO.Al_2O_3$, and $2SiO_2.3Al_2O_3$ as the solid phases. A maximum temperature (1,460°, point *M*) is found on the Zn_2SiO_4, $ZnO.Al_2O_3$ boundary curve in accordance with Alkemade's rule, which states that the temperature along a boundary curve rises toward the line which connects the

compositions of the two solid phases which are in equilibrium with the solution along that boundary. Point *M* is the only point in the ternary system which is a eutectic between two binary compounds, in this case Zn_2SiO_4 and $ZnO.Al_2O_3$.

Figure 3 shows the course of crystallization within the various fields, the arrows pointing in the direction of falling temperatures. For example, with a molten composition represented by point *P* in the $ZnO.Al_2O_3$ field, as the temperature falls, $ZnO.Al_2O_3$ first crystallizes out and the composition of the remaining solution follows along the line *PR* and then along the boundary curve, where Zn_2SiO_4 also crystallizes out, until the ternary temperature (1,305°) and eutectic *E* is reached, where some SiO_2 is deposited and the whole becomes

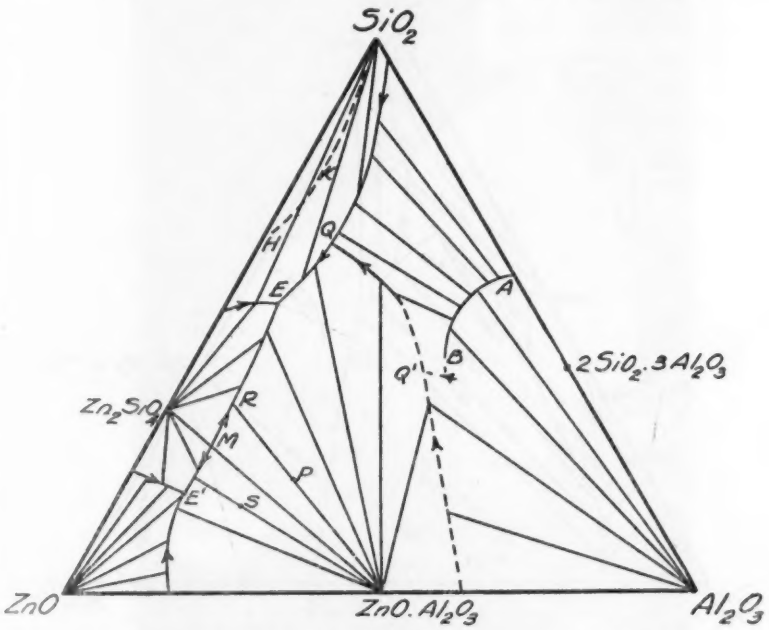

FIGURE 3.—*Diagram indicating the crystallization paths within the various fields, and the eutectic and quintuple points*

solid. Any molten composition lying on the line connecting *M* to $ZnO.Al_2O_3$ becomes completely solid at 1,460° C. when the composition of the liquid reaches point *M*. A molten composition lying below this line, such as *S*, does not become completely crystallized until the temperature of eutectic *E'* is reached (1,440°). All molten compositions in the SiO_2, Al_2O_3, and $2SiO_2.3Al_2O_3$ fields must be cooled to the temperature (1,305°) of eutectic *E* before becoming completely crystallized. The boundary *AB* is an isotherm (1,810°) where $2SiO_2.3Al_2O_3$ breaks down to Al_2O_3 and solution. Compositions to the left of the boundary *HK* separate into two immiscible liquids above 1,695°. A solid model of the temperature-concentration diagram is shown in Figures 4 and 5, and Figure 6 is a projection of the solid model onto the concentration plane.

We can now predict the slagging action on any clay retort when heated in the presence of ZnO. Were the retort composed of only SiO_2 and Al_2O_3 and were no impurities present with the ZnO, the lowest temperature at which slagging would begin is 1,305° C. Suppose that when some of the eutectic liquid is formed it takes up impurities to the extent of 20 mole per cent. Its melting point is lowered to 930° C., as calculated from data obtained from systems involving SiO_2, Al_2O_3, and ZnO. Practically all clay retort bodies contain 70 mole per cent SiO_2 or more, and a line connecting this composition in the $SiO_2.Al_2O_3$ side of the diagram with the ZnO corner of the diagram shows how the composition of the retort changes

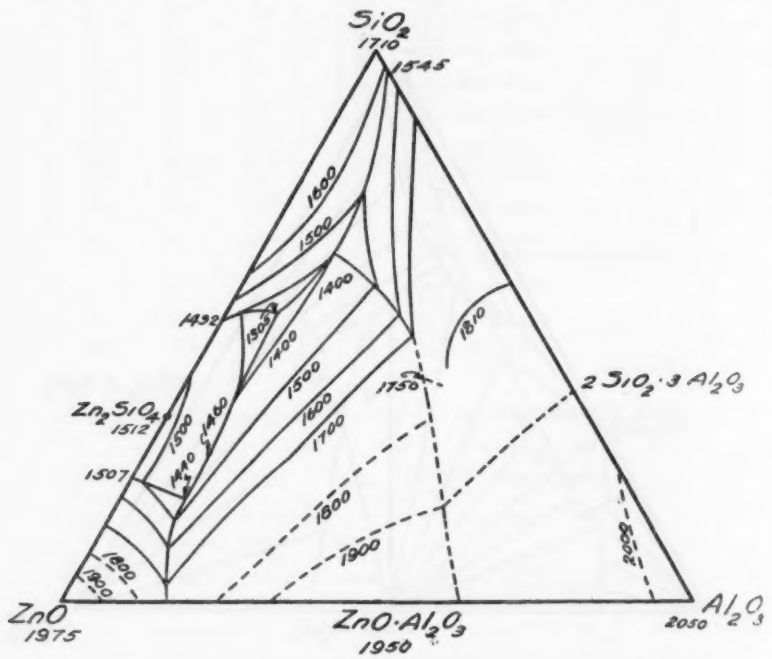

FIGURE 6.—*Projection of concentration-temperature diagram on concentration plane showing isotherms, melting temperatures of compounds, and temperatures of quintuple points and eutectics*

as ZnO is absorbed. Analyses of old zinc retorts[10] show that as much as 20 mole per cent of ZnO may be present in the walls of a retort. A composition of 20 mole per cent ZnO, 20 per cent Al_2O_3 and 60 per cent SiO_2 is totally melted at 1,560° C. When this composition is heated to 1,400° C., the highest temperature reached in firing the retorts, about 75 per cent by weight will be melted. A composition containing only 5 mole per cent ZnO with 25 per cent Al_2O_3 and 70 per cent SiO_2, which is all molten at about 1,725° C., will be 18 per cent melted at 1,400° C.[11] It is thus evident that any clay retort will be subject to considerable slagging at the higher temperatures used in the production of zinc. Were the slagging the only property

[10] Marbaker, J. Am. Ceram. Soc., vol. 14, p. 162; 1931.
[11] For method of calculation, see Rankin and Wright, Am. J. Sci., vol. 39, p. 1; 1915.

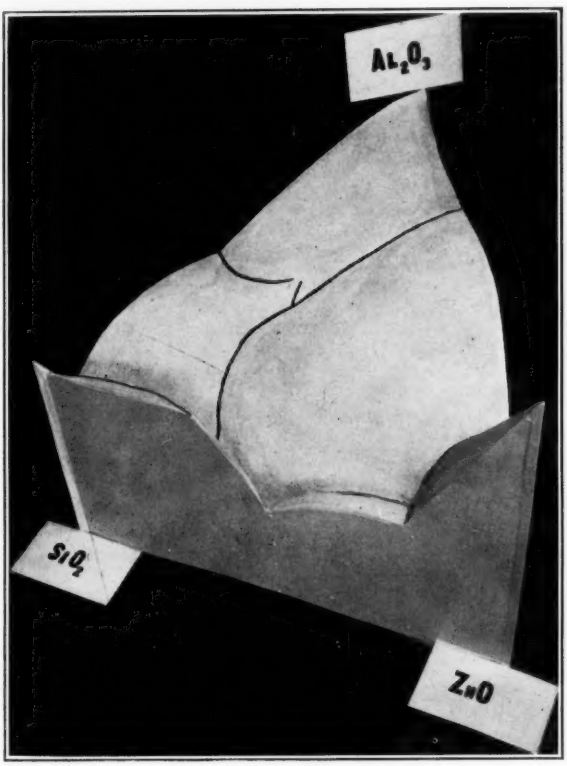

FIGURE 4.—*Solid model of the concentration-temperature diagram*

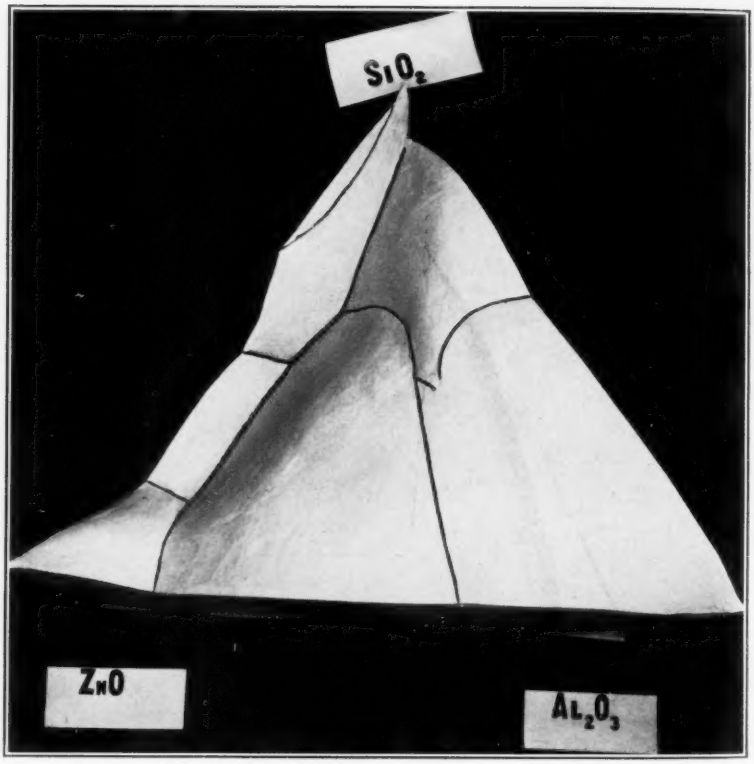

FIGURE 5.—*Photograph of solid model taken from above*

to be considered, a retort of pure alumina, or alumina and zinc oxide, with only enough clay to act as binder and a suitable amount of old retort as grog, would be the most desirable.

The amount of zinc oxide which can be added to a retort batch so that excessive slagging will not occur at high temperatures depends upon the percentages of silica and alumina in the batch. Examination of Figure 6 shows that the addition of 20 per cent of zinc oxide to a high silica batch will give a composition with a much higher molten fraction at 1,400° C. than that of a high alumina batch having the same amount of added zinc oxide. A new retort takes up zinc oxide by the diffusion of metallic zinc vapor through its pores, with the subsequent oxidation of the zinc to oxide in the walls of the retort, where the oxide reacts with the retort body. Although both zinc silicate and aluminate are slowly reduced by carbon at 1,300° to 1,400° C., conditions within the walls of a retort in the furnace are not sufficiently reducing to prevent the formation of zinc oxide. The extent to which zinc oxide penetrates into the retort walls will largely depend upon their porosity and the length of time the retort is in service, and the inclusion of zinc oxide in the retort batch probably would not hinder the absorption of additional zinc. However, a high alumina batch can stand the addition of considerable amounts of zinc oxide without much of it becoming molten at 1,400° C. Another desirable feature of a high-alumina batch, in the neighborhood of a mullite composition, is its very high resistance to spalling on rapid thermal changes, such as occur when fresh charge is put in a retort. Whether or not a high-alumina retort, with or without added zinc oxide, would prove most economical in actual service remains to be determined by factory experiments.

VI. ACKNOWLEDGMENT

This investigation was initiated by E. W. Washburn, chief, chemistry division, under whose general supervision the work was carried on.

WASHINGTON, October 21, 1931.

RP414

SYSTEM CaO-Na_2O-Al_2O_3

By L. T. Brownmiller and R. H. Bogue

ABSTRACT

A part of the system CaO-Na_2O-Al_2O_3, in the region low in Na_2O, has been investigated by the methods of phase equilibria. The stability fields, boundary curves, and invariant points have been defined. Optical and X-ray data are presented and ternary diagrams introduced to indicate the composition and temperature relations and the course of crystallization in the system.

CONTENTS

		Page
I.	Introduction	289
II.	Experimental method	290
III.	Binary systems of the components	292
	1. System CaO-Na_2O	292
	2. System CaO-Al_2O_3	292
	3. System Na_2O-Al_2O_3	295
IV.	Ternary compounds	296
V.	Stability fields	299
VI.	Quintuple points	300
VII.	Boundary curves	300
VIII.	Binary systems within the ternary diagram	302
	1. System $3CaO.5Al_2O_3$-$3CaO.2Na_2O.5Al_2O_3$	302
	2. System $CaO.Al_2O_3$-$3CaO.2Na_2O.5Al_2O_3$	302
	3. System $5CaO.3Al_2O_3$-$3CaO.2Na_2O.5Al_2O_3$	302
	4. System $3CaO.2Na_2O.5Al_2O_3$-$Na_2O.Al_2O_3$	302
	5. System CaO-$Na_2O.Al_2O_3$	303
	6. System $8CaO.Na_2O.3Al_2O_3$-$3CaO.2Na_2O.5Al_2O_3$ + $Na_2O.Al_2O_3$	303
	7. System $5CaO.3Al_2O_3$-$8CaO.Na_2O.3Al_2O_3$	303
	8. System $3CaO.Al_2O_3$-$8CaO.Na_2O.3Al_2O_3$	303
IX.	Course of crystallization	303
X.	Significance of the system CaO-Na_2O-Al_2O_3 in Portland cement	305
XI.	Summary	306
XII.	Acknowledgments	306
XIII.	Bibliography	307

I. INTRODUCTION

The studies reported in this paper are in continuation of a series begun several years ago to determine the constitution of Portland cement clinker and the part played by each of the compounds in the manufacture and utilization of that product. To-day those studies are fairly complete for the principal constituents of Portland cement, namely, for CaO, SiO_2, Al_2O_3, Fe_2O_3 and MgO; and from them the modern ideas on the constitution of cement have been evolved (1).[1]

Besides these components, there are many others occurring in small amounts in cements. Of the minor components, soda is one of the

[1] The figures given in parentheses here and throughout the text relate to the reference numbers in the bibliography at the end of this paper.

more important, since it is common to practically all cements. Therefore a continuation of those studies has been made to determine the combinations which soda is capable of forming with the other constituents of the cement.

The system CaO-Na_2O-Al_2O_3 has now been examined and constitutes the subject of this report. This system, however, was not explored completely. Not only would special methods have to be adopted to solve it entirely, but, in cements, the concentration of soda is small; hence, the studies in the system could be confined to compositions low in Na_2O. Apparently only one compound of CaO and Al_2O_3, $3CaO.Al_2O_3$, occurs in normal Portland cements; accordingly, that region of the diagram CaO-Na_2O-Al_2O_3 in which $3CaO.Al_2O_3$ occurs is the field of greatest importance. Nevertheless, because of the complexity of the system, other portions of the diagram had to be investigated to understand fully the relations in that region.

II. EXPERIMENTAL METHOD

Because of the volatility of Na_2O at temperatures above 900°,[2] somewhat special methods had to be used in preparing the samples. Base compositions of CaO and Al_2O_3 were weighed in various proportions, thoroughly mixed by stirring in a small amount of water and then burned in a platinum resistance furnace. A portion of about 5 g of this base composition was weighed and to it the third component, Na_2O, was added in the form of Na_2CO_3. The compositions of the raw materials are indicated in Table 1.

TABLE 1

Partial analysis by Carlson				Partial analysis by J. T. Baker Chemical Co.	
	Calcium carbonate		Alumina		Sodium carbonate
	Per cent		*Per cent*		*Per cent*
CaO	56.04	Al_2O_3	94.48	Insoluble	0.02
MgO	.07	SiO_2	.01	Cl	.005
R_2O	.06	Fe_2O_3	.002	SO_4	.004
R_2O_3	.05	CaO	Nil.	R_2O_3	.005
SiO_2	.01	Cl	Trace.	SiO_2	.005
Loss	43.71	SO_3	Trace.		
		Loss	1.42		

An excess of the sodium carbonate over that desired in the final sample was required since some Na_2O is volatilized on heating. After dry mixing of the components of the ternary composition, it was burned at a temperature of about 1,400°, pulverized and reburned at a higher temperature. Burning was done in an open platinum boat in a platinum-resistance furnace. After cooling in a desiccator, the sample was weighed and from the difference in weight the amount of Na_2O remaining in the mixture was calculated.

Relatively low temperatures were used for the first burning because this procedure resulted in less loss of Na_2O by volatilization than obtained with high initial burning temperatures.

[2] Temperatures are given in °C.

The amount of Na_2O lost on subsequent heatings at 1,400° to 1,500° was found to vary from less than 1 per cent of the total weight in samples low in soda to somewhat larger percentages in samples high in soda. In making up the compositions for these studies, an excess of about 25 per cent of sodium carbonate above the theoretical amount required was weighed into the base compositions, but this percentage excess could be reduced somewhat if the first burning were made at temperatures as low as about 1,100°. On twice burning such a mixture at 1,400° to 1,500° the composition was found usually to be within 1 per cent of that desired. Further adjustments could then be made to give the precise compositions required.

The second heating of the samples was necessary before final weighing because frequently not all of the carbon dioxide was evolved during the first burning, as evidenced by effervescence on treating with hydrochloric acid. Before final weighing, all samples were heated at least once to temperatures of about 1,500°.

Table 2 gives a few data on the amount of Na_2O volatilized from these samples heated in an open platinum container. The loss usually was less than 1 per cent after the Na_2O was once combined, but the amount of the loss was found to depend somewhat on the composition, the temperature, and the time of heating.

TABLE 2.—*Data showing the per cent loss in Na_2O following several heat treatments*

	Sample HU			Sample HT			Sample HS		
	Temperature	Na_2O	Loss	Temperature	Na_2O	Loss	Temperature	Na_2O	Loss
Na_2O added (per cent)		9.0			20.0			17.0	
Na_2O after first heating	1,450	6.3	2.7	1,450	13.8	6.2	1,450	12.5	4.5
Na_2O after second heating	1,425	5.9	.4	1,400	13.3	.5	1,425	11.8	.7
Na_2O after third heating	1,525	5.0	.9	1,475	12.6	.7	1,425	11.5	.3

These samples were then finely ground and portions taken for determining the temperature relations in the system. Heating curves were not obtained because the thermoelements are attacked by the Na_2O. Hence, the quenching method was used exclusively. In this method a small charge is inclosed in pure platinum foil and suspended in a quenching furnace (2) capable of reaching 1,630°. The samples were usually held in the furnace at desired temperature for 20 minutes, which was sufficient time for the attainment of equilibrium in most cases. Samples were then quenched in mercury or water and examined under a petrographic microscope. Samples dropped in mercury float on the surface and in some regions of the diagram cooling is not rapid enough to prevent quench growths; hence, water was frequently used. Crystallizations during quenching were troublesome in the regions in which the ternary compound $8CaO.Na_2O.3Al_2O_3$ crystallized. They can usually be recognized by wavy extinction under crossed nicols and by a brown color in ordinary light; also the refractive indices of such growths are slightly higher than those of the glass, but never as high as those of the true crystals. Often these growths form concentric bands around the primary phase.

The samples finally obtained as described above were too small for analysis, but the examination of other samples treated at corre-

sponding temperatures indicated that the amount of soda lost due to volatilization from these especially prepared specimens was considerably less than that shown in Table 2. The samples listed in Table 2 were burned in open platinum boats whereas the samples for quenching were always carefully inclosed in platinum foil. Furthermore, in working with samples just above (by one-half per cent of Na_2O) the boundary between the fields of $3CaO.2Na_2O.5Al_2O_3$ and $5CaO.3Al_2O_3$, the primary phase always was $3CaO.2Na_2O.5Al_2O_3$, whereas, if the amount of Na_2O lost were appreciable, the composition, after heating different samples of the same original composition for varying periods, would have been shifted to throw it into the field of $5CaO.3Al_2O_3$. It is felt that if such were the case different quenches of the same composition should have shown different primary phases. Such irregularities did not occur.

Because of the reaction of soda with the thermoelements, frequent calibration was necessary. It is believed that the reaction is principally with the rhodium and not with the platinum. Fused samples containing Na_2O were frequently colored pink or brown and in such cases the samples showed reaction with the metal. No such discoloration was noticed in samples wrapped in the pure platinum foil and the foil could usually be pulled from melted samples leaving a charge with a smooth surface and no indication of reaction.

The optical properties were determined with a petrographic microscope and the powder X-ray diffraction apparatus was employed to obtain the interplanar spacings of the compounds and for the identification of the phases in the samples. The radius of the cassettes is 8 inches and the effective wave length of the rays is 0.712 A.

The principal results of the study are shown diagrammatically in Figure 1.

III. BINARY SYSTEMS OF THE COMPONENTS

1. SYSTEM CaO-Na_2O

No evidence was obtained of the existence of any binary compound in this system. When samples made of these components were heated, the Na_2O was nearly completely volatilized and the optical properties of the CaO were apparently unchanged.

2. SYSTEM CaO-Al_2O_3

This system was studied by Rankin and Wright. The relations are given in their report, The Ternary System CaO-Al_2O_3-SiO_2. (3).

Four compounds were found: $3CaO.Al_2O_3$, which dissociates at $1{,}535° \pm 5°$ into CaO and liquid; $5CaO.3Al_2O_3$, which melts at $1{,}455° \pm 5°$; $CaO.Al_2O_3$, which melts at $1{,}600° \pm 5°$; and $3CaO.5Al_2O_3$, which melts at $1{,}720° \pm 10°$. The $3CaO.Al_2O_3$ does not form a eutectic with CaO, but the composition CaO 57, Al_2O_3 43, is the quadruple point at which the two compounds are stable in contact with liquid and vapor, the equilibrium temperature being $1{,}535° \pm 2°$. $3CaO.Al_2O_3$ forms a eutectic with $5CaO.3Al_2O_3$ having the composition CaO 50, Al_2O_3 50 which melts at $1{,}395° \pm 5°$. $5CaO.3Al_2O_3$ forms a eutectic with $CaO.Al_2O_3$ having the composition CaO 47, Al_2O_3 53 which melts at $1{,}400° \pm 5°$. $CaO.Al_2O_3$ forms a eutectic with $3CaO.5Al_2O_3$ of the composition CaO 33.5, Al_2O_3 66.5 which melts at

1,590° ± 5°. $3CaO.5Al_2O_3$ forms a eutectic with Al_2O_3 of the composition CaO 24, Al_2O_3 76 which melts at 1,700° ± 10°. It should be noted that the composition range within which $3CaO.Al_2O_3$ occurs as a primary phase on the liquidus curve is incorrectly stated on page 10 of the above paper, to be from CaO 50, Al_2O_3 50, to CaO 59, Al_2O_3 41. The range is given correctly in Tables B and C on pages 77

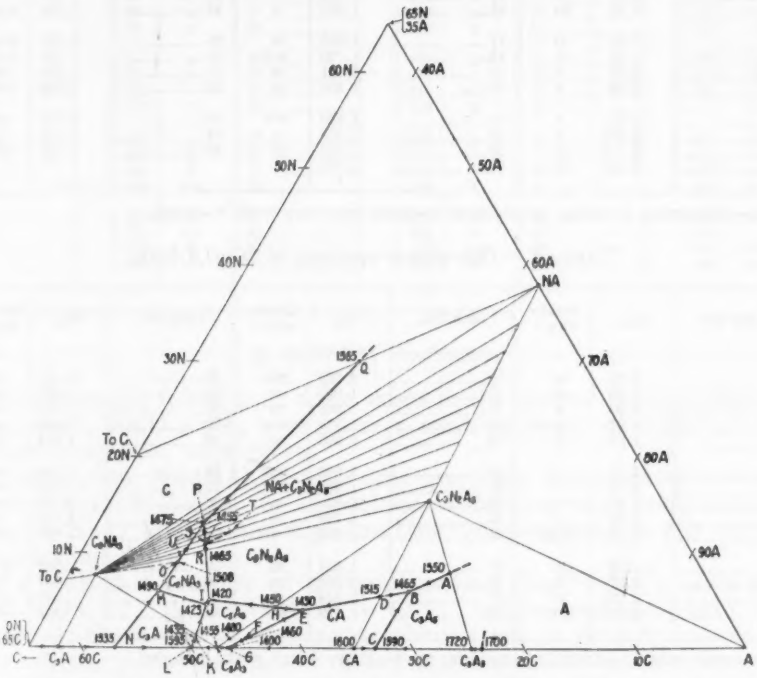

FIGURE 1.—*Diagram showing fields of primary crystallization and the binary systems within the ternary system CaO-Na_2O-Al_2O_3*

C = CaO; A = Al_2O_3; N = Na_2O.

and 78 of the same paper to be from CaO 50, Al_2O_3 50 to CaO 57, Al_2O_3 43.

The interplanar spacings of the X-ray diffraction pattern of $CaO.Al_2O_3$ and $3CaO.5Al_2O_3$ are given in Tables 3 and 4, respectively. Those of CaO, $3CaO.Al_2O_3$, and $5CaO.3Al_2O_3$ have been reported previously from this laboratory (4), but, as more satisfactory patterns of the latter two compounds have recently been obtained, these are given also in Tables 5 and 6.

TABLE 3.—*Interplanar spacings of $CaO.Al_2O_3$*

Line No.	d_{hkl}	Intensity [1]	Line No.	d_{hkl}	Intensity [1]	Line No.	d_{hkl}	Intensity [1]
1	3.70	m	13	2.080	w	25	1.461	m
2	3.40	w	14	2.025	m	26	1.450	m
3	3.31	w	15	1.963	w	27	1.410	m
4	3.18	m	16	1.925	s	28	1.363	wwb
5	2.96	ss	17	1.835	w	29	1.341	wwb
6	2.85	m	18	1.750	ww	30	1.295	wwb
7	2.68	w	19	1.681	w	31	1.278	ww
8	2.52	s	20	1.656	m	32	1.255	ww
9	2.41	s	21	1.605	ww	33	1.181	m
10	2.335	w	22	1.578	m	34	1.153	m
11	2.195	m	23	1.523	sb	35	1.069	ww
12	2.140	m	24	1.481	w			

[1] ss=very strong; s=strong; m=medium; w=weak; ww=very weak; b=broad.

TABLE 4.—*Interplanar spacings of $3CaO.5Al_2O_3$*

Line No.	d_{hkl}	Intensity [1]	Line No.	d_{hkl}	Intensity [1]	Line No.	d_{hkl}	Intensity [1]
1	3.62	m	15	2.055	mb	29	1.451	wb
2	3.50	ss	16	1.998	w	30	1.368	m
3	3.09	s	17	1.960	m	31	1.332	w
4	2.97	s	18	1.923	ww	32	1.306	w
5	2.87	s	19	1.900	m	33	1.284	w
6	2.75	s	20	1.866	ww	34	1.252	w
7	2.72	s	21	1.836	ww	35	1.178	w
8	2.59	ss	22	1.800	m	36	1.153	ww
9	2.52	s	23	1.759	m	37	1.134	w
10	2.43	mb	24	1.679	w	38	1.025	ww
11	2.32	m	25	1.624	m	39	.962	ww
12	2.27	m	26	1.553	m	40	.897	ww
13	2.185	m	27	1.533	sb	41	.893	ww
14	2.125	ww	28	1.479	ww	42	.875	ww

[1] ss=very strong; s=strong; m=medium; w=weak; ww=very weak; b=broad.

TABLE 5.—*Interplanar spacings of $3CaO.Al_2O_3$*

Line No.	d_{hkl}	Intensity [1]	Line No.	d_{hkl}	Intensity [1]	Line No.	d_{hkl}	Intensity [1]
1	4.07	m	19	1.821	w	37	1.204	s
2	3.32	w	20	1.785	ww	38	1.165	w
3	3.03	w	21	1.731	m	39	1.155	ww
4	2.83	w	22	1.693	ww	40	1.099	w
5	2.77	w	23	1.669	ww	41	1.053	ww
6	2.69	ss	24	1.640	w	42	1.034	ww
7	2.57	ww	25	1.611	w	43	1.017	s
8	2.46	ww	26	1.554	ss	44	.998	ww
9	2.400	w	27	1.512	ww	45	.966	ww
10	2.375	w	28	1.486	w	46	.897	m
11	2.270	w	29	1.449	w	47	.850	ww
12	2.200	m	30	1.426	ww	48	.811	ww
13	2.135	ww	31	1.404	w	49	.777	ww
14	2.085	w	32	1.360	w	50	.746	ww
15	2.033	w	33	1.345	s	51	.726	ww
16	1.981	w	34	1.315	ww	52	.694	ww
17	1.947	w	35	1.262	ww	53	.652	ww
18	1.905	s	36	1.231	w	54	.620	ww

[1] ss=very strong; s=strong; m=medium; w=weak; ww=very weak.

TABLE 6.—*Interplanar spacings of* $5CaO.3Al_2O_3$

Line No.	d_{hkl}	Intensity [1]	Line No.	d_{hkl}	Intensity [1]	Line No.	d_{hkl}	Intensity [1]
1	3.77	m	18	1.269	m	35	1.140	ww
2	3.18	m	19	1.599	s	36	1.110	m
3	2.98	s	20	1.554	w	37	1.091	w
4	2.67	ss	21	1.520	m	38	1.084	w
5	2.55	m	22	1.493	w	39	1.066	w
6	2.44	s	23	1.472	m	40	1.057	w
7	2.34	m	24	1.390	s	41	1.048	ww
8	2.180	s	25	1.353	ww	42	1.031	w
9	2.055	w	26	1.336	w	43	1.017	w
10	1.943	s	27	1.305	m	44	.989	ww
11	1.906	w	28	1.290	ww	45	.968	ww
12	1.846	w	29	1.274	w	46	.927	w
13	1.800	ww	30	1.260	w	47	.916	ww
14	1.764	w	31	1.234	w	48	.900	ww
15	1.728	m	32	1.207	w	49	.890	w
16	1.694	w	33	1.187	ww	50	.857	ww
17	1.660	s	34	1.171	w	51	.848	ww

[1] ss=very strong; s=strong; m=medium; w=weak; ww=very weak.

3. SYSTEM Na_2O-Al_2O_3

Matignon (5) found that there exists in the system Na_2O-Al_2O_3 one compound, $Na_2O.Al_2O_3$, which has a melting point at 1,650°. No optical properties were given.

The system Na_2O-Al_2O_3 was only partially investigated by the present authors due to the difficulties of working with compositions high in Na_2O and to the high melting temperatures in the region approaching Al_2O_3.

On heating a mixture of the composition $Na_2O+Al_2O_3$ (37.8 per cent Na_2O; 62.2 per cent Al_2O_3) to 1,630°, a homogeneous phase was obtained; there was no melting or dissociation at that temperature. The melting point could not be determined because of the temperature limitations of the furnace.

The compound $Na_2O.Al_2O_3$ was found to crystallize as colorless rounded grains. It is biaxial negative with indices of refraction: $\alpha=1.566\pm0.003$, $\beta=1.575\pm0.003$, $\gamma=1.580\pm0.003$. The optic axial angle is medium small, about 30°. Twinning commonly occurs. The interplanar spacings of the X-ray diffraction pattern are given in Table 7.

No other binary compounds were detected in the system but, on heating a sample containing 3.5 per cent Na_2O and 96.5 per cent Al_2O_3 for short periods at 1,100°, corundum and βAl_2O_3 were identified. On heating such samples at 1,500°, βAl_2O_3 and $Na_2O.Al_2O_3$ crystallized while corundum was absent. βAl_2O_3 was found to be the stable modification in the system $Na_2O.Al_2O_3$-Al_2O_3 at high temperatures in samples containing as large an amount as 96.5 per cent of Al_2O_3.

βAl_2O_3 was found to be uniaxial negative and to crystallize as plates with the optic axis parallel to the *c*-crystallographic axis. It belongs to the hexagonal crystal system. Determination of the indices of refraction on a sample of the compound furnished by the Norton Co. gave values: $\omega=1.678\pm0.003$; $\epsilon=1.635\pm0.003$. This sample which was made by fusion of Al_2O_3 with Na_2CO_3 appeared under the microscope to be practically pure βAl_2O_3. The crystals

were large and well developed, whereas in the sample referred to above containing 3.5 per cent Na_2O, the small size of the crystals of the βAl_2O_3 prevented satisfactory measurement of the indices of refraction. However, the X-ray diffraction pattern of this sample of βAl_2O_3 and that of the sample furnished by the Norton Co. (6) were identical.

IV. TERNARY COMPOUNDS

Two ternary compounds were found in the system CaO-Na_2O-Al_2O_3—one of a molecular composition $3CaO.2Na_2O.5Al_2O_3$ and the other $8CaO.Na_2O.3Al_2O_3$.

TABLE 7.—*Interplanar spacings of* $Na_2O.Al_2O_3$

Line No.	d_{hkl}	Intensity [1]	Line No.	d_{hkl}	Intensity [1]	Line No.	d_{hkl}	Intensity [1]
1	2.94	s	13	1.599	s	25	1.048	m
2	2.68	s	14	1.523	w	26	1.028	ww
3	2.60	ss	15	1.497	s	27	1.010	w
4	2.55	ss	16	1.471	w	28	.980	ww
5	2.38	w	17	1.458	s	29	.975	ww
6	2.22	ww	18	1.415	m	30	.955	w
7	2.145	w	19	1.362	s	31	.918	ww
8	1.983	ww	20	1.302	w	32	.910	ww
9	1.950	m	21	1.283	w	33	.880	ww
10	1.869	m	22	1.176	ww	34	.805	ww
11	1.805	w	23	1.119	m	35	.782	ww
12	1.762	m	24	1.065	ww	36	.762	ww

[1] ss=very strong; s=strong; m=medium; w=weak; ww=very weak.

By weight percentages the compound $3CaO.2Na_2O.5Al_2O_3$ contains 20.9 per cent CaO; 15.5 per cent Na_2O; 63.6 per cent Al_2O_3. This compound does not dissociate or melt at any temperature up to 1,630°. Optically it is biaxial positive; the mean refractive index is 1.592 ± 0.005; the birefraction is very weak, about 0.005; and it crystallizes as rounded grains. The interplanar spacings of the X-ray diffraction pattern of this compound are given in Table 8.

The compound $8CaO.Na_2O.3Al_2O_3$, having a composition of 54.9 per cent CaO, 7.6 per cent Na_2O, and 37.5 per cent Al_2O_3, dissociates into lime and liquid at 1,508°. Its composition lies outside the field in which it occurs as a primary phase. It is biaxial negative with a medium optic angle; indices of refraction are $\alpha = 1.702 \pm 0.003$, $\gamma = 1.710 \pm 0.003$. When the compound crystallizes as a primary phase, well-formed crystals are readily obtained. They often appear as polyhedrons with hexagonal or octagonal outline. When crystallization of the melt is rapid the compound separates as extremely fine crystalline material. In slowly cooled samples twinning is characteristic.

TABLE 8.—*Interplanar spacings of $3CaO.2Na_2O.3Al_2O_3$*

Line No.	d_{hkl}	Intensity [1]	Line No.	d_{hkl}	Intensity [1]	Line No.	d_{hkl}	Intensity [1]
1	4.20	s	22	1.660	w	43	1.058	w
2	3.91	s	23	1.600	w	44	1.051	m
3	3.41	m	24	1.575	w	45	1.025	ww
4	2.97	w	25	1.544	m	46	1.014	ww
5	2.84	s	26	1.499	s	47	1.000	ww
6	2.67	w	27	1.485	s	48	.975	w
7	2.58	ss	28	1.425	m	49	.951	ww
8	2.49	ww	29	1.391	m	50	.926	ww
9	2.43	w	30	1.363	m	51	.906	ww
10	2.34	w	31	1.333	ww	52	.854	w
11	2.25	m	32	1.302	w	53	.841	ww
12	2.20	m	33	1.288	m	54	.837	ww
13	2.14	m	34	1.263	ww	55	.815	ww
14	2.06	m	35	1.240	ww	56	.812	ww
15	1.990	m	36	1.214	ww	57	.787	ww
16	1.934	m	37	1.188	ww	58	.782	ww
17	1.863	m	38	1.161	m	59	.744	ww
18	1.842	m	39	1.144	m	60	.739	ww
19	1.805	s	40	1.162	w	61	.734	ww
20	1.738	m	41	1.102	w	62	.728	ww
21	1.697	w	42	1.080	wwb			

[1] ss=very strong; s=strong; m=medium; w=weak; ww=very weak; b=broad.

The compound $8CaO.Na_2O.3Al_2O_3$ was never obtained as a perfectly homogeneous phase. Fairly well-crystallized samples were obtained by heating preparations for about two hours just below the dissociation temperature. Longer heating periods were avoided because of possible loss of soda due to volatilization. Neither could the compound be obtained by annealing a glass of its own composition for such a glass could not be prepared since all of the CaO did not go into solution at the temperatures obtainable.

The interplanar spacings of the X-ray diffraction pattern of this compound are given in Table 9.

A consideration of the composition and structure of $8CaO.Na_2O.3Al_2O_3$ is of some interest.

Before the structure of the $8CaO.Na_2O.3Al_2O_3$ had been determined, it was noted that the X-ray diffraction pattern of the new compound was closely similar to that of $3CaO.Al_2O_3$. This suggested that the composition of the compound might lie on the line joining $3CaO.Al_2O_3$ and Na_2O and hence be represented by $3CaO.Al_2O_3$ plus some multiple of Na_2O, just as the ternary compound $3CaO.2Na_2O.5Al_2O_3$ may be represented by a composition $3CaO.5Al_2O_3$ plus $2Na_2O$. Accordingly, a mixture of $3CaO.Al_2O_3$ and Na_2O was prepared and heated at 1,400°; a temperature well below the dissociation temperature of the ternary compound. Following this heat treatment the sample was examined and found to contain considerable free CaO. If the compound were merely an addition product of Na_2O and $3CaO.Al_2O_3$ or a solution of Na_2O in $3CaO.Al_2O_3$, no lime should have been displaced at that temperature. The displacement of CaO in the mixture indicated that the new compound was not such an addition product.

TABLE 9.—*Interplanar spacings of $8CaO.Na_2O.3Al_2O_3$*

Line No.	d_{AAI}	Intensity [1]	Line No.	d_{AAI}	Intensity [1]	Line No.	d_{AAI}	Intensity [1]
1	3.37	w	10	2.03	w	19	1.492	w
2	3.03	w	11	1.915	s	20	1.347	m
3	2.68	ss	12	1.888	s	21	1.235	w
4	2.60	w	13	1.840	ww	22	1.210	m
5	2.53	w	14	1.797	ww	23	1.103	w
6	2.41	w	15	1.746	w	24	1.101	w
7	2.37	w	16	1.692	wb	25	1.055	w
8	2.20	s	17	1.628	w	26	1.019	m [2]
9	2.10	w	18	1.558	ss	27	.899	w

[1] ss=very strong; s=strong; m=medium; w=weak; ww=very weak; b=broad.
[2] Very broad.

If we consider the composition $8CaO.Na_2O.3Al_2O_3$, we observe that it may be represented as $3(3CaO.Al_2O_3)$ in which one CaO has been replaced by Na_2O. Bragg (7) has shown that in the silicates and associated compounds, the X-ray configuration is dependent upon the framework of the oxygen atoms; that is, when packed as closely as possible, the oxygen atoms form the basis of the structure of the compound whereas the other atoms lie between them. One criterion for such close packing is that the index of refraction of a compound with that structure lies above 1.70; $3CaO.Al_2O_3$ and $8CaO.Na_2O.3Al_2O_3$ both have indices above 1.70. The other atoms merely expand this oxygen lattice.

From the similarity of the X-ray diffraction patterns it would seem that the above conditions fit the case here. It might further be remarked that the crystal structure is a function of the unit cell and not of the chemical molecule; that is, the unit cell is some integral multiple of the chemical molecule and hence there is no difficulty encountered in the consideration of the replacement of one Na_2O for one CaO from three molecules of $3CaO.Al_2O_3$. Thus the unit cell of $3CaO.Al_2O_3$ may contain three times as many molecules as the unit cell of $8CaO.Na_2O.3Al_2O_3$. A solution of the structure of both of these compounds to the end of allocating the exact positions of all of the atoms should be of interest.

In its field of primary crystallization, $3CaO.Al_2O_3$ often crystallizes as well-formed polyhedrons with hexagonal or octagonal outline. In ordinary light these crystals appear similar to the well-formed crystals of $8CaO.Na_2O.3Al_2O_3$. Yet $3CaO.Al_2O_3$ is reported as belonging to the isometric system whereas $8CaO.Na_2O.3Al_2O_3$ does not belong to that system, since it is clearly birefracting.

Rankin and Wright (3) have reported that $3CaO.Al_2O_3$ is faintly birefracting, which birefraction they attribute to strain. In this study, the compound $3CaO.Al_2O_3$ showed a distinct but weak birefraction when large grains were available; this was noticeable both in the binary system CaO-Al_2O_3 and in the ternary system CaO-Na_2O-Al_2O_3.

Furthermore Harrington (4) found that his X-ray diffraction patterns of $3CaO.Al_2O_3$ did not altogether conform to the cubic structure and he assigned the compound to a pseudo-cubic system. His samples of $3CaO.Al_2O_3$ were carefully prepared and annealed for long periods in order to avoid strain in the crystals. Such treatment, however, did not alter the X-ray diffraction patterns. Hence, from these

structural considerations, it is suggested that $3CaO.Al_2O_3$ does not belong to the isometric system and only because of its extremely low birefraction has it been so classified.

The nature of the compound $3CaO.2Na_2O.5Al_2O_3$ will be discussed more fully below.

V. STABILITY FIELDS

The fields of stability of the various compounds in the ternary diagram are shown in Figure 1. Each of the components as well as all of the binary and ternary compounds which were found have stability fields in the system.

In the field of $3CaO.5Al_2O_3$ both the stable and unstable forms of that compound were formed. Usually the stable modification crystallized from the melt although occasionally the unstable modification appeared. No definite region of stability was found for either form.

The compound $5CaO.3Al_2O_3$ does not crystallize as such in the presence of Na_2O but as a solid solution of soda, in some form, in $5CaO.3Al_2O_3$. Whenever reference is made in this paper to the compound $5CaO.3Al_2O_3$ in the ternary diagram, this solid solution is indicated. As the amount of solid solution increases to its maximum, containing about 1 per cent of Na_2O, the index of refraction of $5CaO.3Al_2O_3$ is lowered from 1.61 to 1.59. The X-ray diffraction pattern shows a regular shift of the position of its lines as the amount of soda taken up is increased.

Whenever $3CaO.Al_2O_3$ and $8CaO.Na_2O.3Al_2O_3$ crystallized from the melt, well-formed crystals of both of these compounds were found. The crystals showed considerable similarity in appearance, but there was no indication of any solid solution of the two at the liquidus and the boundary curve separating the two fields was easily located.

A boundary separating the fields in which $Na_2O.Al_2O_3$ and $3CaO.2Na_2O.5Al_2O_3$ appear as primary phases could not be located. The properties of the primary phase in the region bounded by the radial lines (fig. 1), but lying to the right of the boundary *RPQ*, varied from those of $3CaO.2Na_2O.5Al_2O_3$ through insensible gradations to those of $Na_2O.Al_2O_3$. Throughout this region, also, the product of final crystallization consisted of two phases: $8CaO.Na_2O.3Al_2O_3$ and a second phase which had properties intermediate between $3CaO.2Na_2O.5Al_2O_3$ and $Na_2O.Al_2O_3$. For these reasons it appears probable that a continuous series of solid solutions exists between those two compounds. The consideration may be simplified by regarding $Na_2O.Al_2O_3$ as taking up $CaO.Al_2O_3$ in solution to a limiting composition of $3(CaO.Al_2O_3)+2(Na_2O.Al_2O_3)$. Since this limit can not be exceeded, it functions as a compound and may properly be regarded as such. The tie line $8CaO.Na_2O.3Al_2O_3$-$3CaO.2Na_2O.5Al_2O_3$ may thus be considered as expanded to include all compositions up to the position $8CaO.Na_2O.3Al_2O_3$-$Na_2O.Al_2O_3$. From the phase-rule viewpoint, that whole area may be regarded as consisting of an infinite number of tie lines passing from the origin, $8CaO.Na_2O.3Al_2O_3$, to the solid solution line $3CaO.2Na_2O.5Al_2O_3$-$Na_2O.Al_2O_3$. It should be pointed out that these tie lines indicate the mean products of final crystallization, but can not be regarded as crystallization curves; that is, the precise composition of the crystals formed at any given

temperature from any given composition of liquid, in this area, can be established only by experimentation (8) which has not been conducted in the present study.

No attempt was made to define a boundary separating the field in which the $Na_2O.Al_2O_3$ appears in solid solution with $3CaO.2Na_2O.5Al_2O_3$ and the field in which $Na_2O.Al_2O_3$ separates as primary phase.

VI. QUINTUPLE POINTS

Three quintuple invariant points were found in the system which represent ternary eutectics; that is, invariant compositions at which three solid phases coexist with liquid and vapor, occurring inside the triangle formed by the three solid phases (9).

The eutectic for $3CaO.5Al_2O_3$, $CaO.Al_2O_3$, and $3CaO.2Na_2O.5Al_2O_3$ (point *B*, fig. 1) occurs at a composition 27.5 per cent CaO, 6.0 per cent Na_2O, 66.5 per cent Al_2O_3, and melts at 1,465°.

The eutectic for $5CaO.3Al_2O_3$, $CaO.Al_2O_3$, and $3CaO.2Na_2O.5Al_2O_3$ (point *E*) occurs at a composition 38.0 per cent CaO, 4.0 per cent Na_2O, 58.0 per cent Al_2O_3, and melts at 1,430°.

The eutectic for $5CaO.3Al_2O_3$, $8CaO.Na_2O.3Al_2O_3$, and $3CaO.2Na_2O.5Al_2O_3$ (point *I*), occurs at a composition 46.0 per cent CaO, 5.0 per cent Na_2O, and 49.0 per cent Al_2O_3, and melts at 1,420°.

Three quintuple invariant points were found in the system which are not eutectics, that is, they are invariant compositions at which three solid phases coexist with liquid and vapor occurring outside the triangle formed by the three solid phases.

The invariant point for $3CaO.Al_2O_3$, $5CaO.3Al_2O_3$, and $8CaO.Na_2O.3Al_2O_3$ (point *J*) occurs at a composition 46.5 per cent CaO, 4.5 per cent Na_2O, and 49.0 per cent Al_2O_3. The melting temperature is 1,423°.

The invariant point for CaO, $3CaO.Al_2O_3$, and $8CaO.Na_2O.3Al_2O_3$ (point *M*) occurs at a composition of 50.0 per cent CaO, 6.0 per cent Na_2O, and 44.0 per cent Al_2O_3. The melting temperature is 1,490°.

The invariant point for CaO, $8CaO.Na_2O.3Al_2O_3$, and solid solutions of $Na_2O.Al_2O_3 + 3CaO.2Na_2O.5Al_2O_3$ (point *P*) occurs at a composition of 42.5 per cent CaO, 13.0 per cent Na_2O, and 44.5 per cent Al_2O_3. The melting temperature is 1,475°.

In addition to the above, some evidence was obtained to indicate that an invariant point occurs along the boundary *PI*, which separates the fields of $8CaO.Na_2O.3Al_2O_3$, and solid solutions of $Na_2O.Al_2O_3$ with $3CaO.2Na_2O.5Al_2O_3$, in the neighborhood of point *S*. This would then represent the composition at which the $Na_2O.Al_2O_3$ had taken up its maximum of $CaO.Al_2O_3$ in solid solution and simultaneously was in equilibrium with $8CaO.Na_2O.3Al_2O_3$. It would thus be the origin of a boundary *ST* separating the field of $3CaO.2Na_2O.5Al_2O_3$ from that in which increasing percentages of $Na_2O.Al_2O_3$ are present in the primary phase.

VII. BOUNDARY CURVES

Many of the boundary curves shown in Figure 1 are normal in all respects and need not be detailed. A few, however, are of especial interest.

At *E* a curve separating the fields of $5CaO.3Al_2O_3$ and $CaO.Al_2O_3$ leaves with temperatures increasing to point *F*, 1,460°, which is a

maximum. From F the temperature again drops to G, 1,400°, the eutectic of $5CaO.3Al_2O_3$ and $CaO.Al_2O_3$. Thus the ternary eutectic E melts at a higher temperature (1,430°) than the binary eutectic of $5CaO.3Al_2O_3$ and $CaO.Al_2O_3$ (1,400°). It may be remarked that point F may be considered the point at which the boundary curve separating the fields of $5CaO.3Al_2O_3$ and $CaO.Al_2O_3$ enters the ternary diagram because $5CaO.3Al_2O_3$ does not exist as such in this ternary system, but only as a solid solution of $5CaO.3Al_2O_3$ with the third component soda. Hence the binary eutectic to be considered in this case is not one of $CaO.Al_2O_3$ with pure $5CaO.3Al_2O_3$ but one of $CaO.Al_2O_3$ with the solid solution of $5CaO.3Al_2O_3+Na_2O$ with a melting point of 1,460° and falling at point F rather than point G.

From I the curve separating the fields of $8CaO.Na_2O.3Al_2O_3$ and $5CaO.3Al_2O_3$ leaves with temperatures increasing to point J, 1,423°, the quintuple point at which $3CaO.Al_2O_3$, $8CaO.Na_2O.3Al_2O_3$, and $5CaO.3Al_2O_3$ are in equilibrium. The temperatures of melting of points I and J are so close as to be practically indistinguishable with the control available. Yet a little consideration will show that point I is the eutectic rather than J, for the eutectic composition must be within the triangle joining the compounds taking part in the eutectic melting. The three solid phases in equilibrium with liquid and vapor at J are $3CaO.Al_2O_3$, $8CaO.Na_2O.3Al_2O_3$, and $5CaO.3Al_2O_3$; but J lies in the triangle $5CaO.3Al_2O_3$–$8CaO.Na_2O.3Al_2O_3$–$3CaO.2Na_2O.5Al_2O_3$; hence it can not be the eutectic. At point I, $5CaO.3Al_2O_3$, $8CaO.Na_2O.3Al_2O_3$, and $3CaO.2Na_2O.5Al_2O_3$ are in equilibrium with liquid and vapor, and since I lies in the triangle joining those compounds it must be the eutectic.

From J the boundary curve separating the field of $5CaO.3Al_2O_3$ from $3CaO.Al_2O_3$ leaves with temperatures increasing to a maximum at point K, 1,435°, and then falling to L, the binary eutectic of $5CaO.3Al_2O_3$ and $3CaO.Al_2O_3$ at 1,395°. This behavior is similar to that discussed above along the boundary curve E–F–G and is due to the existence of a solid solution of Na_2O in this system. Hence point K is the quadruple point at which $3CaO.Al_2O_3$ and solid solution $5CaO.3Al_2O_3+Na_2O$ are at equilibrium with liquid and vapor, and from which the boundary curve separating the fields of crystallization enters the ternary diagram.

From M the boundary M–O leaves with temperatures increasing to O, 1,508°, which is the maximum on the curve M–O–P separating the field of CaO and $8CaO.Na_2O.3Al_2O_3$.

Since O is the maximum on this curve, the compound which is dissociating must lie on a line joining O with the primary phase which separates when the compound dissociates. Inasmuch as O lies on the boundary separating the field of CaO from the field of $8CaO.Na_2O.3Al_2O_3$, the composition of the compound must lie on the line joining O with CaO. While the compound $8CaO.Na_2O.3Al_2O_3$ was never obtained as a perfectly homogeneous phase, yet it was in the neighborhood of this composition that the best samples of the compound were obtained. Final decision as to the composition was then made when the point O was located and O-CaO drawn.

From O the temperatures drop to point P, 1,475°, the quintuple point at which CaO, $8CaO.Na_2O.3Al_2O_3$, and solid solutions of $Na_2O.Al_2O_3+3CaO.2Na_2O.5Al_2O_3$ are in equilibrium. The tempera-

tures of melting then rise along the boundary separating the fields of CaO and $Na_2O.Al_2O_3$ to point *Q*, 1,565° ± 10°, the binary eutectic of CaO and $Na_2O.Al_2O_3$.

From *P* the temperatures drop along the boundary separating the field of $8CaO.Na_2O.3Al_2O_3$ from the field of solid solutions of $Na_2O.Al_2O_3 + 3CaO.2Na_2O.5Al_2O_3$ toward *S*.

Point *R* represents the binary eutectic of $8CaO.Na_2O.3Al_2O_3$ with $3CaO.2Na_2O.5Al_2O_3$ which falls at 1,465°. However, at *S* melting occurs at a temperature of 1,455°. At 1,465° there are still two crystalline phases with liquid and vapor.

If $3CaO.2Na_2O.5Al_2O_3$ and $Na_2O.Al_2O_3$ form a continuous series of solid solutions, as seems probable, then melting might be characterized by a minimum, such as found at 1,455° in the region of point *S*. Until the system $3CaO.2Na_2O.5Al_2O_3$-$Na_2O.Al_2O_3$ is fully established, the boundary curve *P–S–R* must remain only partially explained.

VIII. BINARY SYSTEMS WITHIN THE TERNARY DIAGRAM

1. SYSTEM $3CaO.5Al_2O_3$-$3CaO.2Na_2O.5Al_2O_3$

These two compounds form a true binary system with a eutectic (point *A*) at a composition: 22.8 per cent CaO; 8.0 per cent Na_2O; 69.2 per cent Al_2O_3. This eutectic melts at 1,550°. The unstable modification of $3CaO.5Al_2O_3$ appeared in some of the samples in this system, but no definite region of stabilty of this modification was found.

2. SYSTEM $CaO.Al_2O_3$-$3CaO.2Na_2O.5Al_2O_3$

The eutectic of these two compounds (point *D*) lies at a composition 30.3 per cent CaO, 5.4 per cent Na_2O, and 64.3 per cent Al_2O_3. It melts at 1,515°.

3. SYSTEM $5CaO.3Al_2O_3$-$3CaO.2Na_2O.5Al_2O_3$

There is a eutectic formed in this system (point *H*) at a composition 40.4 per cent CaO, 4.3 per cent Na_2O, and 55.3 per cent Al_2O_3. It melts at 1,450°. The melting temperatures do not decrease regularly from the melting point of $5CaO.3Al_2O_3$ but increase from 1,455°, the melting point of $5CaO.3Al_2O_3$, to 1,480° when about 1 per cent of Na_2O is present. This increase is due to solid solution formation of soda, as previously described, in $5CaO.3Al_2O_3$.

4. SYSTEM $3CaO.2Na_2O.5Al_2O_3$-$Na_2O.Al_2O_3$

No melting was observed in this system up to temperatures of 1,630°. On examination of three samples in the system, a homogeneous phase was found with refractive indices which varied between those of $Na_2O.Al_2O_3$ and $3CaO.2Na_2O.5Al_2O_3$. These samples were plainly striated with an appearance somewhat as exsolid solutions; that is, crystalline material which existed as a solid solution at high temperatures, but, due to reduced solubility at lower temperatures, separated into two phases on cooling. The X-ray patterns of these samples showed a structure similar but not identical to that of $3CaO.2Na_2O.5Al_2O_3$. The system can not be defined with precision from the data at hand as equipment permitting the employment of higher temperatures is required. The correlation of all of the data

indicates, however, that the system consists of a series of solid solutions of $CaO.Al_2O_3$ in $Na_2O.Al_2O_3$ with the end member at the composition $3CaO.2Na_2O.5Al_2O_3$.

5. SYSTEM CaO-$Na_2O.Al_2O_3$

These two compounds form a true binary system with a eutectic (point *Q*) at 20 per cent CaO, 30 per cent Na_2O, and 50 per cent Al_2O_3. It melts at 1,565° ± 10°. Samples of $Na_2O.Al_2O_3$ in this system are highly twinned; polysynthetic twinning is common.

Since the lines connecting the following compositions do not lie wholly within the fields of primary crystallization they do not form true binary systems. The following three systems are of that type:

6. SYSTEM $8CaO.Na_2O.3Al_2O_3$-$3CaO.2Na_2O.5Al_2O_3$+$Na_2O.Al_2O_3$

At the point (*R*) where the tie line of the limiting composition of the solid solution series cuts the boundary separating the fields of primary crystallization, a eutectic appears to be formed having the composition 43.7 per cent CaO, 10.2 per cent Na_2O, and 46.1 per cent Al_2O_3. It melts at 1,465°. $8CaO.Na_2O.3Al_2O_3$ appears along the liquidus in this system from the composition of the eutectic (*R*) to a composition *U*, 46.0 per cent CaO, 9.7 per cent Na_2O, and 44.3 per cent Al_2O_3 where the tie line joining the compounds intersects the boundary *MP*. On the lime side of that region, the $8CaO.Na_2O.3Al_2O_3$ dissociates into CaO and liquid; between *R* and $3CaO.2Na_2O.5Al_2O_3$ the latter compound is the primary phase.

This binary system may be regarded as extending from $8CaO.Na_2O.3Al_2O_3$ to any point on the line $3CaO.2Na_2O.5Al_2O_3$-$Na_2O.Al_2O_3$, but compositions along the line $8CaO.Na_2O.3Al_2O_3$-$Na_2O.Al_2O_3$ were not examined.

7. SYSTEM $5CaO.3Al_2O_3$.-$8CaO.Na_2O.3Al_2O_3$

The compound $8CaO.Na_2O.3Al_2O_3$ does not appear on the liquidus in this system.

8. SYSTEM $3CaO.Al_2O_3$-$8CaO.Na_2O.3Al_2O_3$

In spite of the similarity in structure and habit of these compounds, no evidence of solid solution formation between them was found at the liquidus. The line joining these compositions merely represents one boundary of the limiting areas which determine the final products of crystallization in the adjacent triangles.

The systems CaO-$8CaO.Na_2O.3Al_2O_3$ and $Na_2O.Al_2O_3$+$3CaO.2Na_2O.5Al_2O_3$-Al_2O_3 were not investigated.

IX. COURSE OF CRYSTALLIZATION

Three types of crystallization are found in this system. These will be discussed with the use of the diagram of Figure 2, which shows only a part of the field.

1. The crystallization proceeds to a boundary curve along which one solid phase partially disappears while the other crystallizes, the process becoming complete at the quintuple point for that boundary curve. This type of crystallization may be represented by a composition at point *a*. The primary phase to separate on cooling a melt

of that composition is $8CaO.Na_2O.3Al_2O_3$. As that compound separates, the composition of the liquid follows the line *a b*. When *b* is reached, $3CaO.2Na_2O.5Al_2O_3$ appears with the $8CaO.Na_2O.3Al_2O_3$. These two phases separate together, the mean composition of the solid following the line $8CaO.Na_2O.3Al_2O_3$-$3CaO.2Na_2O.5Al_2O_3$ and that of the liquid following the line *b I*. When *I* is reached the mean composition of the solid phase is represented by point *c*. $5CaO.3Al_2O_3$ then separates with the other crystalline phases and the mean composition of the solid phase follows the line *c a*, ending at *a*.

2. The crystallization curve proceeds to a quintuple point but at that point one solid phase entirely disappears and the crystallization curve proceeds along a boundary to another quintuple point. The primary phase at point *d* is CaO which separates until the liquid

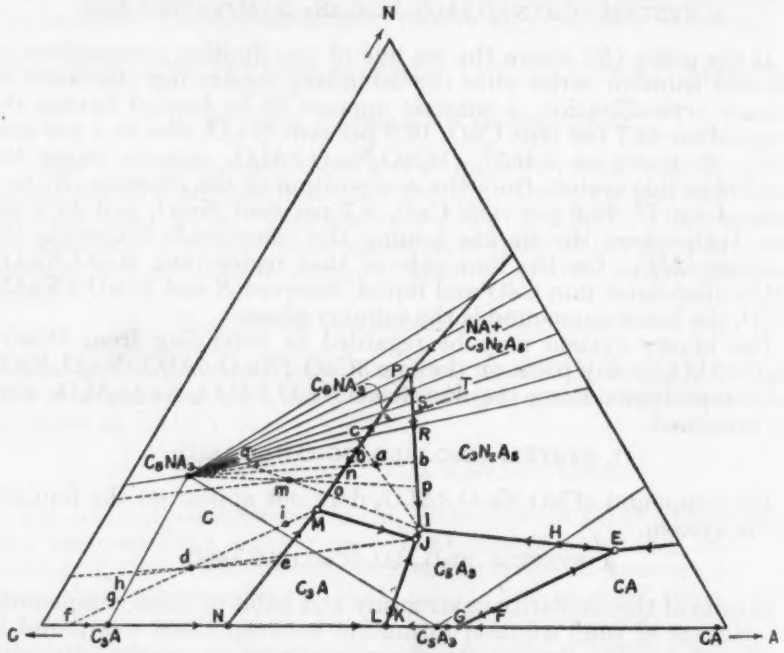

FIGURE 2.—*Diagram showing course of crystallization in a part of the system CaO-Na_2O-Al_2O_3*

reaches the composition *e*. Tricalcium aluminate then crystallizes with CaO along the line CaO-$3CaO.Al_2O_3$ until the mean composition of the solid phases arrives at point *f* when the composition of the liquid will be at *M*. $8CaO.Na_2O.3Al_2O_3$ then appears and the composition of the solid phase follows the line *f g* while the liquid remains at *M*. When the mean composition of the solid phases is represented by point *g*, the CaO disappears, having been dissolved during the simultaneous crystallization of $3CaO.Al_2O_3$ and $8CaO.Na_2O.3Al_2O_3$. The mean composition of the solid then follows the line *g h* while the liquid changes from *M* to *J*. At *J*, $5CaO.3Al_2O_3$ appears and the composition of the solid follows the line *h d*, and ends at *d*.

If the original composition had been located within a restricted area above the line connecting $8CaO.Na_2O.3Al_2O_3$ and $5CaO.3Al_2O_3$,

as at i, the crystallization curve would not have ended at J, but would have proceeded to the ternary eutectic at I.

3. The crystallization curve proceeds to a boundary along which one solid phase entirely disappears before a quintuple point is reached; it then leaves the boundary and crosses a field to another boundary curve along which it proceeds to a quintuple point. The primary phase at point m is CaO which separates until the liquid has the composition of point n. $8CaO.Na_2O.3Al_2O_3$ then appears and the mean composition of the solid phase passes along the line connecting CaO and $8CaO.Na_2O.3Al_2O_3$ until the composition of $8CaO.Na_2O.3Al_2O_3$ is reached. The liquid then has the composition of point o. On further cooling, $8CaO.Na_2O.3Al_2O_3$ separates alone while the composition of the liquid changes from o to p. At p, $3CaO.2Na_2O.5Al_2O_3$ appears and the mean composition of the solid changes from $8CaO.Na_2O.3Al_2O_3$ to point q while the liquid follows $p\,I$ to I. At I, $5CaO.3Al_2O_3$ appears and the mean composition of the solid changes from q to m, where the crystallization ends.

X. SIGNIFICANCE OF THE SYSTEM CaO-Na_2O-Al_2O_3 IN PORTLAND CEMENT

As stated in the introduction of this paper, that portion of the CaO-Na_2O-Al_2O_3 system in the neighborhood of $3CaO.Al_2O_3$ and low in soda is the region which is directly concerned with Portland cement. From this work alone, however, we can not predict the combinations of soda in cement; to do so a study must be made of systems involving the other components of cements with soda. However, we are able to say the following: Of the compounds of CaO, Na_2O, and Al_2O_3 which are important in solving the final status of the Na_2O in cement, $8CaO.Na_2O.3Al_2O_3$ alone is of significance. This is due to the existence in Portland cement of $3CaO.Al_2O_3$ alone, of the compounds of lime and alumina, and the finding in this study that the field of $3CaO.Al_2O_3$ adjoins that of $8CaO.Na_2O.3Al_2O_3$, but not that of $3CaO.2Na_2O.5Al_2O_3$. The stability of $8CaO.Na_2O.3Al_2O_3$ with the other constituents of cement, $3CaO.SiO_2$, $2CaO.SiO_2$, $4CaO.Al_2O_3.Fe_2O_3$, and MgO, must, therefore, be determined before the composition of the compounds of soda in cements can be defined.

Any direct attempt to identify $8CaO.Na_2O.3Al_2O_3$ in a commercial or laboratory cement probably would be unsuccessful. Identification by the microscope would be extremely difficult, since the compound must necessarily be present only in small amounts and the similarity of optical properties of $8CaO.Na_2O.3Al_2O_3$ and the other cement compounds makes difficult its differentiation from them by microscopic means. Likewise, the X-ray method can not be used to advantage because the principal lines of the diffraction pattern of $8CaO.Na_2O.3Al_2O_3$ coincide with those of $3CaO.Al_2O_3$, and only if $8CaO.Na_2O.3Al_2O_3$ were present in excessive amounts could we hope to establish its presence in cements. Hence thermal studies alone furnish the basis for establishing the nature of the soda compounds in cement. If thermal studies show that $8CaO.Na_2O.3Al_2O_3$ is stable in the presence of $3CaO.SiO_2$, $2CaO.SiO_2$, $4CaO.Al_2O_3.Fe_2O_3$, and MgO we are assured that Na_2O may exist in cement in the form of that ternary compound. In that case the Na_2O may replace some of the CaO from $3CaO.Al_2O_3$ and form the new combination $8CaO.Na_2O.3Al_2O_3$. Former studies in this laboratory have indicated

that Na_2O replaces CaO when the former is added to cement compositions, but this does not necessarily mean that the replacement must be in $3CaO.Al_2O_3$. It might be a replacement in $4CaO.Al_2O_3.Fe_2O_3$ or the silicates. All of these questions can be solved only by further study of the soda systems with the other components of cement.

XI. SUMMARY

A part of the system $CaO\text{-}Na_2O\text{-}Al_2O_3$ has been investigated by the method of phase equilibria and the results presented.

Two ternary compounds were found in the system, having the compositions: $3CaO.2Na_2O.5Al_2O_3$ and $8CaO.Na_2O.3Al_2O_3$.

The stability fields of the phases in the system have been defined, the boundary curves indicated and the invariant points located. The compositions and melting points of the compounds and of the invariant points are summarized in Table 10. The optical properties of the ternary compounds and of $Na_2O.Al_2O_3$ and βAl_2O_3 are given in Table 11. The interplanar spacings of the X-ray diffraction patterns are listed for the ternary compounds and for the binary compounds which have not previously been reported. Diagrams are presented which indicate the stability fields, temperature relations, and course of crystallization in the system.

XII. ACKNOWLEDGMENTS

The authors gratefully acknowledge their indebtedness to Dr. W. C. Hansen, formerly of this staff, for his contributions to this study. The investigation was begun by Doctor Hansen and brought by him to partial completion in the region of the compound $3CaO.2Na_2O.5Al_2O_3$. Both for this important contribution and continued interest and advice in the final solution of the system the authors take pleasure in giving full recognition and thanks.

TABLE 10.—*Compositions and melting points*

COMPOUNDS

Composition	CaO	Na_2O	Al_2O_3	Melting point	Authority
				°C.	
C_3A	62.2	-------	37.8	[1] 1,535	Rankin et al.
C_3A_2	47.8	-------	52.2	1,455	Do.
CA	35.4	-------	64.6	1,600	Do.
CA_2	24.8	-------	75.2	1,720	Do.
NA	-------	37.8	62.2	1,650	Matignon.
$C_3N_2A_3$	20.9	15.5	63.6	>1,630	Brownmiller.
C_8NA_3	54.9	7.6	37.5	[1] 1,508	Do.
BINARY EUTECTICS					
$C_3A\text{-}C_5A_3$	50.0	-------	50.0	1,395	Rankin et al.
$C_5A_3\text{-}CA$	47.0	-------	53.0	1,400	Do.
$CA\text{-}CA_2$	33.5	-------	66.5	1,590	Do.
$CA_2\text{-}A$	24.0	-------	76.0	1,700	Do.
$C\text{-}NA$	20.0	30.0	50.0	1,565	Brownmiller.
$C_3N_2A_3\text{-}CA_2$	23.0	8.0	69.0	1,550	Do.
$C_3N_2A_3\text{-}CA$	30.5	5.0	64.5	1,515	Do.
$C_3N_2A_3\text{-}CA_2$	40.0	4.5	55.5	1,450	Do.
$C_3N_2A_3\text{-}C_8NA_3$	43.2	10.3	46.5	1,465	Do.

[1] Dissociation temperatures.

TABLE 10.—*Compositions and melting points*—Continued

QUADRUPLE POINTS NOT EUTECTICS

Compositions	CaO	Na_2O	Al_2O_3	Melting point	Authority
				°C.	
C-C_3A	57.0		43.0	1,535	Rankin et al.
C-C_3NA_3	46.8	9.0	44.2	1,508	Brownmiller.

TERNARY EUTECTICS

C_3A_3-CA-$C_2N_2A_3$	27.5	6.0	66.5	1,465	Brownmiller.
CA-C_3A_3-$C_2N_2A_3$	38.0	4.0	58.0	1,430	Do.
C_3A_3-C_3NA_3-$C_2N_2A_3$	46.0	5.0	49.0	1,420	Do.

QUINTUPLE POINTS NOT EUTECTICS

C_3A_3-C_3A-C_3NA_3	46.5	4.5	49.0	1,423	Brownmiller.
C_3A-C-C_3NA_3	50.0	6.0	44.0	1,490	Do.
C-C_3NA_3-$C_2N_2A_3$+NA	42.5	13.0	44.5	1,475	Do.

TABLE 11.—*Optical properties of some of the compounds examined*

Refractive indices, ±0.003	Optic axial angle	Character	Appearance
NA α=1.566; β=1.575; γ=1.580	About 30°	Biaxial negative.	Colorless, rounded grains; twining common.
βAl_2O_3 ω=1.678; ϵ=1.635	Optic axis parallel to c-crystallographic axis.	Uniaxial negative.	Plates; hexagonal system.
$C_2N_2A_3$ Mean index 1.592; weak birefraction.		Biaxial positive.	Rounded grains.
C_3NA_3 α=1.702; γ=1.710	Medium angle	Biaxial negative.	Polyhedrons with hexagonal or octagonal outline.

The authors are indebted also to Dr. Herbert Insley, of the Bureau of Standards, who gave assistance in the microscopical identification of the phases, and to Dr. Frank C. Kracek, of the Geophysical Laboratory, for his advice and suggestions in the interpretation of data.

XIII. BIBLIOGRAPHY

1. Brownmiller and Bogue, Am. J. Sci., vol. 20, p. 241; 1930. B. S., Jour. Research, vol. 5, p. 813; 1930.
2. Shepherd, Rankin, and Wright, Am. J. Sci., vol. 28, p. 308; 1909.
3. Rankin and Wright, Am. J. Sci., vol. 39, p. 1; 1915.
4. Harrington, Am. J. Sci., vol. 13, p. 467; 1927.
5. Matignon, Compt. rend., vol. 177, p. 23; 1920.
6. Hansen and Brownmiller, Am. J. Sci., vol. 15, p. 225; 1928.
7. Bragg, Trans. Faraday Soc., p. 291; 1929.
8. Bowen, Am. J. Sci., vol. 40, p. 161; 1915.
9. Fenner, J. Geology, vol. 38, p. 159; 1930.

WASHINGTON, April 20, 1931.

RP415

DETERMINATION OF TIN IN IRONS AND STEELS

By J. A. Scherrer

ABSTRACT

Apparently tin is invariably a constituent of irons and steels, usually in amounts ranging from a few thousandths to a few hundredths of 1 per cent. The accurate determination of such small amounts of tin is difficult, and methods that have previously been recommended are unsatisfactory. Practically all of these methods are based on the reduction of tin to the divalent state, followed by oxidation to the quadrivalent state by means of a standard solution of iodine. The chief sources of errors in such methods lie in failure to remove other compounds that are reduced and oxidized, or in incomplete recovery of tin when separations are attempted. As a result of the present study, a method has been developed in which tin is separated from interfering elements, such as chromium, vanadium, and tungsten, by precipitation as sulphide in dilute nitric acid solution, and then separated from elements, such as copper and molybdenum, by precipitation with ammonium hydroxide. These treatments remove the elements that interfere, and the tin is then reduced in a sulphuric-hydrochloric acid solution containing granulated lead, and afterwards oxidized as usual by means of a standard solution of iodine. With proper precautions, results that are accurate to 0.001 per cent can be easily obtained.

CONTENTS

	Page
I. Introduction	309
II. Experimental	310
1. The choice of the method of analysis	310
2. Preliminary separation of tin	312
3. Final separation of tin	313
4. Reduction and titration of tin	313
5. Identification of tin	314
6. Sensitiveness, accuracy, and precision of the recommended procedures	314
III. Recommended procedures	316
1. For irons, plain carbon steels, and alloy steels decomposable by nitric acid	316
(*a*) Treatment when tungsten is absent	316
(*b*) Treatment when tungsten is present	317
(*c*) Precipitation and determination of tin	317
2. For alloy steels not decomposable by nitric acid	319
(*a*) Treatment in the absence of tungsten or other insoluble matter	319
(*b*) Treatment in the presence of tungsten or other insoluble matter	319
IV. Tin contents of representative materials	319
V. Acknowledgment	320

I. INTRODUCTION

Tin is not a significant constituent of iron ores, and in the past it has seldom been added to ferrous materials as an alloying constituent. It is, nevertheless, probably always present in irons and steels, unless

virgin materials have been used. Its source in such materials is either directly or indirectly the tin plate which finds its way into remelting scrap. On the other hand, tin is one of the usual impurities in tungsten ores, and in high-speed steels it is introduced in the ferrotungsten or metallic tungsten. Whether some tin is eliminated during the steel refining process or whether all of it remains and is gradually accumulating is apparently not definitely known. As a general rule, the amount of tin does not exceed 0.01 per cent in cast irons, plain carbon steels, and most alloy steels. High-speed tool steels sometimes contain as much as 0.05 per cent.

The effect of small quantities of tin on the properties of iron and steel has not been exhaustively investigated, but the opinion is growing that tin should not be overlooked. For example, W. Keller [1] has shown that 0.2 to 2.2 per cent of tin has very marked effects on the tensile strength, elongation, rolling properties, and tendency to develop fissures in steel. The effect of tin on the properties of high-speed tool steels has been studied by French and Digges.[2] It is possible that tin may be involved in peculiarities in the behavior of certain steels.[3] It may also have some effect in the nitriding process, for it is well known that nitriding can be prevented by applying a coating of tin.

In addition to the consideration that the metallurgist may need to give to the effect of tin on the properties of steel, the analyst should consider the behavior of tin in methods for the determination of other constituents of steel. For example, in certain methods for the determination of aluminum much, if not all, of the tin is reported as aluminum.

While the conditions in which tin may exist in iron or steel are not established with certainty, there is little doubt that it is largely present in solid solution. Intermetallic compounds, such as Fe_3Sn and $FeSn_2$, are indicated in the iron-tin equilibrium diagram.[4] There is little possibility that any tin is present as carbide or nitride, or that the oxide or other oxygenated compounds of tin could survive in molten carbon-bearing steel.

II. EXPERIMENTAL

1. THE CHOICE OF THE METHOD OF ANALYSIS

The chief methods for the determination of the small amounts of tin that are normally present in ferrous materials are: (1) precipitation as the sulphide and ignition to the oxide, and (2) reduction to the bivalent state and subsequent oxidation to the quadrivalent state by means of a standard solution of iodine. In this study the latter method was chosen because it is fully as accurate as the former, and the preliminary separations are less laborious.

To obtain accurate results by the iodometric method it is, of course, necessary (1) that all of the tin be gathered and then reduced to the divalent state before titrating with iodine and (2) that no iodine be consumed by compounds other than those of tin.

---

[1] Stahl u Eisen, vol. 49, pp. 138–140; 1929.

[2] H. J. French and T. G. Digges, Effect of Antimony, Arsenic, Copper, and Tin in High-Speed Tool Steels, Trans. Am. Soc. Steel Treat., vol. 13, pp. 919–940; 1928.

[3] For example, in a study of "Steel For Casehardening—Normal and Abnormal Steel," S. Epstein and H. S. Rawdon (B. S. Jour. Research, vol. 2, pp. 423–466; 1928), abnormalities were ascribed to the presence of as little as 0.01 per cent of aluminum. If the steels contained tin, more or less of it would have been reported as aluminum after determinations by the method of chemical analysis that was used.

[4] Int. Crit. Tables, vol. 2, p. 452; 1927. McGraw-Hill Book Co. (Inc.).

It might seem, and indeed it has been recommended, that it would suffice to dissolve plain carbon steels in hydrochloric or sulphuric acid under nonoxidizing conditions, and then to titrate with a standard solution of iodine. Such methods yield erratic results. Results for tin in some steels are high because iodine is consumed by gases or other compounds formed from impurities in the steel. With other steels, results are low for reasons that are difficult to ascertain. Typical analyses are shown in Table 1. Somewhat better, though still incorrect and erratic results are obtained if the solution of the iron is boiled with lead, or lead and antimony, as described in the reduction of the purified solution of tin (p. 318). Results obtained by this procedure are shown in Table 2.

TABLE 1.—*The determination of tin by direct titration with iodine following solution of the sample in sulphuric and hydrochloric acids*

Material	Tin		Error	
	Present	Found	By weight	Percentage
	g	*g*	*g*	
B. O. H. steel 1 per cent C	0.0001	0.0044	+0.0043	4,300
Ingot iron	.0008	.0007	−.0001	13
A. O. H. steel 0.2 per cent C	.0012	.0030	+.0018	150
Tin-bearing steel	.0570	.0410	−.0160	28

TABLE 2.—*The determination of tin by direct titration with iodine following solution of the sample in sulphuric and hydrochloride acids and reduction with lead and antimony*

Material	Tin		Error	
	Present	Found	By weight	Percentage
	g	*g*	*g*	
B. O. H. steel 1 per cent C	0.0001	0.0002	+0.0001	100
Ingot iron	.0008	.0007	−.0001	13
A. O. H. steel 0.2 per cent C	.0012	.0003	−.0009	75
Tin-bearing steel	.0570	.0538	−.0032	5.6

Among the substances that consume iodine should be mentioned sulphides and reduced compounds of vanadium, molybdenum, and chromium, all of which are present in steels and in most cast irons. Tungsten also interferes, for during the reduction process it is reduced to a colored compound which obscures the end point in the subsequent titration.

It is therefore evident that separations must be made before tin can be determined by the iodometric method.

TABLE 3.—*The determination of tin by solution of the sample in sulphuric acid and precipitating with hydrogen sulphide*

Material	Tin		Error	
	Present	Found	By weight	Percentage
	g	g	g	
B. O. H. steel 1.0 per cent C	0.00010	0.00006	−0.00004	40
Ingot iron	.0008	.0007	−.0001	13
Cast iron 2.66 per cent C	.0011	.0007	−.0004	36
A. O. H. steel 0.2 per cent C	.0012	.0011	−.0001	8
B. O. H. steel 0.82 C No. 14b [1]	.0018	.0006	−.0012	67
Tin-bearing steel	.0570	.0541	−.0029	5

[1] With this steel it was not possible to obtain more than 0.0014 g of tin by attack with powerful oxidizing agents, such as nitric acid, permanganate, and ammonium persulphate and silver nitrate, following the preliminary solution in sulphuric acid.

2. PRELIMINARY SEPARATION OF TIN

The simplest method for separating tin from iron, as well as from elements, such as chromium, vanadium, and tungsten, is by precipitation as the sulphide. In preliminary experiments it was found that complete precipitation of tin could not be obtained when the sample was dissolved in hydrochloric or sulphuric acids. This was at first ascribed to failure to adjust the solution to the proper acidity. Typical results are shown in Table 3. In tests on solutions of pure ferrous and ferric salts to which known amounts of tin and acids had been added it was found, however, that precipitation was complete in solutions that were much more acid than those of the samples of iron. For example, complete precipitation of tin was obtained in 500 ml of solution containing 10 g of iron as ferrous sulphate, together with as much as 15 ml of sulphuric acid. Further investigation indicated that the incomplete precipitation might be caused by the presence of organic compounds which were derived from the carbides and which formed stable complex ions with the tin. Material containing considerable amounts of carbides or other carbon compounds which are decomposed by dilute nonoxidizing acids, such as hydrochloric or sulphuric, gave more trouble than material containing uncombined carbon, or carbides which are insoluble in these acids. For example, a Bessemer steel containing 0.82 per cent of carbon yielded only about 50 per cent of its tin when dissolved in hydrochloric or sulphuric acid and treated with hydrogen sulphide. On the other hand, a high-speed steel containing 0.66 per cent of carbon, together with tungsten, chromium, and vanadium, which form insoluble carbides, yielded practically all of its tin. The same considerations hold true with cast irons. A cast iron containing 1 per cent of tin, 1.52 per cent of graphite, and 0.72 per cent of combined carbon showed 0.948 per cent of tin when decomposed with sulphuric acid. The complex compound that is formed is so stable that it even resists oxidation by permanganic acid. In view of the uncertainties introduced by the use of hydrochloric or sulphuric acids, it was decided to use the less attractive procedure of dissolving the sample in nitric acid whenever possible. Such an attack permits the complete precipitation of the tin, probably by preventing the formation of objectionable organic compounds. A drawback to the use of nitric acid is that it yields ferric nitrate, which afterwards reacts with hydrogen sulphide and

liberates considerable sulphur. It was found, however, that the mixture of sulphides and sulphur was not difficult to handle. Nitric acid by itself does not react with hydrogen sulphide if the solution is cold and dilute.

Some steels which do not dissolve in dilute nitric acid dissolve readily if a little hydrofluoric acid is added. So far as the determination of tin is concerned, the use of hydrofluoric acid is not permissible, for precipitation by hydrogen sulphide is incomplete, even though boric acid is added. The use of phosphoric acid in conjunction with sulphuric acid, which might seem attractive for the solution of tungsten-bearing steels, also leads to incomplete precipitation of tin.[5]

Precipitation with hydrogen sulphide can be expected to insure separation of tin from elements such as iron, chromium, vanadium, and tungsten, provided they are in solution at the start. Carbides, tungstides, or other insoluble compounds must be decomposed and dissolved before treatment with hydrogen sulphide is begun. If appreciable amounts of tungsten and vanadium are present tartaric acid is needed to avoid partial precipitation of these elements.

3. FINAL SEPARATION OF TIN

Treatment with hydrogen sulphide leaves tin still associated with elements such as copper, molybdenum, antimony, and arsenic. Of these, antimony and arsenic are normally present in only small amount and cause no difficulty in the determination of the small amounts of tin that are involved. The same can be said of selenium or tellurium, should these happen to be present.

Molybdenum interferes and must be removed. Copper is not objectionable unless present in larger amounts than are usually found in steels. Fortunately it is not difficult to separate tin from molybdenum (and also copper), for treatment with an excess of ammonium hydroxide gives a quantitative precipitation of tin with little or no precipitation of molybdenum or copper. In such precipitations it is advantageous to add a little ferric salt to act as a gatherer of the tin and to facilitate the subsequent solution of the precipitate. Incidentally, it should be noted that the precipitate can be expected to contain arsenic and antimony, as well as elements such as tungsten, chromium, and vanadium, if the preliminary treatments have failed to remove them.

4. REDUCTION AND TITRATION OF TIN

Various procedures have been recommended for the reduction of tin preliminary to the titration with iodine. In the analysis of bearing metal the author has had excellent results by the use of granulated lead, together with antimony added as the trichloride. This combination is specified in the recommended method as a matter of preference. Antimony can, no doubt, be dispensed with in most analyses. Its use gives rise to more lead chloride than is

[5] As regards the behavior of tin when steels are dissolved, it is interesting to note that in experiments with a steel containing 0.57 per cent of tin, the residues showed no tin after attack with dilute hydrochloric acid (1:3), 0.03 per cent after attack with dilute sulphuric acid (1:5), 0.06 per cent after attack with dilute nitric acid (1:4), and the full amount (0.57 per cent) after solution in iodine as in determinations of slag. All of the tin in the residues could be put in solution by digesting paper and residue in concentrated nitric and sulphuric acids.

obtained by lead alone, and some analysts may prefer to titrate in a clear solution, rather than against the white background of the lead chloride.[6] The apparatus used in the reduction is shown in Figure 1.

With the small amounts of tin contained in most steels the use of the theoretical titer of the iodine solution leads to no significant error.[7] If extreme accuracy is required, a more accurate titer can, of course, be obtained by carrying a synthetic sample, composed of pure tin and tin-free iron (or a carefully standardized steel, such as No. 22b) in the proportions present in the sample under test, through all steps of the method. For amounts of tin less than 0.005 g (10 g samples containing 0.05 per cent of tin) hundredth normal solutions, and for amounts over this, tenth normal solutions are suitable.

5. IDENTIFICATION OF TIN

Any determination of tin (particularly very small amounts) by a titration method is open to the question as to whether the standard solution was consumed by tin or by something else. To establish the presence of tin in the Bureau's Standard sample of ingot iron No. 55, four 50 g samples were dissolved in dilute sulphuric acid, and the tin, copper, arsenic, antimony, and molybdenum separated as sulphides. The papers and precipitates were combined and dissolved by digestion with nitric and sulphuric acids. Arsenic was removed by distillation, and the copper, antimony, and molybdenum were precipitated in a solution containing oxalic acid, ammonium oxalate and ammonium tartrate in accordance with the Clarke method. The tin was then precipitated by hydrogen sulphide, after the destruction of the oxalic and tartaric acids, and the yellow sulphide tested to confirm the presence of tin. In addition to qualitative verification, the percentage of tin was also determined after this laborious treatment and found to be 0.0067 per cent as compared with 0.0078 per cent obtained by the recommended procedure. The low result was to be expected in view of the incomplete precipitation of tin by hydrogen sulphide in a solution in which the iron was dissolved in sulphuric acid.

6. SENSITIVENSS, ACCURACY, AND PRECISION OF THE RECOMMENDED PROCEDURE

The sensitiveness of the recommended procedure depends (1) on the size of the sample taken, (2) the care with which the end point is obtained, (3) the accuracy to which the volume of the standard solution is read, and (4) the determination of the proper correction. The determination of the latter (iodine needed for impurities in the reagents and for the end point) can be made as usual by carrying the reagents through all steps of the procedure, or by calculating from the volumes of iodine required by samples of different weights, say 5 and 10 g. If small amounts of tin are in question, it is best to use a

[6] According to S. G. Clarke (The Analyst, vol. 56, p. 82; 1931, the use of antimony leads to errors (which may be compensating) because some tin is carried down by the reduced antimony and some of the finely divided reduced antimony may react with iodine. That such errors are of no significance in determinations of the small amounts of tin in most steels is demonstrated by the fact that standardizations of a 0.1 *N* solution of iodine against 100 mg portions of tin which had been reduced by lead in one case and lead-antimony chloride in another gave 0.005956 and 0.005966 g of tin, respectively. For 5 mg portions and a 0.01 *N* solution, the titers were 0.000584 and 0.000591.

[7] For example, the tin titer of a 0.1 *N* solution of iodine as found by actual titration against a known amount of tin carried through all steps of the method may be 0.005960 g of tin as compared with the theoretical titer 0.005935.

burette of small bore, say a 10 ml burette graduated to 0.05 ml. Such a burette can be read to 0.01 ml. Probably the limiting factor in the sensitivity of the method is ability on the part of the analyst to reproduce the end point. With care this need not be in error by more than 0.05 ml. Samples can easily be handled in 25 g units up to the point at which the sulphides have been washed. From this point as many as four papers and residues (representing 100 g) can be combined and carried through the rest of the method with little, if any, disturbance of the end point and correction for reagents. The importance of the size of the sample is evident when it is realized that 0.05 ml of 0.01 *N* iodine solution (equivalent to 0.00003 g of tin) represents 0.0003 per cent of tin in a 10 g, 0.00012 per cent in a 25 g and 0.00006 per cent in a 50 g sample.

The sensitiveness of the recommended procedure was tested by taking four 25 g samples of steel, adding 0.00025 g of tin to each of two samples, and carrying all of the samples through all of the steps of the method. The volumes of 0.01 *N* iodine solution required by the samples to which no tin was added were 0.37 and 0.38 (volume required by the blank and by the tin in the sample), while each of the other samples required 0.81 ml. The difference between the volumes required by the treated and untreated samples was, therefore, 0.43 ml which represented 0.000258 g of tin; or 0.00103 per cent as against the expected 0.001 per cent. In tests on the same steel made at the completion of the work, the volumes of 0.01 *N* iodine solution required by 10, 25, and 50 g samples and by the reagents alone were 0.43 (A), 0.52 (B), 0.70 (C) and 0.37 (D), respectively. B–A, C–A, and C–B, therefore, represent the corrected volumes of iodine required by 15, 40, and 25 g samples, respectively, and represent percentages of 0.00036, 0.00041, and 0.00043, or an average of 0.0004 per cent of tin in the steel. Incidentally, the blank corrections calculated from these titrations are 0.37, 0.36, 0.34, and 0.36, as compared with 0.37 obtained on the reagents alone.

The probable precision and probable accuracy of the method are illustrated by the data shown in Table 4.

TABLE 4.—*Data illustrating the probable accuracy and the precision of the recommended procedures*

[10 g samples]

Type of material	Tin			Tin found	Method used (see pp. 316 to 319
	In sample	Added	Total		
	Per cent	*Per cent*	*Per cent*	*Per cent*	
B. O. H. 1.0 per cent C steel	0.001	0.249	0.25	0.254	III, 1 (*a*).
		.249	.25	.253	
		.009	.01	.011	
High-speed steel (W–Cr–V)	.008	.042	.05	.052	III, 2 (*b*).
		.092	.10	.099	
		.242	.25	.245	
Cast iron	.011	.989	1.00	.998	III, 1 (*a*).
	Percentage of tin found				
Cr–V steel		0.0135	0.0137		III, 1 (*a*).
		.0138	.0137		
B. O. H., 0.8 per cent C steel		.0181	.0181		III, 1 (*a*).
		.0180	.0185		
		.0181	.0180		
		.0194	.0174		
High-speed steel (W–Cr–V)		.0260	.0256		III, 2 (*b*).
		.0263	.0253		
		.0262	------		
		.0252	.0253		III, 1 (*b*).

III. RECOMMENDED PROCEDURES

1. FOR IRONS, PLAIN CARBON STEELS, AND ALLOY STEELS DECOMPOSABLE BY NITRIC ACID

Treat a 10 g sample of the iron or steel in a 600 ml beaker with 250 ml of nitric acid (1:4), cover with a watch glass and warm gently until vigorous action ceases.[8] Bring nearly to the boiling point, continue heating until the sample is completely decomposed, and then boil for about 5 minutes. Gradually add a saturated solution of potassium permanganate until it is present in slight excess (usually 3 to 5 ml is required), and boil for about 5 minutes. Brown oxides of manganese separate if sufficient permanganate has been added. Cautiously add sulphurous acid until the oxides disappear, and boil for 5 to 10 minutes to expel sulphur dioxide.

(a) TREATMENT WHEN TUNGSTEN IS ABSENT

If any undecomposed matter remains, filter, wash, and reserve the filtrate. Occasionally the steel leaves a residue which is so finely divided that it passes through the filter. Such steels should be treated as in (*b*). Transfer the filter paper and residue to a 500 ml Erlenmeyer flask, and add 10 to 12 ml of sulphuric acid (specific gravity 1.84) and about 25 ml of nitric acid (specific gravity 1.42). Heat gently until the first vigorous action is over, then raise the temperature so that the nitric acid is expelled in 30 to 45 minutes and the sulphuric acid is fuming gently. Continue the addition and evaporation of nitric acid in small amounts until the sulphuric acid does not show any evidence of organic matter on fuming. The sulphuric acid should not be too strongly heated, as insoluble chromium sulphate may be formed. Two or three treatments with nitric acid usually suffice. Dilute to about 100 ml with distilled water, add about 10 g of tartaric acid, and boil until all soluble matter is in solution, and filter if necessary. Neutralize with ammonium hydroxide and add to the reserved filtrate.

[8] If very small amounts of tin are in question, larger samples and correspondingly larger amounts of reagents can be used. For example, in some tests, 25 g samples were dissolved in 600 ml of nitric acid (1:4), and the solution diluted to 800 ml before precipitation with hydrogen sulphide. In fact, this modification was used in obtaining the values of steels Nos. 14b, 0.018 per cent tin; 11d, 0.001 per cent tin; 10d, 0.002 per cent tin; 23a, 0.0007 per cent tin; and cast irons Nos. 82, 0.001 per cent tin, and 7b, 0.002 per cent tin. If the material contains an appreciable amount of tin, say over 0.05 per cent, samples smaller than 10 g can be used. The chief consideration then is to use 22.5 ml of nitric acid (1:4) for each gram of iron in addition to 5 ml for each 100 ml of the solution which is prepared for the hydrogen sulphide treatment.

(b) TREATMENT WHEN TUNGSTEN IS PRESENT[9]

Allow the solution to stand overnight, carefully decant the clear liquid and set it aside. Treat the residue[10] and small amount of liquid remaining in the beaker with about 20 ml of sulphuric acid and 30 ml of water. Heat just below the boiling point until no more bubbles of gas are given off and then evaporate until the sulphuric acid fumes gently. Add 10 to 15 ml of nitric acid (specific gravity 1.42) and again evaporate to slight fumes of sulphuric acid. All black residue should be decomposed. Dilute to about 100 ml with distilled water, add a small excess of ammonium hydroxide and about 10 g of tartaric acid. When the tartaric acid is in solution again add a slight excess of ammonium hydroxide. The solution should be clear. Make slightly acid and filter off any insoluble matter which may be present. Neutralize and add to the reserved solution.

(c) PRECIPITATION AND DETERMINATION OF TIN

Cool to room temperature, dilute to about 550 ml or more if desired and treat with a rapid stream of hydrogen sulphide for 30 to 45 minutes. Let settle for 1 to 2 hours, filter and wash with a slightly acid 5 per cent solution of ammonium sulphate which has been saturated with hydrogen sulphide.

Transfer the paper and precipitate to a 500 ml Erlenmeyer flask and decompose with sulphuric and nitric acid as in (*a*). Fume strongly. Cool and dilute to 100 ml with distilled water.

If the sample contains tungsten, add about 10 g of tartaric acid. When the acid has dissolved add a slight excess of ammonium hydroxide and heat to boiling. The solution should be clear. Add an excess of about 10 ml of sulphuric acid (specific gravity 1.84), filter, and wash. Dilute the filtrate to about 550 ml. Again treat with hydrogen sulphide, filter, wash, dissolve paper, and precipitate and dilute to 100 ml as before.

---

[9] This method is recommended for umpire determinations of tin in tungsten steels. Method III, 2 (*b*) has also given good results with such steels as have been tested, but has the possible weakness that is inherent in a sulphuric acid attack. For routine determinations, tungsten steels can be dissolved, and the solution filtered as in method III, 2 (*b*). The residue can then be discarded and the filtrate treated as in the method, except that 10 g of tartaric acid is dissolved, neutralized with ammonia and added to the solution before precipitating with hydrogen sulphide. The following results were obtained by applying the suggested procedures to typical high-speed (W-Cr-V) steels:

Tungsten steel	Percentage of tin found by method—				
	III, 1 (*b*)	III, 2 (*b*)		Modified III, 2 (*b*)	
A	0.0086	0.0081	0.0085	0.0079	0.0080
	------	.0082	.0081	.0074	.0078
	------	------	.0085	------	------
B	.0252	.0260	.0260	.0242	------
	.0253	.0264	.0252	.0233	------
	------	.0262	.0251	.0242	------
	------	.0263	------	------	------
C	.042	.041	.042	.0393	.0390
	.040	.041	.042	.0389	.0400
	------	.042	------	------	------
	------	.042	------	------	------
D	.013	.013	------	.011	------
	.013	.013	------	.013	------
	------	.013	------	------	------
	------	.013	------	------	------

[10] The black residue, chiefly carbides of chromium and vanadium, always contains a little tin. For example, in tests of two high-speed tool steels containing 0.026 and 0.042 per cent of tin, the tin found in the residues represented 0.0011 and 0.0011 per cent.

Boil until the solution is clear or all soluble matter is in solution. Add 15 mg of hydrochloric acid, and filter to remove sulphur [11] (also graphite in the case of cast irons) and wash with water.

Add about 40 mg of iron as chloride or sulphate to the filtrate, which should have a volume of about 200 ml, heat to boiling and add dilute ammonium hydroxide (1:1) until in moderate excess (5 to 10 ml) and boil. Filter and wash three or four times with dilute ammonium hydroxide (2:100), and two or three times with water.[12] The filter should not be allowed to run dry, for this causes filtration to become very slow in some cases. Dissolve the precipitate by passing a hot mixture of 80 ml of hydrochloric acid and 100 ml of distilled water through the paper, catching the solution in a 500 ml Erlenmeyer flask. Dilute to about 350 ml, add a solution of about 10 to 15 mg of antimony as chloride or sulphate (see II, 4) and then about 10 g of test lead. Connect with an air condenser (see fig. 1) and start a stream of carbon dioxide through the apparatus. Heat to boiling and boil gently for 30 to 40 minutes. Cool in a bath of ice water and regulate the current of carbon dioxide so as to prevent back pressure. This may be detected by placing the bubble tube on the end of the air condenser. When the solution has cooled to at least 10° C., add 5 ml of clear starch solution (10 g of soluble starch to 1 liter of water seems to be more sensitive with 0.01 *N* iodine solution) through the air condenser. Remove the plug in the third hole of the stopper and immediately insert the tip of the burette (10 ml capacity in the usual case) containing the standard iodine, or iodate solution. Titrate to the first permanent shade of blue. Deduct the volume required for a blank run, and multiply by the tin titer of the solution.[13]

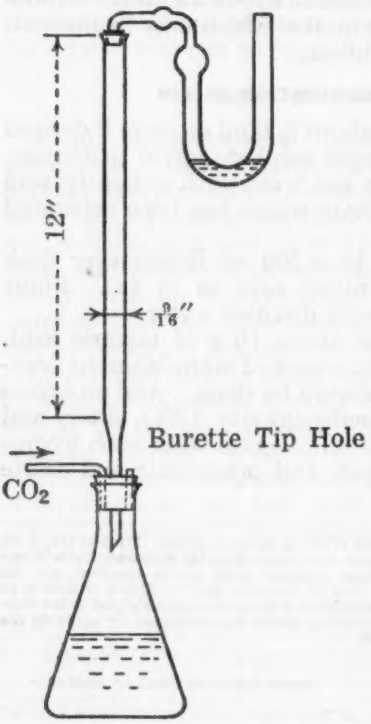

FIGURE 1.—*Apparatus for reduction of tin*

For material containing less than 0.05 per cent of tin use a 0.01 *N* solution; for higher percentages use 0.1 *N* solution. The theoretical titer may be used in the ordinary case. One ml of 0.01 *N* iodine equals 0.0006 g of tin (0.0005935 theoretical). If more than 1 per cent of tin is in question, or exceptional accuracy is required, the titer should be obtained by standardizing against pure tin.

[11] The sulphur contains very little if any tin. For example, the sulphur residues obtained in the analysis of six 10-gram samples of steels containing an aggregate of 0.0150 g of tin showed only 0.00012 g of tin when they were carefully burned and the residues combined and tested for tin.

[12] The filtrate contains practically all of the copper and molybdenum. In routine work, the percentage of copper can be estimated from the color of the solution, and the percentage of molybdenum by acidifying, evaporating to a small volume, and proceeding by the colorimetric method.

[13] The addition of potassium iodide is optional. In either case the end point is distinct, and usually requires about 0.37 ml of 0.01 *N* solution in the absence of added iodide and about 0.1 ml if 1 g of iodide has been added. The iodide can be added with the starch, as, for example, by using 5 ml of a solution prepared as follows: To 500 ml of boiling water add a cold suspension of 5 g of soluble starch in 25 ml of water. Cool, add a cool solution of 5 g of sodium hydroxide in 50 ml of water, then add 15 g of potassium iodide, and mix thoroughly.

2. FOR ALLOY STEELS NOT DECOMPOSABLE BY NITRIC ACID

(a) TREATMENT IN THE ABSENCE OF TUNGSTEN OR OTHER INSOLUBLE MATTER

Treat 10 g of the sample with 130 ml of sulphuric acid (1:5). Heat on the steam bath until vigorous action ceases. Place on a hot plate, heat gently until decomposition is complete, and then boil for about 5 minutes. Gradually add an excess of crystals of potassium permanganate (5 to 7 g is usually required) or oxidize with 25 ml of nitric acid (1:1) and then add an excess of a saturated solution of permanganate. Boil for about 5 minutes. Oxides of manganese should persist. Add 25 to 50 ml of a saturated solution of sulphurous acid, and boil for about 5 to 10 minutes to remove sulphur dioxide. The solution is now ready for treatment with hydrogen sulphide as in III, 1 (c) (p. 317).

(b) TREATMENT IN THE PRESENCE OF TUNGSTEN OR OTHER INSOLUBLE MATTER

Dissolve 10 g of sample in sulphuric acid, filter, treat the filtrate as in (*a*) and reserve it. Decompose the paper and residue with nitric and sulphuric acids as in III, 1 (*b*)[14]. When tungsten is present the darkening of the residue that takes place on fuming with sulphuric acid should not be mistaken for organic matter. Moreover, the sulphuric acid should be fumed very gently when chromium is present, for strong fuming may yield insoluble compounds of chromium. Dilute to 100 ml with distilled water, heat to boiling, and digest for one-half to one hour. Add a small excess of ammonium hydroxide and 10 to 15 g of tartaric acid. When the tartaric acid has dissolved again add a small excess of ammonium hydroxide, and digest on the steam bath until solution is complete or nearly so (usually one-half to one hour). Then add an excess of about 5 ml of sulphuric acid (specific gravity 1.84) and digest on the steam bath for one-half hour. Solution is generally complete at this point. If not, filter, decompose the filter and residue as before, and unite the solution with the other. Neutralize with ammonium hydroxide, add to the reserved filtrate, and treat the combined solutions as in III, 1 (*c*) (p. 317).

IV. TIN CONTENTS OF REPRESENTATIVE MATERIALS

The amounts of tin found in representative ferrous materials are shown in Table 5.

[14] The residue obtained from tungsten steels always contains a little tin. For example, in a determination in which the main solution and the tungstic acid were treated separately, of a total percentage of 0.026 in the steel, 0.024 was found in the solution and 0.0017 per cent in the tungstic acid. In addition to tin and tungsten, the steel also contained chromium and vanadium.

TABLE 5.—*Tin contents of Bureau of Standards standard samples*

Material	Tin	Material	Tin
	Per cent		*Per cent*
Cast iron 4d	[1] 0.011	B. O. H. steel 15b 0.1 per cent C	[1] 0.011
Cast iron 5f	[3] .012	B. O. H. steel 16b 1.0 per cent C	[3] .001
Cast iron 6d	[2] .012	A. O. H. steel 19c 0.2 per cent C	[2] .012
Cast iron 7b	[2] .002	A. O. H. steel 20c 0.4 per cent C	[2] .015
Cast iron 74	[3] .009	A. O. H. steel 21c 0.6 per cent C	[2] .004
Ni, Cr. Iron 82	[2] .001	A. O. H. steel 34a 0.8 per cent C	[2] .007
Bessemer steel 8d 0.10 per cent C	[2] .002	A. O. H. steel 35a 1.0 per cent C	[2] .011
Bessemer Steel 9c 0.2 per cent C	[3] .002	Ingot iron 55	[2] .008
Bessemer steel 10d 0.4 per cent C	[3] .002	Cr V steel 30c	[3] .014
Bessemer steel 22b 0.6 per cent C	[3] .0004	Cr Ni steel 32b	[2] .013
Bessemer steel 23a 0.8 per cent C	[2] .0007	Cr Mo steel 72	[2] .009
Electric steel 51 1.2 per cent C	[2] .005	Cr Ni (18–8) KA2–S 101	[1] .005
Acid electric steel 65a	[1] .024	Nickel steel 33b	[2] .009
B. O. H. steel 11d 0.2 per cent C	[3] .001	Stainless 73	[2] .004
B. O. H. steel 12d 0.4 per cent C	[2] .0006	Rail steel 100	[3] .007
B. O .H. steel 13c 0.6 per cent C	[2] .010	W–Cr–V (high-speed) steel 50	[1] .008
B. O. H. steel 14b 0.8 per cent C	[3] .018	W–Cr–V (high-speed) steel 50a	[3] .026

[1] Denotes the average of 3 or more determinations.
[2] Denotes 1 determination.
[3] Denotes the average of duplicate determinations.

V. ACKNOWLEDGMENT

The author wishes to express his gratitude to Dr. G. E. F. Lundell, of the Bureau of Standards, under whose direction the investigation has been conducted.

WASHINGTON, D. C., December 2, 1931.